

**RESTING-STATE FUNCTIONAL
MAGNETIC RESONANCE IMAGING IN
LATE-LIFE DEPRESSION AND
DEMENTIA**

Eva Rose Kenny

Doctor of Philosophy

Newcastle Magnetic Resonance Centre and
Institute for Ageing and Health

December 2010

Abstract

Introduction

The aim of this research was to use novel functional imaging approaches to investigate connectivity between key brain regions affected in late-life depression (LLD), Alzheimer's disease (AD) and dementia with Lewy bodies (DLB). Using functional magnetic resonance imaging (fMRI), spontaneous low-frequency fluctuations (SLFs) in the blood oxygenation level dependent (BOLD) signal were measured at rest. SLFs represent synchronisation of neuronal activity; therefore differences between subjects reflect differences in underlying networks.

Methods

The first resting-state study investigated connectivity in LLD and involved 33 subjects aged 65 years and over; 17 control and 16 LLD subjects. It was planned to apply this methodology in the dementia study also. However, a global synchronicity pattern was evident in some subjects, which had not previously been seen in the LLD study. Methods were investigated to correct for these spurious fluctuations, thought to be unrelated to neuronal activity (e.g. physiological artefacts), meaning connectivity of neuronal origin only was investigated. The second study investigated connectivity in 47 subjects aged 60 years and over; 16 control, 16 AD and 15 DLB subjects. Additional pre-processing steps were used to remove non-neuronal fluctuations, informed by the previous study. All subjects were scanned using a 3 Tesla MRI System. Functional connectivity was measured by extracting the mean BOLD signal time-series from seed regions in the brain and cross-correlating with all other brain voxels using the FMRIB Software Library (FSL) tools.

Results

In the LLD study, control subjects showed frontal connectivity with the head of caudate nucleus, whereas the LLD group showed a more widespread pattern of connectivity. LLD subjects showed significantly greater connectivity than controls between the bilateral caudate and a number of brain regions, whereas controls showed no brain regions of greater connectivity than LLD subjects. Pre-processing methods, to correct for non-neuronal fluctuations, were found to remove global synchronicity and improve data accuracy. In the second study, AD and DLB subjects showed significantly greater functional connectivity with a number of seed regions compared to the control group. No brain regions showed significantly greater connectivity in control compared

to AD or DLB subjects. Additionally, specific seed regions showed greater connectivity in AD compared to DLB, and vice versa.

Conclusions

This study reported abnormalities in connectivity in LLD, AD and DLB. The potential outcome of these findings is that they will inform greater understanding of the neurobiology of these disorders and in turn aid in early diagnosis and in the development of specific treatments to target the abnormally functioning brain regions.

Acknowledgements

My thanks go to the following people within the Newcastle Magnetic Resonance Centre and the Institute for Ageing and Health, Newcastle University who have helped and contributed to this work.

Firstly, my thanks go to my supervisors, Professor Andrew Blamire and Professor John O'Brien, for their continuous support throughout the course of my PhD. For arranging regular supervision meetings despite their busy schedules and always making time to provide comments and suggestions on my work and ways to take the PhD research forward. Additionally, my thanks go to Professor Blamire for the writing of a Matlab script to make the functional connectivity analysis in the dementia data automated.

Dr David Cousins who had previously carried out initial basic analysis on the late-life depression data and offered helpful suggestions with regards to analysis methods in the initial stages of my PhD. Dr Cousins carried out some of the preparatory work on the depression data, for example the brain extraction, which was extremely useful at the beginning of my PhD. Dr Michael Firbank has provided a great deal of support throughout the course of my PhD with his extensive knowledge on functional MRI and image analysis tools. Dr Firbank provided the volumetric white matter hyperintensity data for the LLD study and helped with the Matlab script to make the functional connectivity analysis of the dementia data automated.

Dr Kieren Hollingsworth and Dr Robert Barber, my internal assessors, who took time to read my yearly reports and arrange meetings to give feedback. Dr Jonathan Richardson and Dr Alan Thomas for subject recruitment and assessment for the late-life depression study, and the radiographers, Ms Carol Smith and Ms Louise Morris who scanned the study subjects. I would like to thank the Medical Research Council who funded my PhD Studentship and the Alzheimer's Research Trust, North East DeNDRoN Network and Biomedical Research Centre for funding subject recruitment and assessment for the studies.

Finally I would like to especially thank Rose and Noel who have offered constant support and encouragement throughout my studies, and to Chris and Tilly who have had to put up with the late nights and early mornings!

All this thesis is my own work apart from; the brain extraction (Dr Cousins), white matter hyperintensity data (Dr Firbank) and the Matlab script for functional connectivity analysis of the dementia data (Dr Firbank and Professor Blamire).

Contents

List of Figures

List of Tables

Abbreviations

Chapter 1 – Clinical Background	1
1.1 Depression	1
1.1.1 <i>Late-Life Depression</i>	2
1.2 Dementia	6
1.2.1 <i>Alzheimer’s Disease</i>	7
1.2.2 <i>Dementia with Lewy Bodies</i>	12
1.2.3 <i>Management of Alzheimer’s Disease and Dementia with Lewy Bodies</i>	19
Chapter 2 – Functional Neuroimaging Background	23
2.1 Magnetic Resonance Imaging	24
2.1.1 <i>The Nuclear Magnetic Resonance Experiment</i>	24
2.2 Functional Magnetic Resonance Imaging	26
2.2.1 <i>The Blood Oxygenation Level Dependent Response</i>	28
2.3 Resting-State Functional Magnetic Resonance Imaging	33
2.3.1 <i>The Default Mode Network</i>	37
2.3.2 <i>Origin of Spontaneous Low-Frequency Fluctuations</i>	40
2.4 Analysis methods for Functional Magnetic Resonance Imaging Data	41
2.4.1 <i>Model-Based Methods</i>	41
2.4.2 <i>Model-Free Methods</i>	42
2.4.3 <i>Pre-Processing Methods</i>	44
Chapter 3 – Neuroimaging Studies in Depression	49
3.1 Structural Magnetic Resonance Imaging	50
3.2 Functional Neuroimaging	53
3.2.1 <i>Positron Emission Tomography</i>	53
3.2.2 <i>Functional Magnetic Resonance Imaging</i>	55

Chapter 4 – Neuroimaging Studies in Alzheimer’s Disease and Dementia with Lewy Bodies	63
4.1 Structural Magnetic Resonance Imaging	64
4.2 Functional Neuroimaging	66
4.2.1 <i>Single Photon Emission Computed Tomography and Positron Emission Tomography</i>	66
4.2.2 <i>Functional Magnetic Resonance Imaging</i>	68
Chapter 5 – Investigation of Functional Connectivity in Late-Life Depression	74
5.1 Rationale for the Study	74
5.2 Aims	75
5.3 Hypotheses	75
5.4 Methods	75
5.4.1 <i>Subjects and Assessment</i>	75
5.4.2 <i>Imaging</i>	76
5.4.3 <i>Selection of the Seed Region</i>	77
5.4.4 <i>Placing of the Seed Region</i>	79
5.4.5 <i>Functional Connectivity Analysis</i>	80
5.4.6 <i>White Matter Hyperintensities and Functional Connectivity</i>	81
5.4.7 <i>Depression Severity and Functional Connectivity</i>	82
5.5 Results	83
5.5.1 <i>Demographics</i>	83
5.5.2 <i>Group Functional Connectivity</i>	85
5.5.3 <i>Brain Hemisphere and Functional Connectivity</i>	89
5.5.4 <i>White Matter Hyperintensities and Functional Connectivity</i>	91
5.5.5 <i>Depression Severity and Functional Connectivity</i>	94
5.6 Discussion	97
5.6.1 <i>Strengths and Limitations</i>	101
5.7 Conclusion	102

Chapter 6 – Methodology to Correct for Non-Neuronal

Fluctuations	103
6.1 Introduction	103
6.2 Aims	105
6.3 Methods	105
6.3.1 <i>Seed Placing</i>	105
6.3.2 <i>Motion Artefact</i>	106
6.3.3 <i>Medications</i>	106
6.3.4 <i>Spurious Fluctuations</i>	107
6.4 Results	115
6.5 Discussion	119
6.6 Conclusion	120

Chapter 7 – Investigation of Functional Connectivity in Alzheimer’s

Disease and Dementia with Lewy Bodies	121
7.1 Rational for this Study	121
7.2 Aims	122
7.3 Hypotheses	122
7.3.1 <i>Seed Regions</i>	122
7.3.2 <i>Neuropsychiatric Measures</i>	125
7.4 Methods	125
7.4.1 <i>Subjects and Assessment</i>	125
7.4.2 <i>Imaging</i>	126
7.4.3 <i>Placing of the Seed Regions</i>	127
7.4.4 <i>Functional Connectivity Analysis</i>	130
7.5 Results	133
7.5.1 <i>Demographics</i>	133
7.5.2 <i>Group Functional Connectivity</i>	136
7.6 Discussion	176
7.6.1 <i>Main Study Findings</i>	176
7.6.2 <i>Findings in Relation to Hypotheses</i>	177
7.6.3 <i>Findings in Relation to other Studies</i>	184
7.6.4 <i>Summary</i>	188
7.6.5 <i>Strengths and Limitations</i>	189
7.7 Conclusion	191

Chapter 8 – Summary	192
8.1 Main Findings	192
8.2 Strengths and Limitations	195
8.3 Future Work	197
8.4 Conclusion	198
Appendices	199
Appendix A FSL Tool Methodology	199
Appendix B Functional Connectivity in Late-Life Depression using Resting-State Functional Magnetic Resonance Imaging (Am J Geriatr Psych, 2010:18)	205
Appendix C Table of Dementia Study Subjects and the Medications Subjects were taking. Subjects showing Global Synchronicity are in Italics.	220
References	223

List of Figures

Chapter 2:

Figure 2.1: Precession of a Magnetic Dipole in a Magnetic Field	25
Figure 2.2: Graph Illustrating the Features of the fMRI BOLD Signal/Haemodynamic Response Function	30
Figure 2.3: Summary Flow Diagram of the Events that Lead to the Generation of the BOLD Signal	31
Figure 2.4: Functional Connectivity Maps of the Anterior (a) and Posterior (b) Default Mode Network Regions	38

Chapter 5:

Figure 5.1: Overview of the Input-Output Organisation of the Basal Ganglia	77
Figure 5.2: Overlay of the Head of Caudate Nucleus in the Axial View on the Functional Image	80
Figure 5.3: Functional Connectivity Maps Showing Regions of Significant Connectivity with the Head of Caudate Nucleus in Late-Life Depression and Control Subjects	86
Figure 5.4: Functional Connectivity Maps Showing Regions of Significantly Greater Connectivity with the Head of Caudate Nucleus in Late-Life Depression versus Control Subjects	87
Figure 5.5: Functional Connectivity Maps Showing Regions of Significantly Greater Connectivity for the Right Head of Caudate Nucleus Compared to the Left in Control and Late-Life Depression Subjects	89
Figure 5.6: Fluid Attenuated Inversion Recovery (FLAIR) Images in a Subject with a High Level of White Matter Hyperintensities (a) and a Subject with a Low Level of White Matter Hyperintensities (b)	93
Figure 5.7: Functional Connectivity Maps for the Left Head of Caudate Nucleus in Late-Life Depression Subjects Split According to High and Low Deep White Matter Hyperintensities	93
Figure 5.8: Functional Connectivity Maps for the Left Head of Caudate Nucleus in Late-Life Depression Subjects Split According to High and Low MADRS Score	95

Chapter 6:

Figure 6.1: Functional Connectivity Maps in Subjects Showing Non-Global Synchronicity and Global Synchronicity	104
Figure 6.2: Functional Connectivity Map for Seed-Based Correlation Analysis with a Seed Placed in the Cerebrospinal Fluid	106
Figure 6.3 Functional Connectivity Maps following Seed-Based Correlation Analysis	111
Figure 6.4: Functional Connectivity Maps of 3 different Subjects (a-c) with Global Synchronicity following Analysis with Methods Summarised in Table 6.1	117
Figure 6.5: Functional Connectivity Maps of 3 different Subjects (d-f) who did not show Global Synchronicity following Analysis with Methods Summarised in Table 6.1	118

Chapter 7:

Figure 7.1: Seed Regions Investigated and Overlaid on the Functional Images	129
Figure 7.2: Functional Connectivity Maps for the Left Head of Caudate Nucleus	137
Figure 7.3: Functional Connectivity Maps for the Right Head of Caudate Nucleus	138
Figure 7.4: Functional Connectivity Maps showing Group Differences for the Head of Caudate Nucleus	139
Figure 7.5: Functional Connectivity Maps for the Left Putamen	142
Figure 7.6: Functional Connectivity Maps for the Right Putamen	143
Figure 7.7: Functional Connectivity Maps showing Group Differences for the Putamen	144
Figure 7.8: Functional Connectivity Maps for the Left Thalamus	147
Figure 7.9: Functional Connectivity Maps for the Right Thalamus	148
Figure 7.10: Functional Connectivity Maps showing Group Differences for the Thalamus	149
Figure 7.11: Functional Connectivity Maps for the Left Hippocampus	152
Figure 7.12: Functional Connectivity Maps for the Right Hippocampus	153
Figure 7.13: Functional Connectivity Maps for the Left Posterior Cingulate	156
Figure 7.14: Functional Connectivity Maps for the Right Posterior Cingulate	157
Figure 7.15: Functional Connectivity Maps showing Group Differences for the Right Posterior Cingulate	158
Figure 7.16: Functional Connectivity Maps for the Left Precuneus	162
Figure 7.17: Functional Connectivity Maps for the Right Precuneus	163

Figure 7.18: Functional Connectivity Maps for the Left Primary Visual Cortex	166
Figure 7.19: Functional Connectivity Maps for the Right Primary Visual Cortex	167
Figure 7.20: Functional Connectivity Maps for the Left Thalamus in DLB Subjects Split by Fluctuation Score	173
Figure 7.21: Functional Connectivity Maps for the Right Thalamus in DLB Subjects Split by Fluctuation Score	173
Figure 7.22: Functional Connectivity Maps for the Left Putamen in DLB Subjects Split by UPDRS Score	175
Figure 7.23: Functional Connectivity Maps for the Right Putamen in DLB Subjects Split by UPDRS Score	175

List of Tables

Chapter 1

Table 1.1: DSM-IV Criteria for Major Depressive Episode	2
Table 1.2: National Institute of Neurological and Communicative Disorders and Stroke/Alzheimer's Disease and Related Disorders Association (NINCDS/ADRDA) Criteria for Clinical Diagnosis of Alzheimer's Disease	10
Table 1.3: Consensus Criteria for the Clinical Diagnosis of Dementia with Lewy Bodies	17

Chapter 2

Table 2.1: Comparison of Functional Neuroimaging Methods to Measure Metabolic and Vascular Parameters	27
Table 2.2: Summary of the Blood Oxygenation Level Dependent Response following Neuronal Activity	29
Table 2.3: Resting-State Networks Identified using Independent Component Analysis	34
Table 2.4: Summary of the Advantages and Disadvantages of Model-Based and Model-Free Methods of Analysis	43
Table 2.5: Summary of Pre-Processing Methods Used in Seed-Based Correlation Analysis	47

Chapter 3

Table 3.1: Summary of Resting-State and Task-State Functional Magnetic Resonance Imaging Studies in Early-Onset and Late-Life Depression	58
--	----

Chapter 4

Table 4.1: Summary of Previous Resting-State Functional Magnetic Resonance Imaging Studies in Alzheimer's Disease and Mild Cognitive Impairment	72
---	----

Chapter 5

Table 5.1: Demographic and Neuropsychological Data of Study Subjects	84
Table 5.2: Brain Regions Showing Greater Functional Connectivity in Late-Life Depression compared to Controls	88

Table 5.3: Brain Regions Showing Greater Connectivity for the Right Head of Caudate Nucleus compared to the Left in Controls and Late-Life Depression Subjects	90
Table 5.4: Brain Regions Showing Greater Connectivity for the Left Caudate in Late-Life Depression Subjects in the High Compared to the Low MADRS Score Group	95
Table 5.5: Summary of the Results from the Model-Based Functional Connectivity Analysis in Late-Life Depression and Control Subjects	96

Chapter 6

Table 6.1: Summary of Methods Used in Previous Studies in Resting-State Functional Connectivity Analysis	109
--	-----

Chapter 7

Table 7.1: Demographic and Neuropsychological Data of Study Subjects	134
Table 7.2: Peak Regions of Functional Connectivity with the Left and Right Head of Caudate Nucleus	140
Table 7.3: Peak Regions of Functional Connectivity with the Left and Right Putamen	145
Table 7.4: Peak Regions of Functional Connectivity with the Left and Right Thalamus	150
Table 7.5: Peak Regions of Functional Connectivity with the Left and Right Hippocampus	154
Table 7.6: Peak Regions of Functional Connectivity with the Left and Right Posterior Cingulate	159
Table 7.7: Peak Regions of Functional Connectivity with the Left and Right Precuneus	164
Table 7.8: Peak Regions of Functional Connectivity with the Left and Right Primary Visual Cortex	168
Table 7.9: Summary of the Differences between Groups in Functional Connectivity for Each Seed Region	169
Table 7.10: Summary of the Brain Regions showing Significant Differences between Groups in Functional Connectivity for Each Seed Region	170

Abbreviations

AD	Alzheimer's Disease
BOLD	Blood Oxygenation Level Dependent
CAFS	Clinical Assessment of Fluctuation Scale
CAMCOG	Cambridge Cognitive Examination
DLB	Dementia with Lewy bodies
DSM	Diagnostic and Statistical Manual of Mental Disorders
FDG	Fluorodeoxyglucose
FEAT	fMRI Expert Analysis Tool
FILM	FMRIB's Improved Linear Model
FLAIR	Fluid Attenuated Inversion Recovery
FLAME	FMRIB's Local Analysis of Mixed Effects
fMRI	Functional Magnetic Resonance Imaging
FMRIB	Functional MRI of the Brain
FLIRT	FMRIB's Linear Registration Tool
FP-CIT	2 β -carbomethoxy-3 β -(4-iodophenyl)- <i>N</i> -(3-fluoropropyl)nortropane
FSL	FMRIB Software Library
FWHM	Full Width at Half Maximum
GDS	Geriatric Depression Scale
LB	Lewy Body
LLD	Late-Life Depression
MADRS	Montgomery-Asberg Depression Rating Scale
MCI	Mild Cognitive Impairment
MMSE	Mini Mental State Examination
MNI	Montreal Neurological Index
MRI	Magnetic Resonance Imaging
NPI	Neuropsychiatry Inventory
PD	Parkinson's Disease
PDD	Parkinson's Disease with Dementia
PET	Positron Emission Tomography
SLFs	Spontaneous Low-frequency Fluctuations
SPECT	Single Photon Emission Computed Tomography
SPM	Statistical Parametric Mapping
SPSS	Statistical Package for Social Sciences

Tc-HMPAO	Technetium-99m-hexamethylpropylene amine oxime
TE	Echo Time
TR	Repetition Time
UPDRS	Unified Parkinson's Disease Rating Scale

Chapter 1

Clinical Background

1.1 Depression

Depression is a clinical disorder of mood which can occur at any age. There are different approaches to classifying depression, but the Diagnostic and Statistical Manual of Mental Disorders, Fourth Edition (DSM-IV) is widely used in clinical and research settings to classify mood disturbances (American Psychiatric Association, 1994). The DSM-IV criteria categorise depression as either major or minor based on duration, number of symptoms and severity. Table 1.1 summarises the DSM-IV criteria required for diagnosis. Five of the symptoms listed in Table 1.1 must be present for at least two weeks for a diagnosis of major depression to be fulfilled; one symptom must be depressed mood or loss of interest/enjoyment in everyday activities (anhedonia). The symptoms must have a significant impact on occupational and/or social functioning in order for criteria to be fulfilled (American Psychiatric Association, 1994).

Depression can be unipolar, where patients have a depressive disorder only, or bipolar, where patients have both depressive disorder and mania (mood alternates between 2 emotional extremes). Once a diagnosis has been made, more detailed information about the disorder can be provided in the form of specifiers which can aid in effective treatment. Specifiers include whether the depression is with psychotic features (hallucinations and/or delusions) or not, or with melancholic features (loss of pleasure in most activities and the depressed mood are distinct) or not (American Psychiatric Association, 1994).

Using positron emission tomography (PET), studies have shown increased metabolism/activation of limbic regions (Mayberg et al., 1999) and decreased activity of cortical regions in depression (Mayberg et al., 1999; Drevets et al., 1997). These findings led to the proposal that a mood regulating circuit exists and that depression arises due to communication imbalances in this circuit (Mayberg et al., 1999; Drevets et al., 1997). Previous imaging studies in depression are discussed in greater detail in Chapter 3 of this thesis.

Table 1.1: DSM-IV Criteria for Major Depressive Episode
(American Psychiatric Association, 1994)

Five or more symptoms are needed for diagnosis:

- Depressed mood
- Markedly diminished interest or pleasure in all or almost all activities
- Abnormal weight loss or gain
- Sleep disturbance, either insomnia or hypersomnia
- Activity disturbance, either abnormal agitation or abnormal slowing
- Fatigue or loss of energy
- Feelings of worthlessness or inappropriate guilt
- Diminished concentration or indecisiveness
- Recurrent thoughts of death or suicide

1.1.1 Late-Life Depression

A) Epidemiology and Clinical Features

Late-life depression (LLD) is a common psychiatric disorder which typically occurs after 60 years of age. Prevalence rates for major depression range from 1 to 4% and minor depression up to 13% (Blazer, 2003). LLD is associated with changes in frontostriatal circuits (Alexopoulos, 2002), which is supported by findings from structural magnetic resonance imaging (MRI) studies showing significant volume reductions in frontal regions (Ballmaier et al., 2004; Almeida et al., 2003a) and the medial temporal lobe (hippocampus) (Hickie et al., 2005; O'Brien et al., 2004b; Steffens et al., 2000). Additionally, studies have shown that volume reductions in the hippocampus are linked with memory deficits (Hickie et al., 2005; O'Brien et al., 2004b).

White matter hyperintensities are associated with increasing age (Raz et al., 2007), but in LLD a higher burden and greater severity are reported (Herrmann et al., 2008; Taylor et al., 2005), specifically in frontal regions where they have been shown to

be ischaemic (Firbank et al., 2004; Thomas et al., 2002; O'Brien et al., 1996). White matter hyperintensities have also been associated with greater memory impairment and executive dysfunction (Kohler et al., 2010a; Sheline et al., 2008) (see Chapter 3).

LLD frequently differs from early-onset depression in its clinical characteristics. LLD is generally characterised by greater impairments in executive function and processing speed (Herrmann et al., 2007; Sheline et al., 2006; Alexopoulos et al., 2002), more severe anhedonia (Alexopoulos et al., 2002), poorer response to treatment (Alexopoulos et al., 2000) and greater association with medical comorbidities, for example cerebrovascular diseases (Blazer, 2000). Family history has been shown to be a less common risk factor in LLD than in early-onset depression (Brodaty et al., 2001).

B) Cognitive Changes

Cognitive deficits in memory, executive function and processing speed are a core feature of depression, both early-onset depression and LLD (Thomas and O'Brien, 2008). Most studies suggest that cognitive deficits in LLD are trait rather than state dependent. In a 4 year follow-up study, cognitive impairments were found to persist despite recovery from depressive symptoms, though cognition did not decline any further (Kohler et al., 2010a).

Depression, including LLD, is known to be a risk factor for subsequent development of dementia. The reasons for this link are not clear, but one possibility is that the two psychiatric disorders have similar underlying neurobiological changes, or that brain changes that occur as a result of depression increase the risk for subsequent dementia.

Three main hypotheses have been proposed to attempt to explain the causes of structural brain changes in LLD:

i. The Toxic Stress Hypothesis

Smaller brain volumes in LLD could be due to increased glucocorticoid levels (McEwen, 1997) caused by an earlier age of disease onset and longer exposure to toxic levels of cortisol (hypercortisolaemia) (Sheline et al., 1996). In contrast, other studies report no link between cortisol levels and atrophy rates, and consequently cognitive deficits in LLD (Kohler et al., 2010b; O'Brien et al., 2004b).

ii. The Dementia Prodrome Hypothesis

This hypothesis proposes that depression develops as an early clinical presentation of dementia (Devanand et al., 1996). In contrast to the toxic stress hypothesis, the dementia prodrome hypothesis is supported by findings showing volume loss is associated with later age of onset and/or a shorter duration of illness and such atrophy may be caused by vascular lesions or neurodegeneration, rather than steroid mediated toxicity (O'Brien et al., 2004b; Steffens et al., 2000; Alexopoulos et al., 1993). Others report depression to be a risk factor for subsequent development of dementia rather than a prodrome (Green et al., 2003). It is highly likely that depression is both a prodrome and a risk factor.

iii. The Vascular Depression Hypothesis

Recent research has largely focussed on the vascular depression hypothesis which states that vascular disease in key brain areas (frontal lobes and basal ganglia) predisposes to, precipitates, or perpetuates depression (Alexopoulos et al., 1997). In support of this hypothesis, deep white matter hyperintensities in frontal regions in LLD show ischaemic damage reflecting an underlying condition, cerebrovascular disease. This predisposes individuals to the development of LLD by disrupting the fibre tracts connecting frontostriatal structures (Thomas et al., 2002).

A number of studies support this hypothesis (Firbank et al., 2004; Thomas et al., 2002); though others have questioned the validity of some of the supporting data (Almeida, 2008; Rainer et al., 2006). Rainer *et al.* (2006) reported that there was no evidence that cerebrovascular disease predisposes to LLD as no link was found between levels of white matter hyperintensities and LLD (Rainer et al., 2006). Almeida (2008) also disputed the hypothesis stating that using the Alexopoulos definition (Alexopoulos et al., 1997) anyone who develops LLD will have vascular depression if they have a history of cerebrovascular disease, and as prevalence of cerebrovascular disease increases with age, very few LLD subjects would fail to meet these criteria (Almeida, 2008).

C) Transmitter Changes

It could also be that transmitter deficits are responsible for the pathophysiological changes that occur in LLD. The monoamine hypothesis proposes that depression is caused by a deficiency in monoamine neurotransmitter levels; namely serotonin, noradrenaline and/or dopamine (Schildkraut, 1965). These neurotransmitters play a key role in the regulation of mood and behaviour.

D) Treatment

The monoamine hypothesis has been key to the development of pharmacological interventions for the treatment of depression, for example antidepressants which alleviate symptoms by elevating neurotransmitter levels. Early depression treatments involved the use of tricyclic antidepressants which act by blocking the reuptake pumps for serotonin and noradrenaline, and to a lesser extent dopamine. However, they also block adrenergic, muscarinic cholinergic and histamine receptors causing side effects of dizziness and blurred vision. Selective serotonin reuptake inhibitors have more recently become the treatment of choice as they do not cause the side effects associated with tricyclic antidepressants. They act on the serotonin transporter inhibiting the reuptake of serotonin and remove the noradrenaline reuptake blocking properties. Studies show that selective serotonin reuptake inhibitors decrease platelet aggregation which could reduce vascular disease progression (Maurer-Spurej et al., 2004). Others report negative effects of tricyclic antidepressants and selective serotonin reuptake inhibitors, and have shown, using magnetic resonance imaging, that they are linked with greater white matter burden (Steffens et al., 2008).

The action of antidepressants is still not fully understood. Further research is necessary, particularly for the development of treatments specific for LLD, as currently the same treatments are used as in early-onset depression and as the neurobiology differs the same treatments may not be appropriate.

1.2 Dementia

The most commonly used criteria for the diagnosis of dementia are the Diagnostic and Statistical Manual of Mental Disorders, Fourth Edition (DSM-IV). These criteria classify dementia as a clinical syndrome characterised by global cognitive impairment (American Psychiatric Association, 1994). Symptoms affect memory, communication, mood and behaviour, and impair daily functioning, social skills and emotional control. Onset can be progressive, or sudden, followed by long plateaus of no change, depending on the cause. Dementia is age-related and affects 5% of those over 65 years of age and 20% of those over 80. Currently there are an estimated 820,000 sufferers in the UK, though numbers are increasing rapidly and by 2051 the number of sufferers is estimated to be close to 1.7 million (Alzheimer's Research Trust, 2010). The impact on the individual with dementia is profound, but additionally the disorder puts a great burden on families and carers, and the health and social care systems, where the estimated annual cost is in excess of £23 billion (Alzheimer's Research Trust, 2010). There are many different causes of dementia, but greater than 90% are caused by either Alzheimer's disease (AD) (50-60%), dementia with Lewy bodies (DLB) or vascular dementia (15-20% each). Other less common causes include metabolic and endocrine disorders and infections (Eastley and Wilcock, 2005).

A clear distinction between normal ageing and the pathological features of dementia is difficult as clinical and pathological brain changes associated with the normal ageing brain are also common features of dementia, e.g. mild cognitive decline, decreased brain weight and volume, widening of ventricles, neuritic plaques and neurofibrillary tangles. Differentiation between the subtypes of dementia is also problematic as there is no definitive clinical (or antemortem) diagnosis, therefore, currently, diagnosis can only be confirmed at autopsy. Over recent years, however, consensus clinical diagnostic criteria have been developed and studies have demonstrated that careful application results in high diagnostic accuracy. Diagnosis of AD shows high sensitivity (proportion of positives that are correctly identified) and specificity (proportion of negatives that are correctly identified) for probable AD (roughly 80%) (Blacker et al., 1994; Kazee et al., 1993). For DLB, the criteria show high specificity (79-100%), however sensitivity is low (32%), so diagnosis can be easily missed (Nelson et al., 2010; Litvan et al., 2003). Additionally, it has been shown that the accuracy of the clinical diagnosis can be greatly enhanced by the use of neuroimaging methods, for example single photon emission computed tomography

(SPECT), positron emission tomography (PET), and structural and functional magnetic resonance imaging (MRI).

1.2.1 Alzheimer's Disease

Alzheimer's disease (AD) accounts for 50-60% of dementia cases (McKeith, 1996) and is characterised by prominent impairment in memory, aphasia (language disturbance), apraxia (impaired ability to carry out motor activities despite intact motor function), agnosia (failure to recognise or identify objects despite intact sensory function) and executive functioning (planning and organising) (American Psychiatric Association, 1994). The National Institute of Neurological and Communicative Disorders and Stroke/Alzheimer's Disease and Related Disorders Association (NINCDS/ADRDA) criteria for the clinical diagnosis of AD are summarised in Table 1.2 (McKhann et al., 1984).

The main risk factor for AD is old age, with incidence reported to increase exponentially up to 90 years of age (Jorm and Jolley, 1998), though others have reported a levelling off of incidence in the very old (Gao et al., 1998). Some studies report women have a higher risk of developing AD (Gao et al., 1998), whereas others report higher incidence in women at very old age but not in younger old subjects (Jorm and Jolley, 1998). Other risk factors include family history, Down's syndrome, vascular factors (e.g. hypertension, smoking, raised cholesterol, diabetes), depression and possession of the ApoE4 genotype.

The neuropathological features of AD are amyloid-rich senile plaques, neurofibrillary tangles, neurodegeneration and synaptic loss. Plaques are extracellular aggregates, ranging in size from 50-200 μm (Terry et al., 1981) and mainly consist of aggregated amyloid beta protein ($\text{A}\beta$), which is derived from amyloid precursor protein (a transmembrane protein of unknown function) (Kang et al., 1987) by β - and γ -secretase cleavage (Haass et al., 1992). This process does not normally cause problems, as amyloid beta protein is present in many healthy body tissues. However, in AD, the more toxic forms are produced which form monomers then oligomers and polymers, which consequently form plaques. Plaques are mainly located in grey matter and to a lesser extent in adjoining areas of white matter (Masters et al., 1985). Neurofibrillary tangles contain paired helical and straight filaments both consisting of abnormally phosphorylated and aggregated tau protein (Braak et al., 1994). When functioning normally, tau builds and stabilises microtubules, but in AD it twists up into pairs and

distorts the cell physically. Ageing causes tau to aggregate inside neurones, neurofibrillary tangles form and ultimately this causes neuronal death.

The Braak and Braak (1991) staging system was derived to detect neurofibrillary changes at post-mortem in AD subjects. The staging system measures how many neurofibrillary tangles there are and where in the brain they are located. There are 6 Braak stages ranging from 1 where the brain is intact to 6 when patients are always demented. At Braak stage 1, tau begins to clump into neurofibrillary tangles, but there are no external symptoms and it can be over 30 years before dementia is noticeable; however from this point onwards decline is inevitable. Neurofibrillary tangles first form in the transentorhinal region (the relay station between the neo-cortex and the hippocampus which is critical for memory), as they accumulate further they spread to the hippocampus and by stage 6 neurofibrillary tangles have caused extensive neuronal death and spread across the transentorhinal region, the hippocampus and the neo-cortex (Braak and Braak, 1991).

The neurotransmitter acetylcholine plays a key role in memory (Drachman and Leavitt, 1974), and as memory is impaired in AD, this has led to the investigation of the cholinergic system. It is now well established that there is an abnormality in the cholinergic system in AD, with studies reporting:

- Reduced levels of the enzyme responsible for acetylcholine production, choline acetyltransferase (Perry et al., 1977; Bowen et al., 1976).
- Reduced acetylcholine uptake (Rylett et al., 1983) and release (Nilsson et al., 1986).
- Loss of neurones from the nucleus of Meynert (the principal cholinergic nucleus innervating the neocortex) (Whitehouse et al., 1982).
- Reduced levels of nicotinic and muscarinic acetylcholine receptors (Court et al., 2001; Lai et al., 2001).

It is important to determine at what stage cholinergic deficits develop in AD to inform when treatment is optimal.

The transition from normal cognition to dementia in AD is gradual and individuals often pass through a state of mild cognitive impairment (MCI). MCI is a condition where isolated cognitive impairment(s), most usually involving memory, is/are seen not associated with functional decline (Petersen et al., 1999). Annual conversion rates of 10-15% for MCI to AD have previously been reported (Petersen et al., 1999), therefore identification of MCI could be a means of studying AD in its earliest stages where drug treatment is more beneficial. However, others have reported that the criteria for predicting AD in MCI is not robust and at follow-up, up to 40% of those with MCI were reclassified as normal (Ritchie et al., 2001).

Table 1.2: National Institute of Neurological and Communicative Disorders and Stroke/Alzheimer's Disease and Related Disorders Association (NINCDS/ADRDA) Criteria for Clinical Diagnosis of Alzheimer's Disease (McKhann et al., 1984)

1) Criteria for the clinical diagnosis of probable AD:

- Dementia established by clinical examination and documented by the Mini-Mental Test, Blessed Dementia Scale, or some similar examination, and confirmed by neuropsychological tests
- Deficits in two or more areas of cognition
- Progressive worsening of memory and other cognitive functions
- No disturbance of consciousness
- Onset between ages 40 and 90, most often after age 65
- Absence of systemic disorders or other brain diseases that could account for the progressive deficits in memory and cognition

2) The diagnosis of probable AD is supported by:

- Progressive deterioration of specific cognitive functions such as language (aphasia), motor skills (apraxia) and perception (agnosia)
- Impaired activities of daily living and altered patterns of behaviour
- Family history of similar disorders, particularly if confirmed neuropathologically; and laboratory results of :
 - Normal lumbar puncture as evaluated by standard techniques
 - Normal pattern of non-specific changes in EEG; such as increased slow-wave activity
 - Evidence of cerebral atrophy on CT with progression documented by serial observation

Table 1.2 (Contd.): National Institute of Neurological and Communicative Disorders and Stroke/Alzheimer's Disease and Related Disorders Association (NINCDS/ADRDA) Criteria for clinical diagnosis of Alzheimer's disease (McKhann et al., 1984)

<p>3) Other clinical features consistent with the diagnosis of probable AD, after exclusion of causes of dementia other than AD, include:</p> <ul style="list-style-type: none">• Plateaus in the course of progression of the illness• Associated symptoms of depression, insomnia, incontinence, delusions, illusions, hallucinations, catastrophic verbal, emotional, or physical outbursts, sexual disorders, and weight loss• Other neurological abnormalities in some patients, especially with more advanced disease and including motor signs such as increased muscle tone, myoclonus, or gait disorder• Seizures in advanced disease• Computed tomography normal for age
<p>4) Features that make the diagnosis of probable AD uncertain or unlikely include:</p> <ul style="list-style-type: none">• Sudden apoplectic onset• Focal neurological findings such as hemiparesis, sensory loss, visual field deficits, and incoordination early in the course of the illness• Seizures or gait disturbances at the onset or very early in the course of the illness

Abbreviations: AD=Alzheimer's disease, CT=Computed tomography, EEG=Electroencephalography

1.2.2 Dementia with Lewy Bodies

Dementia with Lewy Bodies (DLB) is the second most common form of degenerative disease after AD in older people and accounts for approximately 20% of dementia cases at autopsy (McKeith et al., 1996). In 1996, the DLB Consortium published guidelines for the clinical and pathological diagnosis of DLB in order to establish a common framework (McKeith et al., 1996). These guidelines were revised in 2005 to incorporate new information on improved methods of assessment to identify the core clinical features of DLB (McKeith et al., 2005). Table 1.3 outlines the DLB Consortium guidelines.

A) Central Feature – Progressive Cognitive Decline

The central feature for DLB diagnosis is progressive cognitive decline leading to global dementia over a period of months or more commonly several years. Symptoms of prominent or persistent memory impairment may not be present in early DLB, but generally develop as the disease progresses. DLB patients are usually more impaired on memory retrieval tests, whereas in AD the major deficit lies in memory acquisition and consolidation (McKeith et al., 1996). Studies show greater deficits in visual attention and visuospatial (e.g. the clock drawing task) working memory in DLB patients compared to AD (Calderon et al., 2001; Mori et al., 2000). In late stage DLB, differential diagnosis from AD is increasingly difficult due to the overlapping deficits in cognition (McKeith et al., 1996).

B) Pathological Feature – Lewy Bodies

The essential pathological feature of DLB is the presence of LB (alpha synuclein fibrillary aggregates) in the brain of a patient with a clinical history of dementia (McKeith et al., 1996). LB are spherical, intracytoplasmic, eosinophilic neuronal inclusion bodies commonly located in the substantia nigra and locus coeruleus, though they can also be found extracellularly and be multiocular (with many small compartments) in shape (McKeith et al., 1996). Plaques, neurofibrillary tangles and neurone loss are also evident in most DLB cases, but are not essential for diagnosis (McKeith et al., 1996). These criteria alone are not sensitive enough to differentiate between DLB and AD, as up to 60% of AD cases could also be considered to meet pathological criteria for DLB, though their LB are limited to the amygdala (Litvan et al., 2003). More recent recommendations take into account the extent of Lewy and AD-type

pathology to increase diagnostic specificity, so cases in which LB are detected in the setting of extensive AD-type pathology are classified as having a low possibility of DLB (McKeith et al., 2005). This is because studies have shown that AD pathology has a mediating effect on the clinical expression of DLB, therefore a greater burden of AD pathology, in the presence of similar LB pathology, means the person is less likely to show classic DLB characteristics of hallucinations, fluctuation and parkinsonism and more likely an AD clinical picture. Immunohistochemical staining for alpha-synuclein is the most sensitive and specific method for detecting LB and Lewy-related pathology, with grading of lesion density advised and the pattern of regional involvement more important than the total count (McKeith et al., 2005).

C) Core Features

The core clinical features for the diagnosis of probable and possible DLB are fluctuating cognitive impairment, recurrent complex visual hallucinations and spontaneous motor features of parkinsonism (McKeith et al., 1996). The presence of two core features is essential to diagnose probable DLB and one to diagnose possible DLB (McKeith et al., 1996). There were no major amendments to the core features of DLB in the 2005 DLB Consortium Report, though a suggestive feature can replace a core feature providing one core feature is present. However, improved methods of assessment are recommended to aid in diagnosis and determine symptom severity.

i. Fluctuating Cognitive Impairment

Fluctuating cognitive impairment occurs in 50-75% of DLB patients (McKeith et al., 2005). In the early stages of DLB, deficits in cognitive function and global performance can alternate with periods of normal or near normal performance. The periodicity and amplitude of fluctuations varies between and within subjects. Guidelines recommend the use of at least one formal measure of fluctuation. The Clinical Assessment of Fluctuation Scale (CAFS) consists of a series of screening questions put to an informant regarding fluctuating cognition and impaired consciousness during the month prior to assessment. Fluctuating cognition is judged as present if the informant can give a clear example, the clinician then assesses severity based on frequency and duration over the previous month. The One Day Fluctuation Assessment scale can be carried out by a less experienced rater and is based on the day prior to assessment. The scale consists of seven features of confusional behaviour; falls, fluctuation, drowsiness, attention, disorganised thinking, altered level of consciousness and communication. A

score is generated which enables distinction between DLB, AD and vascular dementia (Walker et al., 2000).

Studies have shown that DLB patients with fluctuating cognition have higher [3H]epibatidine binding to high affinity nicotinic receptors in the temporal cortex and hippocampus (Ballard et al., 2002), and higher nicotinic receptor density in the thalamus (Pimlott et al., 2006) than patients without fluctuating cognition, though significantly less than controls. The differentiation of DLB subjects with and without fluctuating cognition was specific to nicotinic receptors, implying that cholinergic mechanisms are involved in the process of maintaining attentional function (Ballard et al., 2002).

ii. Recurrent Complex Visual Hallucinations

Recurrent complex visual hallucinations appear to be the only psychotic symptom that reliably discriminates DLB from AD (Ballard et al., 1996). At autopsy, DLB patients have high levels of LB in the anterior and inferior temporal lobe and the amygdala. These areas are involved in the generation of complex images (Harding et al., 2002). At presentation, one third of DLB patients report visual hallucinations which rises to nearly half of DLB patients reporting visual hallucinations at some point in the course of the disorder (McKeith et al., 2005). The Neuropsychiatry Inventory (NPI) is a useful screening tool for assessing the severity of visual hallucinations. The NPI can be performed by a caregiver and assesses ten behavioural disturbances which occur in dementia including delusions and hallucinations (Cummings et al., 1994).

The perception and attention deficit model aims to account for why people hallucinate, what they see and when and where they see it (Collerton et al., 2005). The model is based on results from functional magnetic resonance imaging (fMRI) studies showing that normal scene perception depends on the interaction between frontal and posterior visual areas, therefore subjects with visual hallucinations exhibit dysfunction in these areas (Collerton et al., 2005; Haxby et al., 2000).

iii. Spontaneous Motor Features of Parkinsonism

Spontaneous motor features of parkinsonism are reported in 25-50% of patients at diagnosis, with 75-80% of DLB patients experiencing symptoms during the course of the illness (McKeith, 2005). The common symptoms are rigidity and bradykinesia (Galasko and Hansen, 1992), others include hypophonic speech, expressionless face, stooped posture and a slow and shuffling gait, with resting tremor less common (McKeith et al., 1996). Severity of motor features in DLB is similar to age-matched Parkinson's disease (PD) patients (Aarsland et al., 2005). DLB can present as a primary neuropsychiatric syndrome, or it can develop later in a patient diagnosed as having PD, i.e. dementia in PD (PDD). DLB consensus criteria suggest that DLB and PDD should be differentiated on the basis of parkinsonism features prior to the onset of dementia. DLB is diagnosed if dementia develops within 12 months of parkinsonism whereas PDD is diagnosed if the clinical history of parkinsonism is greater than 12 months (McKeith et al., 1996).

D) Suggestive Features

The revised guidelines in 2005 included suggestive features in the diagnosis of DLB. If one or more suggestive feature and one or more core feature is present probable DLB can be diagnosed. Currently, there is not enough evidence in support of suggestive features to diagnose probable DLB in the absence of a core feature. Suggestive features are rapid eye movement sleep behaviour disorder, severe neuroleptic sensitivity and reduced striatal dopamine transporter activity on SPECT or PET imaging (McKeith et al., 2005).

E) Supportive Features

Supportive features can be used to increase diagnostic sensitivity. They include severe autonomic dysfunction, depression (McKeith et al., 2005), repeated falls, syncope, and transient loss of consciousness (McKeith et al., 1996). They are commonly present in DLB but lack sufficient diagnostic specificity to be categorised as core or suggestive. Exclusion of other systemic or neurological disorders (e.g. stroke) which could account for the patients' symptoms and characteristics is essential (McKeith et al., 1996).

F) Special Investigations

Assessment of the original DLB Consortium diagnostic guidelines showed they have high specificity but low sensitivity, so diagnosis can easily be missed (Nelson et al., 2010; Litvan et al., 2003). Therefore, it is necessary to establish additional markers which when combined with clinical assessment can improve diagnostic accuracy, and for this neuroimaging is a clear choice. The use of SPECT and PET to measure striatal abnormalities in the dopaminergic system has already been discussed under suggestive features, but other imaging markers have also been established for DLB which can aid in diagnosis. Structural MRI studies demonstrate preservation of the medial temporal lobe (hippocampus) in DLB, which enables differentiation from AD which is characterised by hippocampal atrophy (Burton et al., 2002; Barber et al., 2000). SPECT studies show a distinct pattern of hypoperfusion in DLB compared to AD, with DLB subjects showing greater hypoperfusion in occipital and posterior parietal cortex (Firbank et al., 2003a; Colloby et al., 2002). Scintigraphy with (¹²³I) metaiodobenzylguanidine (MIBG), which enables the quantification of post-ganglionic sympathetic cardiac innervations, shows decreased MIBG uptake in DLB, demonstrating diffuse loss of sympathetic terminal innervations and enabling differentiation from AD which shows normal MIBG uptake (Taki et al., 2004) (see Chapter 4 for more detail).

Table 1.3: Consensus Criteria for the Clinical Diagnosis of Dementia with Lewy Bodies (McKeith et al., 2005; McKeith et al., 1996)

<p>1) Central features</p> <p><i>Essential for the diagnosis of DLB</i></p> <ul style="list-style-type: none">• Progressive cognitive decline of sufficient magnitude to interfere with normal social or occupational function• Prominent or persistent memory impairment may not necessarily occur in the early stages but it is usually evident with progression• Deficits on tests of attention, executive function, and visuo-spatial ability may be especially prominent
<p>2) Core Features</p> <p><i>Two are sufficient for a diagnosis of probable DLB, one for possible DLB</i></p> <ul style="list-style-type: none">• Fluctuating cognition with pronounced variations in attention and alertness• Recurrent visual hallucinations that are typically well formed and detailed• Spontaneous motor features of parkinsonism
<p>3) Suggestive Features</p> <p><i>One or more and one or more core feature = probable DLB, one or more and no core features = possible DLB</i></p> <ul style="list-style-type: none">• Rapid eye movement sleep behaviour disorder• Marked neuroleptic sensitivity• Reduced striatal dopamine transporter activity in the basal ganglia on SPECT and PET

Table 1.3 (Contd.): Consensus Criteria for the Clinical Diagnosis of Dementia with Lewy Bodies (McKeith et al., 2005; McKeith et al., 1996)

<p>4) Supportive Features</p> <ul style="list-style-type: none">• Repeated falls and syncope• Transient loss of consciousness• Neuroleptic sensitivity• Systemised delusions• Hallucinations in other modalities• Severe autonomic dysfunction• Depression• Relative preservation of medial temporal lobe structures on CT/MRI scan• Generalised low uptake on SPECT/PET perfusion scan with reduced occipital activity• Abnormal (low uptake) MIBG myocardial scintigraphy• Prominent slow wave activity on EEG with temporal lobe transient sharp waves
<p>5) A diagnosis of DLB is less likely in the presence of:</p> <ul style="list-style-type: none">• Stroke disease, evident as focal neurological signs or on brain imaging• Evidence on physical examination and investigation of any physical illness or brain disorder sufficient to account for the clinical picture

Abbreviations: DLB = Dementia with Lewy bodies, SPECT = single photon emission computed tomography, PET = positron emission tomography, CT = computed tomography, MRI = magnetic resonance imaging, MIBG = (¹²³I) metaiodobenzylguanidine, EEG = electroencephalography

1.2.3 Management of Alzheimer's Disease and Dementia with Lewy Bodies

In dementia, management generally involves a multidisciplinary approach to determine environmental and/or health-related factors which could enhance an individual's condition and optimise their quality of life and daily functioning (Barber et al., 2001).

Accurate diagnosis is key as AD and DLB require disease specific management, which differs from other causes of dementia (e.g. vascular and frontotemporal) and other conditions that can mimic dementia (space occupying lesions, depression, metabolic and endocrine disorders). It is important that the disclosure of the diagnosis should be individually tailored and accompanied by further information and counselling (Hort et al., 2010; Barber et al., 2001).

- Identification of the most prominent symptoms and the stage of dementia are crucial to inform management of the disorder. This is normally via a collaborative approach between the patient, carer and health professionals (Barber et al., 2001).
- Administering non-pharmacological interventions is a highly favourable approach as studies have reported adverse effects to drug interventions. Non-pharmacological interventions include education of patients and caregivers about the nature of their symptoms, and suggesting strategies to cope with them, and cognitive stimulation therapy, which aims to actively stimulate and engage people with dementia. In DLB specifically, this can include improving the patient's hearing and vision to reduce falls and hallucinations. However, these approaches are highly dependent on the patient, carer and environment, therefore research is limited (Barber et al., 2001).
- Pharmacological interventions also have a limited evidence base. Currently there is insufficient evidence to support the use of any drugs purely for the primary prevention of dementia. It is important that prior to pharmacological intervention, realistic expectations are discussed with the patient and caregivers and also the potential side effects (Hort et al., 2010). Serial interventions are recommended, allowing improvements or side effects to be directly monitored.

Pharmacological Interventions

i. Acetylcholinesterase Inhibitors

Both AD and DLB are associated with acetylcholine deficits, though deficits in DLB have been shown to be even more profound than in AD (Perry et al., 1994). Acetylcholinesterase inhibitors (e.g. donepezil, rivastigmine and galantamine) are the most well developed approaches to alleviate cholinergic deficits (Francis et al., 1999). Acetylcholinesterase inhibitors have been shown to be relatively safe and effective in treating cognitive and neuropsychiatric symptoms. However, they cannot ‘cure’ dementia, but can delay the deterioration of symptoms.

In DLB subjects, a randomised control trial with rivastigmine (McKeith et al., 2000a) and non-randomised trials with donepezil and galantamine (Edwards et al., 2007; Thomas et al., 2005) have shown that all 3 cholinesterase inhibitors improve cognitive measures (measured by mini-mental state examination score [MMSE]) and have a positive effect on treatment of neuropsychiatric symptoms, especially psychosis (measured by neuropsychiatric inventory [NPI] score) (Bhasin et al., 2007; Edwards et al., 2007; Thomas et al., 2005; McKeith et al., 2000a). Though, as results are from different studies and methodologies vary, it is difficult to directly compare and determine which cholinesterase inhibitor is the best choice for treatment (Bhasin et al., 2007).

Additionally, cholinesterase inhibitors have been shown to slow dementia progression in AD and patients diagnosed as AD + DLB. Patients taking cholinesterase inhibitors showed a slower rate in decline of MMSE score compared to patients not taking cholinesterase inhibitors (Nelson et al., 2009). However, treatment with cholinesterase inhibitors has not been shown to prevent or delay the onset of AD. A meta-analysis of 8 studies involving donepezil, rivastigmine and galantamine showed no significant difference in the rate of conversion from MCI to AD in subjects taking cholinesterase inhibitors and those not (Raschetti et al., 2007).

ii. N-methyl-D-aspartate Antagonists

The neurotransmitter glutamate plays a key role in cognition and memory. In AD, the postsynaptic glutamate receptors, N-methyl-D-aspartate (NMDA), are hypothesised to be over stimulated by glutamate. Memantine, a non-competitive NMDA-receptor antagonist, has been shown to have positive effects in AD (Reisberg et al., 2003). Memantine is an open channel blocker, as glutamate increases causing channels to open, memantine blocks more, and as glutamate decreases it blocks less, thus modulating glutamatergic activity (Rogawski and Wenk, 2003).

A recent randomised controlled trial tested the safety and efficacy of memantine in DLB and was shown to be well tolerated, and patients taking memantine showed better clinical global impression of change scores (measures change in symptoms from baseline) than those taking placebo. It should be noted that these are preliminary findings and a large-scale study is needed to provide further confirmation (Aarsland et al., 2009).

There may be a synergistic benefit to co-administer drugs that target both cholinergic and glutamatergic systems. A study which administered donepezil and memantine showed improved cognition in AD (Tariot et al., 2004). These findings however have not been replicated, and recently it was shown that patients who were administered memantine and cholinesterase inhibitors showed no evidence of improved cognitive or non-cognitive symptoms (Porsteinsson et al., 2008).

iii. Levodopa

Post-mortem studies in DLB have shown decreased levels of dopamine (Perry et al., 1990). Levodopa, the most effective oral therapy for the treatment of PD, has been investigated in the management of DLB (Molloy et al., 2006; Molloy et al., 2005). Levodopa did not cause significant or irreversible side effects and was found to relieve parkinsonian symptoms in roughly a third of DLB patients (Molloy et al., 2006; Molloy et al., 2005). The poorer response to dopaminergic treatments in DLB could be due to striatal alpha-synuclein pathology (Duda et al., 2002) or decreased levels of dopamine D2 receptors in the caudate and putamen (Piggott et al., 1999).

iv. Neuroleptics (antipsychotics)

Previously, neuroleptics were commonly used to treat agitation and anxiety in dementia, but recent concerns regarding increased risk of stroke and mortality has resulted in greater caution in their use. In addition to these problems, it has long been established, that in roughly half of DLB patients they can cause side effects of increased rigidity, immobility, confusion, sedation and postural falls (Ballard et al., 1998; McKeith et al., 1992). This is thought to be due to the reduction in D2 receptors in the caudate, putamen (Piggott et al., 1999) and temporal cortex, which correlates with greater cognitive decline, and inversely with cortical LB pathology (Piggott et al., 2007).

Another area for promising future research is to actually prevent the onset of dementia, for example by reducing blood pressure to prevent cerebrovascular disease. Though not specific to dementia, blood pressure lowering may be preventative, however further research is needed in this area. In summary, no intervention has been shown to prevent dementia, but it is important that individuals with dementia are treated on a case by case basis as an approach that works for one patient will not necessarily be directly applicable to another.

Chapter 2

Functional Neuroimaging Background

Functional neuroimaging methods are techniques which enable spatial and temporal mapping of brain activity (Villringer, 1999). There are two approaches which are generally used:

Electrophysiological Methods

Electroencephalography (EEG) and magnetoencephalography (MEG) are examples of electrophysiological methods which measure electrical or magnetic signals from active neurones (Yang et al., 1993). These methods directly measure neuronal activity, are non-invasive and have excellent temporal resolution (Villringer, 1999). However, a considerable disadvantage of these methods is that as measurements are made at the brain surface they may not represent activity in the underlying cortex, therefore an inversion step is required to determine active brain regions which is complex and without a unique solution (Stok, 1987).

Metabolic or Vascular Methods

Single photon emission computed tomography (SPECT), positron emission tomography (PET) and functional magnetic resonance imaging (fMRI) are examples of functional neuroimaging techniques which can be used to measure metabolic and/or vascular parameters. The main advantage of these methods over electrophysiology is their higher spatial resolution; they enable good delineation of the spatial extent of the activated area and accurate matching to anatomical structures. Additionally, they offer greater flexibility, for example PET can study neurotransmitter systems. The drawback is their temporal resolution which is poor compared to electrophysiological approaches.

SPECT and PET can measure regional cerebral blood flow or the metabolic rate of glucose or oxygen depending on the radioactively labelled tracer administered. For example, to measure glucose metabolism, the glucose analogue 2-[¹⁸F] fluoro-2-deoxy-D-glucose (FDG) is administered and taken up by metabolically active neurones, radioactive decay occurs and positrons are emitted. Positrons collide with electrons causing the production of photons which are detected by the scanner. Areas of high radioactivity are associated with brain activity. Similarly, (¹⁵O) labelled water can be used as a tracer for blood flow.

The main advantage of SPECT compared to PET is that the radioisotopes used have longer half lives; a few hours to a few days, versus 2 to 100 minutes for PET. For SPECT, this means that radioisotopes can be produced elsewhere and transported, whereas for PET it means that they have to be made on the scanner site using an expensive cyclotron. However, the spatial resolution and sensitivity of PET is far superior to SPECT. The main disadvantage of both methods is that they are invasive as they involve the use of radioisotopes therefore repeatability is limited (see Table 2.1). This has subsequently led to the use of fMRI to examine brain function, which is a non-invasive method with high spatial resolution (Villringer, 1999).

2.1 Magnetic Resonance Imaging

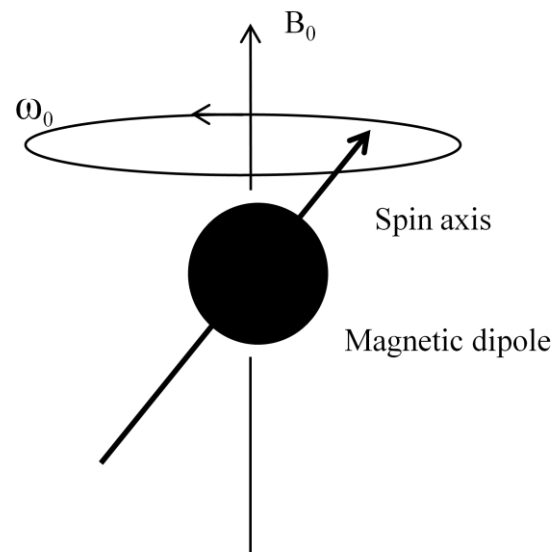
2.1.1 The Nuclear Magnetic Resonance Experiment

Spin

The MRI technique is based on nuclear magnetic resonance, i.e. magnetic properties of atomic nuclei, specifically hydrogen, which, as part of water and lipids, makes up 75-80% of the human body. Hydrogen, with only a single proton in its nucleus, possesses intrinsic angular momentum (spin). This causes the hydrogen nuclei, or protons, to behave like magnetic dipoles, which is the source of resonance. In the scanning procedure, subjects are placed inside a large magnet which exerts a powerful magnetic field with a magnetic flux density, usually between 1.5 and 4.0 Tesla. The magnetic field inside the scanner causes the hydrogen nuclei in water, which are normally randomly orientated, to become aligned with the direction of the field (B_0) (though full alignment is never reached). A net vertical internal magnetic field called longitudinal magnetisation is produced. Nuclei precess around the axis of the field at a frequency proportional to the strength of the magnetic field, the precession frequency (or Larmor frequency, ω_0), which is the resonant frequency of nuclear magnetic resonance. Figure 2.1 illustrates the above process (Buxton, 2002b).

Figure 2.1: Precession of a Magnetic Dipole in a Magnetic Field

Adapted from (Buxton, 2002b)



B_0 = Magnetic frequency

ω_0 = Precession/Resonant frequency (Larmor frequency)

Radio Frequency Pulse

The net longitudinal magnetisation cannot be directly detected. However, the application of a radio frequency (RF) pulse (generated by an oscillating current in a coil) in a horizontal direction (at the precession/resonant frequency) tips the longitudinal magnetisation into the transverse plane. This results in precessing transverse magnetisation and a detector located in the transverse plane can measure the oscillating signal. In summary, MRI measures the changes in the longitudinal and transverse magnetisation components as the nuclei/protons respond to the applied magnetic fields and radio frequency pulses. The strength of the signal detected is dependent on the amount of protons in the tissue and the timing parameters used during imaging (Buxton, 2002b).

Signal Contrast

The contrast between one tissue and another in an MR image is varied by the properties of the pulse sequences and by careful selection of their timings; repetition time (TR) and echo time (TE), which control the sensitivity to the local tissue relaxation times. In MRI, 3 relaxation times are of interest; T_1 , T_2 and T_2^* . These describe the time constant of the recovery of longitudinal magnetisation (T_1 relaxation) and the time constants associated with loss of transverse magnetisation (T_2 and T_2^*). The combined T_2 and detrimental effects of magnetic field inhomogeneity is called T_2^* , which is the

most relevant relaxation time for understanding contrast in an fMRI image (Matthews et al., 2004; Buxton, 2002b).

There are two main types of pulse sequence used in MRI; spin echo and gradient echo:

- Spin echo sequences use 2 radio frequency pulses to create a signal echo, during which the signal intensity is measured. They generally produce the best quality images but take a relatively long time (several minutes).
- Gradient echo sequences use a single radio frequency pulse followed by a gradient pulse to create the echo, during which the signal intensity is again measured. Gradient echo sequences generally have shorter repetition times than spin echo, therefore the scan time is shorter (Buxton, 2002b).

2.2 Functional Magnetic Resonance Imaging

Early MRI studies focussed mainly on structural brain changes, but more recently techniques have been developed to also measure brain function. Using fMRI, it is possible to determine the location and magnitude of neuronal activation either following the performance of a specific task (e.g. visual, motor or cognitive) or when a subject is at rest. fMRI is a non-invasive procedure and the subject is not exposed to ionising radiation, unlike in SPECT and PET. This means the frequency with which experiments can be repeated is not limited and treatment responses can be tested within a few days whereas with SPECT and PET, radiation exposure limits scan frequency to every few months. The fMRI technique enables high quality anatomical images to be acquired in the same scanning session and additionally, in comparison to SPECT and PET, the method has finer spatial resolution, gives temporal data output and generates within subject measures. The main disadvantage of fMRI is that it is more sensitive to subjects head motion than SPECT and PET (Villringer, 1999). Table 2.1 directly compares the functional neuroimaging methods of SPECT, PET and fMRI.

Table 2.1: Comparison of Functional Neuroimaging Methods to Measure Metabolic and Vascular Parameters

Adapted from (Matthews et al., 2004)

	SPECT	PET	FMRI
Spatial resolution	9-12 mm	5-7 mm	1-3 mm
Temporal resolution	3-4 mins	1-2 mins	4-10 sec
Exposure to ionising radiation	Yes	Yes	No
Cost	Low	High	Medium

There are 2 main image acquisition techniques used in fMRI;

Conventional Techniques

The image is assembled using multiple data collections, for example the fast low angle shot (FLASH) method (Haase et al., 1986). FLASH uses multiple radio frequency pulses to excite the MRI signal which are then used to encode the spatial distribution of the signal and form the complete image of the slice. The main advantage is high spatial resolution as you have longer to encode more detail about localisation, but acquisition time is long (typically between 2 and 10 seconds per slice), therefore it is difficult to image the whole brain and the technique is highly sensitive to motion.

High Speed Techniques

Echo planar imaging is an example of single-shot imaging (Mansfield, 1977), where the full data for a low resolution image are acquired from the signal generated by a single radio frequency pulse. Acquisition time for echo planar imaging is extremely short (normally less than 0.1 seconds); therefore it is ideal for whole brain mapping. However, it is more sensitive to geometric distortions and spatial resolution is poor in comparison to conventional techniques. The speed of echo planar imaging means that it is the method of choice for blood oxygenation level dependent fMRI (Buxton, 2002b).

2.2.1 *The Blood Oxygenation Level Dependent Response*

The most common method of fMRI scanning uses the blood oxygenation level dependent (BOLD) response to map brain activity. The BOLD response was first described by Ogawa *et al.* (Ogawa et al., 1990) and is based on:

- The differential magnetic properties of oxygenated and deoxygenated haemoglobin, and
- The coupling of oxygenated blood flow and neuronal activity.

When neuronal activity increases in a brain region, blood flow to that region also increases and oxygen is delivered to the area by haemoglobin in red blood cells to keep up with the increased metabolic demand. Haemoglobin is diamagnetic (i.e. non magnetic) when oxygenated, but paramagnetic when deoxygenated (Pauling and Coryell, 1936). The difference in magnetic properties of oxygenated and deoxygenated haemoglobin causes a change in the MR signal from water in tissue surrounding the capillaries depending on the degree of oxygenation, which varies according to the levels of neuronal activity. When neurones are active, more oxygenated blood is supplied than is immediately necessary and deoxhaemoglobin levels decrease. This causes slower dephasing of the hydrogen nuclei/protons (slower loss of transverse magnetisation), T_2^* is longer, the MR signal decays more slowly and therefore the measured MR signal at the echo time is stronger. This is known as the BOLD effect (Ogawa et al., 1990). The BOLD effect is summarised in Table 2.2.

Table 2.2: Summary of the Blood Oxygenation Level Dependent Response following Neuronal Activity

Unstimulated Tissue	Stimulated Tissue
<ul style="list-style-type: none"> • Little activation of neurones • Blood flow is not increased • Promotes dephasing (loss of transverse magnetisation) of rotating protons • T_2^* is shorter • MRI signal is weaker 	<ul style="list-style-type: none"> • Activation of neurones • \uparrow blood flow, volume and oxygen delivery • \uparrow oxygenated to deoxygenated haemoglobin ratio • \downarrow deoxyhaemoglobin levels • De-phasing of rotating protons is slower • T_2^* is longer • MRI signal is stronger

The BOLD signal does not directly measure neuronal activity but is sensitive to the changes in cerebral blood flow, volume and oxygen metabolism rate. These physiological responses are referred to collectively as the haemodynamic response to activation (Ogawa, 1998; Ogawa et al., 1998; Ogawa et al., 1993). A critical goal for interpreting fMRI data is to understand the underlying link between neuronal activity and the haemodynamic response.

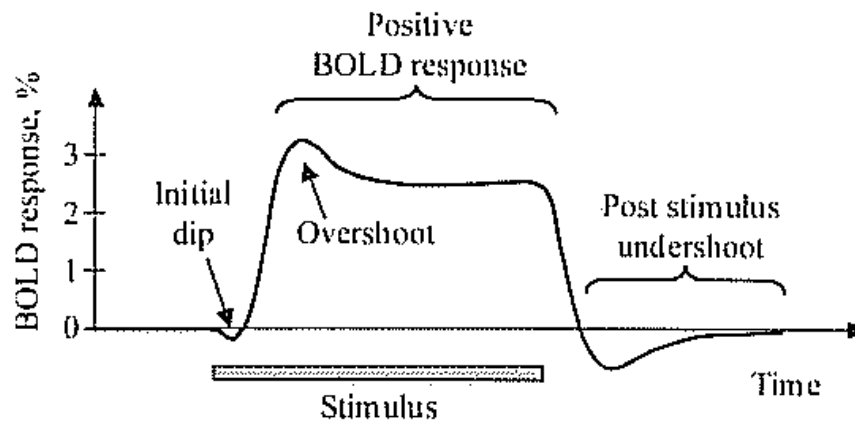
This relationship has been investigated using simultaneous fMRI and electrophysiological recordings in monkeys. This work showed that the haemodynamic response correlated with local field potentials (the summation of postsynaptic potentials; neuronal input), rather than multi-unit activity (outgoing action potentials). The haemodynamic response is therefore proposed to be a measure of the input and intrinsic processing of a given area rather than the output (Logothetis et al., 2001).

The temporal limits of the haemodynamic response were first investigated by Blamire *et al.* (1992) who showed that an fMRI BOLD signal change could be detected even following a visual stimulus of only 2 seconds, with the observed signal change occurring after the stimulus ceased. Regardless of the period of stimulation, the increase in signal was always delayed, 3.5 ± 0.5 seconds in this study, which determines the scan repeat time (TR) (Blamire et al., 1992).

The BOLD response is illustrated in Figure 2.2, with the events that lead to the BOLD response summarised in Figure 2.3.

Figure 2.2: Graph Illustrating the Features of the fMRI BOLD Signal/Haemodynamic Response Function

Extracted from (Hoge and Pike, 2001)



Initial Dip

Upon neural activation, a decrease in the BOLD signal is seen caused by the increased oxygen consumption in active neurones and the consequent decreased ratio of oxygenated to deoxygenated haemoglobin. However, this decrease in BOLD signal is only brief, and is caused by the time lag from when a brain region is activated and when blood flow increases to it (Hu et al., 1997; Menon et al., 1995).

Positive BOLD Response

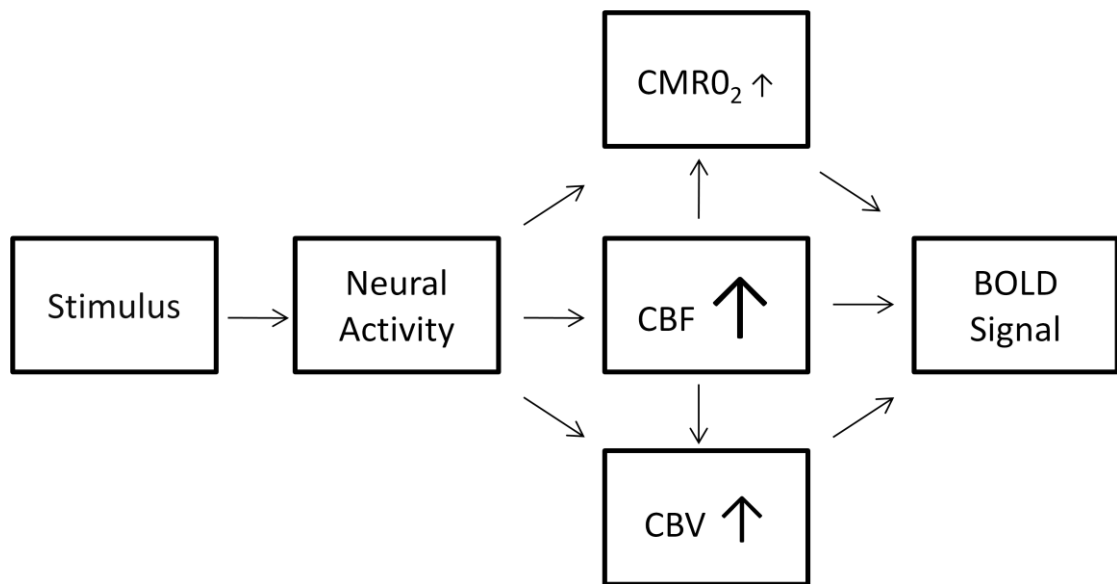
Following the dip, the BOLD signal increases as blood flow increases by 50-70%, however the increase in oxygen utilisation is only 5-20%, therefore an oversupply of oxygenated haemoglobin is delivered and a higher than normal ratio of oxygenated to deoxygenated haemoglobin occurs. This causes a decrease in magnetic susceptibility and consequently an increase in the MR signal (Bandettini et al., 1993; Fox and Raichle, 1986). It is not fully understood why this overcompensation occurs, with blood flow increasing disproportionately to the oxygen demand.

Post Stimulus Undershoot

After the stimulus stops, synaptic activity decreases, blood flow and the oxygenated to deoxygenated haemoglobin ratio return to baseline. There is a brief decrease in the signal below the initial baseline which is thought to be due to a more slowly resolving increase in blood volume (Hu et al., 1997; Menon et al., 1995).

Figure 2.3: Summary Flow Diagram of the Events that Lead to the Generation of the BOLD Signal

Adapted from (Buxton, 2002a)



Abbreviations: BOLD = blood oxygenation level dependent; CBF = cerebral blood flow; CBV = cerebral blood volume; CMRO₂ = cerebral metabolism rate of oxygen.

Most studies measuring the BOLD signal have focussed on the positive BOLD response following task performance, but during a task performance a decrease from resting baseline in other areas of the brain is also observed. In an attention demanding cognitive task, increases in frontal and parietal cortical regions (Corbetta and Shulman, 2002; Cabeza et al., 2000) and decreases from resting baseline in the posterior cingulate and medial prefrontal cortices (Gusnard et al., 2001; Shulman et al., 1997) are observed. A negative BOLD response results from an increase in deoxyhaemoglobin concentration, which causes a decrease in local venous oxygenation level because of a reduction in cerebral blood flow. The exact cause of the negative BOLD response is unclear; however three main theories have been proposed:

i. Haemodynamic effect

Neuronal activation causes blood to be diverted to specific areas meaning blood drains from neighbouring areas to supply the increased demand and consequently the BOLD signal is reduced in the inactive areas (Woolsey et al., 1996).

ii. Active neuronal suppression

Areas with reduced activation are supplied with less oxygenated blood and therefore show a reduced BOLD signal during the stimulus period (Shmuel et al., 2002).

iii. Extension of the initial dip

Negative BOLD response areas have increased neuronal activity during the stimulus period but they do not receive a corresponding increase in blood flow. The increased activation therefore depletes local oxygen levels (Hu et al., 1997).

Investigations to determine whether the positive and negative BOLD responses were coupled showed that the negative response is an exact mirror image of the positive and varying stimuli generate positive and negative responses in different locations. Therefore, the negative response results from a decrease in BOLD signal linked with the level of stimulus and with the positive response, implying that the negative response has either a neuronal or a haemodynamic origin, or both (Shmuel et al., 2002).

Further investigations of the negative BOLD response measured the response from 2 baseline conditions; normal resting baseline and a lower baseline, induced by a sustained negative response (negative baseline). For resting and negative baseline conditions, cerebral blood flow and oxygen metabolism increases reached the same peak amplitude. Therefore, responses from the negative baseline are larger than those from the resting baseline. The ratio of cerebral blood flow and oxygen metabolism remained approximately the same, thus showing tight coupling between haemodynamic and metabolic components. It can therefore be concluded that the blood flow increase is accounted for entirely by the oxygen consumption increase and the negative BOLD response results entirely from active neuronal suppression, thus areas with decreased activation are supplied with less oxygenated blood (Pasley et al., 2007).

BOLD fMRI is advantageous as it is non-invasive, the ratio of contrast to noise is high and it is sensitive to perfusion and metabolic measures. A disadvantage of the BOLD technique is that it is an indirect measure, as it measures the haemodynamic response function triggered by neuronal activity and not neuronal activity directly, however SPECT and PET are also indirect measures. Additionally, interpreting the signal can be difficult as the haemodynamic response is caused by multiple physiological parameters (blood volume, flow and oxygen metabolism) and the images can be affected by head motion and/or magnetic susceptibility artefacts (Bandettini, 2001).

2.3 Resting-State Functional Magnetic Resonance Imaging

Previous fMRI studies have mainly focussed on brain regions showing neuronal activity when an experimental task is performed, however spontaneous low-frequency fluctuations (SLFs) in the BOLD signal are observed even when the subject is at rest and these have become a target of investigation in their own right, termed the resting-state BOLD signal. Biswal *et al.* (1995) were the first group to report SLFs in the BOLD signal at frequencies of < 0.10 Hz using resting-state fMRI (Biswal *et al.*, 1995). SLFs in the left somatomotor cortex were found to correlate with SLFs in the right somatomotor cortex and with medial motor areas, in the absence of overt motor behaviours. This correlation of SLFs between brain regions is termed functional connectivity (Biswal *et al.*, 1995), a measure used to describe the spatiotemporal correlations between spatially distinct regions of cerebral cortex (Strother *et al.*, 1995; Friston *et al.*, 1993). Further studies confirmed these findings, showing that high correlations are preserved in lower sampling rate multislice echo-planar data, allowing the assessment of whole brain functional connectivity (Lowe *et al.*, 1998). Spectral decomposition of the correlated SLFs showed that only frequencies of < 0.10 Hz contribute to functional connectivity (Cordes *et al.*, 2000), with physiological noise sources (respiratory or cardiac pulsations) occurring at higher frequencies (Cordes *et al.*, 2001).

Brain regions showing these coherent SLFs have been termed resting-state networks. A number of studies have focussed on identifying resting-state networks, and it is now believed that there are at least 8 networks which comprise grey matter brain regions. Table 2.3 outlines the most commonly identified resting-state networks using a model-free analysis approach, independent component analysis (see section 2.4.2) (Fox and Raichle, 2007; Damoiseaux *et al.*, 2006; De Luca *et al.*, 2006; Beckmann *et al.*, 2005).

Table 2.3: Resting-State Networks Identified using Independent Component Analysis [axial view, images taken from (Beckmann et al., 2005)]

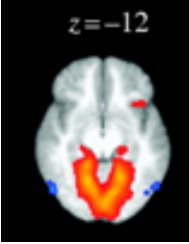
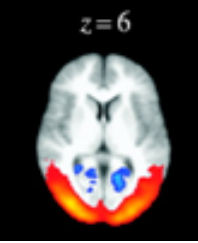
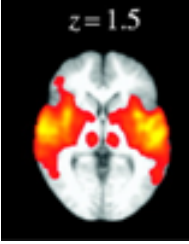
Resting-State Network	Brain Regions
<p data-bbox="443 424 636 451">Medial visual</p>  <p data-bbox="510 485 600 512">z = -12</p>	<ul data-bbox="981 424 1570 632" style="list-style-type: none"> • Primary visual areas (calcarine sulcus) • Medial extrastriate regions (lingual gyrus) • Precuneus (inferior division) • Thalamus (lateral geniculate nucleus)
<p data-bbox="443 743 636 770">Lateral visual</p>  <p data-bbox="517 804 584 831">z = 6</p>	<ul data-bbox="981 743 1547 951" style="list-style-type: none"> • Occipital lobe • Visual cortex (non-primary regions) • Superior parietal regions • Posterior cingulate cortex (deactivation)
<p data-bbox="421 1062 658 1090">Auditory System</p>  <p data-bbox="510 1123 600 1150">z = 1.5</p>	<ul data-bbox="981 1062 1547 1382" style="list-style-type: none"> • Primary and secondary auditory cortices • Lateral occipital temporal gyrus • Posterior insular cortex • Anterior cingulate cortex • Anterior supramarginal gyrus • Thalamus

Table 2.3 (Contd.): Resting-State Networks Identified using Independent Component Analysis [axial view, images taken from (Beckmann et al., 2005)]

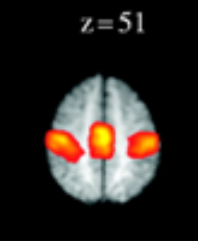
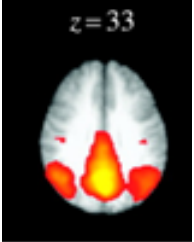
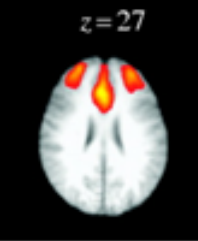
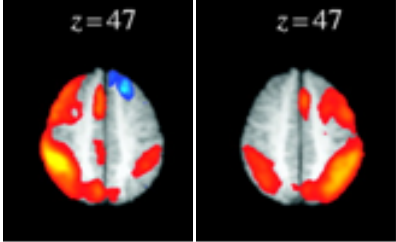
Resting-State Network	Brain Regions
<p data-bbox="383 533 689 564">Sensory Motor System</p>  <p data-bbox="517 592 584 616">z = 51</p>	<ul data-bbox="987 536 1346 568" style="list-style-type: none"> • Pre and post central gyri
<p data-bbox="383 852 689 884">Default Mode Network</p>  <p data-bbox="517 911 584 935">z = 33</p>	<ul data-bbox="987 855 1547 999" style="list-style-type: none"> • Precuneus and posterior cingulate cortex • Medial prefrontal cortex • Lateral parietal cortex

Table 2.3 (Contd.): Resting-State Networks Identified using Independent Component Analysis [axial view, images taken from (Beckmann et al., 2005)]

Resting-State Network	Brain Regions
<p data-bbox="412 533 663 560">Executive Control</p> 	<ul data-bbox="987 533 1559 735" style="list-style-type: none"> • Superior and middle prefrontal cortices • Anterior cingulate and paracingulate gyri • Venterolateral prefrontal cortex • Thalamus
<p data-bbox="389 852 685 879">Dorsal Visual Stream</p> 	<ul data-bbox="987 852 1518 1118" style="list-style-type: none"> • Right lateral occipital • Right inferior parietal cortex • Bilateral intraparietal sulcus • Right middle and superior frontal gyri • Complimentary pattern in left

2.3.1 *The Default Mode Network*

The default mode network (see Table 2.3) has received considerable attention in resting-state studies. PET studies first showed the existence of the default mode network, a network of brain regions which deactivate (sub-baseline signal deflections) in response to cognitive and attentional tasks (Raichle et al., 2001; Shulman et al., 1997), and activate at rest (Raichle et al., 2001).

Following on from these findings the default mode network has been investigated using resting-state fMRI and a seed-based correlation approach (see section 2.4.1) to identify which regions make up this network. Seeds were placed in 2 brain regions previously identified as comprising the default mode network; the posterior cingulate cortex and ventral anterior cingulate cortex. Functional connectivity was assessed by examining the spatial patterns and strength of correlation between SLFs in each seed and all other brain regions. Significant functional connectivity was found between:

- The posterior cingulate cortex and medial prefrontal, ventral anterior cingulate, orbitofrontal, dorsolateral prefrontal (left), inferior parietal, inferotemporal cortices (left) and parahippocampal gyrus (left)
- The ventral anterior cingulate cortex and the posterior cingulate, medial prefrontal, orbitofrontal cortices, nucleus accumbens and the hypothalamus/midbrain (Greicius et al., 2003).

Additionally, others have reported the involvement of the cerebellar tonsils (Fox et al., 2005) and the hippocampus (Koch et al., 2010; Greicius et al., 2004) in the default mode network.

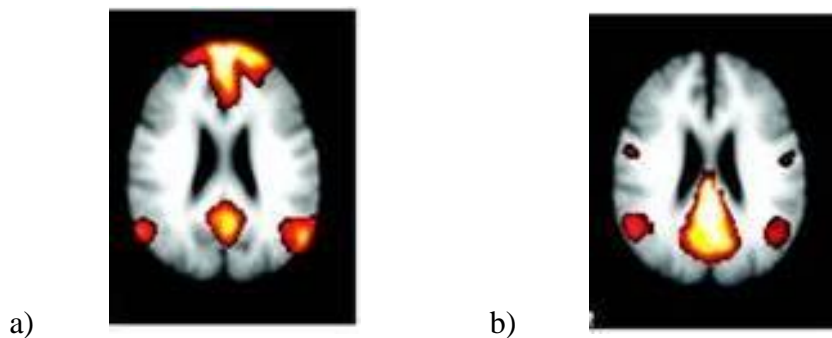
Brain regions showing anticorrelations with the default mode network have also been reported. Using the posterior cingulate cortex as a seed, the intraparietal sulcus, frontal eye field, middle temporal region, supplementary motor area and insula were all shown to anticorrelate (Fox et al., 2005). These findings demonstrate strong coupling between the default mode network and task-positive network regions, as these regions are shown to activate in response to attention and working memory tasks (Fox et al., 2005; Corbetta et al., 2002). Additionally, this study investigated anticorrelations during a low-level task (fixation), and eyes closed versus open. Results were shown to be consistent over resting-state conditions, thus showing that anticorrelations cannot be due to a low-level task (Fox et al., 2005).

More recently the default mode network has been proposed to be composed of at least 2 components, anterior and posterior (Damoiseaux et al., 2008), as illustrated in Figure 2.4;

- The anterior default mode network consists of superior and middle frontal gyrus, posterior cingulate, bilateral middle temporal gyrus and bilateral superior parietal regions (Figure 2.4a).
- The posterior default mode network consists of posterior cingulate cortex and bilateral superior parietal regions (Damoiseaux et al., 2008; Damoiseaux et al., 2006) (Figure 2.4b).

Figure 2.4: Functional Connectivity Maps of the Anterior (a) and Posterior (b) Default Mode Network Regions

Images taken from (Damoiseaux et al., 2008)



Anticorrelations in the anterior and posterior components of the default mode network were further investigated by Uddin *et al.* (2009) using the medial prefrontal and posterior cingulate cortices as seeds. Regions which correlated with the seeds showed some similarities, but anticorrelations were very different. The medial prefrontal cortex generally correlated more strongly with frontal and temporal regions and the posterior cingulate cortex with mid and lateral parietal regions. Anticorrelations were reported between medial prefrontal cortex and task-positive network regions (e.g. intraparietal sulcus) and between the posterior cingulate cortex and motor planning areas (e.g. frontal areas). These findings confirmed that important differences in functional connectivity exist between the anterior and posterior regions of the default mode network (Uddin et al., 2009).

The default mode network is affected by both ageing and disease, with decreased functional connectivity reported in older (mean age 71 years) versus younger (mean age 23 years) subjects, which was not accounted for by the decreased grey matter volume in the older subjects (Damoiseaux et al., 2008). In Alzheimer's disease (AD), decreased default mode network activity has also been reported in the hippocampus and posterior cingulate cortex (Greicius et al., 2004), and between the hippocampus (right) and a number of brain regions (medial prefrontal, ventral anterior cingulate and posterior cingulate cortices and the precuneus) (Wang et al., 2006).

The exact role of the default mode network is not fully known, but studies have shown it is involved in attending to environmental stimuli (Gusnard et al., 2001; Raichle et al., 2001), mediating processes such as reviewing past knowledge or preparing future actions (Binder et al., 1999), and episodic memory processing (Greicius et al., 2004).

The involvement of the default mode network in memory processing and the abnormal functioning of the network in AD (Wang et al., 2006; Greicius et al., 2004) has led to the proposal of the metabolism hypothesis (Buckner et al., 2005). This hypothesises that default mode network activity may set the stage for AD. The continuous activity of this network at rest is linked with either an activity or metabolism-dependent cascade that contributes to AD pathology (Buckner et al., 2005). The metabolism hypothesis is supported by PET studies which have localised amyloid beta plaques in early stage AD (Klunk et al., 2004) and these locations show close matching with default mode network regions (Buckner et al., 2005). Though this hypothesis is still considered highly speculative, the role the default mode network is thought to play in memory processing would offer an explanation as to why memory structures (i.e. the medial temporal lobe) are particularly vulnerable in AD (Buckner et al., 2008; Buckner et al., 2005).

2.3.2 *Origin of Spontaneous Low-Frequency Fluctuations*

Various theories have been proposed regarding what actually causes SLFs in the resting-state, and whether they are solely neuronal in origin. Support that SLFs are of neuronal origin comes from studies combining fMRI and electroencephalography (EEG) techniques showing correlation between the BOLD signal and cortical electrical activity (Goldman et al., 2002), and studies in subjects with neurological disease (e.g. AD) showing changes in resting-state networks, specifically decreased functional connectivity in the default mode network (Greicius et al., 2004).

Others report that SLFs are independent of neuronal function and that they are due to changes in underlying brain physiology, for example blood pulsations induced by the heart beat and arterial CO₂ changes due to respiration. Studies measuring arterial CO₂ fluctuations have shown significant changes in key brain regions of resting-state networks; occipital, parietal and temporal lobes, and the cingulate, which suggests that vascular processes do contribute to the generation of resting-state networks (Wise et al., 2004).

More recently, studies propose that SLFs are a combination of both neuronal and non-neuronal artefacts, meaning that SLFs of neuronal origin can be obscured (Lund et al., 2006). Various methods have been explored to attempt to correct for non-neuronal SLFs, which can artificially inflate and over-estimate functional connectivity, for example measuring cardiac and respiratory traces during acquisition of fMRI data and filtering of the data (Glover et al., 2000; Hu et al., 1995).

Resting-state studies are advantageous over task-based studies, particularly in cognitively impaired subjects, as no complicated experimental design is required and no task has to be practised therefore patient compliance and tolerance is high, head motion is reduced, scan time is relatively short, and studies can be easily standardised. However, it can be difficult to control resting-state during scanning as brain activity will vary greatly depending on how active a subject's mind is at rest, and may vary greatly between separate scans in the same subject.

It has been confirmed that during resting-state the brain is not inactive, but very dynamic showing coherent SLFs in the BOLD signal in anatomically and functionally plausible networks. It is of great importance to investigate whether these networks are affected by disorders such as depression and dementia, which could help to explain the neurobiological changes and brain dysfunction.

2.4 Analysis Methods for Functional Magnetic Resonance Imaging Data

Following an fMRI experiment, data has to be passed through various analysis steps before experimentally related activations can be determined. Analytical methods applied to fMRI data include model-based, which examine each voxel individually, and model-free which separate the data into spatial patterns enabling the analysis of coactivation.

2.4.1 Model-Based Methods

Model-based, univariate or hypothesis driven approaches, test a specific hypothesis/hypotheses about the BOLD response at certain voxel locations, for example seed-based correlation analysis. In this analysis, data can be acquired during a task and from this output a region or voxel which activates significantly is identified and used to define a seed in the resting-state data. Alternatively, a seed can be selected based on prior knowledge of how this brain region is affected by disease, for example a region known to atrophy as a consequence of disease. The time-series is then extracted from the seed and used as a regressor in a general linear model (Worsley and Friston, 1995) approach in order to calculate whole brain connectivity. The data in each voxel is regressed against the model separately from every other voxel (Poline et al., 1997). A statistical map is then generated of all brain regions which show a similar time-series to the seed (Lowe et al., 1998; Biswal et al., 1995).

Seed-based correlation analysis is advantageous because a prior hypothesis is required therefore there is sound background knowledge behind what is being investigated. The drawback of this approach is that analysis can be limited to correlations specifically searched for and the strongest correlations may be missed, i.e. if they do not show connectivity with the seed. However, more recent methods investigate functional connectivity with all brain regions which attempts to overcome this problem. Also, as general linear modelling is based on linear decomposition of the data, functional connectivities with non-linear relationships can be missed.

2.4.2 *Model-Free Methods*

Model-free, multivariate or data driven methods simultaneously separate the data into individual spatial maps which enables the analysis of all voxels' time-courses at the same time and interactions between voxels, without the need to specify a seed region of interest. Principal and independent component analysis (Comon, 1994) are examples of model-free methods. They decompose two-dimensional data matrices (time \times voxels) into time-series and associated spatial maps which jointly describe the temporal and spatial characteristics of underlying signals. These methods assume that the sources of resulting features are statistically independent and enable unknown, yet structured spatiotemporal processes to be detected (Beckmann et al., 2005).

Extensions of independent component analysis include probabilistic independent component analysis which solves the problem of over-fitting by including a noise model (Beckmann and Smith, 2004) and tensorial probabilistic independent component analysis which extracts signals of interest in the spatial, temporal and subject domain (Beckmann and Smith, 2005). A number of studies have successfully used independent component analysis to measure SLFs (Greicius et al., 2004; Goldman, 2003; Kiviniemi et al., 2003) and to produce spatial maps with different time-series enabling separation from noise-related signal variations (e.g. head motion, cardiac pulsations or the respiratory cycle) (De Luca et al., 2006; Lowe et al., 1998).

Model-free approaches do not require the identification of a seed voxel; therefore no prior assumptions of the importance of any brain region are made. The flexibility of independent component analysis is ideal in situations where the effects of interest cannot be predicted accurately, but this also has disadvantages as no prior hypothesis is needed so in general terms everything is searched for. This means that the results can be hard to interpret as there can be a large number of components, and networks can be split into a number of sub-networks. The method is biased by the number of independent components selected and when matching the independent components to resting-state networks, components of interest can be easily ignored or missed. Similar to model-based analysis, the method is based on linear decomposition of the data, therefore functional connectivities with non-linear relationships are not taken into account. Table 2.4 summarises the advantages and disadvantages of the two techniques.

Table 2.4: Summary of the Advantages and Disadvantages of Model-Based and Model-Free Methods of Analysis

Model-Based (E.g. Seed-Based Correlation Analysis)	Model-Free (E.g. Independent Component Analysis)
Advantages:	
<ul style="list-style-type: none"> • Direct answer to a direct question – easily interpretable • Moderately fast • Produces voxels of high temporal synchronicity 	<ul style="list-style-type: none"> • Flexible, no temporal model needed • Good separation of fluctuations from other physiological signals • High spatial sensitivity and specificity
Disadvantages:	
<ul style="list-style-type: none"> • Selecting a representative time-series can be lengthy • Choice of the seed location is biased • Physiological signals can be present in the data 	<ul style="list-style-type: none"> • The order of different components can vary between separate runs of the same data • Large number of components, time consuming • Selecting the components of interest is subjective • Networks can be split over a number of components

2.4.3 *Pre-Processing Methods*

As discussed previously, resting-state data can be contaminated by spurious fluctuations unrelated to neuronal activity which can hide the SLFs of neuronal origin. Spurious fluctuations can be cardiac related; caused by pulsations of the blood induced by the heartbeat, or respiratory related; caused by a change in the arterial level of CO₂, a potent vasodilator (Wise et al., 2004). Recently it has become evident that these confounders can cause artifactual signal changes and mask the fluctuations of interest.

When the studies that comprise this thesis were started (2006), research on the removal of these types of confounders was limited, and only through the course of this research has it become clear that it is important to remove these fluctuations from the data so that SLFs of neuronal origin only are analysed. This has involved validation of pre-processing methods to remove confounders from the data (this work is covered in Chapter 6).

One approach is to simultaneously record physiological parameters (e.g. cardiac and respiratory cycles) at the time of scanning. A model is then derived from the time-series of the physiological noise and subtracted from the fMRI time-series (Birn et al., 2006; Glover et al., 2000), or used as a covariate of no interest (or nuisance variable) in general linear modelling analysis (Lund et al., 2006). The drawback of this approach is that physiological parameters must be recorded at the time of scanning as they cannot be estimated retrospectively from the images.

Resting-state SLFs of the BOLD signal are known to occur at low frequencies, < 0.08 Hz. Though, SLFs occur in the presence of various other signal fluctuations caused by physiological processes, e.g. cardiac (0.6-1.2 Hz) and respiratory cycles (0.1-0.5 Hz) (Cordes et al., 2001; Cordes et al., 2000). Therefore filtering of the data is recommended to only include SLFs of neuronal origin. Some studies band-pass filter the data using low-pass (to remove high frequency noise) and high-pass (to remove low frequency drift) filter cut-offs (e.g. 0.08 and 0.009 Hz) (Weissenbacher et al., 2009; Fox et al., 2005), whereas others use a low pass cut-off of 0.1 Hz only (Chang and Glover, 2009) (see Table 2.5). Generally the consensus is that the time-series need to be filtered at < 0.1 Hz to reduce the effect of noise on the resting-state data. However, even after filtering, fluctuations from physiological artefacts may still be present, e.g. arterial CO₂ fluctuations have been shown to occur at approximately 0.03 Hz (Wise et al., 2004), which has led to the use of additional pre-processing and regression steps.

Pre-processing can involve including covariates of no interest in the general linear modelling analysis, for example a global brain mask (the average time-series across all voxels in the brain) and seed regions placed in the white matter and cerebrospinal fluid (Weissenbacher et al., 2009; Margulies et al., 2007; Fox et al., 2005). Including the global brain mask as a covariate of no interest involves the removal/regression of the global signal from the data. This is based on the assumption that to investigate functional connectivity, local changes in neuronal signal are only of interest, global activation in the data represents noise and therefore local neuronal changes and global signal must be uncorrelated. White matter and cerebrospinal fluid signal are assumed to carry mainly noise and minimal signal of interest, and to investigate resting-state networks only grey matter activity is of interest (Weissenbacher et al., 2009; Margulies et al., 2007; Fox et al., 2005).

A number of studies report noise reduction and improved fMRI results following global signal regression (Fox et al., 2009; Weissenbacher et al., 2009; Margulies et al., 2007; Fox et al., 2005). Weissenbacher *et al.* (2009) showed that when no global signal regression was performed strong correlations were found throughout the brain between functionally non-related regions (e.g. a seed in the right primary motor cortex and primary and secondary visual cortices); whereas when global signal regression was performed significant positive correlations were found in motor network regions and correlations found prior to global signal regression in functionally non-related regions were completely suppressed. They showed that global signal regression also removed white matter functional connectivity, but significant connectivity in the cerebrospinal fluid still remained, which was only suppressed if white matter and cerebrospinal fluid signal regression were also carried out (Weissenbacher et al., 2009).

Another method which aims to remove global brain connectivity is global normalisation, which scales the mean intensity of each image to the mean intensity of the first image. This was also tested by Weissenbacher *et al.* (2009) and was found to increase the significance and specificity of functional connectivity results, but was outperformed by global signal regression. In summary, global signal regression was found to suppress false correlations and double the specificity of functional connectivity results. The use of additional covariates of no interest (e.g. white matter and cerebrospinal fluid) increased the specificity of connectivity results further, however this also reduces statistical significance (Weissenbacher et al., 2009).

Conversely, it has been reported that global signal regression can artificially introduce anticorrelations into the data and as these anticorrelations are only observed when global signal regression is carried out they should be viewed with some caution (Murphy et al., 2009; Weissenbacher et al., 2009). On the other hand, anticorrelations may truly represent neuronal activity and may exist in the data before regression but are too weak to pass statistical significance. Additionally, anticorrelations cannot be solely a result of pre-processing using global signal regression, as global signal is by definition global and not localised to specific brain regions. Another disadvantage of global signal regression is that the global signal can carry a substantial part of the signal of interest and so remove some functional connectivity. Without simultaneously taking physiological recordings at the time of scanning, it is impossible to know whether the confounding signals identified are physiologically related. These findings show that methodology has a high impact on resting-state fMRI studies. Table 2.5 summarises the pre-processing methods that have been used in previous resting-state studies to correct for noise in the data.

An alternative approach is to use model-free methods, for example independent component analysis, to extract the global signal from the data. Independent component analysis will identify global signal as independent components, i.e. separately from brain activity or signals of interest so they can be eliminated from the data (Beckmann et al., 2005). The disadvantage of this method however is that it is investigator biased as it relies on the independent components being identified visually (Beckmann et al., 2005).

In conclusion, fMRI has become a valuable tool in the investigation of human brain function. Early studies typically examined brain activity changes associated with performance of a task, but more recently resting-state SLFs in BOLD fMRI signals have generated a great deal of interest. At rest, the brain is very active and it is possible to study this activity whilst the subject rests in the scanner. The application of resting-state fMRI is ideal in disease states as it does not require a complicated experimental set-up or task compliance. It is clear that careful handling of the data is required in order to investigate only the SLFs of neuronal origin and so that functional connectivity is not over-estimated. However, the true meaning of these SLFs remains to be elucidated.

Table 2.5: Summary of Pre-Processing Methods Used in Seed-Based Correlation Analysis Studies

Study	Pre-Processing	Filtering	Nuisance Covariates	Global Signal Removed
(Fox et al., 2009) (Fox et al., 2005)	Slice timing and head motion correction, intensity scaling, registration, smoothing (6 mm FWHM), linear trend removal	Lowpass of 0.1 Hz or $0.009 < f < 0.08$ Hz	Motion correction parameters (6), CSF and WM seeds, global brain mask	Yes
(Murphy et al., 2009)	RETROICOR (physiological noise correction tool), slice timing and head motion correction, smoothing (5 mm FWHM), registration	$0.01 < f < 0.1$ Hz	None	No (as it introduces deactivations)
(Weissenbacher et al., 2009)	Slice timing and head motion correction, smoothing (9 mm FWHM), registration	$0.009 < f < 0.08$ Hz	Motion correction parameters, CSF and WM seeds, global brain mask	Yes
(Chang and Glover, 2009)	RETROICOR, slice timing and head motion correction, smoothing (5 mm FWHM), registration	Lowpass of 0.1 Hz	CSF and WM seeds, global brain mask	Yes

Table 2.5: Summary of Pre-Processing Methods Used in Seed-Based Correlation Analysis

Study	Pre-Processing	Filtering	Nuisance Covariates	Global Signal Removed
(Roy et al., 2009)	Slice timing and head motion correction, despiking (time-series outliers removed), spatial smoothing (6 mm FWHM), intensity normalisation	Highpass = 100s (sigma) Lowpass = 2.8s (HWHM)	Motion correction parameters, CSF and WM seeds, global brain mask	Yes
(Zhang et al., 2009)	Slice timing and head motion correction, smoothing (5 mm FWHM), voxel intensity scaling, registration	$0.01 < f < 0.08$ Hz	No	No
(Castellanos et al., 2008) (Margulies et al., 2007) (Uddin et al., 2009)	Slice timing and head motion correction, smoothing (6 mm FWHM), registration	Highpass = 100s (sigma) Lowpass = 2.8s (HWHM)	Motion correction parameters, CSF and WM seeds, global brain mask	Yes
(Greicius et al., 2003)	Head motion correction, intensity normalisation, smoothing (4 mm FWHM), registration	$0.0083 < f < 0.15$ Hz	No	No

Abbreviations = Cerebrospinal fluid (CSF), full width half maximum (FWHM), global signal (GS), half width half maximum (HWHM), RETROspective Image CORrection (RETROICOR), white matter (WM).

Chapter 3

Neuroimaging Studies in Depression

Late-life depression (LLD) is a common disorder which can cause great suffering in the elderly and reduce their quality of life. LLD is frequently comorbid with physical illnesses, for example it is common in patients recovering from myocardial infarction (Blazer, 2000), and when present can delay recovery and lengthen hospital stay. Diagnosis and treatment is therefore of key importance to improve quality of life, but current treatments are empirically based and the biological causes of depression remain largely unknown, though there are several theories all supported by evidence (see Chapter 1). It is now understood that there are a number of contributors, or causes, which increase susceptibility to LLD, including environmental and genetic factors, prior psychiatric history and overall medical burden, which can all affect brain structures and functioning.

Neuroimaging can be used to investigate the underlying brain changes that are associated with depression. Imaging studies have focussed on investigating the functioning of circuits of brain regions and on determining if abnormalities here are associated with the behavioural signs and symptoms of depression. Studies have shown that depression is associated with abnormalities in the volumes and functioning of limbic-cortical-striatal-pallidal-thalamic (mood regulating) circuits formed by connections between the orbital and medial prefrontal cortex, amygdalae, hippocampi, ventromedial striatum (caudate and putamen), mediodorsal and midline thalamic nuclei and ventral pallidum (globus pallidus) (Sheline, 2003; Mayberg, 1997; Mayberg, 1994; Alexander et al., 1986).

The hypothesis of dysfunction of the limbic-cortical-striatal-pallidal-thalamic circuits was initially described in early-onset depression but studies suggest that these circuits are also involved in LLD. Along with emotional dysfunction, LLD is often accompanied by cognitive impairments (executive dysfunction), characterised by decreased interest in activities and more profound psychomotor retardation (Herrmann et al., 2007; Alexopoulos, 2002). Cognitive impairments have been linked with fronto-striatal-limbic network abnormalities in a number of LLD studies (Sheline et al., 2006; Alexopoulos et al., 2002; Alexopoulos et al., 1997).

Neuroimaging studies can be structural or functional in nature. The main structural imaging studies summarised here have investigated region of interest volumes, voxel based morphometry (which enables whole brain volumetric analysis), and analysis of the burden of white matter hyperintensities. Functional imaging techniques can involve the use of positron emission tomography (PET) or functional magnetic resonance imaging (fMRI), for example, and brain function can be investigated at rest, or when a subject performs a cognitive or emotional task.

3.1 Structural Magnetic Resonance Imaging

Volumetric measures, using T1-weighted MR images, are the most common method used to examine differences in brain structures. These methods involve measuring the volume of a specific brain region guided by relevant neuroanatomical parameters. Volumetric measures generally show high reliability, if they are carried out within the same research group and/or by a small number of investigators, and are easy to implement. However, they can be time consuming and as there is a lack of standardised guidelines for the delineation of brain regions it can be difficult to compare findings between studies. More recent methods involve placing a region of interest in standard space and then overlaying this region onto individual subject scans. However, the drawback of this approach is that it can be difficult to overlay the regions on brain images of older subjects because they have greater brain atrophy (e.g. surrounding the ventricles) than a standardised brain template takes into account. Therefore it is important that appropriate templates are used.

LLD has been linked with significant abnormalities in frontostriatal circuits (Alexopoulos, 2002). Cross-sectional MRI studies report significant volume reductions in frontal brain regions in LLD (Almeida et al., 2003a; Kumar et al., 2000); namely the anterior cingulate and orbitofrontal cortices (Andreescu et al., 2008; Ballmaier et al., 2004), and the medial temporal lobe (specifically the hippocampus) (Andreescu et al., 2008; Ballmaier et al., 2008b; Hickie et al., 2005; Lloyd et al., 2004; O'Brien et al., 2004b; Steffens et al., 2000). Longitudinal studies have also demonstrated greater loss in hippocampal volume in LLD over a 2 year period compared to control subjects (Steffens et al., 2010). Volume losses in the hippocampus in LLD have been linked with memory deficits (Steffens et al., 2010; O'Brien et al., 2004b), thus showing these subjects are at greater risk of cognitive decline. Though, in contrast, others have reported no hippocampal volume reductions in LLD (Greenberg et al., 2008).

Additionally, studies comparing volumes in late-onset with early-onset depression show greater atrophy in the medial temporal lobe (hippocampus) in late-onset compared to early-onset depression (Hickie et al., 2005; Lloyd et al., 2004; Steffens et al., 2000; Greenwald et al., 1997). However there are also negative studies reporting no difference in hippocampal volume between late-onset and early-onset depression (Ballmaier et al., 2008b). Though, the study by Ballmaier *et al.* (2008) did report significantly decreased volumes in late-onset compared to early-onset depression in subregions of the hippocampus; CA1-CA3 and the subiculum (Ballmaier et al., 2008b).

The finding of greater medial temporal lobe atrophy in late-onset could be linked with subsequent development of Alzheimer's disease, which is characterised by greater hippocampal atrophy compared to other dementia subtypes and age-matched controls (Jack et al., 2002; Du et al., 2001; Killiany et al., 2000; Jack et al., 1997). This would provide support for the dementia prodrome hypothesis; depression develops as an early clinical presentation of dementia (Devanand et al., 1996) (see Chapter 1.1.1).

The caudate nuclei have also been shown to be affected in depression (mean age 48 years), with smaller volumes reported compared to controls (Krishnan et al., 1992). More recently, studies have shown significantly decreased (13.1%) caudate nucleus volumes (left, right and total) in LLD (mean age 71 years) compared to control subjects (Butters et al., 2009). The volume decreases in LLD were localised to the head of caudate nucleus and showed correlation with depression severity (Butters et al., 2009). This is supported by findings from an earlier study which reported decreased right and total caudate volume in bipolar older depressed patients (mean age 58 years) compared to controls (Beyer et al., 2004). In contrast, others report no significant differences in caudate volume in younger depressed (mean age 41 years) (Lacerda et al., 2003) or in LLD (mean age 70 years) (Hannestad et al., 2006). Similar to hippocampal volume measurements, the caudate (left only) has also been shown to be more affected in late-onset compared to early-onset depression (Greenwald et al., 1997). Volumetric abnormalities in the caudate in LLD are supported by recent pathological studies showing decreased neuronal density in the caudate nucleus in LLD (Khundakar et al., 2010).

Brain changes have also been investigated in white matter regions in depression. Significant differences in atrophy of the corpus callosum were reported between late-onset depression, early-onset depression and control subjects. Late-onset depression subjects showed greater atrophy in the splenium of the corpus callosum compared to

early-onset depression subjects and greater atrophy of both the genu and the splenium compared to controls (Ballmaier et al., 2008a).

Using longitudinal measures, subthreshold levels of LLD have been associated with smaller volumes and a faster rate of volumetric decline (over a 9 year period) in frontal and temporal areas, specifically the cingulate, orbitofrontal cortex and hippocampus. This study suggests that even depressive symptoms at subthreshold levels are associated with atrophy of specific brain regions which increases with advancing age (Dotson et al., 2009).

Voxel based morphometry is another approach to image analysis, which also typically uses anatomical T1-weighted scans. This method involves registration to standard space, images are typically segmented into grey matter, white matter and cerebrospinal fluid and this enables the analysis of the entire brain at once. Due to age-related increases in the variability of the shape and size of structures it is important to use age appropriate templates. The method is highly dependent on the image registration quality, but advantages are that it is an automated approach. Studies using voxel based morphometry support findings from volumetric region of interest studies showing significantly decreased volumes in LLD compared to controls subjects in a number of brain regions including the anterior cingulate cortex, hippocampus, prefrontal and orbitofrontal cortices (Ballmaier et al., 2004; Bell-McGinty et al., 2002).

T2-weighted MR images can also be analysed and used in the investigation of depression by studying levels of white matter hyperintensities in the brain. White matter hyperintensities are associated with increasing age (Raz et al., 2007), but in LLD a higher burden and greater severity are reported (Herrmann et al., 2008; Taylor et al., 2005). In LLD, similar to regions showing greater atrophy in volumetric studies, increased white matter hyperintensities have been localised to frontal regions (Firbank et al., 2004; O'Brien et al., 1996), specifically the dorsolateral prefrontal cortex, where they have been shown to be ischaemic in a post-mortem study (Thomas et al., 2002).

A study matching LLD subjects and subjects with similar vascular risk factors showed LLD was characterised by greater white matter hyperintensities in the deep white matter underlying cortical regions (in 7 regions) and by interruptions in white matter connections in the cingulate, insula and amygdala (Sheline et al., 2008). Others report an association between increased burden of white matter hyperintensities in anterior brain regions (where frontostriatal circuits are located) and reduced caudate volume in LLD (Hannestad et al., 2006). Severe deep white matter hyperintensities in LLD have been shown to predict poor disease outcome in terms of poor recovery from

the initial illness, cognitive decline and relapses (O'Brien et al., 1998). Approaches to measure the burden of white matter hyperintensities are simple to implement but they are highly dependent on the investigator rating the images, therefore this can introduce variability between studies.

To summarise, structural MRI studies using approaches to measure region of interest volumes and voxel based morphometry techniques, have reported volume losses in LLD in a consistent set of brain regions including the frontal and the medial temporal lobes. Volume losses in LLD have been linked with memory deficits and also specific brain regions; hippocampus and caudate nucleus, have been shown to be more affected in late-onset than early-onset depression. Further to this, volume losses, for example in frontal brain regions, have been associated with increased levels of white matter hyperintensities in these regions in LLD.

3.2 Functional Neuroimaging

Chapter 2 of this thesis covers the background of functional neuroimaging methods in detail. Briefly, functional neuroimaging can be used to measure brain function, either as a subject rests or when a task is performed in the scanner.

3.2.1 Positron Emission Tomography

Positron emission tomography (PET) studies in depression using the ligand (^{18}F) fluorodeoxyglucose (FDG) to measure glucose metabolism have shown increased activity in limbic regions, specifically the amygdala, pallidostriatum and medial thalamus, and decreased activity in cortical regions, namely the dorsal lateral prefrontal cortex and anterior cingulate cortex (Mayberg et al., 1999; Drevets et al., 1997).

In a resting-state PET study Mayberg *et al.* (1999) measured cerebral blood flow with (^{15}O) water in sad and neutral mood states in controls, and glucose metabolism using FDG in patients with unipolar depression (mean age 44 years) prior and following treatment with the antidepressant fluoxetine. In controls, induction of transient sadness caused increased activity in limbic regions; namely the subgenual cingulate and ventral, mid- and posterior insula, and decreased activity in cortical regions; namely the dorsal lateral prefrontal (right), inferior parietal, dorsal anterior cingulate and posterior cingulate cortices. In depression, treatment with fluoxetine and consequent recovery from depression caused metabolism to decrease in limbic regions and increase in cortical regions, i.e. the reverse of what was seen in controls when sadness was induced.

These findings have led to the theory that these brain regions form part of a mood regulating circuit, and in depression imbalances in the functional connectivity of this circuit occur (Mayberg et al., 1999).

In younger depressed subjects the subgenual anterior cingulate cortex (primarily Brodmann area [BA] 25, and also caudal portions of BA32 and BA24) has become a key area of interest. PET studies of the subgenual anterior cingulate cortex report significantly decreased cerebral blood flow in bipolar depressed patients compared to controls and significantly decreased glucose metabolism in both bipolar and unipolar depressives compared to controls. The subgenual anterior cingulate cortex connects with key emotional processing regions; the hypothalamus, amygdala and medial thalamus, therefore dysfunctions in this region are linked with emotional disturbances which are characteristic of depression (Drevets et al., 2002; Drevets et al., 1997).

PET studies show increased metabolism in LLD compared to controls in anterior (superior and middle frontal gyrus and anterior cingulate cortex) and posterior (precuneus, superior and inferior parietal regions) cortical regions (Smith et al., 2009; Smith et al., 2004a). Smith *et al.* (2009) investigated whether functional abnormalities in LLD (mean age 65 years) were related to structural abnormalities. They showed that increased cerebral glucose metabolism was associated with increased cerebrospinal fluid volumes and decreases in grey and white matter volumes in LLD compared to controls. Increased cerebral metabolism in LLD matched with grey matter regions where atrophy was observed, specifically the caudate, thalamus and precuneus. Additionally, severity of depression had an effect on cerebral metabolism, with increased cerebral metabolism showing positive correlation with depression severity (Smith et al., 2009).

Though in contrast to these findings, an earlier PET study by Kumar *et al.* (1993) reported decreased glucose metabolism in LLD (mean age 71 years) compared to controls in a number of brain regions including frontal, temporal and parietal lobes, the caudate and putamen and the anterior cingulate cortex (Kumar et al., 1993). Similarly, Nobler *et al.* (2000) also reported decreased activity in LLD in frontal cortical regions compared to control subjects (Nobler et al., 2000).

3.2.2 *Functional Magnetic Resonance Imaging*

More recently, blood oxygenation level dependent (BOLD) fMRI has been used in the investigation of patients with depression. This application is advantageous as spatial and temporal resolution is high, and subjects are not exposed to ionising radiation. In addition, the technique enables the application of resting-state measures which is highly favourable as the scanning time is relatively short, and comparisons between studies are more accurate as there is less variability compared to task-based studies (see Chapter 2.2.1).

Anand *et al.* (2005a) used BOLD fMRI to investigate the mood regulating circuit brain regions in younger unipolar depressed patients (mean age 28 years). Spontaneous low-frequency fluctuations (SLFs) in the BOLD signal were acquired during resting-state and in a task-state when subjects viewed neutral, positive and negative pictures. Using a model-based analysis approach, correlations in SLFs were investigated between specific seed regions previously shown to form part of the mood regulating circuitry; cortical (anterior cingulate cortex) and limbic (medial thalamus, amygdala and pallidostriatum). In both resting and task-states, correlations in SLFs were decreased between cortical and limbic regions in depression compared to controls (Anand *et al.*, 2005a). The authors subsequently showed that antidepressant (sertraline) treatment over a 6 week period in depressed patients was associated with a significant increase in connectivity between the anterior cingulate cortex and limbic regions (Anand *et al.*, 2005b).

Bluhm *et al.* (2009) also used a model-based seed correlation approach in early-onset depression (mean age 22 years), in subjects who had a very recent onset of depression. A seed was placed in the posterior cingulate/precuneus, with the aim of identifying the default mode network, and correlations in SLFs investigated with all other brain regions. They showed good identification of the default mode network and, similar to Anand *et al.* (2005a), they reported decreased functional connectivity, specifically between the posterior cingulate/precuneus and the caudate (head and body) in the depressed group compared to controls. No regions of greater connectivity were found in depressed versus controls (Bluhm *et al.*, 2009).

Similarly, a study by Veer *et al.* (2010) also reported decreased resting-state functional connectivity in depressed subjects (mean age 36 years) compared to age-matched controls. However, this study reported decreased functional connectivity in different brain regions compared to the Anand *et al.* (2005) and Bluhm *et al.* (2009)

studies. Functional connectivity was found to be decreased in 3 resting-state networks in depression; specifically in the amygdala, insula, lingual gyrus and frontal regions. In contrast to the model-based studies (seed-based correlation analysis) carried by Anand *et al.* (2005) and Bluhm *et al.* (2009), this study used a model-free analysis approach of independent component analysis (Veer *et al.*, 2010).

Conversely, others have reported increases in functional connectivity in depression in the resting-state. Similar to Veer *et al.* (2010), Greicius *et al.* (2007) used independent component analysis, though they carried out the analysis on individual subject data sets whereas Veer *et al.* (2010) analysed at the group level. Greicius *et al.* (2007) investigated the default mode network and showed increased functional connectivity within the subgenual cingulate, thalamus, medial frontal cortex and precuneus in younger depressed subjects compared to controls. Additionally, increased functional connectivity in the subgenual cingulate positively correlated with the length of depressive episode. In the control group no brain regions showed significantly greater connectivity than in depressed patients. In contrast to the Bluhm *et al.* (2009) study the patients in this study were slightly older (mean age of 39 years) and had a longer duration of illness (Bluhm *et al.*, 2009; Greicius *et al.*, 2007).

In support of the findings by Greicius *et al.* (2007), other groups have also reported increased functional connectivity in depression compared to controls in the resting-state. Sheline *et al.* (2010) investigated 3 networks; the default mode network, cognitive control network, and the affective network, in the resting-state in depressed patients (mean age 36 years). Consistently across all networks functional connectivity was increased in depressed versus controls subjects, with each network showing increased connectivity with the dorsal medial prefrontal cortex (Sheline *et al.*, 2010). Others also support these findings of increased resting-state functional connectivity in the default mode and cognitive control networks in depression compared to controls (mean age 39 years) (Zhou *et al.*, 2010).

Task-based studies provide further support for increased functional connectivity in depression. Younger depressed patients (mean age 40 and 34 years respectively) were shown to have a failure to decrease the activity of the default mode network, specifically the anterior cingulate, prefrontal cortex, lateral parietal and lateral temporal regions, when an emotional task was performed. Abnormally increased activity of default mode network regions during task-performance correlated with depression severity (Grimm *et al.*, 2009; Sheline *et al.*, 2009).

Resting-state BOLD fMRI studies in LLD are limited. A resting-state study by Yuan *et al.* (2008) used a model-free method of analysis (termed “regional homogeneity”) to investigate functional connectivity in LLD (mean age 67 years). This method measures the coherence of the regional BOLD signal time-series, and is based on the assumption that a given voxel is temporally similar to neighbouring voxels. This study reported both increases and decreases in functional connectivity in LLD. Functional connectivity increases were reported in the putamen, frontal and parietal lobes, whereas functional connectivity was also found to be decreased in frontal and parietal lobes, and additionally in the temporal lobe in LLD compared to controls (Yuan *et al.*, 2008).

A task-based fMRI study by Aizenstien *et al.* (2009) showed decreased activity and connectivity using a model-based analysis approach in LLD (mean age 69 years). Decreased activity was reported in the dorsolateral prefrontal cortex and decreased connectivity between this region and the dorsal anterior cingulate cortex in LLD compared to control subjects. Following antidepressant (paroxetine) treatment, activity in the dorsolateral prefrontal cortex was increased in the LLD group, but treatment had no effect on functional connectivity (Aizenstein *et al.*, 2009). Table 3.1 summarises the findings from resting and task-state fMRI studies in early-onset depression and LLD.

Table 3.1: Summary of Resting-State and Task-State Functional Magnetic Resonance Imaging Studies in Early-Onset and Late-Life Depression (in Italics)

Research Study	Patients Mean Age	Methodology	Results in Depression
(Anand et al., 2005a)	28 years	Resting-state and task-state Model-based analysis: Cortical and limbic seeds	↓ connectivity between cortical and limbic regions
(Bluhm et al., 2009)	22 years	Resting-state Model-based analysis: Posterior cingulate/Precuneus as seed	↓ connectivity between posterior cingulate/precuneus and the caudate (head and body)
(Sheline et al., 2010)	36 years	Resting-state Model-based: Seeds in dorsal lateral prefrontal cortex, precuneus and subgenual anterior cingulate	↑ connectivity between 3 networks and the dorsal medial prefrontal cortex
(Zhou et al., 2010)	39 years	Resting-state Model-based: Seeds in dorsal lateral prefrontal cortex, and posterior cingulate/precuneus	↑ connectivity in default mode network
(Greicius et al., 2007)	39 years	Resting-state Model-free: Independent component analysis	↑ connectivity in default mode network regions
(Veer et al., 2010)	36 years	Resting-state Model-free: Independent component analysis	↓ connectivity in 3 resting-state networks

Table 3.1 (Contd.): Summary of Resting-State and Task-State Functional Magnetic Resonance Imaging Studies in Early-Onset and Late-Life Depression (in Italics)

Research Study	Patients Mean Age	Methodology	Results in Depression
<i>(Yuan et al., 2008)</i>	<i>67 years</i>	<i>Resting-state</i> <i>Model-free: Regional homogeneity</i>	<i>↑ connectivity in putamen, frontal, parietal</i> <i>↓ connectivity in frontal, temporal, parietal</i>
<i>(Sheline et al., 2009)</i>	<i>34 years</i>	<i>Task-state</i> <i>Model-based: Seeds in medial prefrontal, posterior cingulate/precuneus, lateral parietal cortices</i>	<i>↑ connectivity/failure to down-regulate the default mode network</i>
<i>(Grimm et al., 2009)</i>	<i>40 years</i>	<i>Task-state</i> <i>Model-based: Seeds in medial prefrontal cortex, posterior cingulate, pregenual anterior cingulate</i>	<i>↑ connectivity/failure to down-regulate the default mode network</i>
<i>(Aizenstein et al., 2009)</i>	<i>69 years</i>	<i>Task-state</i> <i>Model-based: Seeds in dorsal lateral prefrontal and dorsal anterior cingulate cortices</i>	<i>↓ connectivity between dorsolateral prefrontal and dorsal anterior cingulate cortices</i>

Abnormalities in levels of key excitatory and inhibitory neurotransmitters have previously been reported in depression, for example glutamate and gamma aminobutyric acid (GABA). Decreased glutamate has been reported in the anterior cingulate (Auer et al., 2000) and prefrontal cortices in depression (Hasler et al., 2007) (mean age 50 and 34 years respectively) and decreased GABA in prefrontal (mean age 34 years) (Hasler et al., 2007) and occipital regions (mean age 43 years) (Sanacora et al., 1999). More recently, combined methods of analysis have been carried out using fMRI and proton nuclear magnetic resonance spectroscopy to investigate whether activity and/or connectivity abnormalities are associated with metabolite level abnormalities.

A task-based study by Walter *et al.* (2009) used BOLD fMRI to investigate activity, and magnetic resonance spectroscopy to measure metabolite levels, in the pregenual anterior cingulate cortex in younger depressed subjects (mean age 40 years). The pregenual anterior cingulate cortex has been linked with anhedonia in depression, therefore it was hypothesised that there would be abnormalities in activity and metabolite concentration in this region. In depressed subjects, negative BOLD responses in the pregenual anterior cingulate cortex correlated with glutamate and N-acetylaspartate concentrations, whereas in control subjects correlation was with GABA. In depressed subjects, decreased concentrations of glutamine were reported in the pregenual anterior cingulate cortex, whereas glutamate and GABA concentrations were normal (Walter et al., 2009).

A study by Horn *et al.* (2010) also investigated the pregenual anterior cingulate cortex in similarly aged younger depressed subjects (mean age 39 years) (Horn et al., 2010). They used resting-state fMRI measures to investigate functional connectivity between the pregenual anterior cingulate and the anterior insular cortex, and also measured glutamate/glutamine levels using magnetic resonance spectroscopy. Consistent with the Walter *et al.* (2009) study, they showed significantly decreased glutamine levels in the pregenual anterior cingulate in depression versus controls. Additionally, contrary to the Walter *et al.* (2009) study, they also showed that glutamate levels were significantly decreased. In depressed subjects, the decreased levels of glutamate and glutamine correlated with abnormalities in resting-state connectivity with the left anterior insular cortex. Additionally, altered metabolism and functional connectivity were linked with depression severity (Horn et al., 2010). These studies suggest a key role of glutamatergic deficits in the development of depression.

Findings between fMRI studies investigating functional connectivity vary, with some studies reporting increases and some reporting decreases in connectivity in both LLD and early-onset depression. It is difficult to directly compare findings between the studies, as the analysis methods used vary. For example, Greicius *et al.* (2007) and Veer *et al.* (2010) both used model-free approaches of independent component analysis, but one analysed individual subject data sets and the other group data, whereas Yuan *et al.* (2008) also used a model-free analysis approach but not independent component analysis, regional homogeneity (Veer *et al.*, 2010; Yuan *et al.*, 2008; Greicius *et al.*, 2007). In contrast, Anand *et al.* (2005a) and Bluhm *et al.* (2009) used model-based methods, but again the types used were different with correlation investigated between specific seeds versus a seed and all other brain regions respectively (Bluhm *et al.*, 2009; Anand *et al.*, 2005a). Additionally, the age of study subjects varies; Bluhm *et al.* (2009) and Anand *et al.* (2005a) studied younger depressed subjects; mean ages of 22 and 28 years respectively (Bluhm *et al.*, 2009; Anand *et al.*, 2005a), whereas the Veer *et al.* (2010) and Greicius *et al.* (2007) studies were carried out in subjects of similar ages (36 and 39 years respectively) and similar methods of analysis were used, though the studies report conflicting results (Veer *et al.*, 2010; Greicius *et al.*, 2007). The Yuan *et al.* (2008) and Aizenstein *et al.* (2009) studies were both carried out in subjects with LLD, mean age of 67 and 69 years respectively, though one study was a resting-state study and the other was a task-state study (Aizenstein *et al.*, 2009; Yuan *et al.*, 2008) (see Table 3.1 for a summary).

There can also be great variability between studies investigating LLD depending on subject selection, for example whether the subjects have had depression earlier in life, and if so, their exposure and response to treatment, and whether they are taking medication and their mental state (depressed or euthymic) at the time of scanning. LLD is often associated with medical comorbidities, particularly cardiovascular diseases, and cognitive impairments, either as a result of depression itself or a co-existing condition such as Alzheimer's disease, and this can cause further variability between studies in terms of patient groups.

In summary, increasing evidence from different neuroimaging techniques suggests abnormalities in a reasonably consistent set of brain regions in depression. Studies show that emotional disturbances, characteristic of the depressed state, are associated with a distributed neuronal network involving cortical and limbic regions and not solely on the activity of a discrete brain region. Functional connectivities between

limbic and cortical regions, and the volume size or the extent of atrophy of these regions, are therefore considered critical in the formation of complex behaviours.

Further research is necessary, particularly in LLD, as few studies have been carried out investigating connectivity in this disorder. The majority of resting-state fMRI studies have measured activity/connectivity in early-onset depression. However, it is not known whether changes that occur in early-onset depression also occur in LLD, or if certain brain regions are more affected in LLD. The aim would be to guide pharmacological intervention as currently treatments used in early-onset depression are applied also in LLD and as structural studies have shown, there are significant differences in terms of brain atrophy, and therefore the same treatments may not be applicable.

The use of functional connectivity is an ideal application in subjects with depression as it enables the investigation of correlations between brain regions, therefore abnormalities previously shown in structural and some PET studies in frontostriatal brain regions can be investigated. The method offers advantages over structural MRI as it enables the investigation of correlations between brain regions, and over PET in terms of spatial and temporal resolution and repeatability (see Chapter 2 for more detail). Resting-state is an ideal application in subjects with cognitive impairments, for example, as the scanning time is short and no task has to be practised or performed, therefore patient compliance is generally high and head motion is reduced.

Therefore it was planned to investigate resting-state functional connectivity using BOLD fMRI measures in subjects with LLD. Based on findings from structural MRI studies showing volume reductions (Butters et al., 2009) and pathological studies showing decreased neuronal density (Khundakar et al., 2010), the head of caudate nucleus was selected as the seed region and functional connectivity investigated with all other brain regions (see Chapter 5).

Chapter 4

Neuroimaging Studies in Alzheimer's Disease and Dementia with Lewy Bodies

Differential diagnosis between Alzheimer's disease (AD) and dementia with Lewy bodies (DLB) can be difficult as there can be great overlap in clinical symptoms, especially in the early stages. Diagnosis of AD using the National Institute of Neurological and Communicative Disorders and Stroke/Alzheimer's Disease and Related Disorders Association (NINCDS/ADRDA) criteria (McKhann et al., 1984) (see Chapter 1, Table 1.2) shows high sensitivity (proportion of positives that are correctly identified) and specificity (proportion of negatives that are correctly identified) for probable AD (roughly 80%) (Blacker et al., 1994; Kazee et al., 1993). The consensus criteria for DLB to assist with ante-mortem diagnosis (McKeith et al., 1996) (see Chapter 1, Table 1.3), show high specificity (79-100%), however sensitivity is low (32%), therefore diagnosis can be easily missed (Nelson et al., 2010; Litvan et al., 2003). The DLB consensus criteria were revised in 2005 to incorporate new information on methods of assessment to improve case detection (see Chapter 1), but the accuracy of the new criteria have not yet been systematically assessed (McKeith et al., 2005).

Diagnosis is important as it aids in the management of the patient, which varies between the dementias. AD and DLB patients both respond well to acetylcholinesterase inhibitors (Perry et al., 1994), but antipsychotics which can be used in the treatment of AD (though they do increase stroke risk) can cause additional serious, sometimes life threatening, side effects in up to 50% of DLB cases (McKeith et al., 1992).

The cognitive profile varies between the disorders; AD is characterised by greater impairments in memory (Ferman et al., 2006; Calderon et al., 2001), whereas DLB is associated with greater deficits on attentional and visuo-perceptual tasks (Collerton et al., 2003; Calderon et al., 2001). Neuroimaging studies have provided important information on differences in specific structures between the disorders which attempt to explain the varying symptoms. In general, neuroimaging changes have been less well investigated in DLB compared to AD.

4.1 Structural Magnetic Resonance Imaging

Structural magnetic resonance imaging (MRI) can involve manual anatomical methods; measuring region of interest volumes, surface area, tissue density or topology. Alternatively, it can involve methods that enable tissue differentiation; white and grey matter, and cerebrospinal fluid, and either looking at global brain structure or specific regions. These methods can be cross-sectional or longitudinal, where rates of change are measured.

In early AD, the hippocampus is one of the first regions to be affected by neurofibrillary tangles and neuritic plaques (Jack et al., 1992). It is expected that these deposits would affect functioning here and consequently the hippocampus has been a key region of investigation in imaging studies of AD. Structural MRI studies have shown that AD is characterised by atrophy of medial temporal lobe structures, specifically the hippocampus and entorhinal cortex (Kenny et al., 2008; Jack et al., 2002; Du et al., 2001; Killiany et al., 2000; Jack et al., 1997), whereas DLB is characterised by relative preservation of the hippocampus (Burton et al., 2009; Ballmaier et al., 2004; Barber et al., 2000; Barber et al., 1999). Atrophy of subregions of the hippocampus has also been investigated, with greater atrophy reported in AD compared to DLB and controls in anterior portions of the hippocampus (CA1 and subiculum) (Firbank et al., 2010). Additionally, the hypointense line that runs between hippocampus subregions, which represents the fibres in the stratum moleculare, lacunosum and radiatum, was shown to be significantly less distinct in AD compared to DLB and controls (Firbank et al., 2010).

Other brain regions that have been investigated in dementia include the caudate nucleus, putamen and substantia innominata. Almeida *et al.* (2003) reported no significant differences in caudate nucleus volume between AD, DLB and controls (Almeida et al., 2003b), whereas for the putamen significantly smaller volumes have been reported in DLB compared to AD and controls (Cousins et al., 2003). Similarly, significantly reduced substantia innominata volume has been reported in DLB compared to AD (Hanyu et al., 2007).

Voxel based morphometry is another approach which has been used in the investigation of dementia. This is an automated method that looks throughout the whole brain to show differences in global or large-scale brain structures, and therefore there is no prior decision on which structures to assess. Using voxel based morphometry, distinct patterns of grey matter loss have been reported in AD and DLB. In AD, a

widespread pattern of grey matter loss is evident in temporo-parietal cortex and the medial temporal lobes (hippocampus). In contrast, DLB is characterised by grey matter loss involving the dorsal midbrain, substantia innominata and hypothalamus, with preservation of the medial temporal lobe (hippocampus) in roughly 40% of cases (Whitwell et al., 2007; Burton et al., 2004; Burton et al., 2002).

Longitudinal or serial MRI enables the investigation of structural changes over time within the same subject. The method allows a subject to act as their own control via registration of one scan to another, i.e. a baseline scan and a 2 year follow-up scan. Longitudinal measures increase sensitivity, as individual differences in neuroanatomy are removed and paired statistics are used. Using longitudinal measures, significantly higher rates of atrophy have been reported in AD (2% per year) compared to controls (0.25-0.5%) (O'Brien et al., 2001; Fox et al., 1996). DLB patients also showed greater rates of atrophy (1.4%) than controls but lower compared to AD, although this was not significant (O'Brien et al., 2001). Additionally, higher atrophy rates are reported in the hippocampus, entorhinal cortex, ventricles and whole brain of normal subjects who converted to mild cognitive impairment (MCI) (a syndrome which is linked with higher risk of developing AD) and AD compared to those that remained stable, and greater rates are reported in fast AD progressors compared to slow (Jack et al., 2004).

More specifically, the diagnostic accuracy of medial temporal lobe atrophy has been investigated in AD and DLB by measuring how well atrophy matches confirmation at autopsy. Medial temporal lobe atrophy was rated visually using the Scheltens scale (Scheltens et al., 1992), which is based on hippocampus height and cerebrospinal fluid space width. Visual rating of medial temporal lobe atrophy was greater in AD compared to DLB which correlated with the Braak stage and percentage area of neurofibrillary tangles in the autopsy confirmed cases. Therefore, medial temporal lobe atrophy was found to differentiate AD from DLB with high accuracy for autopsy confirmed cases (91% sensitivity and 94% specificity) (Burton et al., 2009).

Brain regions shown to be atrophied in DLB (substantia innominata, dorsal midbrain and hypothalamus) contain neurones which are major components of the cholinergic system, for example the nucleus basalis of meynert in the substantia innominata. Both AD and DLB are associated with deficits in the cholinergic system, but profound cholinergic loss and severely depleted choline acetyltransferase levels occur earlier in the disease course in DLB than AD (Perry et al., 1994). Therefore, these regions are expected to be more severely affected in DLB and are a potentially important target for investigation in the differentiation of DLB and AD.

4.2 Functional Neuroimaging

Functional neuroimaging can be used to measure brain function, either as a subject rests or when a task is performed in the scanner (see Chapter 2). The main functional neuroimaging techniques which have been used in AD and DLB are single photon emission computed tomography (SPECT) and positron emission tomography (PET), and more recently functional magnetic resonance imaging (fMRI). The previous findings from studies in AD and DLB using functional neuroimaging methods are covered in this section.

4.2.1 *Single Photon Emission Computed Tomography and Positron Emission Tomography*

SPECT studies using the ligand technetium-99m hexamethylpropylene amine oxime (Tc-HMPAO) report decreased blood flow in the parietal and frontal lobes in both AD and DLB compared to controls (Colloby et al., 2002). AD is characterised by greater deficits in temporal regions, whereas in DLB occipital (visual areas) and posterior parietal cortices (precuneus) are more affected (Colloby et al., 2002). Occipital hypoperfusion on SPECT has been robustly associated with DLB, for a review see (O'Brien, 2007). However, its utility as a diagnostic marker in individual cases has been questioned.

Some studies report good diagnostic accuracy. Using SPECT to measure perfusion and (^{123}I) metaiodobenzylguanidine (MIBG) myocardial scintigraphy to measure sympathetic nerve damage, Hanyu *et al.* (2006a) showed significantly decreased occipital perfusion and lower cardiac MIBG uptake in DLB compared to AD. Dysfunction of the sympathetic nervous system was specific to DLB, enabling differentiation between DLB and AD. Additionally, MIBG myocardial scintigraphy showed stronger discriminating power in differentiating DLB from AD than SPECT (Hanyu et al., 2006a). A further study by the same group showed that the combined use of SPECT and mini-mental state examination (MMSE) score also achieved high sensitivity and specificity for discriminating DLB from AD (>80%) in terms of medial occipital hypoperfusion specific to DLB (Hanyu et al., 2006b). In contrast, to these studies others have shown low sensitivity and specificity of HMPAO-SPECT in the differential diagnosis of DLB (Colloby et al., 2008; Kemp et al., 2007).

Consistent with findings from perfusion SPECT studies, FDG-PET studies measuring cerebral metabolism have reported hypometabolism/reduced activity in the occipital lobes in DLB compared to AD, which differentiated the disorders with high sensitivity and specificity (92%) (Ishii et al., 1998). The decreased blood flow in DLB to occipital/visual areas has been associated with the core feature of visual hallucinations, which is characteristic of this disorder (Colloby et al., 2002; Lobotesis et al., 2001; Ishii et al., 1999). Occipital hypoperfusion on SPECT is now included in the revised guidelines as a supportive feature for the diagnosis of DLB (McKeith et al., 2005).

Similar to findings from structural imaging studies (Cousins et al., 2003), SPECT studies show the putamen is affected in DLB, and, in contrast to structural findings which show preservation of caudate volume (Almeida et al., 2003b), SPECT studies show abnormalities in DLB (O'Brien et al., 2004a; Walker et al., 2002). These SPECT studies reported decreased binding of the (¹²³I)-2b-carbomethoxy-3b-(4-iodophenyl)-N-(3-fluoropropyl)nortropine (¹²³I-FP-CIT) ligand to the dopamine transporter reuptake site in both the caudate and putamen in DLB compared to AD and control subjects (O'Brien et al., 2004a; Walker et al., 2002). Differentiation between DLB and AD using FP-CIT SPECT showed high specificity (90%) and sensitivity (78%) (McKeith et al., 2007).

PET studies using Pittsburgh compound B to image amyloid burden in the brain showed increased amyloid in the majority (approximately 90 %) of subjects meeting clinical criteria for probable AD. However, a more variable pattern was reported in DLB, with some patients showing a similar burden to AD, and in MCI, subjects were characterised by either an AD-like pattern (60%) or a normal pattern. In AD and DLB, binding was highest in the frontal lobes, the caudate, posterior cingulate cortex and the precuneus, therefore suggesting that these regions are most affected by amyloid (Rowe et al., 2007).

PET and SPECT studies have consistently shown decreased activity (measured by cerebral glucose metabolism and perfusion/blood flow) in the posterior cingulate cortex in AD (Johnson et al., 1998; Minoshima et al., 1997). This was initially a surprising finding as early studies showed the first regions to demonstrate neuropathological changes in AD are medial temporal lobe structures (Braak and Braak, 1991). Consequently, this has led to the theory that a distributed brain network exists which plays a role in memory. This network involves the posterior cingulate and medial temporal lobe structures and is affected in early stage AD. This hypothesis has been

confirmed by further SPECT studies which propose a remote effect hypothesis; abnormalities in the posterior cingulate cortex are caused by degeneration in distant but connected areas, i.e. the entorhinal cortex (Hirao et al., 2006).

4.2.2 Functional Magnetic Resonance Imaging

Blood oxygenation level dependent (BOLD) fMRI can also be used to measure brain function through the measurement of deoxyhaemoglobin concentrations as a result of changes in blood flow, caused by neuronal activity. A major advantage of this method over PET and SPECT is that it does not require the injection of a contrast agent and can therefore be repeated many times.

As discussed in Chapter 2, fMRI studies have shown that during a task, e.g. memory performance, specific brain regions activate and at the same time other brain regions deactivate, i.e. exhibit a decrease in BOLD signal. Brain regions which show activation with task performance have been investigated in patients to see if their activation differs from control subjects. Additionally, brain regions which deactivate with the performance of a task have also been investigated for abnormalities in disease states. Further still, regions which show an increase in BOLD signal when no task is performed (i.e. resting-state), have also become key areas of interest. Studies have mainly been carried out in AD, and at the time of this research, no studies had investigated resting-state connectivity in DLB and only one task-based study had been carried out in DLB.

Task-based studies, e.g. involving the encoding of new information into memory, report decreased activation of the hippocampus and parahippocampal areas in AD compared to controls, confirming these regions are critical for successful memory functioning (Dickerson et al., 2005; Sperling et al., 2003; Rombouts et al., 2000). Additionally, regions showing increases in activation have also been reported in AD compared to controls in the medial parietal and posterior cingulate cortices (Sperling et al., 2003). In subjects with mild cognitive impairment (MCI) reduced hippocampal activity has also been reported compared to control subjects (Johnson et al., 2006). In contrast, other studies have reported greater hippocampal activation in MCI compared to controls, and in the same study reduced activation of both the hippocampus and entorhinal cortex in AD. These findings propose a stage of increased activity in the medial temporal lobe early in the disease course, followed by a subsequent decrease as the disease progresses (Dickerson et al., 2005).

Other task-based studies have investigated brain regions which deactivate with the performance of a task, specifically the default mode network regions, and have shown that there are also alterations in deactivations in AD. Lustig *et al.* (2003) reported differences in activity in the medial parietal and posterior cingulate regions. Younger adults showed deactivations in these regions whilst a task was being performed, whereas AD patients showed activation in these regions. In older adults without dementia a trend towards positive activation was seen, but the AD group showed significantly greater activations (Lustig *et al.*, 2003).

Resting-state studies have shown that AD is linked with changes in spontaneous low-frequency fluctuations (SLFs) and consequently abnormalities in functional connectivity. The majority of studies have used the hippocampus as the seed region, as it is known to be affected early in the course of the disease (Du *et al.*, 2001; Jack *et al.*, 1992), or other brain regions that are known to form part of the default mode network, e.g. the posterior cingulate cortex (Raichle *et al.*, 2001). Studies investigating activity in the default mode network in AD have generally shown that it is decreased compared to controls, specifically in the posterior cingulate and medial temporal lobe structures (hippocampus) (Greicius *et al.*, 2004).

AD patients have been shown to have significantly lower functional connectivity within the hippocampus than MCI and control subjects, with the MCI group also showing significantly lower connectivity than controls. The approach used in this resting-state study involved selecting pairs of voxels within the hippocampus and measuring the mean of the cross-correlation coefficient of spontaneous low-frequency (COSLOF) fluctuations to determine functional connectivity within the structure (Li *et al.*, 2002).

Others also report similar findings; Wang *et al.* (2006) found reduced functional connectivity between the right hippocampus and several brain regions; medial prefrontal, ventral anterior cingulate, inferior, superior and middle temporal, and posterior cingulate cortices and the precuneus. However, they also reported increases in functional connectivity in the AD group between the left hippocampus and right lateral prefrontal cortex (Wang *et al.*, 2006). A study by Allen *et al.* (2007) showed that in controls the hippocampus (bilaterally) had extensive connectivity between frontal, parietal, occipital and temporal cortices, whereas in AD a more restricted pattern of connectivity is seen and a complete absence of connectivity with the frontal lobes (Allen *et al.*, 2007).

The regional homogeneity (ReHo) method has also been used in resting-state fMRI studies. This model-free approach measures the functional connectivity of a voxel with its nearest neighbours, as significant brain activities are thought to more likely occur in clusters rather than a single voxel (Zang et al., 2004). Using this method, decreased functional connectivity was reported in the posterior cingulate and precuneus in AD compared to controls, which correlated with disease progression (measured by mini mental state examination score [MMSE]). Brain regions showing increased functional connectivity were also found in AD in occipital and temporal lobe regions of the cuneus, lingual and fusiform gyrus. These findings support the compensatory recruitment hypothesis which proposes that decreases in the posterior cingulate and precuneus are compensated for by the recruitment of the occipital and temporal lobes (He et al., 2007).

A study by Zhang *et al.* (2009) using the posterior cingulate cortex as the seed region showed reduced functional connectivity in AD compared to controls with several brain regions; ventral medial prefrontal cortex, visual cortex, dorsal lateral prefrontal cortex, infero temporal cortex, precuneus, hippocampus (left), thalamus (right) and posterior orbital frontal cortex. Conversely, increased functional connectivity with the posterior cingulate cortex was observed in AD compared to controls in medial prefrontal cortex, primary motor cortex (left), dorsal lateral prefrontal cortex, orbital frontal cortex (right) and inferior temporal cortex (left) (Zhang et al., 2009). These findings support the view that functional connectivity within the default mode network is decreased in AD. Similar to the He *et al.* study (He et al., 2007), the findings of increased functional connectivity provide further support for the compensatory recruitment hypothesis in that frontal-parietal cortices are recruited to play a compensatory role in early stage AD. This is confirmed by findings from pathological examinations showing impairments in these brain regions occur later in the disease course (Braak and Braak, 1997; Braak and Braak, 1991). Table 4.1 summarises findings from previous resting-state fMRI studies in AD and MCI.

DLB is characterised by greater attentional deficits than AD (Collerton et al., 2003; Calderon et al., 2001), therefore it might be expected that the default mode network would be more dysfunctional (affected) in DLB compared to AD. In DLB and AD, following the performance of colour and motion tasks, deactivation of the default mode network was decreased compared with controls, however there were no significant differences in deactivation between DLB and AD (Sauer et al., 2006). Previous studies have shown that AD and DLB patients have greater rates of atrophy

than controls (O'Brien et al., 2001), but the effect this greater atrophy has on functional connectivity is not fully known and whether functional connectivity abnormalities occur before structural or vice versa.

In summary, DLB is generally characterised by changes affecting subcortical structures whereas AD is characterised by abnormalities in medial temporal lobe structures. These characteristics are considered an important tool in the differentiation of DLB from AD and have been included in the revised guidelines for DLB diagnosis (McKeith et al., 2005). Resting-state fMRI studies, for example, generally show decreased functional connectivity in AD in the default mode network including the hippocampi. In contrast, other brain regions show increased functional connectivity and this has led to the compensatory recruitment theory that certain brain regions show increased activity to compensate for the decreased activity of other brain regions.

It is difficult to directly compare findings between studies because there can be great variation in group size, age range of subjects, stage of dementia, scanning procedure and the methods of analysis. No resting-state fMRI studies, to date, have investigated functional connectivity in DLB. The findings from studies which have been carried out in AD are not consistent, with some reporting increases and others reporting decreases in functional connectivity. Resting-state fMRI is an ideal application in subjects with dementia as no task has to be performed, which is advantageous as cognitive impairments may make it more difficult for subjects to adhere to a task.

The investigation of connectivity in AD and DLB is of key importance in order to better understand the neurobiology of the disorders to inform diagnosis. Currently definitive diagnosis is only possible at autopsy and many studies lack pathological confirmation. Connectivity measures are hoped to be able to inform disease-modifying therapies which could target brain abnormalities to slow cognitive decline and also to enable differentiation between the disorders, which require different management. Chapter 7 of this thesis covers the investigation of functional connectivity in AD, DLB and control subjects. Additionally, as the methods of analysis vary greatly between studies it is important that methodology becomes more consistent so that studies can be compared more directly and the accuracy of the data is improved (see Chapter 6).

Table 4.1: Summary of Previous Resting-State Functional Magnetic Resonance Imaging Studies in Alzheimer’s Disease and Mild Cognitive Impairment

Research Group	Methods	Results and Conclusions
(Zhang et al., 2009)	Method: Seed (posterior cingulate) correlation analysis Subjects: AD	<ul style="list-style-type: none"> • ↓ FC between posterior cingulate and ventral medial prefrontal cortex, visual cortex, dorsal lateral prefrontal cortex (r), inferotemporal cortex, hippocampus (l), thalamus (r) precuneus • ↑ FC between posterior cingulate and medial prefrontal cortex, primary motor cortex, dorsal lateral prefrontal cortex, orbital frontal cortex (r), inferotemporal cortex (l)
(Allen et al., 2007)	Method: Seed (hippocampus) Subjects: AD	<ul style="list-style-type: none"> • ↓ FC of hippocampus, cortical limbic, subcortical and cerebellar regions • No FC between hippocampus and frontal brain regions
(Wang et al., 2006)	Method: Seed (hippocampus) correlation analysis Subjects: AD	<ul style="list-style-type: none"> • ↓ FC between hippocampus (r) and medial prefrontal cortex, ventral anterior cingulate cortex, posterior cingulate and precuneus • ↑ FC between hippocampus (l) and dorsolateral prefrontal cortex (r) • Right > left FC in controls, diminished in AD
(Wang et al., 2007)	Method: Whole brain divided into 116 regions Subjects: AD	<ul style="list-style-type: none"> • ↓ FC between prefrontal and parietal lobes • ↑ FC within the prefrontal lobe, parietal lobe and occipital lobe • ↓ negative correlations with anti-correlated network

Table 4.1 (Contd.): Summary of Previous Resting-State Functional Magnetic Resonance Imaging Studies in Alzheimer’s Disease and Mild Cognitive Impairment

Research Group	Methods	Results and Conclusions
(He et al., 2007)	Method: Regional Homogeneity Subjects: AD	<ul style="list-style-type: none"> • ↓ FC in posterior cingulate and precuneus, correlates with disease progression • ↑ FC in occipital and temporal lobe: cuneus, lingual gyrus (r), fusiform gyrus (l)
(Gili et al., 2010)	Method: Independent Component Analysis Subjects: AD, MCI and Controls	<ul style="list-style-type: none"> • ↓ FC between DMN regions (posterior cingulate and medial prefrontal cortex) and the rest of the brain in AD and MCI compared to controls • Greater grey matter atrophy in posterior cingulate in AD vs MCI • Loss of FC precedes grey matter atrophy
(Sorg et al., 2007)	Method: Independent Component Analysis Subjects: MCI	<ul style="list-style-type: none"> • Absence of FC between hippocampus and posterior cingulate (l) • ↓ FC of selected areas of DMN and executive attention network
(Greicius et al., 2004)	Method: Independent Component Analysis Subjects: AD and Controls	<ul style="list-style-type: none"> • Coactivation of the hippocampus showing the DMN is involved in episodic memory • ↓ FC between the posterior cingulate and left hippocampus in AD

Abbreviations: AD – Alzheimer’s disease; DMN – Default mode network; FC – Functional connectivity; MCI – mild cognitive impairment; RSN – resting-state network.

Chapter 5

Investigation of Functional Connectivity in Late-Life Depression

5.1 Rationale for this Study

Structural and functional imaging studies have shown abnormalities in a number of brain regions in subjects with depression (see Chapter 3). The methods used in functional imaging studies (resting and task state) have varied greatly, with some studies using model-based (hypothesis driven) approaches of seed-based correlation analysis whereas others have used model-free approaches, for example independent component analysis. Most previous resting-state functional connectivity studies have been carried out in younger depressed subjects (Bluhm et al., 2009; Greicius et al., 2007; Anand et al., 2005a), with only one study in late-life depression (LLD), and this study used a model-free analysis approach (Yuan et al., 2008). No study to date has investigated resting-state functional connectivity using a model-based analysis approach of correlating a seed region with all other brain voxels in LLD, and only one study has used this approach in early-onset depression (Bluhm et al., 2009).

As discussed in Chapter 2, using fMRI, resting-state images can be acquired over a period of minutes and show small amplitude, spontaneous low-frequency fluctuations (SLFs) in the blood oxygenation level dependent (BOLD) signal, which are correlated between functionally related brain regions (Cordes et al., 2001; Lowe et al., 1998). Related brain regions can therefore be investigated by determining the level of cross-correlation between SLFs in the BOLD signal in a seed region and the rest of the brain. Resting-state functional connectivity measures may provide key insights in the investigation of neurobiological changes in depression by measuring activity between brain regions, for example in frontostriatal circuits. These measures may also be used to support findings from previous structural imaging studies in depression, and could determine whether such structural changes are related to functional abnormalities. Additionally, measures may supplement other research data on clinical and neuropsychological features and from structural imaging studies to help clarify whether there are important differences between LLD and early-onset depression. Resting-state fMRI does not require patient compliance in task performance and is therefore ideal for

application in older subjects and patient groups who may have cognitive problems, for example, which can limit their ability to comply with fMRI activation paradigms.

5.2 Aims

- To examine functional connectivity between the head of caudate nucleus and the rest of the brain in LLD and age-matched controls by cross-correlation of the BOLD signal time-series.
- To investigate whether there are differences in functional connectivity between LLD and control subjects, and whether functional connectivity measures can differentiate the two groups.
- To determine in the LLD group whether white matter pathology, as indicated by white matter hyperintensities on MRI, or depression severity has an effect on functional connectivity.

5.3 Hypotheses

LLD subjects were hypothesised to show abnormal functional connectivity between the head of caudate nucleus and other brain regions compared to controls based on the role of the caudate in regulating mood, emotion and cognition. Functional connectivity was predicted to be increased in LLD compared to control subjects because of the characteristic features of heightened emotional responses and self-reflective tendencies in this disorder. This hypothesis was supported by prior resting-state studies in younger subjects showing increased functional connectivity in sub-lobar regions in depression (Greicius et al., 2007).

5.4 Methods

5.4.1 Subjects and Assessment

The study involved 33 subjects aged 65 years and over. Subjects were community dwelling in the North East of England. Sixteen patients were recruited from referrals to Newcastle and Gateshead Old Age Psychiatry Services and met diagnostic criteria for Major Depression according to DSM-IV, as assessed during a standardised interview by an experienced psychiatrist (Dr Jonathan Richardson). Seventeen similarly aged controls were recruited by advertisement; none of the control subjects had past or

present history of depression. All subjects were cognitively intact, had no history or clinical evidence of dementia, and all scored ≥ 24 on the Mini-Mental State Examination (MMSE) (Roth et al., 1986). Patients were assessed using a standardised interview and received a structured physical examination. Current depression severity was rated using the Montgomery-Asberg Depression Rating Scale (MADRS) (Montgomery and Asberg, 1979). Exclusion criteria were; co-morbid or previous history of drug or alcohol misuse, previous head injury, history of epilepsy, myocardial infarction in the preceding 3 months, a carotid bruit on physical examination, or any contraindication to MRI. The study received ethics committee approval and all subjects gave verbal and written consent.

5.4.2 Imaging

Subjects were scanned in a 3 Tesla Philips Intera Achieva MRI System at the Newcastle Magnetic Resonance Centre, Newcastle University. An 8 channel head coil was used to collect anatomical 3D T1-weighted, fluid attenuated inversion recovery (FLAIR) and resting-state functional MRI (fMRI) scans. The scanning protocol involved asking subjects to lie still in the scanner, to keep their eyes closed, to think of nothing in particular, but not to fall asleep.

The timing and parameters used to collect anatomical scans were as follows;

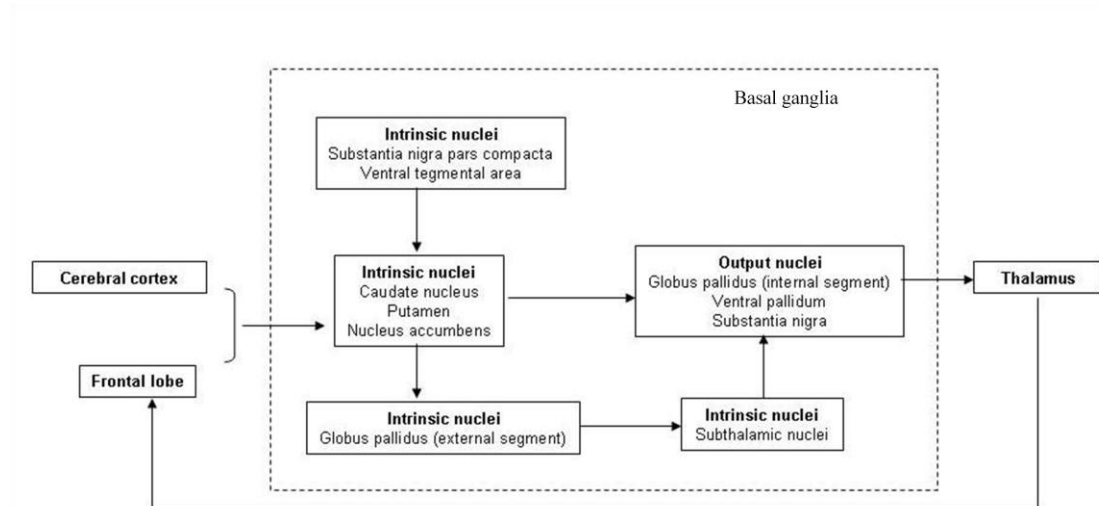
- Anatomical 3D T1-weighted: Magnetisation-prepared rapid acquisition with gradient echo (MPRAGE), sagittal acquisition, slice thickness = 1.2 mm, voxel size = 1.15 x 1.15 mm, repetition time (TR) = 9.6 ms, echo time (TE) 4.6 ms, flip angle = 8°, sensitivity encoding (SENSE) factor = 2.
- FLAIR: Number of slices = 60, slice thickness = 2.5 mm, voxel size = 1.02 x 1.02, TR = 11000 ms; TE = 125 ms, inversion time (TI) = 2800 ms; SENSE factor = 1.5.
- Resting-state fMRI scans were collected using a gradient-echo echo-planar imaging (GE-EPI) sequence. The timing and parameters used were similar to those that have been used in previous studies to detect resting-state networks (De Luca et al., 2006); 25 axial slices, 128 volumes, anterior-posterior acquisition, in-plane resolution = 2 x 2 mm, slice thickness = 6 mm, TR = 3000 ms, TE = 40 ms, field of view = 260 x 150 x 260 mm, and acquisition time = 6.65 minutes.

5.4.3 Selection of the Seed Region

The head of caudate nucleus was used as the seed region in this study. The caudate is a basal ganglia structure. The basal ganglia are a collection of subcortical nuclei involved in controlling motor, cognitive and emotional functions. The caudate nucleus, putamen and nucleus accumbens, collectively termed the striatum, are the input nuclei for signal circuits that originate in the cerebral cortex. These input nuclei project to the intrinsic nuclei (external segment of the globus pallidus, subthalamic nucleus, substantia nigra pars compacta, ventral tegmental area) and output nuclei (internal segment of the globus pallidus, ventral pallidum, substantia nigra). The caudate nucleus is C-shaped and is a continuous structure although three separate names are given to its portions; head, body and tail. The caudate nucleus is connected to the putamen by cell bridges and the nucleus accumbens is located ventromedially. Figure 5.1 illustrates the organisation of the basal ganglia (Martin, 1996).

Figure 5.1: Overview of the Input-Output Organisation of the Basal Ganglia

Figure extracted from (Martin, 1996)



Early studies investigating the role of the basal ganglia nuclei suggested they integrate influences from cortical association and sensorimotor areas to common thalamic target zones and contribute to the initiation and control of movement (Allen and Tsukahara, 1974; Kemp and Powell, 1971; Evarts and Thach, 1969). Though subsequently, it has been shown that there are at least 5 basal ganglia thalamocortical

circuits; motor, oculomotor, prefrontal (2 circuits) and limbic (Alexander and Crutcher, 1990; Alexander et al., 1986):

- i. Motor circuit:
 - Focussed on the precentral motor fields
 - Controls skeletal musculature
- ii. Oculomotor circuit:
 - Focussed on the frontal and supplementary eye fields
 - Controls extraocular muscles
- iii. Prefrontal circuits (2 circuits):
 - Focussed on the dorsal lateral prefrontal cortex and lateral orbitofrontal cortices
 - Control cognition and spatial memory
- iv. Limbic circuit:
 - Focussed on the anterior cingulate and medial orbitofrontal cortices
 - Controls motivational regulation of behaviour and emotions

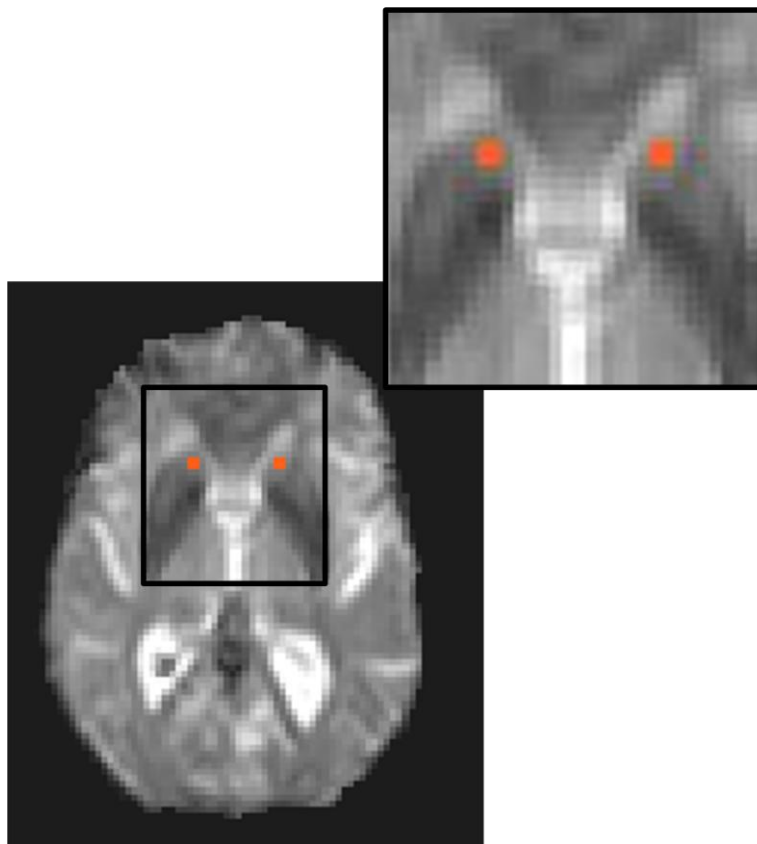
Each individual circuit is organised in parallel and the basic design is similar; output is received from the cerebral cortex and projections are then sent to the input and output nuclei, the thalamus, and a portion of the frontal lobe (as outlined in figure 5.1).

As was discussed in detail in Chapter 3, a number of studies have investigated the caudate nuclei in depression. Decreased caudate volumes have been reported in LLD (mean age 71 years) (Butters et al., 2009), in older depressed subjects (mean age 58 years) (Beyer et al., 2004) and in younger depressed subjects (mean age 48 years) (Krishnan et al., 1992). Caudate volumes have also been shown to be smaller in LLD compared to early-onset depression (Greenwald et al., 1997) and anterior white matter lesion volumes have been negatively associated with total and right caudate nuclei volumes in LLD (mean age 70 years) (Hannestad et al., 2006). Conversely, other studies have reported no significant differences in caudate volumes between depressed patients and controls, though these subjects had early-onset depression (mean age 41 years) (Lacerda et al., 2003). The methods used to delineate the caudate nucleus vary between studies, with some studies measuring the head of caudate nucleus only (Butters et al., 2009), whereas others have measured the whole caudate volume (Lacerda et al., 2003), which could explain the differences found between studies.

5.4.4 *Placing of the Seed Region*

The Functional MRI of the Brain (FMRIB) Software Library (FSL) (www.fmrib.ox.ac.uk/fsl) tools were used for analysis (FMRIB Analysis Group, 2007) (version 4.1). Brain extraction, using the FSL Brain Extraction Tool (BET) (version 2.1) (Smith, 2002), which segments brain from non-brain, was previously carried out by Dr. David Cousins. Using the FSLView tool (version 3.1), the head of caudate nuclei seed regions were placed directly on the first volume of the resting-state fMRI scans. The seeds, of 2 by 2 voxels, were placed on one slice only in both the left and right hemispheres, with the images in the axial view and radiological orientation noted (i.e. right side of the computer is the left hemisphere of the brain) (see Figure 5.2). The seeds were placed by a sole investigator (the author) blinded to the identity and diagnosis of each scan and guided by a standard brain atlas (DeArmond et al., 1989). In a second display window, the FSL tools were used to display an echo planar image in standard space with the head of caudate nucleus overlaid for further reference. The seeds were placed on the most inferior slice where the head of caudate nucleus and the putamen are separated by the internal capsule, similar to guidelines used in previous studies (Beyer et al., 2004; Aylward et al., 2003). In some subjects, placing the seed was more difficult than in others due to greater ventricular atrophy. However, on reviewing all seeds after placement, in all cases the seed was observed to be accurately placed and within the caudate nucleus boundaries. To check for motion in the images the movie mode function was used which enables all volumes of the brain to be viewed. No study subjects exhibited a significant amount of head motion.

Figure 5.2: Overlay of the Head of Caudate Nucleus in the Axial View on the Functional Image



5.4.5 Functional Connectivity Analysis

FMRI data pre-processing steps of motion correction (Jenkinson et al., 2002), spatial smoothing (5 mm full width at half maximum) and high-pass temporal filtering (cut-off = 125 s) (Smith et al., 2004b) were performed using FMRI Expert Analysis Tool (FEAT) (version 5.92). The mean BOLD signal time-series were extracted from the left and right (separately) head of caudate nuclei (using the command line tool `fslmeants` which outputs the average time-series of a set of voxels) and these time-series were then used as the model response function in first-level (i.e. individual subject) general linear modelling time-series analysis; FMRIB's Improved Linear Model (FILM) (Woolrich et al., 2001). This effectively cross-correlates the time-series of SLFs in the BOLD signal in the head of caudate nucleus with all other brain areas, and searches for voxels which are showing similar time-series. The FSL recommended default setting for statistical analysis were used with functional connectivity thresholded at $z > 2.3$ and $p < 0.05$ (Worsley, 2001). Images were registered to the standard space echo planar

imaging template from Statistical Parametric Mapping (SPM) (Wellcome Trust Centre for Neuroimaging, 2005) using FMRIB's Linear Image Registration Tool (FLIRT) (Jenkinson and Smith, 2001). For a more detailed outline of the methods carried out please refer to Appendix A.

Following the individual subject analysis, a study specific standard brain template was created. The subjects in this study were elderly so we would expect them to have more brain atrophy than a general standard space template which is based on younger subjects. To create the study specific brain template, one subject was registered to the standard space echo planar imaging template from SPM (Wellcome Trust Centre for Neuroimaging, 2005), all other study subjects were registered to this subject (using FLIRT) (Jenkinson and Smith, 2001) and then averaged (using the `fslmaths` command which enables mathematical manipulation of images).

FEAT higher-level (group) analysis was then run on the registered data. Using FMRIB's Local Analysis of Mixed Effects (FLAME), a two-sample unpaired t-test was carried out to investigate differences between the functional connectivity results for control and LLD subjects using a voxel by voxel comparison (Woolrich et al., 2004). Z (Gaussianised T/F) statistic images were thresholded using clusters of pixels determined by $z > 2.3$ and $p < 0.05$ (Worsley, 2001). Connectivity differences between the left and right head of caudate nuclei within each group were also investigated, with z and p thresholds as above.

The coordinates from FSL are in Montreal Neurological Institute (MNI) space, to assign specific brain regions to these coordinates they were converted to Talairach space (Talairach and Tournoux, 1988) using GingerALE (Lancaster et al., 2007) and entered into Talairach Client which assigns Talairach labels (hemisphere, lobe, gyrus, tissue and cell type) (Lancaster et al., 2000; Lancaster et al., 1997).

5.4.6 White Matter Hyperintensities and Functional Connectivity

The relationship between functional connectivity and levels of white matter hyperintensities were investigated in LLD subjects using structural MRI and fluid attenuated inversion recovery (FLAIR) images. Volumes of white matter hyperintensities in the LLD subjects had previously been calculated from FLAIR images by Dr. Michael Firbank using a published and validated method (Firbank et al., 2004; Firbank et al., 2003b). This work involved using SPM (Wellcome Trust Centre for Neuroimaging, 2005) to segment subjects' T1 scans into images showing the

distribution of grey and white matter and cerebrospinal fluid (Firbank et al., 2004; Firbank et al., 2003b). Registration was performed, and from the segmentations the total brain (grey plus white matter) and intracranial (brain volume plus cerebrospinal fluid) volumes were calculated for each subject, and intersubject differences in head size were corrected for. FLAIR scans for each subject were registered to their corresponding T1 image, and white matter hyperintensities identified using a previously automated procedure (Firbank et al., 2004; Firbank et al., 2003b). Non-brain regions of the FLAIR image were removed using the T1 brain segmentation, and the white matter hyperintensities were segmented on a slice by slice basis (with the images in native space) using a threshold determined from the histogram of pixel intensities for each image slice. White matter hyperintensities in the periventricular regions (frontal, occipital and lateral) were distinguished from deep white matter hyperintensities (volume outside the periventricular regions), and were expressed as a percentage of the total brain volume.

The LLD subjects were split into 2 groups (low and high) based on their median value for deep white matter hyperintensities, using a cut-off of 0.10%. The LLD subjects were also split into 2 groups (low and high) based on their median value for deep plus periventricular white matter hyperintensities, using a cut-off of 0.60%, to determine whether there was a regional difference in white matter burden.

5.4.7 Depression Severity and Functional Connectivity

The relationship between depression severity and functional connectivity was investigated in the LLD group using the Montgomery-Asberg Depression Rating Scale (MADRS) (Montgomery and Asberg, 1979). LLD subjects were split into 2 groups using the mean MADRS score (7.1):

- For the low MADRS score group a cut-off of ≤ 7 was used
- For the high MADRS score group a cut-off of ≥ 8 was used (a higher MADRS score indicates greater depression severity).

5.5 Results

5.5.1 Demographics

Table 5.1 shows the clinical characteristics of the subjects. Statistical analysis was carried out using Statistical Package for Social Sciences (SPSS), version 15.0.1 (SPSS for Windows, 2006). Groups were comparable for gender ($p=0.38$, $\chi^2 = 0.76$, $df = 1$), age ($p=0.76$, $df=31$, $t=-0.31$), MMSE score ($p=0.17$, $df=31$, $t=-1.43$) and total brain volume normalised to total intracranial volume ($p=0.85$, $df=31$, $t=-0.19$). Mean MADRS score for LLD subjects was 7.1, indicating that most had recovered from their episode of depression by the time of scanning. Mean age at onset of depression was 47.4 years and the mean number of previous episodes of depression was 2.5. At the time of the study, 12 subjects in total were taking antidepressants (citalopram, mirtazapine, trazodone, venlafaxine, paroxetine and lofepramine), 2 subjects were taking antipsychotics (flupenthixol and prochlorperazine) (1 of these subjects was also taking antidepressants), 2 subjects were taking benzodiazepines (zopiclone and temazepam) (both subjects were also taking antidepressants) and 2 subjects were taking antiepileptic medication (carbamazepine and sodium valproate) (both subjects were also taking antidepressants).

Table 5.1: Demographic and Neuropsychological Data of Study Subjects

Demographic and Neuropsychological Data	Controls	Late-Life Depression	<i>P</i> Value
<i>n</i>	17	16	
Age (Years)	75.7±7.6	76.4±7.2	0.76 ^a
Sex (Male:Female)	11:6	8:8	0.38 ^b
Age at Onset of Depression (Years)		47.4±18.5	
Montgomery-Asberg Depression Rating Scale		7.1±4.8	
Number of Previous Episodes of Depression		2.5±2.1	
Mini-Mental State Examination Score	28.8±1.2	28.0±1.8	0.17 ^a
Brain Volume Normalised to Total Intracranial Volume	0.79±0.052	0.79±0.048	0.85 ^a

Values expressed as mean ± standard deviation. ^a*P* values calculated using Independent-Samples T Test. ^b*P* value calculated using Chi-Square Test.

5.5.2 *Group Functional Connectivity*

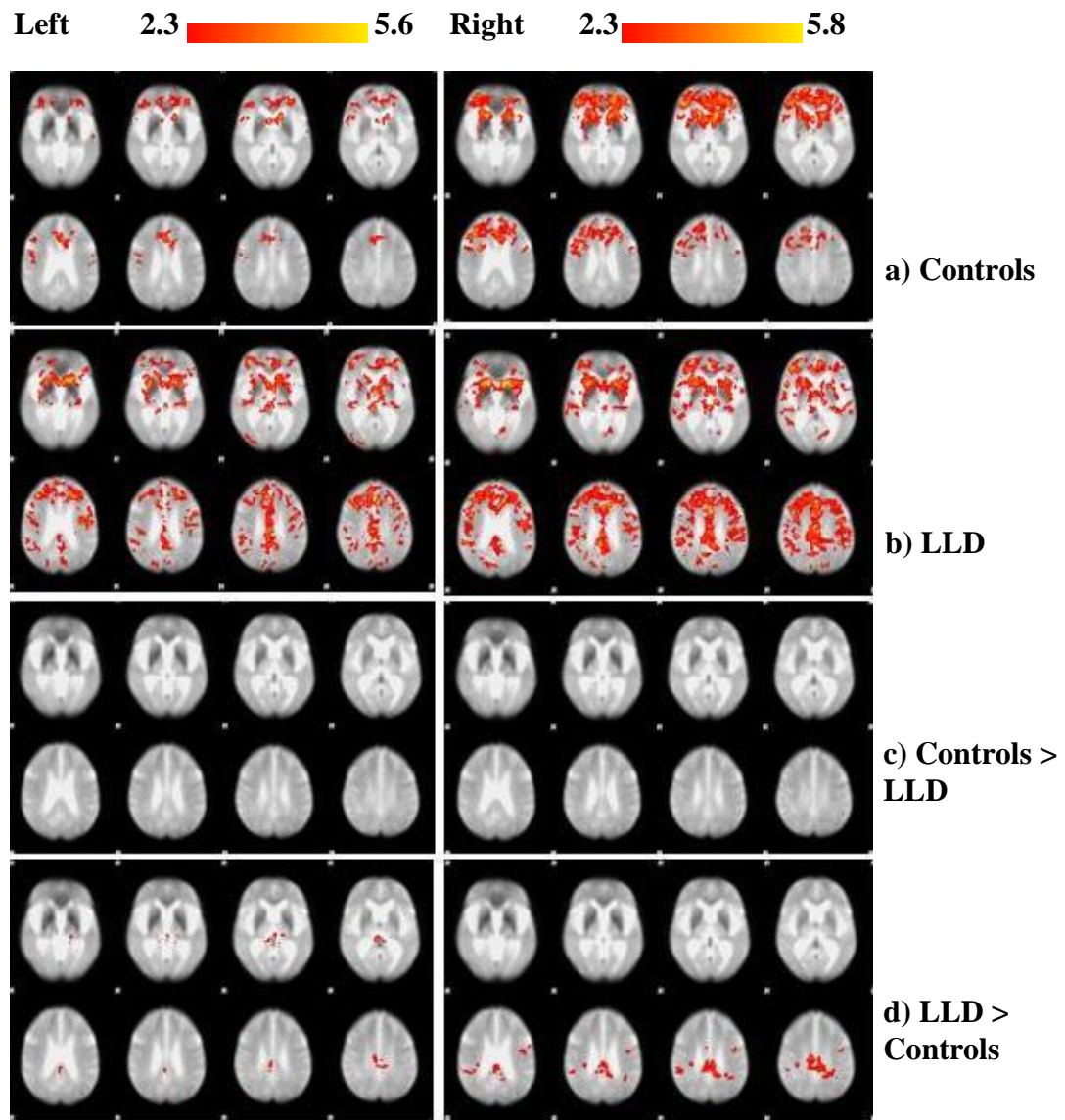
The mean functional connectivity maps for control subjects showed that areas of significant connectivity with the head of caudate nucleus were predominately frontal areas; including inferior, middle and the precentral gyrus, and also limbic (cingulate) and sub-lobar regions (caudate head and body and the insula) (Figure 5.3a). In contrast, the LLD group showed functional connectivity over a much wider area. The brain regions with the most peak connectivity clusters in LLD for the left head of caudate nucleus were; frontal (precentral gyrus), sub-lobar (thalamus) and parietal (precuneus), and for the right head of caudate nucleus; frontal (precentral gyrus) and limbic (cingulate). The LLD group showed connectivity with temporal and parietal regions which were not shown in the control group (Figure 5.3b).

When the groups were compared, brain regions showing significantly greater connectivity (z statistic >2.3 , $p < 0.05$) in LLD compared to control subjects for both left and right head of caudate nucleus were the following:

- Frontal (precentral, sub-gyral, middle frontal and paracentral lobule)
- Sub-lobar (thalamus and insula)
- Limbic (cingulate)
- Parietal (postcentral gyrus, precuneus, inferior parietal lobule and supramarginal gyrus)
- Temporal (superior temporal gyrus)

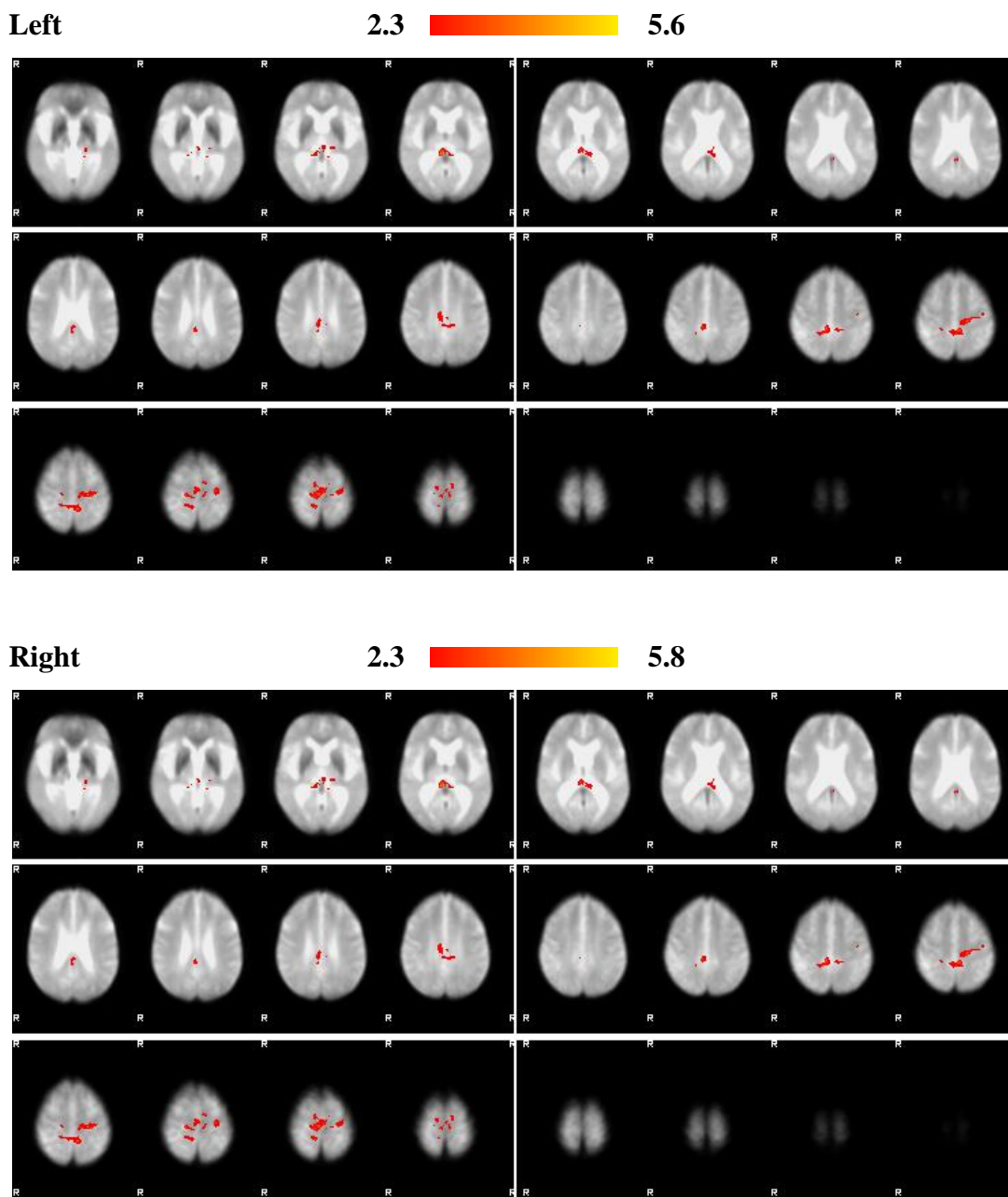
These brain regions are illustrated in Figure 5.3d and in more detail in Figure 5.4, with the corresponding brain regions listed in Table 5.2. There were no brain regions of significantly greater connectivity with the left or right head of caudate nucleus in controls compared to LLD subjects (Figure 5.3c).

Figure 5.3: Functional Connectivity Maps Showing Regions of Significant Connectivity with the Head of Caudate Nucleus in Late-Life Depression and Control Subjects



Images are registered to standard space. Threshold levels are shown at the top of the figure. Voxels with a z score of > 2.3 ($p < 0.05$) were considered to show significant connectivity. Slices are $z = 33, 35, 37, 39, 49, 51, 53, 55$. Note radiological orientation, i.e. left hemisphere in the image is right hemisphere in the brain.

Figure 5.4: Functional Connectivity Maps Showing Regions of Significantly Greater Connectivity with the Head of Caudate Nucleus in Late-Life Depression versus Control Subjects (Figure 5.3d but with slices covering more of the brain)



Images are registered to standard space. Threshold levels are shown at the top of the figure. Voxels with a z score of > 2.3 ($p < 0.05$) were considered to show significant connectivity. Odd slices, $z = 33 - 77$. Note radiological orientation, i.e. left hemisphere in the image is right hemisphere in the brain.

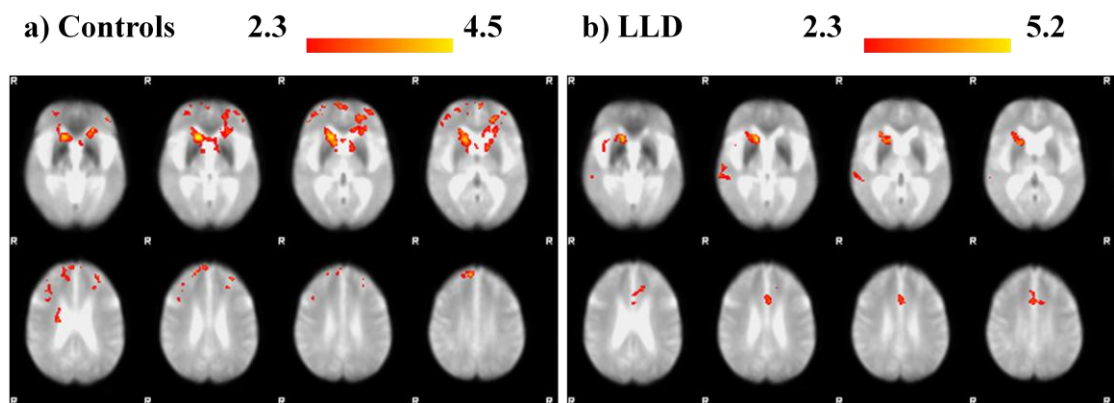
Table 5.2: Brain Regions Showing Greater Functional Connectivity in Late-Life Depression compared to Controls

Left Head of Caudate Nucleus						
Brain Region		Left/ Right	Talairach			Z Score
Lobe	Gyrus		Coordinates (mm)			
			x	y	z	
Frontal	Precentral	L	-16	-27	50	3.44
	Sub-Gyral	R	16	-27	56	3.15
	Paracentral Lobule	L	-7	-40	48	3.28
		R	18	-40	50	3.01
Sub-lobar	Thalamus	L	-11	-34	8	2.92
		R	6	-34	5	3.83
Limbic	Cingulate	R	14	-44	42	3.19
Parietal	Postcentral	L	-24	-29	52	3.48
	Precuneus	L	-7	-48	51	3.09
		R	6	-36	43	3.39
Right Head of Caudate Nucleus						
Brain Region		Left/ Right	Talairach			Z Score
Lobe	Gyrus		Coordinates (mm)			
			x	y	z	
Frontal	Precentral	L	-43	-6	24	3.19
	Middle Frontal	L	-37	-7	41	3.19
	Paracentral Lobule	L	-7	-40	48	3.48
Sub-lobar	Insula	R	37	-39	23	3.79
Limbic	Cingulate	L	-7	-41	30	3.87
		R	12	-20	36	3.87
Parietal	Postcentral	R	31	-32	38	3.56
	Inferior Parietal	R	50	-36	30	3.21
	Supramarginal	R	46	-39	32	3.08
Temporal	Superior Temporal	R	44	-43	22	3.09

5.5.3 Brain Hemisphere and Functional Connectivity

In control and LLD subjects, a number of regions showed significantly greater connectivity for the right head of caudate nucleus compared to the left (Figure 5.5), whereas no regions showed significantly greater connectivity for the left head of caudate nucleus compared to the right in either control or LLD subjects. In the control group, peak areas showing greater right caudate functional connectivity than left were mainly in frontal and to a lesser extent sub-lobar brain regions (Figure 5.5a and Table 5.3), whereas in LLD sub-lobar, followed by limbic and temporal regions showed the greatest functional connectivity (Figure 5.5b and Table 5.3).

Figure 5.5: Functional Connectivity Maps Showing Regions of Significantly Greater Connectivity for the Right Head of Caudate Nucleus Compared to the Left in Control and Late-Life Depression Subjects



Images are registered to standard space. Threshold levels are shown at the top of the figure. Voxels with a z score > 2.3 ($p < 0.05$) were considered to show significant connectivity. Slices are $z = 33, 35, 37, 39, 49, 51, 53, 55$. Note radiological orientation, i.e. left hemisphere in the image is right hemisphere in the brain.

Table 5.3: Brain Regions Showing Greater Connectivity for the Right Head of Caudate Nucleus compared to the Left in Controls and Late-Life Depression Subjects

Controls: Right Head of Caudate Connectivity > Left						
Brain Region Lobe	Gyrus	Left/ Right	Talairach Coordinates (mm)			Z Score
			x	y	z	
Frontal	Inferior Frontal	L	-22	28	-2	4.15
	Medial Frontal	L	-20	41	9	3.90
		R	8	46	39	3.68
	Superior Frontal	R	24	55	14	3.54
Sub-lobar	Caudate (Head)	R	14	18	1	4.58
	Caudate (Body)	R	14	14	6	3.97
	Thalamus	L	-12	-3	12	3.87
LLD: Right Caudate Connectivity > Left						
Brain Region Lobe	Gyrus	Left/ Right	Talairach Coordinates (mm)			Z Score
			x	y	z	
Sub-lobar	Caudate (Head)	R	16	18	-4	5.27
	Putamen	R	22	16	2	4.25
	Clastrum	R	28	26	-2	3.69
	Extra-nuclear	R	32	16	-12	3.4
	Insula	R	48	8	-12	3.08
Limbic	Cingulate	L	0	18	30	3.63
		R	4	16	40	3.91
	Anterior Cingulate	L	-6	28	20	3.34
Temporal	Superior Temporal	R	64	-26	-2	3.63
	Middle Temporal	R	66	-30	-4	3.59

5.5.4 White Matter Hyperintensities and Functional Connectivity

To assess whether the level of white matter hyperintensities affected connectivity, the LLD group was split according to median values in two ways:

- i. Low and high levels of deep white matter hyperintensities as a percentage of the total brain volume. The low deep white matter hyperintensities group had $\leq 0.10\%$ (9 subjects) (mean = 0.08%), and the high group had $> 0.10\%$ (7 subjects) (mean = 0.28%) (mean for all subjects = 0.16%).
- ii. Low and high levels of deep plus periventricular white matter hyperintensities as a percentage of the total brain volume. The median was used as a cut-off to split the LLD subjects. The low group had $< 0.60\%$ (8 subjects) (mean = 0.40%) and the high group $> 0.60\%$ (8 subjects) (mean = 1.13%) (mean for all subjects = 0.76%).

The overlap of subjects between the 2 groups (low and high) for deep only and deep plus periventricular white matter hyperintensities were as follows:

- Low deep only white matter hyperintensity group and the low deep plus periventricular group comprised 5 of the same subjects
- High deep only white matter hyperintensity group and the high deep plus periventricular group comprised 4 of the same subjects
- Low deep only white matter hyperintensity group and the high deep plus periventricular group comprised 4 of the same subjects
- High deep only white matter hyperintensity group and the low deep plus periventricular group comprised 3 of the same subjects.

FLAIR images for 2 subjects are shown in Figure 5.6, a subject with high levels of white matter hyperintensities (Figure 5.6a) and a subject with low levels of white matter hyperintensities (Figure 5.6b).

Deep white matter hyperintensities

For the left and right head of caudate seeds, functional connectivity visibly looked greater in the high (Figure 5.7a for the left caudate seed) compared to the low (Figure 5.7b for the left caudate seed) white matter hyperintensity groups. However, on statistical testing no significant differences in functional connectivity were found

between the groups based on levels of white matter hyperintensities for either the left or right caudate seeds.

For the left head of caudate nucleus the high deep white matter hyperintensity group showed functional connectivity with (see Figure 5.7a):

- Frontal (precentral, inferior frontal)
- Sub-lobar (thalamus, caudate head, putamen, insula, claustrum)
- Limbic (parahippocampal gyrus)
- Parietal (postcentral, inferior parietal, supramarginal)
- Temporal (caudate tail, superior temporal)

For the left head of caudate nucleus the low deep white matter hyperintensity group showed functional connectivity with (see Figure 5.7b):

- Frontal (precentral, inferior frontal, superior, middle and medial)
- Sub-lobar (caudate head, putamen, claustrum)
- Limbic (cingulate)
- Parietal (precuneus, supramarginal)
- Temporal (middle temporal)
- Occipital (cuneus)

Deep plus Periventricular White Matter Hyperintensities

Similar to the results for deep white matter hyperintensities only, there were no significant differences between the high and low burden groups in deep plus periventricular white matter hyperintensities for the left or right head of caudate nucleus.

Figure 5.6: Fluid Attenuated Inversion Recovery (FLAIR) Images in a Subject with a High Level of White Matter Hyperintensities (a) and a Subject with a Low Level of White Matter Hyperintensities (b)

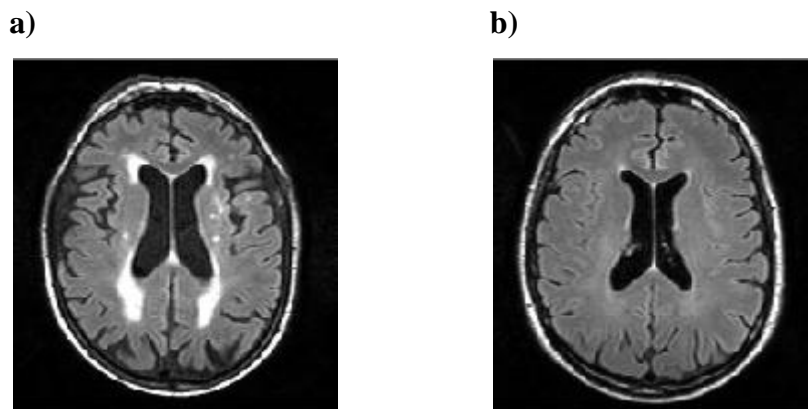
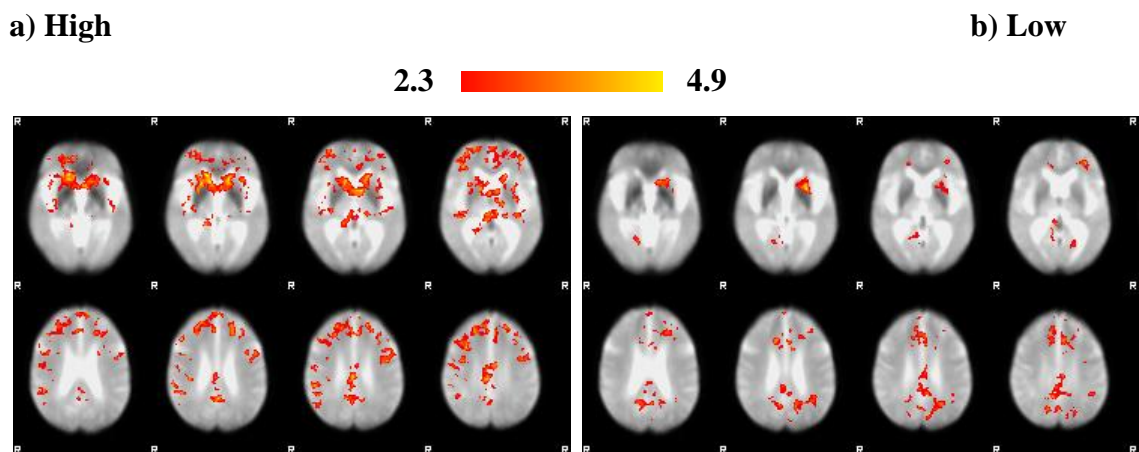


Figure 5.7: Functional Connectivity Maps for the Left Head of Caudate Nucleus in Late-Life Depression Subjects Split According to High and Low Deep White Matter Hyperintensities



Images are registered to standard space. Threshold levels are shown at the top of the figure. Voxels with a z score of 2.3 ($p < 0.05$) were considered to show significant connectivity. Slices are $z = 33, 35, 37, 39, 49, 51, 53, 55$. Note radiological orientation, i.e. left hemisphere in the image is right hemisphere in the brain.

5.5.5 *Depression Severity and Functional Connectivity*

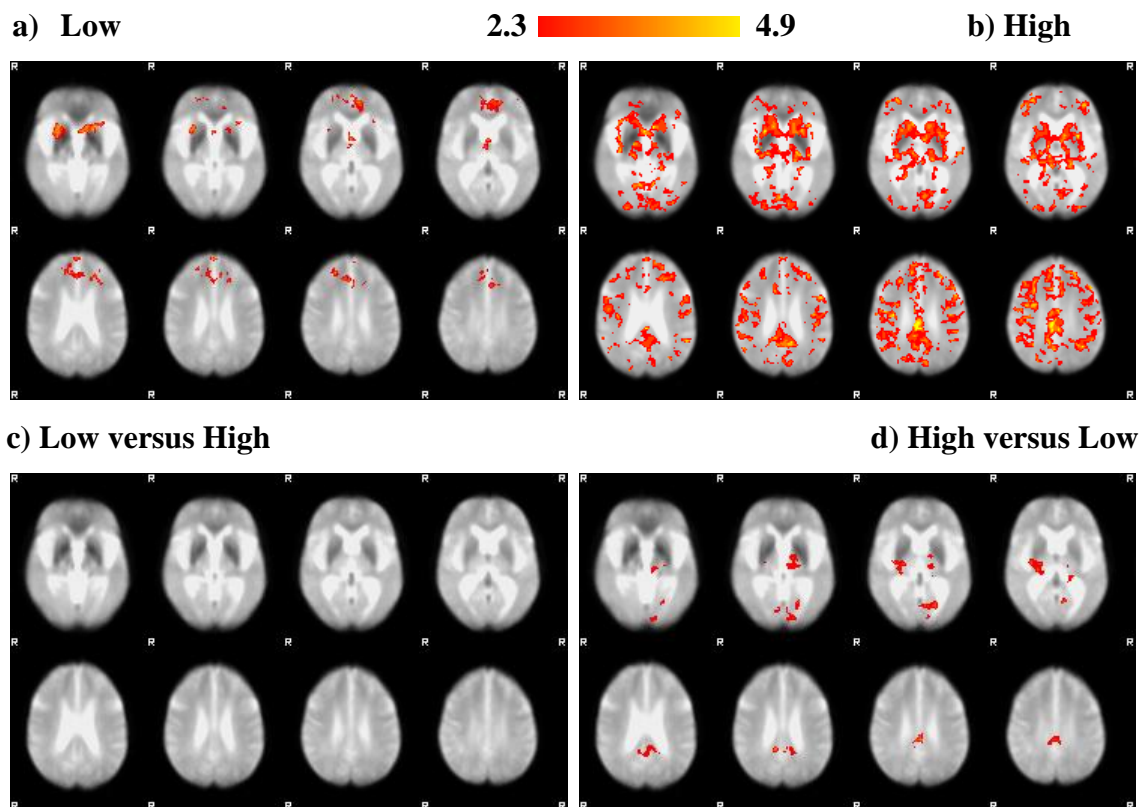
To assess whether differences in functional connectivity might reflect state rather than trait changes, the LLD group was split based on depression severity as measured by their score on the Montgomery-Asberg Depression Rating Scale (MADRS). The mean MADRS score for all subjects was 7.1, so ≤ 7 and ≥ 8 were used as the cut-offs to split the LLD subjects into 2 groups. Subjects with a MADRS score of ≤ 7 were assigned to the low MADRS score group (7 subjects) (Figure 5.8a for the left caudate) and subjects with a score of ≥ 8 were assigned to the high MADRS score group (9 subjects) (high score signifies greater depression severity) (Figure 5.8b for the left caudate).

Significantly greater connectivity for the left head of caudate nucleus was found in the high MADRS score group compared to the low MADRS score group in a number of brain regions; sub-lobar (putamen and thalamus), limbic (cingulate), midbrain (substantia nigra), anterior (culmen), occipital (lingual gyrus) and parietal (precuneus and superior parietal lobule) regions (see Figure 5.8d and Table 5.4). There were no regions of significantly greater connectivity in the low versus high MADRS score group for the left head of caudate nucleus (Figure 5.8c). There were no significant differences between the low and high MADRS score groups for the right head of caudate nucleus.

Summary

In summary, significant differences in functional connectivity with the head of caudate nucleus were observed between groups (LLD > controls for left and right seeds), hemispheres (right > left seed in LLD and controls) and for depression severity (high > low MADRS score for the left seed). Table 5.5 provides a summary of the model-based functional connectivity analysis carried out on the data.

Figure 5.8: Functional Connectivity Maps for the Left Head of Caudate Nucleus in Late-Life Depression Subjects Split According to High and Low MADRS Score



Images registered to standard space. Threshold levels are at the top of the figure. Significant connectivity = z score > 2.3 and $p < 0.05$. Slices are $z = 33, 35, 37, 39, 49, 51, 53, 55$. Note radiological orientation, i.e. left hemisphere in the image is right hemisphere in the brain.

Table 5.4: Brain Regions Showing Greater Connectivity for the Left Caudate in LLD Subjects in the High Compared to the Low MADRS Score Group

Brain Region		Left/ Right	Talairach Coordinates			Z Score
Lobe	Gyrus		x	y	z	
Sub-Lobar	Putamen	R	22	-17	4	3.32
	Thalamus	L	-16	-31	3	2.89
Limbic	Cingulate	R	22	-23	9	3.05
		L	-13	-50	25	2.71
	Posterior Cingulate	R	10	-44	26	3.67
		L	-3	-44	15	3.16
Midbrain	Substantia Nigra	L	-7	-27	-9	3.09
Anterior	Culmen	L	-12	-28	-15	2.92
Occipital	Lingual Gyrus	L	-18	-65	-7	3.15
Parietal	Precuneus	L	-17	-46	49	3.57
	Superior Parietal	L	-15	-46	60	3.1

Table 5.5: Summary of the Results from the Model-Based Functional Connectivity Analysis in Late-Life Depression and Control Subjects

Variable	Comparisons	Significant Difference ($z > 2.3$, $p < 0.05$)
Group	LLD > Control for L Seed	✓
	LLD > Control for R Seed	✓
	Control > LLD for L Seed	✗
	Control > LLD for R Seed	✗
Hemisphere	R > L Seed in Control	✓
	R > L Seed in LLD	✓
	L > R Seed in Control	✗
	L > R Seed in LLD	✗
White Matter Hyperintensities in LLD (Deep only and Deep plus PVH)	Low > High for L Seed	✗
	Low > High for R Seed	✗
	High > Low for L Seed	✗
	High > Low for R Seed	✗
MADRS Score in LLD	High > Low MADRS score for L Seed	✓
	High > Low MADRS score for R Seed	✗
	Low > High MADRS score for L Seed	✗
	Low > High MADRS score for R Seed	✗

Abbreviations: LLD=Late-Life depression, L=Left, MADRS=Montgomery-Asberg Depression Rating Score, PVH = Periventricular; R=Right.

5.6 Discussion

This resting-state fMRI study showed increased functional connectivity between the head of caudate nucleus and specific brain regions in LLD compared to age-matched control subjects. Increased connectivity was reported in frontal (precentral, sub-gyral, middle frontal and paracentral lobule), sub-lobar (thalamus and insula), limbic (cingulate), parietal (postcentral gyrus, precuneus, inferior parietal lobule and supramarginal gyrus) and temporal (superior temporal gyrus) brain regions in LLD compared to control subjects. No brain regions showed greater connectivity in control compared to LLD subjects.

In both the control and LLD groups, greater right head of caudate connectivity was shown than left, and no regions of greater left connectivity than right. Similarly, previous studies have shown rightward asymmetry in elderly controls with the hippocampus, which was absent in Alzheimer's disease (Wang et al., 2006). These findings could suggest that the right hemisphere of the brain is more important for resting-state brain activity, for example mind-wandering/daydreaming, whereas the left hemisphere has been shown to be more strongly activated for task-based functions such as language processing (Desmond et al., 1995). It could also be that ageing, and/or disease, affect connectivity in the right hemisphere, and functioning in the left hemisphere is preserved, though maybe only initially. Therefore, the left hemisphere is characterised by lower connectivity as brain regions are functioning more efficiently.

The effect of white matter hyperintensities on functional connectivity in LLD were investigated, however no significant differences in connectivity were found between the high and low level groups for deep only or deep plus periventricular hyperintensities. Though, functional connectivity did appear to be greater in the group with high deep white matter hyperintensities and it is likely that the group size of between 7 and 9 subjects was too small for statistical significance to be reached.

In the LLD subjects, the effect of depression severity on functional connectivity was also investigated to see whether functional connectivity might reflect mood state, rather than trait changes. LLD subjects who had a greater severity of depression (as assessed by score on the MADRS) showed increased functional connectivity with the left head of caudate nucleus compared to LLD subjects who had a lower MADRS score and less severe depression. This finding indicates that the mood state of individuals at the time of scanning does have an effect on the functional connectivity observed.

The finding of increased functional connectivity in LLD between the head of caudate nucleus and a number of brain regions supports results from previous studies of abnormal functioning of mood regulating circuits in depression, specifically limbic-cortical-striatal-pallidal-thalamic circuits (Drevets et al., 2002; Mayberg et al., 1999; Drevets et al., 1997). These circuits are known to be formed by connections between several brain regions which match regions that were shown in this study to have abnormally increased functional connectivity in LLD, for example the thalamus.

Previous PET studies have shown that depression is characterised by increased activity (glucose metabolism) in limbic regions (Mayberg et al., 1999). Consistent with previous studies, this study reports increased activity in the same regions, specifically the thalamus, cingulate and insula. PET studies have also reported decreased activity in cortical regions in depression (Mayberg et al., 1999; Drevets et al., 1997), however decreased connectivity was not found in this study, but similarly, other resting-state fMRI studies have also reported no regions of significantly greater connectivity in control versus depression subjects (Greicius et al., 2007).

Increased connectivity was found in a number of brain regions which have previously been demonstrated to form part of a resting-state network, the default mode network (Raichle et al., 2001), namely frontal regions, the cingulate, precuneus and inferior parietal regions. Additionally, this study showed that LLD subjects with more severe depression (high MADRS score) had increased functional connectivity compared to patients who had a lower MADRS score. The regions showing increased connectivity corresponded with default mode network regions of the thalamus, posterior cingulate and precuneus.

The default mode network is more active at rest and is deactivated during task performance (Raichle et al., 2001). This network is involved in the processing of internal self-reflective thoughts, i.e. daydreaming (Gusnard et al., 2001) (see Chapter 2). Abnormally increased activity of the default mode network in LLD could cause emotional dysregulation, characteristic of LLD, due to increased levels of unconstrained mental activity. Over activity of this network at rest may mean there is no, or reduced, suppression of this network during task performance. Therefore the task state could also be characterised by more mind-wandering and less adherence to the task being performed.

Similar to the findings in this study, a previous study in depression by Greicius *et al.* (2007) showed increased connectivity in default mode network regions. Greicius *et al.* (2007) reported increased connectivity within frontal regions, the cingulate,

thalamus and precuneus in depression compared to controls, regions where this study also reported increased functional connectivity (Greicius et al., 2007).

A resting-state study by Sheline *et al.* (2010) also reported increased functional connectivity in depression. Similarly, using a seed-based correlation approach, Sheline *et al.* (2010) reported increased functional connectivity in 3 networks in depression, which suggests that abnormalities in depression affect connections between a number of brain regions. Using the precuneus as the seed region Sheline *et al.* (2010) reported increased functional connectivity in the default mode network. This LLD study also reported increased functional connectivity in the precuneus and again similar to this study, Sheline *et al.* (2010) also observed positive correlation between increased connectivity and depression severity (Sheline et al., 2010).

There has only been one resting-state study to date investigating functional connectivity in LLD and the findings here, in part, match this study. Yuan *et al.* (2008) reported increased connectivity in frontal, striatal (putamen) and parietal regions, but they also reported decreased functional connectivity in frontal, temporal and parietal regions. The regions where Yuan *et al.* (2008) reported decreased connectivity match with some of the regions where they also reported increased connectivity, and also regions where this study showed increased connectivity (Yuan et al., 2008). The mean age of depressed subjects in the Yuan *et al.* (2008) study was younger (67 years) compared to this study (76 years) and as they used a model-free analysis approach it is possible that these factors could explain the differences between study findings.

Contrary to the findings reported here, Bluhm *et al.* (2009) reported decreased functional connectivity in depression compared to control subjects. In depression, functional connectivity was decreased between a seed placed in the posterior cingulate/precuneus and the bilateral caudate (head and body). In contrast to this study, the subjects in the Bluhm *et al.* (2009) study were younger (mean of 22 years) and also had a recent onset of depression (Bluhm et al., 2009). Others have also reported decreased connectivity in depression. Anand *et al.* (2005) used a seed placed in the anterior cingulate and investigated connectivity with the thalamus, amygdala and pallidostriatum and found decreased connectivity compared to control subjects (Anand et al., 2005a). The subjects in the Anand *et al.* (2005) study had early-onset depression (mean age 28 years) and connectivity between specific seeds only was investigated, unlike the approach used in this study which investigated connectivity with all brain regions. A model-free analysis study using independent component analysis also reported decreased connectivity in early-onset depression (mean age 36 years). Though,

decreased connectivity was reported in different regions to the Bluhm *et al.* (2009) and Anand *et al.* (2005) studies; namely the amygdalae, insula, lingual gyrus and frontal regions (Veer *et al.*, 2010).

The reasons why control subjects were characterised by a frontal predominance of connectivity whereas LLD subjects had a more diffuse pattern are not clear. No significant differences in brain volumes were found between control and LLD subjects, therefore it is not thought that connectivity differences can be related to greater brain atrophy in LLD. In support of this, functional connectivity was increased in LLD subjects with a greater severity of depression (higher MADRS score), which implies that some changes in connectivity appear to be mood related and suggests that structural changes cannot be the only explanation for functional connectivity abnormalities.

One possible cause of abnormal functional connectivity in LLD could be microvascular damage. Microvascular damage would alter neurovascular coupling and consequently affect the BOLD response (D'Esposito *et al.*, 2003). However, if this was the case, a delay, or a decrease in the BOLD response would be expected and thus reduced connectivity, rather than increased functional connectivity as reported here.

The widely distributed connectivity seen in LLD may represent a departure from frontally coordinated suppression of brain activity, seen in the control group, which is necessary for normal brain functioning at rest. The caudate is involved in the processing of rewarding stimuli involved in pleasure and emotion, therefore abnormalities here could be linked with a characteristic feature of depression, anhedonia; the inability to experience interest or pleasure in activities (Haruno *et al.*, 2004). This study showed abnormal functioning of the default mode network in LLD, which was further increased in the LLD patients who had higher severity of symptoms. This network is activated in free thinking including remembering the past, thinking about future events and considering the thoughts and views of others (Buckner *et al.*, 2008; Buckner and Vincent, 2007; Raichle *et al.*, 2001). The abnormal functioning of this network in LLD and the role this network plays in memory function could be linked with cognitive impairments that are often associated with LLD and also a contributing factor to subsequent development of dementia.

There has been a great deal of discussion as to whether SLFs represent neuronal activity or if they represent fluctuations due to non-neuronal physiological noise, for example. In support of their neuronal origin, SLFs have been shown to be affected in neurological diseases, for example in Alzheimer's disease (Greicius *et al.*, 2004), and the BOLD signal has been shown to correlate with cortical electrical activity (Goldman

et al., 2002). However, it has also been shown that noise from the cardiac and respiratory cycles can introduce fluctuations into the fMRI time-series, into the low-frequency ranges at which resting-state functional connectivity is investigated (Lowe et al., 1998). Filtering techniques have been developed to remove cardiac (at 0.6-1.2 Hz) and respiratory fluctuations (at 0.1-0.5 Hz) prior to functional connectivity analysis as they are easily separable from neuronal SLFs (at <0.1 Hz) (Cordes et al., 2001; Cordes et al., 2000). However, variations in respiration depth from breath to breath occur at much lower frequencies (approx 0.03 Hz), which are not filtered out by typical physiological correction techniques (Wise et al., 2004) and thus can over-estimate functional connectivity (Birn et al., 2008; Birn et al., 2006).

Therefore, it has now become clear that monitoring and/or removal of non-neuronal physiological signals leads to significant improvement in the quality of the data (Birn et al., 2006; Fox et al., 2005). It can be concluded that resting-state networks are distinct neuronal processes, but it is important that non-neuronal fluctuations are removed for greatest accuracy of the functional connectivity results. Chapter 6 of this thesis will discuss this area in detail.

5.6.1 Strengths and Limitations

Strengths of this study are that the control and LLD groups were well matched in terms of subject numbers, gender and age. The model-based analysis method used in this study enables the investigation of the correlation of SLFs between the head of caudate nucleus and all other brain regions based on an *a priori* hypothesis to select the seed region. In this study, the hypothesis was based on findings from previous studies showing that the caudate nucleus is abnormal in depression, and specifically in LLD, for example structural studies showing decreased volume (Butters et al., 2009) and pathological studies showing decreased neuronal density (Khundakar et al., 2010). In contrast, other studies have only looked at correlations between a few specific regions in depression, or have used model-free methods where no prior hypothesis is required and all connectivity is searched for. Resting-state studies benefit from simplicity of experimental design, no task has to be practised or performed, therefore patient compliance and tolerance is high and head motion is reduced.

Limitations of this study are that model-based techniques can be biased by the choice of seed region which means functional connectivities of interest can be missed if they do not show connectivity with the seed. Model-free methods do not require

predefined seeds or a temporal model, and this can be advantageous in ageing studies as the measured BOLD response in these subjects, and particularly in patients, may not necessarily match the standard haemodynamic response function (Rombouts et al., 2005; D'Esposito et al., 2003). However, the lack of specificity of model-free approaches means that results can be hard to interpret as resting-state networks can be split into a number of separate components and the order of these can vary between separate runs of the same data. Further limitations include the effects of psychoactive medications in the LLD group, which previous task state studies have shown can modulate the BOLD response and therefore may affect connectivity (Anand et al., 2007; Anand et al., 2005b), however obtaining a drug naïve patient group with LLD would be difficult to achieve.

5.7 Conclusion

In conclusion, this study reports abnormal (increased and more widespread) resting-state functional connectivity with the head of caudate nucleus in LLD compared to control subjects. Further studies are required to replicate these findings and to determine the time course of the development of changes, and the effects of a change in mood state and treatment on functional connectivity. Of importance will be to determine whether functional connectivity changes precede structural changes and therefore could be used as an early marker for subsequent atrophy, or whether structural changes occur prior, and are responsible for, functional connectivity abnormalities.

Chapter 6

Methodology to Correct for Non-Neuronal Fluctuations

6.1 Introduction

The aim of resting-state functional magnetic resonance imaging (fMRI) is to investigate connectivity between brain regions by measuring spontaneous low-frequency fluctuations (SLFs) in the blood oxygenation level dependent (BOLD) signal. SLFs in the BOLD signal are believed to be caused by neuronal activity of the brain (see Chapter 2). When the methodology used in the late-life depression (LLD) study (Chapter 5) was applied to the next study, investigating connectivity in Alzheimer's disease (AD) and dementia with Lewy bodies (DLB), an unexpected pattern of global synchronicity was observed in some subjects. Functional connectivity maps in these subjects showed synchronicity between the seed regions and the majority of brain voxels, across grey and white matter (see Figure 6.1). This pattern of global synchronicity had not been observed in the previous study in any of the subjects (LLD or controls) when the head of caudate nucleus was used as the seed (Chapter 5).

Global synchronicity was not seed region specific, meaning that in subjects where we saw this it generally occurred for all seed regions, and there was no anatomical seed region where global synchronicity was not observed in these subjects. Global synchronicity was most commonly seen in the AD group followed by the DLB group, but was also seen in control subjects. Five AD subjects showed global synchronicity across all the seed regions investigated (generally with more than one seed region), 3 DLB subjects and 2 control subjects; totalling over 20% of subjects in the study. Figure 6.1 illustrates examples of this global synchronicity (right side of the page) compared to subjects showing a 'normal'/non-global pattern (left side of the page) of connectivity with seeds placed in the left thalamus (a), head of caudate nucleus (b) and precuneus (c).

The finding of global synchronicity in a number of subjects was surprising, as a seed region placed in the grey matter would not be expected to show correlation with white matter also. Additionally, a seed region would not be expected to show correlation with almost every voxel of the brain. Therefore, possible contributors to the global synchronicity pattern were investigated as the aim of resting-state functional connectivity is to measure SLFs in the BOLD signal between grey matter regions only.

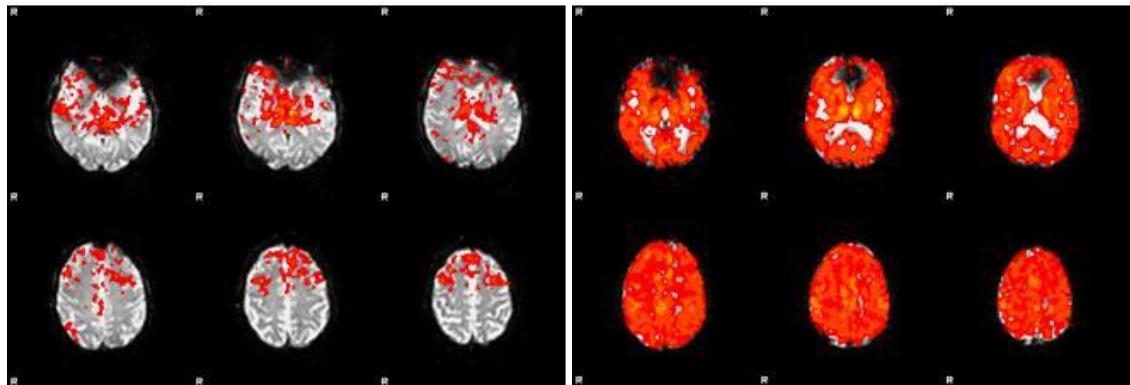
In recent years, other studies investigating functional connectivity have reported these global effects (Fox et al., 2009; Weissenbacher et al., 2009). A number of different ways to correct for non-neuronally related fluctuations have been proposed, which will be discussed in detail in this chapter.

Figure 6.1: Functional Connectivity Maps in Subjects Showing Non-Global Synchronicity and Global Synchronicity

a) Left Thalamus

Non-Global Synchronicity (Control)

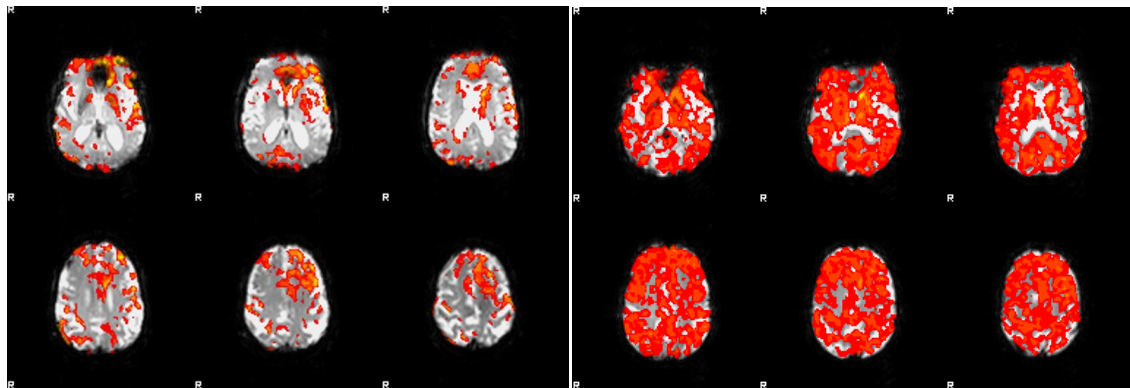
Global Synchronicity (DLB)



b) Left Head of Caudate Nucleus

Non-Global Synchronicity (DLB)

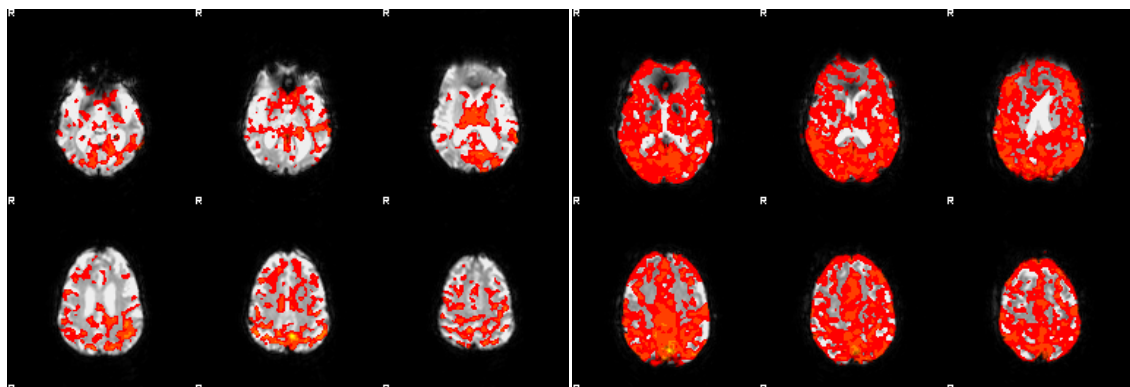
Global Synchronicity (AD)



c) Left Precuneus

Non-Global Synchronicity (AD)

Global Synchronicity (Control)



6.2 Aims

The main aim of this investigation was to optimise the methodology for the analysis of the dementia study data, with the aim of eliminating or minimising what appeared to be aberrant connectivity patterns in the data, which have also been reported in previous studies.

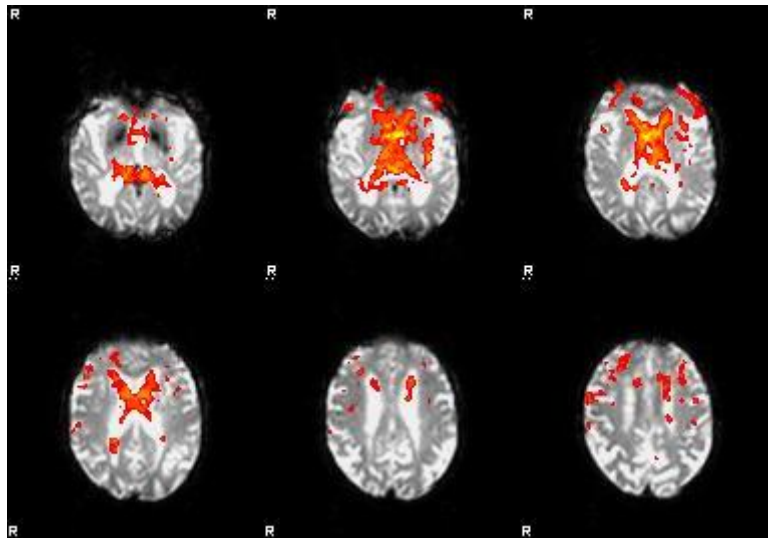
6.3 Methods

6.3.1 Seed Placing

The first step in the investigation of why some subjects were showing global synchronicity involved verifying the placing of the seed regions to ensure that seeds were correctly placed within the structure boundaries. One concern was that as the subjects in this study were older, they have greater brain atrophy, which is known to be even greater in AD and DLB (O'Brien et al., 2001). This could mean that the seed voxels for certain brain regions, for example the thalamus or head of caudate nucleus, which are located close to the ventricles, may actually be in the cerebrospinal fluid due to the greater ventricular atrophy in dementia (O'Brien et al., 2001). However, if this was the case it would be expected for connectivity to be observed in the cerebrospinal fluid, and not in grey and white matter brain regions. This is demonstrated in Figure 6.2 which shows the pattern of functional connectivity observed following the placing of a seed of 2 by 2 voxels in the ventricles/cerebrospinal fluid.

All seeds were re-checked in the subjects showing global synchronicity and accurate placing of the seeds within the structure boundaries was confirmed. Moving the seed within the structure (a few voxels in all directions) was investigated, though still making sure the seed was within the structure boundaries, but this had no effect on the pattern of global synchronicity seen in these subjects. It was therefore concluded that the seed regions had been accurately placed.

Figure 6.2: Functional Connectivity Map for Seed-Based Correlation Analysis with a Seed Placed in the Cerebrospinal Fluid



6.3.2 Motion Artefact

It was also checked whether this pattern of global synchronicity could be caused by motion-related artefacts in these subjects. Motion correction had previously been carried out in the pre-processing stage of the FMRIB Expert Analysis Tool (FEAT) analysis (Jenkinson et al., 2002), and tools in the FMRIB Software Library (FSL) had been used to view all volumes through the brain (<http://www.fmrib.ox.ac.uk/fsl/>) (FMRIB Analysis Group, 2007). In no subjects was a high level of motion clearly visibly. Additionally, the mean displacement in subjects showing global synchronicity was <1 mm and previous studies have used guidelines of a mean displacement of >3.125 mm to exclude subjects (Greicius et al., 2007). Also, the mean displacement in subjects showing global synchronicity (mean = 0.51 mm) was compared with subjects who did not show global synchronicity (mean = 0.42 mm) and was not found to be significantly different between the 2 groups.

6.3.3 Medications

It was investigated whether medications could be contributing to the global synchronicity effect. However, as global synchronicity was also observed in control subjects it was not thought likely that it was medication related. Additionally, when investigating the subjects who showed global synchronicity, no medication was found

to be consistent across all subjects that could explain the results. The most common medication across the global synchronicity subjects was the acetylcholinesterase inhibitor donepezil (5 subjects), which alleviates cholinergic deficits. However in the study there were 14 subjects taking donepezil. Appendix C shows the medications taken by study subjects, with the global synchronicity subjects in italics.

Therefore it was concluded from these investigations that the seed regions had been accurately placed within the structure boundaries and that global synchronicity was not likely to be caused by excessive motion, as tools had been used to correct for this and the mean displacement measurements were low and comparable with subjects who did not show global synchronicity. Global synchronicity was not thought to be related to subject medication as no medication was common across all global synchronicity subjects, other subjects taking the same medications did not show global synchronicity and the pattern was also observed in control subjects.

6.3.4 *Spurious Fluctuations*

Recently, fMRI studies have begun to report the occurrence of global synchronicity in resting-state data. Similar to the results shown in Figure 6.1, these fluctuations have been shown by other studies to occur across grey and white matter regions (Fox et al., 2009; Weissenbacher et al., 2009; Fox et al., 2005). Global synchronicity is also illustrated in Figure 6.3b, taken from (Fox et al., 2009). Studies have shown that spurious fluctuations contaminate the resting-state fMRI BOLD signal by introducing false correlations in the data and consequently over-estimating functional connectivity. A combination of factors are thought to be responsible for these spurious fluctuations including physiological signals, scanner related artefacts (field drifts) and head motion.

As was discussed in Chapter 2, early resting-state fMRI studies showed that SLFs occur at low-frequencies, < 0.08 Hz (Cordes et al., 2001). Physiological signals, for example cardiac and respiratory-related fluctuations, occur at higher frequencies; 0.1-0.5 Hz (respiratory) 0.6-1.2 Hz (cardiac). SLFs were therefore deemed separable from physiological signals using methods to temporally filter the data (Cordes et al., 2001; Cordes et al., 2000). More recently however, variations in respiration depth from breath to breath have been shown to occur at much lower frequencies, which are not filtered out by typical physiological correction techniques (Birn et al., 2006; Wise et al.,

2004). Respiration has been shown to affect the BOLD signal time-series by changing the arterial level of CO₂, a potent vasodilator. CO₂ can fluctuate during the scan due to changes in depth and rate of breathing. Small fluctuations in end tidal CO₂ level have been shown at frequencies of 0.03 Hz, which therefore correlate significantly with SLFs in the BOLD signal. These CO₂ fluctuations occur naturally during normal breathing at rest and have been shown in grey matter brain regions, specifically they have been shown to overlap with default mode network regions (Birn et al., 2006; Wise et al., 2004). Cardiac related signals have been reported in brain regions expected to be more susceptible to cardiac pulsatility, for example major vessels and cerebrospinal fluid, and additionally, more recently, they have also been localised to grey matter regions (Chang and Glover, 2009; Shmueli et al., 2007; Birn et al., 2006). Since these fluctuations do not reflect neuronal activity it is important that they are removed from the data.

Over recent years, a number of studies have proposed various methods to attempt to correct for spurious fluctuations in the BOLD signal and consequently remove false correlations in resting-state data using model-based methods, specifically seed-based correlation analysis (Murphy et al., 2009; Weissenbacher et al., 2009; Margulies et al., 2007; Fox et al., 2005; Greicius et al., 2003). These methods are investigated in this chapter, and are summarised in Table 6.1. The Fox *et al* (2005) method is summarised in Figure 6.3, taken from (Fox et al., 2009; Fox et al., 2005). To test and compare the effect of different methods on the dementia study data, each method was run on 6 subjects using the left thalamus as the seed region. Three subjects were selected which had shown the greatest pattern of global synchronicity with the left thalamus; 2 AD subjects and 1 DLB subject, and 3 subjects who did not show this pattern of global synchronicity with the left thalamus; 1 control, 1 AD and 1 DLB subject, using the previous method described in Chapter 5.

Table 6.1: Summary of Methods Used in Previous Studies in Resting-State Functional Connectivity Analysis

Study	Pre-processing	Filtering	Covariates of No Interest	Global signal Removed
(Kenny et al., 2010)	<ul style="list-style-type: none"> • Motion correction • Spatial smoothing, Gaussian kernel of FWHM 5 mm • Registration 	High-pass temporal filtering (125s)	✘	✘
(Fox et al., 2005)	<ul style="list-style-type: none"> • Motion correction • Spatial smoothing, Gaussian kernel of FWHM 6 mm • Registration 	Band-pass temporal filtering between 0.009 and 0.08 Hz	<ul style="list-style-type: none"> • Motion parameters • Ventricular seed • White matter seed • Global mask 	✓
(Murphy et al., 2009)	<ul style="list-style-type: none"> • RETROICOR – Physiological noise correction tool • Motion correction • Spatial smoothing, Gaussian kernel of FWHM 5 mm • Registration 	Band-pass temporal filtering between 0.01 and 0.1 Hz	✘	✘

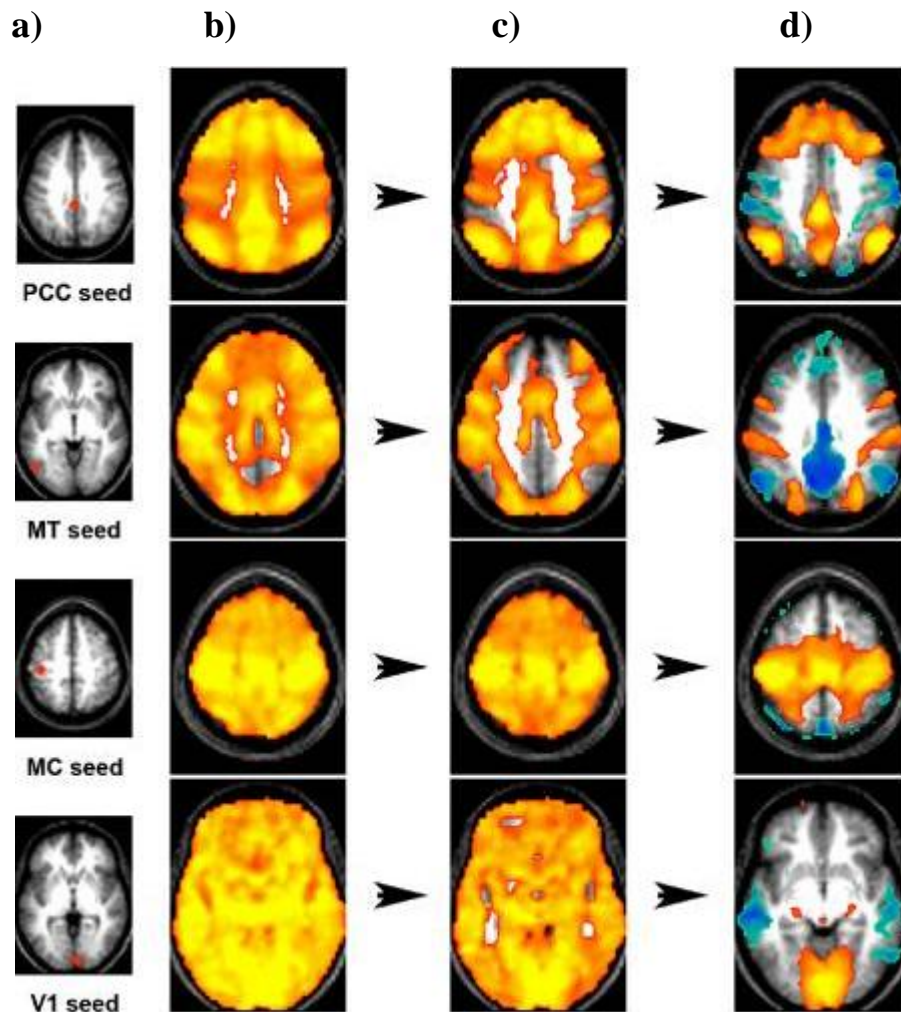
Table 6.1 (Contd.): Summary of Methods Used in Previous Studies in Resting-State Functional Connectivity Analysis

Study	Pre-processing	Filtering	Covariates of No Interest	Global signal Removed
(Weissenbacher et al., 2009)	<ul style="list-style-type: none"> • Motion correction • Spatial smoothing, Gaussian kernel of FWHM 9 mm • Registration 	Band-pass temporal filtering between 0.009 and 0.08 Hz	<ul style="list-style-type: none"> • Motion parameters • Ventricular seeds (5) • White matter seeds (4) • Global signal 	✓
(Greicius et al., 2003)	<ul style="list-style-type: none"> • Motion correction • Spatial smoothing, Gaussian kernel of FWHM 4 mm • Intensity normalisation • Registration 	Band-pass temporal filtering between 0.0083 and 0.15 Hz	✗	✗
(Margulies et al., 2007)	<ul style="list-style-type: none"> • Motion correction • Spatial smoothing, Gaussian kernel of FWHM 6 mm • Registration 	High-pass temporal filtering (100s) Low-pass temporal filtering (2.8s)	<ul style="list-style-type: none"> • Motion parameters • Ventricular • White matter • Global signal 	✓

Abbreviations = FWHM = Full width at half maximum; RETROICOR = Retrospective correction of physiological motion effects.

Figure 6.3: Functional Connectivity Maps following Seed-Based Correlation Analysis

Figure extracted from (Fox et al., 2009)



- a) Seed regions used for correlation analysis
 - b) Connectivity maps following model-based analysis (no regression)
 - c) Connectivity maps following regression for movement, white matter and ventricular signal
 - d) Connectivity maps following global signal regression
- Yellow/Orange = positive correlations with the seed (z score of 2 to 6)
Blue/Green = negative correlations with the seed (z score of -2 to -6)

The Functional MRI of the Brain (FMRIB) Software Library (FSL) (www.fmrib.ox.ac.uk/fsl) tools were used for analysis (FMRIB Analysis Group, 2007) (version 4.1). Firstly, the thalamus seeds were placed in the left and right hemispheres on the first volume of the resting-state functional scans using FSLView (version 3.1) (see Chapter 7 for guidelines used to place the thalamus).

The FSL tool FMRI Expert Analysis Tool (FEAT) (version 5.92) was used to analyse the data with each method (Smith et al., 2004b), following the methodology outlined in Table 6.1 as closely as possible. Below is a description of some of the analysis steps described in Table 6.1 and how they were implemented in this study:

Motion Correction

All of the methods outlined in Table 6.1 corrected for subject head motion. The FSL tool, motion correction FMRIB's linear image registration tool (MCFLIRT) was used which attempts to remove the effects of subject head motion which can occur during the scan procedure. This tool is designed for use on fMRI time-series. Through time, each voxel in the brain should be located at a consistent anatomical point, MCFLIRT realigns to a common reference using FLIRT, an automated tool for brain image registration (Jenkinson et al., 2002).

Spatial Smoothing

All of the study methodologies outlined in Table 6.1 carried out spatial smoothing of the data. Spatial smoothing averages a voxel with its neighbour(s), so that each voxel's intensity is replaced by a weighted average of neighbouring intensities. The advantages are that the signal to noise ratio is increased (if the size of smoothing is less than the size of activation), it enables the application of Gaussian random field theory for thresholding and correlation/connectivity analysis, and can improve comparisons across subjects by decreasing the anatomic variability in brain regions between subjects. However, a disadvantage of spatial smoothing is that it can reduce activation in small brain areas.

The methods in Table 6.1 differed on the extent of smoothing they used. Greicius *et al.* (2003) smoothed the data at 4 mm full width at half maximum (FWHM), whereas Weissenbacher *et al.* (2009) smoothed much higher at 9 mm FWHM (Weissenbacher et al., 2009; Greicius et al., 2003). The level of smoothing is also dependent on the resolution of the data, which may in part explain the different levels of smoothing used. Each level of smoothing was applied using the FEAT tool. FEAT has a default setting of 5 mm for smoothing and recommends lowering below 5 mm to

investigate small activation areas and above 10 mm for the investigation of larger areas (Smith et al., 2004b).

Registration

All methods performed registration which enables the localisation of anatomical landmarks and multi-subject analysis. Registration was carried out to the standard space echo planar imaging template from SPM (Wellcome Trust Centre for Neuroimaging, 2005) using the FLIRT tool in FEAT (Jenkinson et al., 2002).

Filtering

All the study methodologies outlined in Table 6.1 applied temporal filtering to the data. In the previous analysis method (Chapter 5) the data were high-pass temporally filtered only, to remove low-frequency artefacts. Others have used band-pass filtering which involves high and low-pass filtering (to remove high frequency noise). The methods by Fox *et al.* (2005) and Weissenbacher *et al.* (2009) both band-pass filtered at 0.009 and 0.08 Hz. The `fslmaths` command line tool (which enables mathematical manipulation of images) was used to band-pass filter the fMRI data using the `-bptf` option (FMRIB Analysis Group, 2007).

Time-Series Extraction

Following the pre-processing steps (motion correction, smoothing, registration and filtering), the thalamus mean time-series (left and right separately) were extracted from the seed regions and used as the model response function in first-level (i.e. individual subject) general linear modelling time-series analysis; FMRIB's Improved Linear Model (FILM) (Woolrich et al., 2001). This cross-correlates the time-series of SLFs in the BOLD signal in the thalamus with all other brain areas and searches for voxels which are showing similar time-series. The FSL recommended default setting for statistical analysis were used with functional connectivity thresholded at z statistic > 2.3 and p value < 0.05 (Worsley, 2001) (see Chapter 5 and Appendix A for more detail).

Covariates of No Interest

Another approach which has been used in model-based analysis studies is to include covariates of no interest (or nuisance covariates) (Weissenbacher et al., 2009; Margulies et al., 2007; Fox et al., 2005). This involves including time-series information from seeds and masks in specific regions which would not be expected to correlate with the seed under investigation, and are assumed to contain information on global physiological and/or scanner-related effects. These can be included in the first-level general linear modelling analysis for the seed region under investigation, and regressed out of the time-series of interest. Including covariates of no interest has been shown to

improve the accuracy of functional connectivity results, and enables the investigation of SLFs localised to grey matter only (Weissenbacher et al., 2009; Margulies et al., 2007; Fox et al., 2005) (see Figure 6.2) (Fox et al., 2009). Examples of covariates of no interest that previous studies have used are:

- **Global Brain Mask**

Including a global brain mask as a covariate of no interest has been carried out by a number of the studies in Table 6.1 (Weissenbacher et al., 2009; Margulies et al., 2007; Fox et al., 2005). This involves creating a seed or mask of the global signal, i.e. using a binary mask showing activity in all brain voxels. Studies by Greicius *et al.* (2003) and Murphy *et al.* (2009) did not include the global signal as a covariate of no interest. The study by Murphy *et al.* (2009) strongly recommended against including this in the analysis as they believe it introduced anti-correlations in the data which are not present before global signal was removed (Murphy et al., 2009). Alternatively, Greicius *et al.* (2003) performed intensity normalisation whereby each voxel in every volume is divided by the mean value of this volume and multiplied by the intensity of the first volume. This gives a constant mean volume intensity over time (Greicius et al., 2003). The study by Weissenbacher *et al.* (2009) showed that global signal regression (i.e. using the global signal as a covariate of no interest) outperformed intensity normalisation in terms of significance and specificity of results (Weissenbacher et al., 2009).

- **Seeds Placed in the White Matter and Cerebrospinal Fluid**

Linear regression for white matter and cerebrospinal/ventricular signal has been shown to correct for fluctuations in non-grey matter regions (Weissenbacher et al., 2009; Margulies et al., 2007; Fox et al., 2005). This involved using FSLView to place seeds in the white matter (cerebellum) and cerebrospinal fluid (lateral ventricles) on the first volume of subjects' resting-state fMRI scans. The time-series from the white matter and cerebrospinal fluid seeds were then extracted (as described above for the thalamus seed), included in the general linear modelling analysis and regressed out of the time-series of interest.

- **Motion Parameters**

This was carried out by some of the previous studies (Weissenbacher et al., 2009; Margulies et al., 2007; Fox et al., 2005). Movement regressors from head motion correction were included in the general linear modelling analysis and regressed out of the time-series of interest.

6.4 Results

Figures 6.4 and 6.5 show the results from the functional connectivity analysis using the methods outlined in Table 6.1 and the left thalamus as the seed region. Figures 6.4 (a), (b) and (c) are the subjects who had shown global synchronicity and Figures 6.5 (d), (e) and (f) are subjects who had shown non-global/non-noisy connectivity using the method from the previous study (Chapter 5).

The connectivity maps for the Fox *et al.* (2005) method for subjects (a), (b) and (c) (Figure 6.4) showed a considerable difference compared to the maps from the Kenny *et al.* (2010) method (Kenny *et al.*, 2010; Fox *et al.*, 2005). Connectivity was greatly reduced using the Fox *et al.* (2005) method and localised to more specific brain regions. In the subjects who had not previously shown global synchronicity, Figure 6.5 (d), (e) and (f), following analysis with the Fox *et al.* (2005) method, the maps look similar to the maps following the Kenny *et al.* (2010) method. The Fox *et al.* (2005) method appears to have removed some of the smaller clusters, slightly decreased the z statistic and removed connectivity from the edges of the brain. This is an interesting finding as it has been shown that cardiac pulsations are often localised in the edges of the brain (Glover *et al.*, 2000). Therefore, it appears from the connectivity maps that the Fox *et al.* (2005) method is correcting the global signal pattern (Figure 6.4 (a), (b) and (c)) and in the subjects showing a non-global pattern (Figure 6.5 (d), (e) and (f)) it is not dramatically changing their connectivity maps, but is also removing non-neuronal signal (Fox *et al.*, 2005).

The connectivity maps for the Murphy *et al.* (2009) method for subjects (a), (b) and (c) (Figure 6.4) show that the method has removed some of the global synchronicity, though the z statistic has been increased and the signal at the edges of the images is still high. In subjects (d), (e) and (f) (Figure 6.5), correlations with the seed region are shown to have increased, and this method seems to be introducing correlations into the data in the subjects who previously did not show global synchronicity. It was not possible to follow all the steps in the Murphy *et al.* (2009) method, as to run the retrospective correction of physiological motion effects (RETROICOR) (Glover *et al.*, 2000) requires respiratory and cardiac data to have been collected at the time of scanning, and then subsequently regressed out. As RETROICOR could not be carried out on the data, this may in part explain why the Murphy *et al.* (2009) method did not entirely remove global synchronicity in this data.

The results for the global synchronicity subjects using the Weissenbacher *et al.* (2009) method look similar to the Fox *et al.* (2005) results. In subjects (b) and (c)

(Figure 6.4), more connectivity is evident at the brain edges following the Weissenbacher *et al.* (2009) method than the Fox *et al.* (2005) method, therefore the Weissenbacher *et al.* (2009) method does not appear to be correcting as accurately for potential cardiac related fluctuations. The non-global synchronicity maps for subjects (e) and (f) (Figure 6.5) look similar to the Kenny *et al.* (2010) method, which is what would be expected as these subjects were viewed to have non-noisy maps. In subject (d) some correlations seem to have been introduced following the Weissenbacher *et al.* (2009) method (Weissenbacher *et al.*, 2009).

The functional connectivity results for subjects (b) and (c) (Figure 6.4) following the Greicius *et al.* (2003) method are similar to the Fox *et al.* (2005) and Weissenbacher *et al.* (2009) methods, but the z statistic for correlations in subject (a) (Figure 6.4) have increased greatly and the areas showing connectivity are very different, with a loss of connectivity with the thalamus. For subjects (e) and (f) correlations are decreased, but for subject (d) they were increased compared to the Kenny *et al.* (2010) results (Figure 6.5).

The results using the Margulies *et al.* (2007) method are similar to the Fox *et al.* (2005) method showing that the method filtered the global synchronicity in subjects (a), (b) and (c) (Figure 6.4) and did not change the connectivity maps for the subjects showing non-global synchronicity, (d), (e) and (f) (Figure 6.5). Both the Margulies *et al.* (2007) and Fox *et al.* (2005) methods involved similar steps using covariates of no interest in the linear regression analysis.

In summary, if looking at the subjects who previously showed a relatively non-noisy pattern of functional connectivity (Figure 6.5), the Fox *et al.* (2005) and Margulies *et al.* (2007) methods changed the connectivity the least, only removing connectivity from the edges of the brain and not introducing or increasing correlations (Margulies *et al.*, 2007; Fox *et al.*, 2005). The Fox *et al.* (2005) and Margulies *et al.* (2007) methods were also shown to be the most accurate methods to remove global synchronicity and limit the connectivity seen to grey matter regions only in the subjects originally showing a noisy pattern of connectivity (Figure 6.4). Additionally, the Fox *et al.* (2005) method has been widely used by many studies investigating resting-state functional connectivity and has also been previously used by studies investigating resting-state in older subjects (Hedden *et al.*, 2009) and in Alzheimer's disease (Wang *et al.*, 2007). Therefore, it was decided that the Fox *et al.* (2005) method would be used for the analysis of functional connectivity on the dementia study data.

Figure 6.4: Functional Connectivity Maps of 3 Different Subjects (a-c) with Global Synchronicity following Analysis with Methods Summarised in Table 6.1

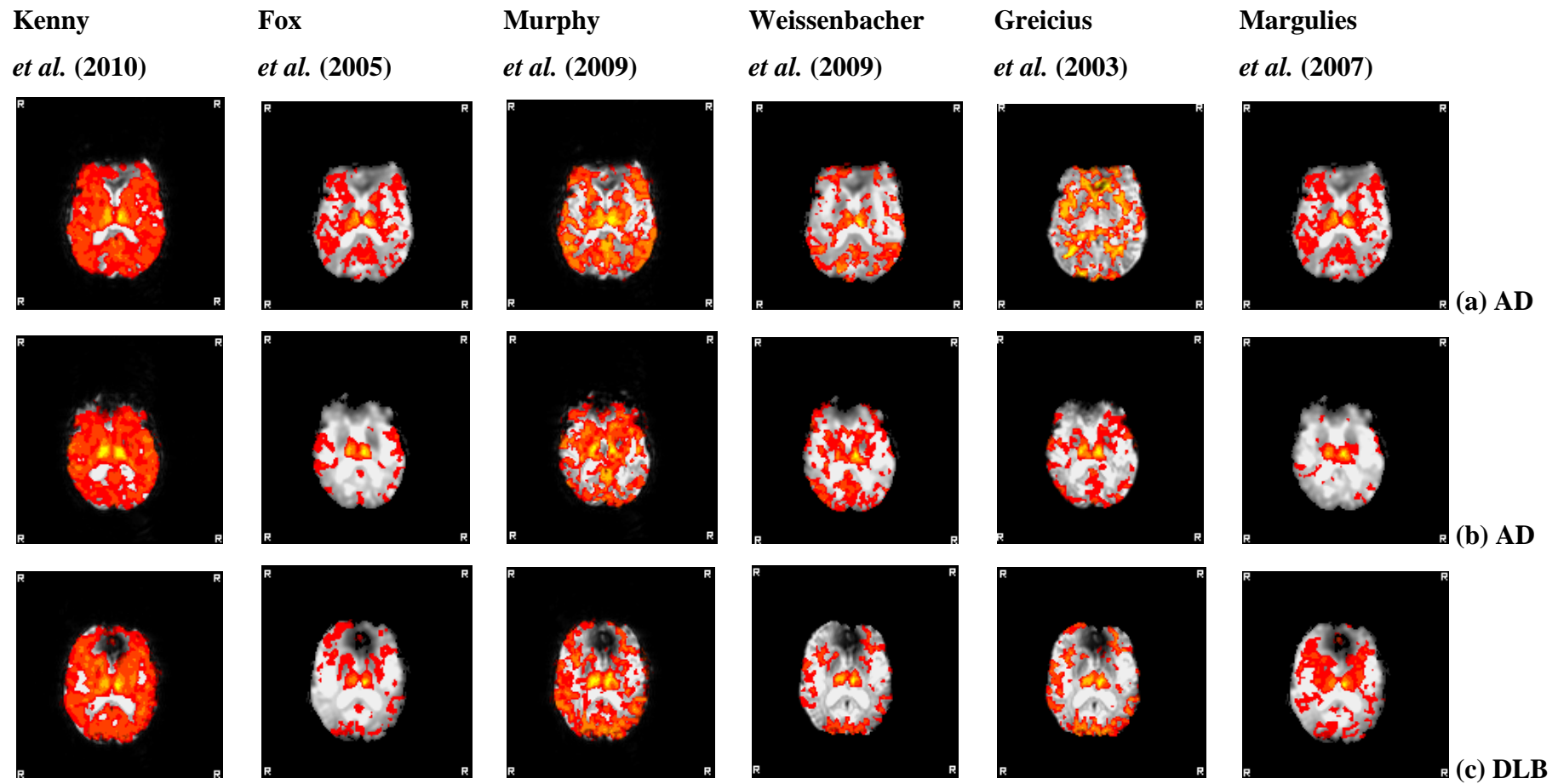
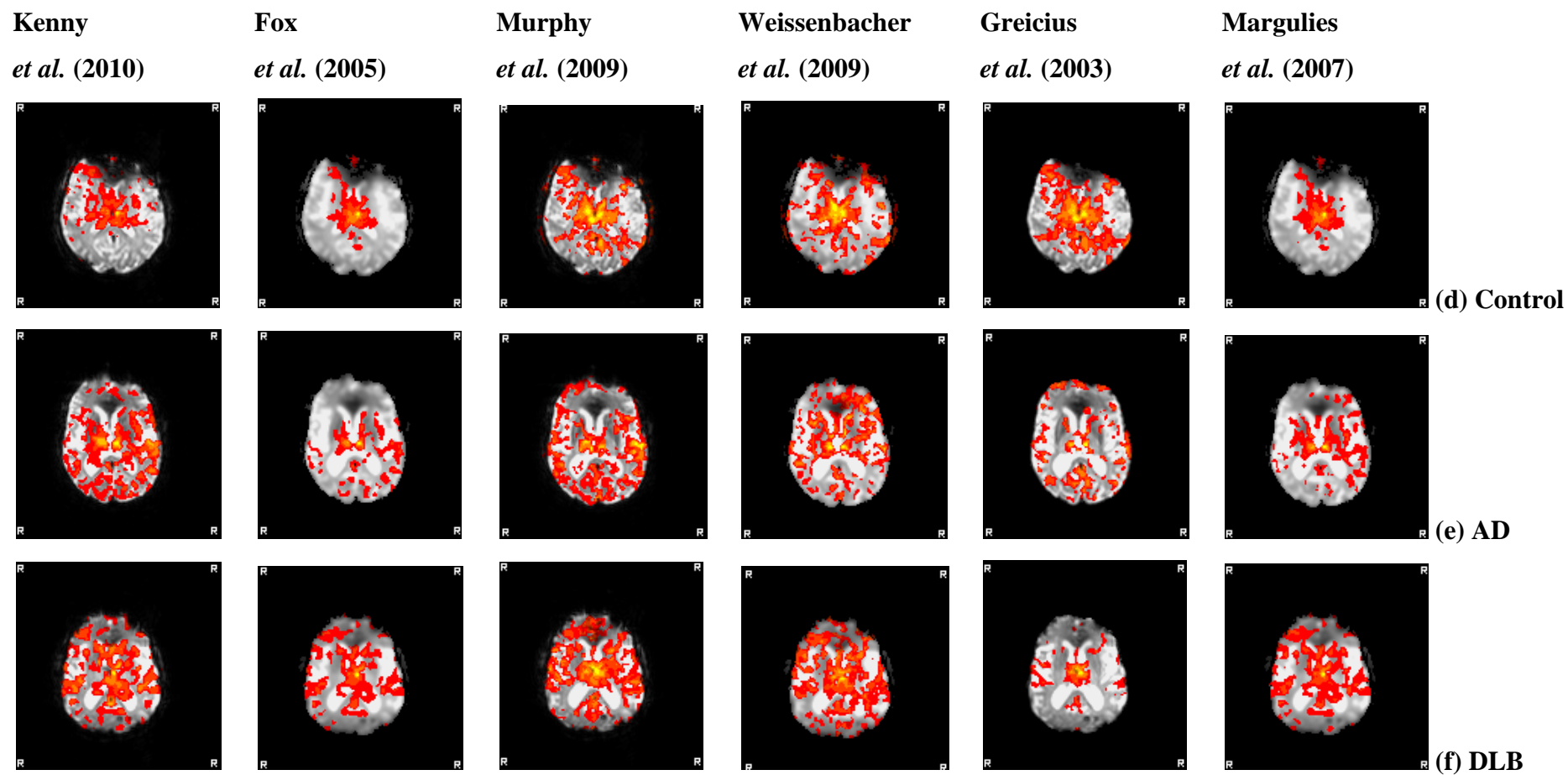


Figure 6.5: Functional Connectivity Maps of 3 Different Subjects (d-f) who did not show Global Synchronicity following Analysis with Methods Summarised in Table 6.1



6.5 Discussion

In summary, when the method used in the LLD study (Chapter 5) was applied to the resting-state BOLD data from dementia subjects a pattern of global synchronicity was observed in some control, AD and DLB subjects across the seed regions investigated (Figure 6.1). This global synchronicity had not been previously observed in the LLD study (Chapter 5). Initially, it was thought that it could be due to the different seed regions investigated, however global synchronicity was also observed with the head of caudate nucleus (the same seed that was used in the LLD study). It was also investigated whether it could be due to the seed regions being placed inaccurately, i.e. in the cerebrospinal fluid. The seed regions were re-checked and placing was viewed accurate, and if the seeds were in the cerebrospinal fluid, synchronicity in the cerebrospinal fluid would be expected and not in grey and white matter regions (see Figure 6.2).

Another possibility was that this could be related to the patient groups, as the subjects in this study had dementia therefore this synchronicity could be related to the disorder. However, global synchronicity was also shown in the control subjects in this study. Related to this, it could be an age related effect, but then the same result would have been expected in the LLD study, and other studies also report global synchronicity in younger control subjects (Fox *et al.*, 2005). Global synchronicity may not have been seen in the LLD study because there were fewer subjects investigated and/or because the analysis methods in the FEAT tool for motion correction, spatial smoothing and temporal filtering were accurate enough in this cohort to remove spurious fluctuations. In support of this, when the Fox *et al.* (2005) method was applied to non-noisy data (Figures 6.5d, e, and f), the method had almost no effect on the functional connectivity maps.

The results from the investigation and comparison of methodologies to correct for spurious fluctuations showed that the best method for the dementia study data was the Fox *et al.* (2005) method. This method involved regression for the global signal. It has been shown that signal changes caused by variations in respiration (rate and depth) and heart rate occur throughout the brain, i.e. in grey matter regions and blood vessels (Chang and Glover, 2009; Birn *et al.*, 2006). Therefore it is expected that these signals would be major contributors to the global signal, but resting-state signals may also contribute to the global signal, meaning regression can also remove neuronally related connectivity and possibly result in under estimation of connectivity.

Some of the other methods investigated did not involve regression of the global signal using covariates of no interest (Murphy et al., 2009; Greicius et al., 2003) and although these methods were found to remove part of the global signal, in this data it seemed that some spurious fluctuations still remained. These methods were also shown to introduce correlations in the non-noisy data (Murphy et al., 2009; Greicius et al., 2003).

Preventing respiratory or cardiac changes from influencing the data in the first place would be ideal, but this involves monitoring breathing and heart rate at the time of scanning and regressing from the signal of interest, which cannot be estimated retrospectively. Recent studies have reported respiratory and cardiac-related haemodynamic response functions/models which can be used to regress out the signal from respiratory and cardiac related noise and these should be considered essential for future investigations (Chang and Glover, 2009; Birn et al., 2008).

6.6 Conclusion

In conclusion, various methods to correct for spurious fluctuations in resting-state fMRI data were investigated. The findings here concluded on a method which corrected for noise caused by physiological signals, scanner related artefacts and head motion, for example. Chapter 7 of this thesis applies the methodology selected here on the dementia data.

Chapter 7

Investigation of Functional Connectivity in Alzheimer's Disease and Dementia with Lewy Bodies

7.1 Rationale for this Study

As discussed in Chapter 1, Alzheimer's disease (AD) and dementia with Lewy Bodies (DLB) are the 2 most common causes of degenerative dementia in older people. AD and DLB have distinct clinical profiles and a different clinical course, but, compared to AD, neurobiological changes in DLB have not been studied in great detail. Chapter 4 of this thesis discusses findings from imaging studies showing brain changes that occur in AD and DLB. However, the neural substrates which underpin the core features of fluctuating cognition and visual hallucinations in DLB are still relatively unknown.

Using resting-state functional magnetic resonance imaging (fMRI), this study investigated functional connectivity in AD and DLB by measurement of the time-series of spontaneous low-frequency fluctuations (SLFs) in the blood oxygenation level dependent (BOLD) signal in seed regions of the brain, the rationale for which has been described in Chapter 2. Resting-state fMRI methods do not require patient compliance in task performance and scanning time is short, therefore they are ideal for application in cognitively impaired subjects, for example AD and DLB subjects. A small number of studies have applied these methods in AD, but studies have generally focussed on using seeds in the posterior cingulate cortex or the hippocampus only (Zhang et al., 2009; Wang et al., 2006; Li et al., 2002). Results from such connectivity studies to date are conflicting, with some reporting decreases in functional connectivity in AD (Gili et al., 2010; Allen et al., 2007; Greicius et al., 2004), whereas others report both increases and decreases in AD compared to controls (Zhang et al., 2009; Wang et al., 2007; Wang et al., 2006). No studies to date have investigated resting-state functional connectivity in DLB.

7.2 Aims

Functional connectivity in AD and DLB was investigated using a seed-based correlation analysis approach. This hypothesis driven approach used seeds placed in brain regions which have been reported, or are hypothesised, to be abnormal in DLB and/or AD. The main aims were to investigate differences between DLB and AD and to determine how these might relate to the neurobiological differences between the disorders. It was hoped that this would inform better understanding of the mechanisms of symptom formation in these disorders and lead to improved methods for diagnosis and aid in directing therapeutic strategies.

7.3 Hypotheses

7.3.1 Seed Regions

The following patterns of functional connectivity were expected with the seed regions investigated:

- i. Head of Caudate Nucleus:
 - Abnormal connectivity in DLB versus Control and AD subjects

It was hypothesised that DLB patients would show abnormal connectivity with the head of caudate nucleus compared to AD and control subjects. It was not certain whether abnormal connectivity would be demonstrated as increased or decreased connectivity in DLB subjects, as functional connectivity studies have reported both results in patient groups. However, it was predicted that connectivity would be most likely demonstrated as decreased in DLB subjects compared to AD and control subjects. This hypothesis was based on findings from structural (e.g. diffusion tensor imaging) and functional (e.g. SPECT) studies investigating the caudate in DLB subjects. Diffusion tensor imaging, which enables the investigation of white matter connections, has shown tissue abnormalities in the caudate nucleus in DLB compared to control subjects (Bozzali et al., 2005). SPECT studies have shown significantly reduced ligand binding, indicating dopamine transporter loss, in the caudate nucleus in DLB compared to AD and controls (O'Brien et al., 2004a). In contrast, others have reported no significant differences in structural measures such as caudate volume between DLB, AD and control subjects (Almeida et al., 2003b).

ii. Putamen:

- Abnormal connectivity in DLB versus Control and AD subjects

DLB patients were hypothesised to show abnormal functional connectivity with the putamen compared to AD and controls, most likely decreased connectivity. This hypothesis was based on the motor features of parkinsonism associated with DLB. SPECT studies show significantly greater dopaminergic degeneration in the putamen, as demonstrated by decreased ligand binding to the dopamine transporter, in DLB and Parkinson's disease compared to AD and control subjects (O'Brien et al., 2004a; Walker et al., 2002). Structural MRI studies also show abnormalities in the putamen in DLB, with significantly greater atrophy in DLB compared to AD (Cousins et al., 2003).

iii. Thalamus (Mediodorsal nucleus):

- Abnormal connectivity in DLB versus Control and AD subjects

Similar to the hypotheses for the head of caudate nucleus and the putamen, functional connectivity with the thalamus was hypothesised to be more abnormal in DLB subjects compared to AD and controls. It was hypothesised that this connectivity abnormality in DLB subjects would be characterised by decreased connectivity. The thalamus has been implicated as playing a major role in the maintenance of consciousness (Perry and Perry, 2004) and post-mortem studies of brain tissue have shown higher nicotinic receptor binding in the mediodorsal nucleus in DLB subjects with disturbances of consciousness/cognitive fluctuation than DLB without and control subjects (Pimlott et al., 2006).

iv. Hippocampus:

- Abnormal connectivity in AD versus Control and DLB subjects

A very consistent finding from structural imaging studies is greater atrophy of the hippocampus in AD compared to DLB, which is thought to be responsible for the relative preservation of memory in DLB compared to AD (Ballmaier et al., 2004; Burton et al., 2002; Barber et al., 2000). Some studies have reported reduced functional connectivity in the hippocampus in AD subjects (Allen et al., 2007; Greicius et al., 2004; Zang et al., 2004; Li et al., 2002), whereas others have reported that this is the case for the right hippocampus, but for the left hippocampus functional connectivity is actually increased (Wang et al., 2006). Based on these findings it was hypothesised that AD patients would show abnormal functional connectivity with the hippocampus compared to DLB and control subjects, and for there to be no significant difference in hippocampus functional connectivity between DLB and control subjects.

v. Posterior Cingulate Cortex:

- Abnormal connectivity in DLB and AD versus Control subjects

Studies in AD have generally reported decreased functional connectivity in the posterior cingulate in AD (Zhang et al., 2009; He et al., 2007; Greicius et al., 2004; Zang et al., 2004), though increased functional connectivity between the posterior cingulate and several brain regions has also been reported (Zhang et al., 2009). The posterior cingulate forms part of the default mode network which is involved in attending to environmental stimuli (Raichle et al., 2001). DLB is characterised by greater attentional deficits than AD (Ballard et al., 2001), therefore it was expected that functional connectivity with the posterior cingulate would also be affected in DLB and possibly to a greater extent than in AD.

vi. Precuneus:

- Abnormal connectivity in DLB and AD versus Control subjects

The precuneus also forms part of the default mode network (Raichle et al., 2001) and previous studies in AD have reported reduced functional connectivity in this region (Zhang et al., 2009; He et al., 2007; Zang et al., 2004). SPECT studies in DLB report decreased perfusion compared to AD (Colloby et al., 2002), and it was expected this would be reflected in the functional connectivity with this region. It was hypothesised that functional connectivity would be decreased in AD and DLB compared to control subjects, and additionally more affected in DLB compared to AD.

vii. Primary Visual Cortex (V1):

- Abnormal connectivity in DLB versus Control and AD subjects

For the seed placed in the primary visual cortex, it was hypothesised that DLB subjects would show abnormal connectivity compared to AD and control subjects. The primary visual cortex was expected to be functioning normally in AD subjects, as vision is not affected in this disorder. In DLB, resting-state SPECT studies have reported decreased perfusion in DLB compared to AD in the primary visual cortex (Colloby et al., 2002), and these abnormalities are thought to be associated with the core feature of visual hallucinations in DLB (McKeith et al., 1996). Therefore it was hypothesised that this would affect the functional connectivity with this region in DLB subjects, and most likely cause a decrease in connectivity in these subjects.

7.3.2 Neuropsychiatric Measures

Although group sizes were modest, it was examined in an exploratory post hoc way the relationship between functional connectivity and severity of cognitive impairments and neuropsychiatric features. It was expected that patients who had a higher burden of cognitive and non-cognitive symptoms would show more abnormalities in functional connectivity to those who had less severe dementia.

7.4 Methods

7.4.1 Subjects and Assessment

The study involved 47 subjects all aged over 60 years: 16 Control, 16 AD and 15 DLB subjects. AD and DLB patients were recruited from clinical Old Age Psychiatry, Geriatric Medicine and Neurology outpatient services and controls were recruited by local advertisement. The study was approved by the local ethics committee, and all subjects gave signed informed consent for participation. AD patients fulfilled National Institute of Neurological and Communicative Diseases and Stroke, and the Alzheimer's Disease and Related Disorders Association (NINCDS/ADRDA) criteria for probable AD (McKhann et al., 1984) and DLB patients met DLB consensus criteria for probable DLB, including the presence of 2 or more core features (fluctuating cognition, visual hallucinations and/or parkinsonism) (McKeith et al., 2005; McKeith et al., 1996). Diagnoses were made by consensus between two experienced clinicians, a method which has previously been validated against autopsy diagnosis (McKeith et al., 2000b). Detailed physical, neurological and neuropsychiatric examinations were carried out. Cognitive and neuropsychiatric examinations involved:

- Mini-mental state examination (MMSE) as a measure of global cognitive impairment and to assess dementia severity. This very widely used test assesses orientation, registration, short-term memory and language function. The maximum score is 30, a score of ≥ 24 is conventionally taken as the cut-off indicating normal cognition, ≥ 21 signifies mild dementia, ≥ 10 moderate, and < 10 severe (Folstein et al., 1975).
- Cambridge cognitive (CAMCOG) examination was carried out to assess cognitive status. CAMCOG is made up of 8 subscales to assess orientation, language, memory, praxis, attention, abstract thinking, perception and

calculation. The CAMCOG total score can range from 0 to 105, with a score of < 80 considered indicative of dementia (Roth et al., 1986).

- The 15 item geriatric depression score (GDS) was developed as a screening tool for the measurement of depressive symptoms in elderly populations and derived from the original 30 item scale. It is a self-completed assessment, with a maximum possible score of 15 (Sheikh and Yesavage, 1986). A score of ≥ 5 is normally used as a cut-off for depression (D'Ath et al., 1994).
- Neuropsychiatric inventory (NPI) assesses 12 neuropsychiatric domains common in dementia, including delusions, hallucinations, agitation and depression, based on the frequency and severity of each symptom over the last month, according to the carer report (Cummings et al., 1994).
- Fluctuating cognition was assessed using the clinical assessment of fluctuation scale (CAFS), which is judged present if a clear-cut example can be given. Frequency and duration of episodes are rated and the two scores multiplied to give severity. A score of 0 signifies no fluctuating cognition and 12 shows severe fluctuating cognition (Walker et al., 2000).
- The motor subsection of the unified Parkinson's disease rating scale (UPDRS III) was carried out to assess severity of motor features of parkinsonism (e.g. speech, facial expression and tremor at rest) (Fahn et al., 1987).

Exclusion criteria for the study were; severe concurrent illness (apart from dementia in the AD and DLB groups), the presence of space occupying lesions on MRI, stroke history and any contraindications to MRI. Control subjects had no history of psychiatric illnesses.

7.4.2 Imaging

Subjects were scanned using a 3 Tesla MRI system at the Newcastle Magnetic Resonance Centre, Newcastle University. Resting-state fMRI scans were acquired whilst subjects lay still in the scanner. The same imaging parameters used in the LLD study were also used in this study (see Chapter 5 for details).

7.4.3 *Placing of the Seed Regions*

The FMRIB Software Library (FSL) tools, www.fmrib.ox.ac.uk/fsl (version 4.0.4) were used for analysis (FMRIB Analysis Group, 2007). Firstly, all non-brain structures were removed using the brain extraction tool (BET) (Smith, 2002). Seed regions were then placed manually using the FSLView tool. For reference and help with seed placing a standard brain atlas (DeArmond et al., 1989) and the FSL brain atlas tool (which overlays specified brain regions on a standard brain template) were used. Seeds were placed on the first volume of the resting-state functional scans (in the axial view) by a sole investigator who was blinded to subject diagnosis. Seeds were placed in both the left and right hemispheres and the radiological orientation was noted, i.e. left hemisphere of the brain is the right side of the computer screen. The guidelines used for seed placing are summarised below and the seeds overlayed on the functional images are shown in Figure 7.1.

The size of the seeds placed was selected based on the structure under study to ensure the seed could confidently be placed within the structure boundaries. The thalamus is approximately 3 cm (or 15 voxels) in length and the mediodorsal nucleus is approximately 1.2 cm (6 voxels) in length, therefore a seed of 2 by 2 voxels (4x4 mm) should easily fit inside the structure. Although the ventral anterior nucleus of the thalamus was also of potential interest, because of the higher nicotinic receptor binding reported here in DLB subjects with disturbances of consciousness than DLB subjects without (Pimlott et al., 2006), it was considered to be too small a structure for accurate placing, as the nucleus is only 0.5 cm (2.5 voxels). In addition, due to this structures close proximity to the ventricles it may be affected by dementia-related ventricular atrophy. All seeds were considered to be placed accurately and no subjects were excluded due to difficulty in seed region placing. In order to view all brain volumes and check for subject motion in the image time-series, the movie mode function was used. No subjects were found to have moved excessively during the scanning procedure.

Guidelines used for Seed Placing:

i. Head of Caudate Nucleus

A seed of 2x2 voxels was placed in the mid-region on the most inferior slice where the caudate and putamen are separated by the internal capsule. The anterior commissure was located, and as this structure disappears the head of caudate becomes the body of caudate. These are the same guidelines that were used for seed placing in the LLD study (Chapter 5) (see Figure 7.1.i).

ii. Putamen

A seed of 2x2 voxels was placed on the slice inferior to where the caudate and putamen are separated by the internal capsule. Ventricle III and the insula were used as guidelines to identify the inner and outer borders. The seed was placed in the upper putamen as this is the widest part of the structure, therefore it was thought that placement here would be most accurate (see Figure 7.1.ii).

iii. Thalamus (mediodorsal nucleus)

A seed of 2x2 voxels was placed on the slice where ventricle III and the internal capsule separate the head of caudate nucleus and the putamen, in line with the base of the putamen (the widest part of the thalamus) (see Figure 7.1.iii).

iv. Hippocampus

The mammillary body and cerebral peduncle were located, and the hippocampus is adjacent to these structures, a seed of 2x2 voxels was placed (see Figure 7.1.iv).

v. Posterior Cingulate Cortex

A seed of 2x2 voxels was placed on the same slice as where the head of caudate, putamen and ventricle III are present, and where the posterior cingulate is separated by the cerebellum (see Figure 7.1.v).

vi. Precuneus

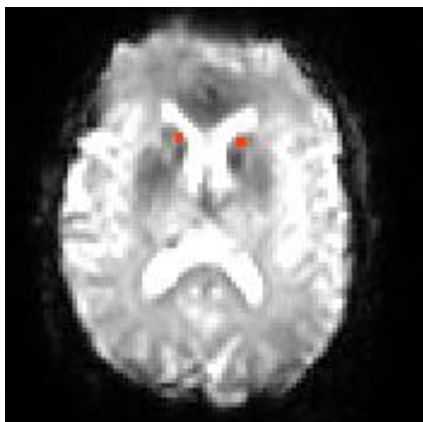
A seed of 4x4 voxels was placed on the first slice after the ventricles have disappeared, as the precuneus is easily identifiable here and comprises a large area. The seed was placed in the lower precuneus, towards the centre (see Figure 7.1.vi).

vii. Primary Visual Cortex

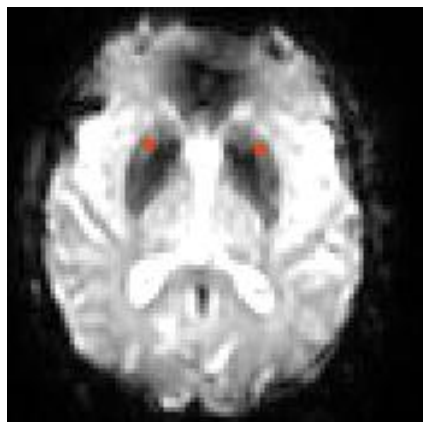
A seed of 4x4 voxels was placed in the lower area of the primary visual cortex on the same slice where the head of caudate nucleus and the putamen are present (see Figure 7.1.vii).

Figure 7.1: Seed Regions Investigated and Overlaid on the Functional Images

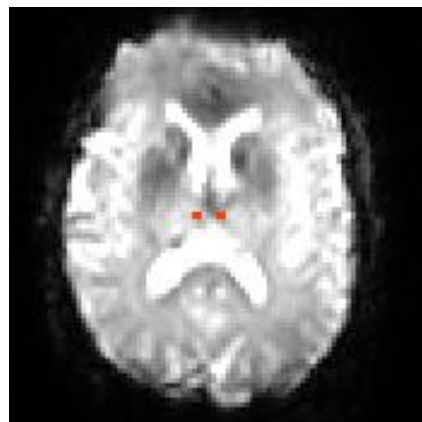
i) Head of Caudate Nucleus



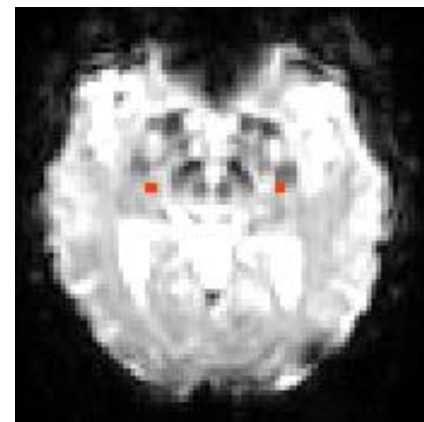
ii) Putamen



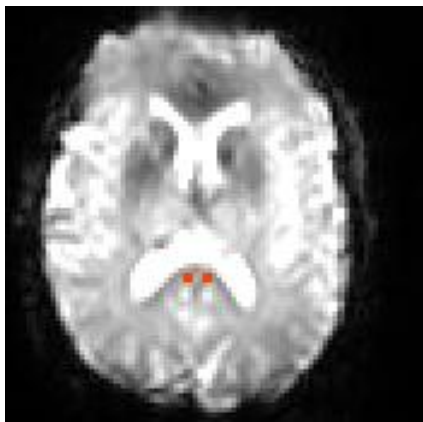
iii) Thalamus



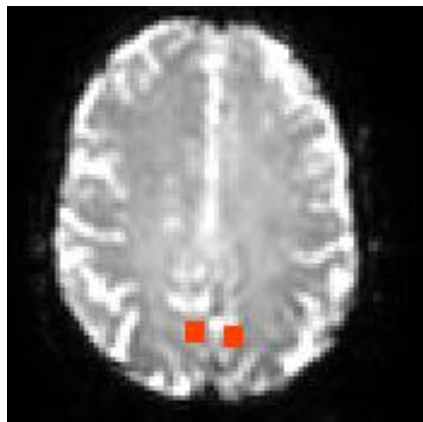
iv) Hippocampus



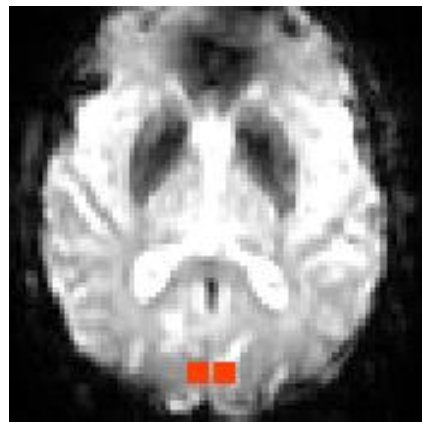
v) Posterior Cingulate Cortex



vi) Precuneus



vii) Primary Visual Cortex



7.4.4 Functional Connectivity Analysis

The FSL tool, FMRI Expert Analysis Tool (FEAT) was used to carry out the following data analysis:

- Data pre-processing (i.e. filtering and smoothing)
- First-level general linear modelling time-series analysis; FMRIB's Improved Linear Model (FILM) (Woolrich et al., 2001)
- Higher-level/group analysis; FMRIB's Local Analysis of Mixed Effects (FLAME) (Beckmann et al., 2003).

The method used by Fox *et al.* (2005) was followed for analysis. This method involves additional pre-processing steps to remove spurious fluctuations from the data which are known to over-estimate functional connectivity (Fox et al., 2005), see Chapter 6 for more detail on why this method was selected. The steps for pre-processing and model-based analysis of the data were as follows:

A) Pre-processing Steps:

- i. Motion Correction: The resting-state fMRI data were corrected for head motion using Motion Correction FMRIB's Linear Image Registration Tool (MCFLIRT). The tool attempts to remove the effects of subject head motion which can occur during the scan procedure. Through time, each voxel in the brain should be located at a consistent anatomical point, MCFLIRT realigns to a common reference using FLIRT, an automated tool for brain image registration (Jenkinson et al., 2002).
- ii. Spatial Smoothing: Data were spatially smoothed using a 6 mm full width at half maximum (FWHM) Gaussian kernel. Spatial smoothing averages a voxel with surrounding voxels, so that each voxel's intensity is replaced by a weighted average of surrounding intensities (Smith et al., 2004b).

The Fox *et al.* (2005) method requires a specific setting of the low pass and high pass filters and additional registration steps, which cannot be run through the FEAT graphical user interface; therefore the analysis was performed through a command line script written by AMB and MJF.

- iii. Temporal Band-pass Filtering: The fMRI data were temporally band-pass filtered at 0.009 and 0.08 Hz using the 'fslmaths' (a tool which enables mathematical manipulation of images) command. High-pass filtering enables the removal of low-frequency drift and low-pass filtering removes high frequency noise and physiological fluctuations (Smith et al., 2004b).

- iv. Registration: A study specific functional brain template was created as the subjects in this study are elderly, therefore they would be expected to have more brain atrophy than a general standard space template, which is based on younger subjects. To create the study specific brain template, one subject was registered to the standard space echo planar imaging template from Statistical Parametric Mapping (SPM) (Wellcome Trust Centre for Neuroimaging, 2005), all other study subjects were registered to this subject (using FLIRT) (Jenkinson and Smith, 2001) and then averaged using fslmaths (a tool which enables mathematical manipulation of images). The seeds which had been placed in patient space were transformed to standard space for analysis.

B) First-level/Subject FEAT Analysis:

- v. First-level analysis was carried out which is a model-based fMRI analysis tool. The data modelling that FEAT uses is based on general linear modelling, or multiple regression. FEAT allows you to provide a model of the predicted BOLD response and finds voxels in the brain that match this response, with a good match showing positive correlation with the seed (Woolrich et al., 2001). The mean BOLD signal time-series was extracted from each seed region and used as the model response function, enabling cross-correlation of SLFs in the seed with signal variations in all other brain regions to determine functional connectivity.

Covariates of no interest, i.e. spurious fluctuations, were removed from the data using a linear regression approach. This involved extracting the time-series from:

- a. Seeds placed in the white matter (left and right cerebellum)
- b. A seed in the cerebrospinal fluid
- c. A whole brain mask to remove the global signal

The z statistic threshold was set at > 2.3 and the p threshold at < 0.05 .

C) Higher-level/Group FEAT Analysis:

- vi. A three group comparison (control, AD and DLB groups) was carried out to investigate whether there were significant differences in connectivity between groups for each of the seed regions, by comparing their data on a voxel by voxel basis (FMRIB's Local Analysis of Mixed Effects [FLAME]) (Woolrich et al., 2004; Beckmann et al., 2003). FEAT first-level analysis directories were selected, with left and right seeds run separately. Z (Gaussianised T/F) statistic images were thresholded using clusters of pixels determined by $z > 2.3$ and

$p < 0.05$ (corrected cluster significance threshold) (Worsley, 2001). Higher-level FEAT analysis was run through the graphical user interface.

vii. Scores on neuropsychiatric measures were investigated to see whether a poor score was associated with greater abnormalities in functional connectivity:

- Clinical Assessment of Fluctuation Scale (CAFS):

The effect of fluctuating cognition on functional connectivity with the mediodorsal nucleus of the thalamus was investigated in the DLB group. Previous studies have shown that the thalamus plays a key role in maintaining consciousness (Pimlott et al., 2006), it was therefore predicted that subjects with a poor score on the clinical assessment of fluctuation scale would show greater abnormalities in functional connectivity with the thalamus. The mean CAFS score of 6.7 was used as a cut-off and subjects grouped as either low (8 subjects with a score ≤ 6) or high fluctuators (7 subjects with a score ≥ 8).

- Unified Parkinson's Disease Rating Scale (UPDRS):

The DLB subjects were split according to a high and low score on the UPDRS and functional connectivity investigated with the putamen. DLB subjects were split based on the median UPDRS score; 7 subjects scored ≤ 16 and were classified in the low group (less severe parkinsonian symptoms) and 8 subjects scored ≥ 19 and were allocated to the high UPDRS score group. Higher-level FEAT analysis was then run to compare functional connectivity between the two groups based on their scores on the neuropsychiatric measures. The z statistic threshold was set at > 2.3 and the p threshold at < 0.05 .

viii. The peak connectivity cluster coordinates from the FEAT analysis are in Montreal Neurological Institute (MNI) space. Coordinates were converted to Talairach space (Talairach and Tournoux, 1988) using GingerALE (Lancaster et al., 2007) and entered into Talairach Client which assigns Talairach labels (hemisphere, lobe, gyrus, tissue and cell type) (Lancaster et al., 2000).

Appendix A outlines the above analysis steps in more detail.

7.5 Results

7.5.1 Demographics

Table 7.1 shows the clinical characteristics of the study subjects. Statistical analysis was performed using Statistical Package for Social Sciences (SPSS) (version 15.0.1) (SPSS for Windows, 2006). Groups were comparable for age ($p=0.294$, $df=2$, $F=1.26$) and sex ($p=0.466$, $\chi^2=0.532$, $df=1$). As expected, controls had significantly higher scores on cognitive tests (MMSE and CAMCOG) and lower scores on measures of motor features (UPDRS) and depression (GDS) compared to AD and DLB subjects. There were no significant difference between the AD and DLB groups in MMSE or total CAMCOG score, age at onset of dementia or duration of dementia, but (consistent with the known preservation of memory in DLB) DLB subjects had significantly higher scores than AD subjects on CAMCOG memory subscore ($p=0.022$). UPDRS scores were significantly higher in DLB subjects compared to AD ($p<0.001$), indicating greater severity of the motor features of parkinsonism in DLB. NPI scores were also significantly higher in DLB compared to AD subjects ($p=0.002$), indicating greater severity of neuropsychiatric disturbances in DLB. DLB subjects scored significantly higher than AD subjects on the CAFS ($p=0.01$), a measure of fluctuating cognition. Scores for the GDS were significantly higher in DLB subjects compared to AD subjects ($p<0.001$), which signifies greater severity of depressive symptoms in the DLB group. All of these differences were expected given the known symptom profile of DLB compared to AD.

At the time of study, 24 subjects were taking acetylcholinesterase inhibitors; 14 AD subjects (donepezil [9 subjects] and galantamine [5 subjects]) and 10 DLB subjects (donepezil [5 subjects], galantamine [4 subjects] and rivastigmine [1 subject]). Eight subjects (6 DLB) were taking antidepressants (citalopram, mirtazapine, trazodone, venlafaxine and paroxetine), and 1 DLB subject was taking a benzodiazepine (zopiclone) as a hypnotic.

Table 7.1: Demographic and Neuropsychological Data of Study Subjects

Demographic and Neuropsychological Data	Controls	AD	DLB	P Value
<i>n</i>	16	16	15	
Age (Yrs)	76.3±8.3	77.3±8.9	80.6±6.0	=0.294 ^b
Sex (M:F)	9:7	8:8	9:6	=0.466 ^a
Age at Onset of Dementia (Yrs)	n/a	73.9±8.9	77.2±6.7	=0.256 ^c
Duration of Dementia (Months)	n/a	40.4±24.8	40.2±20.3	=0.981 ^c
MMSE	28.6±1.3	21.1±3.5	19.5±4.2	<0.001 ^{b*}
CAMCOG Total	96.9±3.5	68.9±11.4	69.0±12.9	<0.001 ^{b*}
CAMCOG Memory	24.1±2.1	12.1±4.0	16.0±4.9	<0.001 ^{b*}
UPDRS	2.7±3.6	6.1±4.4	22.1±11.9	<0.001 ^{b*}
NPI	n/a	8.5±11.8	23.1±11.5	=0.002 ^{c*}
CAFS	n/a	1.6±3.4	6.7±5.3	=0.01 ^{c*}
GDS	1.3±1.4	3.4±2.4	7.1±3.3	<0.001 ^{b*}

Values expressed as mean ± standard deviation.

Abbreviations: CAMCOG = Cambridge cognitive examination; CAFS = Clinical assessment of fluctuation scale; GDS = Geriatric Depression Score; MMSE = Mini-Mental State Examination; NA = not applicable; NPI = Neuropsychiatric Inventory; UPDRS = Unified Parkinson's Disease Rating Scale (subsection III).

Table 7.1: Demographic and Neuropsychological Data of Study Subjects

^aThe *P* value was calculated using the Chi-Square Test

^bThe *P* values were calculated using the One-Way ANOVA

^cThe *P* values were calculated using the Independent-Samples T Test

*The *P* value is ≤ 0.05

- MMSE: Con > AD and DLB ($p < 0.001$, $df=2$, $F=36.61$)^b
- CAMCOG Total: Con > AD, DLB ($p < 0.001$, $df=2$, $F=40.46$)^b
- CAMCOG Memory: Con > AD, DLB ($p < 0.001$, $df=2$, $F=41.09$)^b; DLB > AD ($p=0.022$, $df=29$, $t=-2.42$)^c
- UPDRS: Con, AD < DLB ($p < 0.001$, $df=2$, $F=29.24$)^b (i.e. DLB subjects performed significantly worse)
Con < AD ($p=0.023$, $df=30$, $t=-2.40$)^c (i.e. AD subjects performed significantly worse)
- NPI: DLB vs AD ($p=0.002$, $df=27$, $t=-3.38$)^c (i.e. DLB subjects performed significantly worse)
- CAFS: DLB vs AD ($p=0.01$, $df=24$, $t=-2.8$)^c (i.e. DLB subjects performed significantly worse)
- GDS: Con vs AD ($p=0.006$, $df=30$, $t=-2.95$)^c
AD vs DLB ($p=0.001$, $df=29$, $t=-3.60$)^c
Con vs DLB ($p < 0.001$, $df=29$, $t=-6.39$)^c

7.5.2 *Group Functional Connectivity*

Seed Regions

i. Head of Caudate Nucleus

Group Means:

Across all groups, the head of caudate nucleus (bilateral) showed connectivity with the head and body of caudate nucleus and the cingulate (anterior/posterior). For the left head of caudate nucleus, the DLB group (Figure 7.2c) showed connectivity with the greatest number of brain regions. Control (Figure 7.2a) and AD (Figure 7.2b) subjects showed connectivity with a similar number and set of brain regions.

For the right head of caudate nucleus the DLB group (Figure 7.3c) showed significant connectivity with the fewest brain regions, and like the left seed the control (Figure 7.3a) and AD (Figure 7.3b) groups showed connectivity with a similar number of brain regions. The controls and AD patients both showed connectivity between the left head of caudate nucleus and sub-lobar and limbic areas and between the right head of caudate nucleus and frontal, sub-lobar and limbic areas, whereas in the DLB group the reverse was the case. Table 7.2 provides a summary of the peak brain regions showing connectivity with the left and right head of caudate nuclei seeds.

Group Differences:

The left head of caudate nucleus showed significantly greater connectivity in DLB subjects compared to controls in several brain regions; parahippocampal gyrus (left), posterior cingulate (right) and precuneus (bilateral) (see Figure 7.4a).

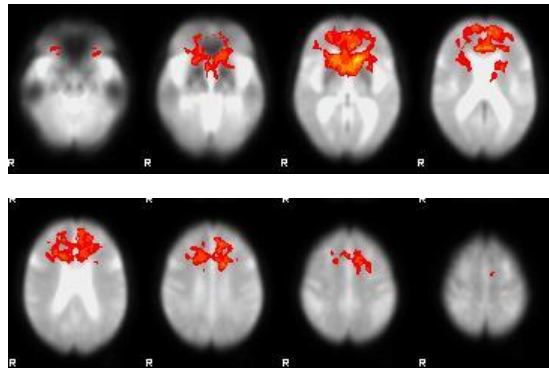
Whereas the right head of caudate nucleus showed greater connectivity in both dementia groups compared to controls. The AD group showed greater connectivity than controls with the posterior cingulate (bilateral) and precuneus/cuneus (bilateral) (Figure 7.4b). The DLB group showed greater connectivity than controls in similar regions; posterior cingulate (bilateral) and precuneus (left), and also the culmen (right) (Figure 7.4c). The control group did not show significantly greater connectivity than either dementia group.

Summary:

- Left Head of Caudate Nucleus: DLB > Controls
- Right Head of Caudate Nucleus: AD and DLB > Controls

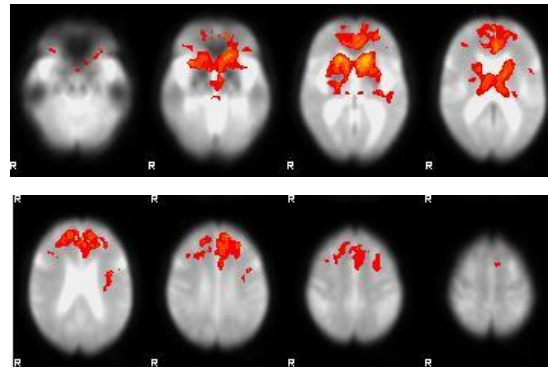
Figure 7.2: Functional Connectivity Maps for the Left Head of Caudate Nucleus

a) Controls Mean



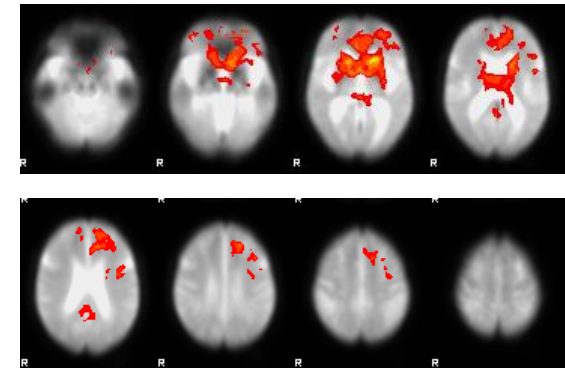
Brain Region	Coordinates	Z Stat
Caudate Body	-12, 15, 6	6.63
A. Cingulate	-1, 27, 18	5.45
Caudate Head	-8, 6, 5	5.42
A. Cingulate	10, 23, 23	5.39

b) AD Mean



Brain Region	Coordinates	Z Stat
Caudate Head	-14, 15, 5	6.5
Caudate Body	16, 17, 6	5.83
Caudate Body	-8, 0, 10	5.5
Thalamus	4, -2, 10	5.4
A. Cingulate	-5, 31, 13	5.25
Clastrum	31, 12, -5	5.19

c) DLB Mean

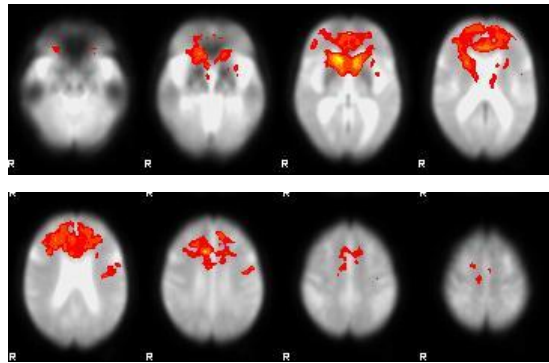


Brain Region	Coordinates	Z Stat
Putamen	-19, 15, 5	6.83
Caudate Body	-16, 13, 5	6.59
Caudate Body	14, 11, 6	6.11
G. Pallidus	-10, 1, -1	5.31
Caudate Head	1, 2, 4	4.88
Insula	-47, -1, 14	3.74
Inf. Frontal	-46, 16, 16	3.43
Precentral	-38, 14, 37	3.35
Mid. Frontal	-33, -10, 46	3.34
P. Cingulate	1, -55, 10	3.09

Abbreviations: A. Cingulate = Anterior Cingulate Cortex; G. Pallidus = Globus Pallidus; Inf. Frontal = Inferior Frontal Gyrus; Mid. Frontal = Middle Frontal Gyrus; P. Cingulate = Posterior Cingulate Cortex

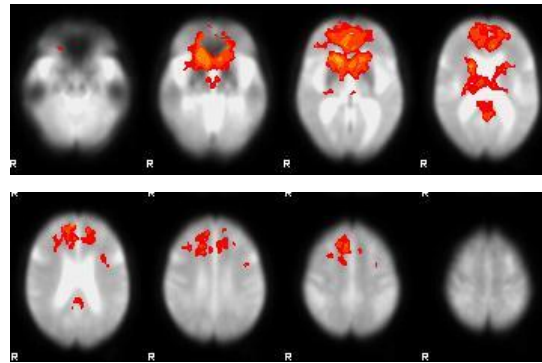
Figure 7.3: Functional Connectivity Maps for the Right Head of Caudate Nucleus

a) Controls Mean



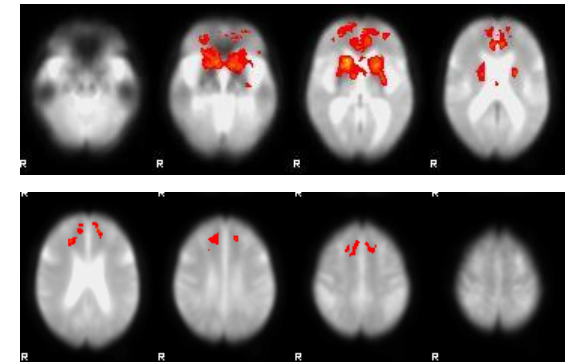
Brain Region	Coordinates	Z Stat
Caudate Body	10, 15, 6	7.14
Caudate Head	-10, 13, 5	5.94
Inf. Frontal	18, 24, -9	5.71
Cingulate	8, 12, 38	5.54
Putamen	21, 11, 11	5.43
A. Cingulate	10, 25, 23	5.10
Insula	-38, -12, 19	3.79
Precentral	-48, -6, 30	3.65

b) AD Mean



Brain Region	Coordinates	Z Stat
Caudate Head	8, 14, 0	6.11
Caudate Body	14, 15, 6	5.89
Medial Frontal	6, 46, 30	5.75
Caudate Head	-8, 14, 0	5.69
A. Cingulate	-5, 29, 12	5.25
P. Cingulate	1, -57, 10	3.4
P. Cingulate	-1, -45, 22	3.21

c) DLB Mean



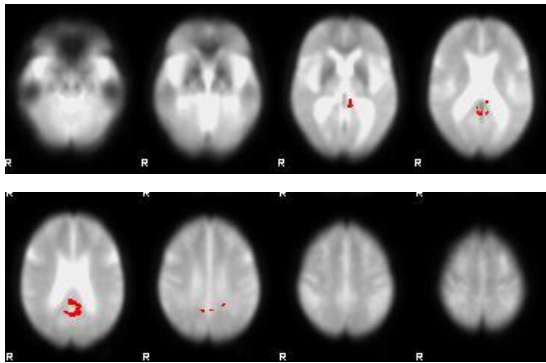
Brain Region	Coordinates	Z Stat
Caudate body	16, 13, 6	6.02
Caudate head	-14, 14, 0	5.05
Putamen	-25, 6, -1	5.00
A. Cingulate	-7, 33, 18	4.67

Abbreviations: A. Cingulate = Anterior Cingulate Cortex; Inf. Frontal = Inferior Frontal Gyrus; P. Cingulate = Posterior Cingulate Cortex

Figure 7.4: Functional Connectivity Maps Showing Group Differences for the Head of Caudate Nucleus

Left Caudate

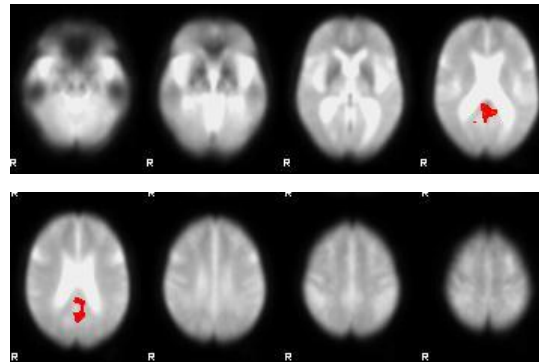
a) DLB > Con



Brain Region	Coordinates	Z Stat
PHG	-9, -40, 6	3.21
Precuneus	-11, -49, 26	3.2
Precuneus	10, -57, 26	2.96
P. Cingulate	2, -49, 21	2.92

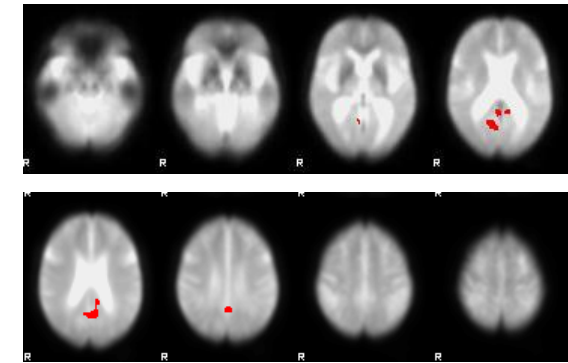
Right Caudate

b) AD > Con



Brain Region	Coordinates	Z Stat
P. Cingulate	-7, -51, 10	3.65
P. Cingulate	2, -55, 10	3.40
Precuneus	-7, -63, 20	2.98
Cuneus	2, -69, 14	2.81

c) DLB > Con



Brain Region	Coordinates	Z Stat
P. Cingulate	8, -68, 9	3.11
Precuneus	-7, -65, 36	3.06
Culmen	4, -60, 4	3.02
P. Cingulate	-11, -51, 10	2.94

Abbreviations: Culmen = Culmen of Vermis; PHG = Parahippocampal Gyrus; P. Cingulate = Posterior Cingulate Cortex

Table 7.2: Peak Regions of Functional Connectivity with the Left and Right Head of Caudate Nucleus

Group Mean/ Difference	Left Head of Caudate Nucleus	Right Head of Caudate Nucleus
Control Mean	<ul style="list-style-type: none"> • Sub-lobar: Caudate Head and Body • Limbic: Anterior Cingulate 	<ul style="list-style-type: none"> • Frontal: Inferior, Precentral Gyrus, Cingulate • Sub-lobar: Caudate Head and Body, Putamen, Insula • Limbic: Anterior Cingulate
AD Mean	<ul style="list-style-type: none"> • Sub-lobar: Caudate Head and Body, Thalamus, Claustrum • Limbic: Anterior Cingulate 	<ul style="list-style-type: none"> • Frontal: Medial • Sub-lobar: Caudate Head and Body • Limbic: Anterior, Posterior Cingulate
DLB Mean	<ul style="list-style-type: none"> • Frontal: Inferior, Precentral, Middle • Sub-lobar: Caudate Head and Body, Putamen, Globus Pallidus, Insula • Limbic: Posterior Cingulate 	<ul style="list-style-type: none"> • Sub-lobar: Caudate Head and Body, Putamen • Limbic: Anterior Cingulate
AD > Con		<ul style="list-style-type: none"> • Limbic: Posterior Cingulate • Occipital: Precuneus, Cuneus
DLB > Con	<ul style="list-style-type: none"> • Limbic: Parahippocampal Gyrus, Posterior Cingulate • Parietal: Precuneus • Occipital: Precuneus 	<ul style="list-style-type: none"> • Limbic: Posterior Cingulate • Parietal: Precuneus • Anterior Lobe: Culmen of Vermis

ii. Putamen

Group Means:

Mean functional connectivity maps with a seed placed in the putamen are shown in figures 7.5a (left seed) and 7.6a (right seed) for controls, 7.5b (left seed) and 7.6b (right seed) in AD and 7.5c (left seed) and 7.6c (right seed) in DLB. The peak brain regions which showed connectivity with the left and right putamen are summarised in Table 7.3. All groups showed bilateral putamen connectivity, i.e. a seed in the left putamen showed connectivity with the right putamen and a seed in the right putamen showed connectivity with the left putamen. The right putamen showed connectivity with more brain regions in all groups than the left putamen. For the left putamen all groups only showed sub-lobar connectivity. Controls and AD subjects showed similar patterns of connectivity for the right putamen; frontal, sub-lobar and limbic (Figures 7.6a and b). The DLB group showed connectivity with frontal and sub-lobar regions similar to controls and AD, but in contrast did not show limbic connectivity and showed connectivity with parietal and temporal regions (Figure 7.6c).

Group Differences:

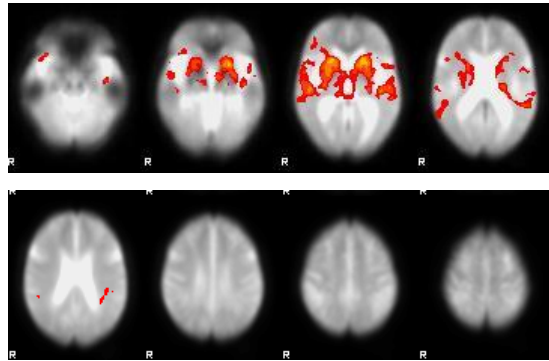
DLB subjects showed greater connectivity than controls with the left putamen and the pre and postcentral gyrus and inferior parietal regions (all left hemisphere) (Figure 7.7a). DLB subjects also showed greater functional connectivity than AD subjects for both the left and right seeds in similar regions; pre and postcentral gyrus, inferior parietal and transverse temporal regions (all left hemisphere) (Figures 7.7b and 7.7c). Controls did not show greater functional connectivity than AD or DLB between the putamen and any brain region, and there were no brain regions of significantly greater functional connectivity in AD compared to DLB.

Summary:

- Left Putamen: DLB > Controls and AD
- Right Putamen: DLB > AD

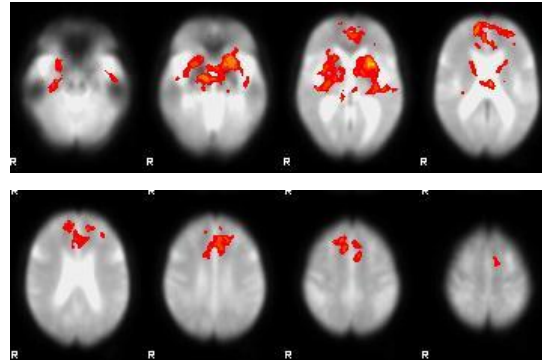
Figure 7.5: Functional Connectivity Maps for the Left Putamen

a) Control Mean



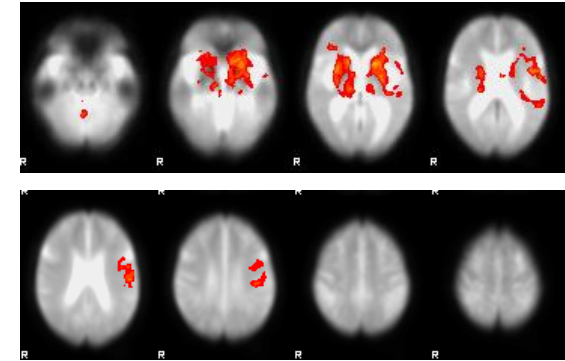
Brain Region	Coordinates	Z Stat
Putamen	-23, 8, -1	6.42
Putamen	21, 8, 0	6.32

b) AD Mean



Brain Region	Coordinates	Z Stat
Putamen	-23, 6, -1	6.15
Putamen	29, -2, 5	5.53
Clastrum	-27, 23, 6	4.02

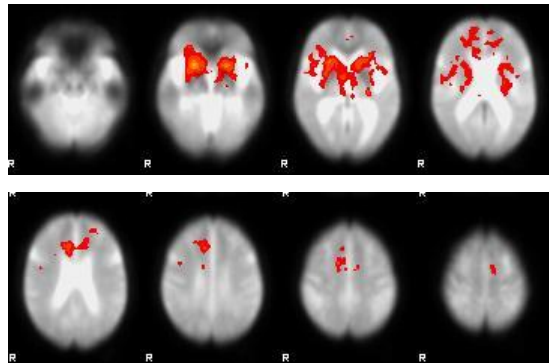
c) DLB Mean



Brain Region	Coordinates	Z Stat
Putamen	-23, 6, 1	6.07
Putamen	29, 2, 5	4.87
Clastrum	-27, 23, 6	4.46

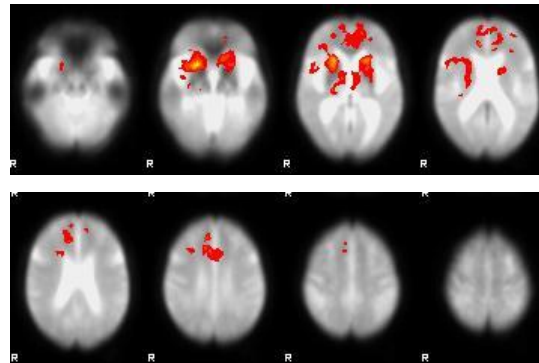
Figure 7.6: Functional Connectivity Maps for the Right Putamen

a) Control Mean



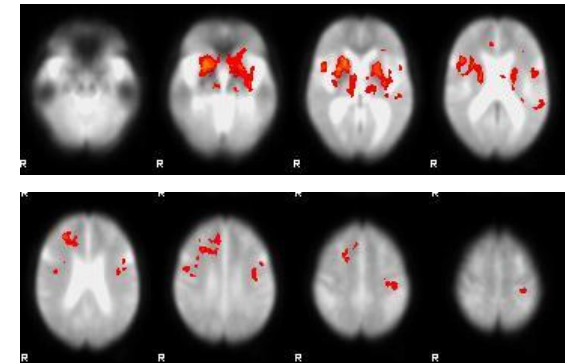
Brain Region	Coordinates	Z Stat
Putamen	21, 8, -5	6.63
Putamen	-19, 9, -6	5.44
Thalamus	-25, -26, 1	4.51
Cingulate	10, 22, 28	4.19
A. Cingulate	-5, 33, 13	3.95
Med. Frontal	6, 21, 44	3.73
Sup. Frontal	-27, 46, 14	3.61
Med. Frontal	-9, -5, 52	3.59

b) AD Mean



Brain Region	Coordinates	Z Stat
Putamen	20, 8, -5	8.52
Insula	40, -26, -3	4.61
Thalamus	21, -22, 3	3.73
Cingulate	8, 33, 18	3.66
A. Cingulate	-10, 31, 12	4.70
Med. Frontal	8, 15, 44	4.14
Putamen	-18, 17, 0	5.51
Caudate Head	-12, 12, 0	4.53
Hypothalamus	-7, -5, -2	3.89

c) DLB Mean



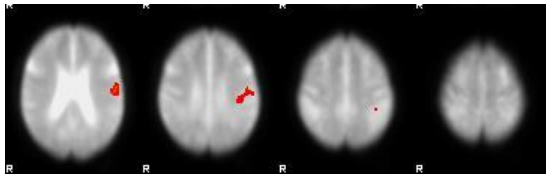
Brain Region	Coordinates	Z Stat
Putamen	21, 6, 0	6.46
Putamen	-19, 4, -1	4.71
Sup. Frontal	28, 33, 30	4.42
Insula	41, 12, 17	4.32
Clastrum	34, 0, -1	3.93
Postcentral	-46, -9, 19	3.63
Precentral	-37, -16, 35	3.53
Sup. Temporal	-49, 4, 4:	3.50
Insula	-47, -3, 14	3.40

Abbreviations: A. Cingulate = Anterior Cingulate Cortex; Med. Frontal = Medial Frontal Gyrus; Sup. Frontal = Superior Frontal Gyrus; Sup. Temp. = Superior Temporal Gyrus

Figure 7.7: Functional Connectivity Maps Showing Group Differences for the Putamen

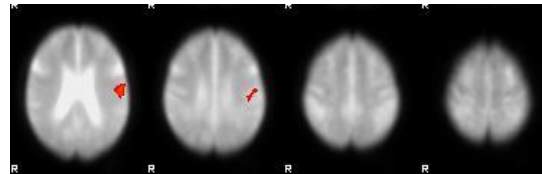
Left Putamen

a) DLB > Con



Brain Region	Coordinates	Z Stat
Precentral	-55, -13, 24	3.46
Inf. Parietal	-53, -20, 23	3.43
Postcentral	-48, -19, 29	3.06

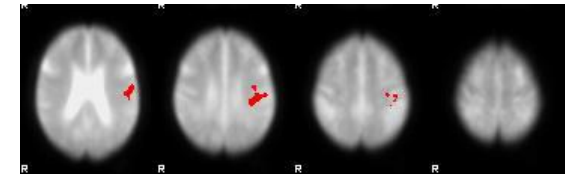
b) DLB > AD



Brain Region	Coordinates	Z Stat
Inf. Parietal	-53, -20, 23	3.75
Postcentral	-55, -15, 24	3.45
Trans. Temp.	-57, -12, 13	2.84

Right Putamen

c) DLB > AD



Brain Region	Coordinates	Z Stat
Inf. Parietal	-42, -33, 38	3.04
Postcentral	-55, -15, 24	2.99
Precentral	-38, -10, 30	2.78

Abbreviations: Inf. Parietal = Inferior Parietal Lobule; Trans. Temp. = Transverse Temporal Gyrus

Table 7.3: Peak Regions of Functional Connectivity with the Left and Right Putamen

Group Mean/Difference	Left Putamen	Right Putamen
Control Mean	<ul style="list-style-type: none"> • Sub-lobar: Putamen 	<ul style="list-style-type: none"> • Frontal: Medial, Superior • Sub-lobar: Putamen, Thalamus • Limbic: Cingulate, Anterior Cingulate
AD Mean	<ul style="list-style-type: none"> • Sub-lobar: Putamen, Claustrum 	<ul style="list-style-type: none"> • Frontal: Medial • Sub-lobar: Caudate Head, Putamen, Thalamus, Hypothalamus, Insula • Limbic Lobe: Cingulate, Anterior Cingulate
DLB Mean	<ul style="list-style-type: none"> • Sub-lobar: Putamen, Claustrum 	<ul style="list-style-type: none"> • Frontal Lobe: Superior, Precentral • Sub-lobar: Putamen, Insula, Claustrum • Parietal Lobe: Postcentral • Temporal Lobe: Superior
DLB > Con	<ul style="list-style-type: none"> • Frontal: Precentral Gyrus • Parietal: Inferior, Postcentral 	
DLB > AD	<ul style="list-style-type: none"> • Parietal: Inferior, Postcentral • Temporal: Transverse 	<ul style="list-style-type: none"> • Frontal: Precentral Gyrus • Parietal: Inferior, Postcentral

iii. Thalamus (Mediodorsal nucleus)

Group Means:

The mean connectivity maps for all subjects showed significant connectivity between the left and the right thalamus, and vice versa. The control (Figures 7.8a and 7.9a) and AD (Figures 7.8b and 7.9b) groups showed significant connectivity between the thalamus (left and right) and frontal regions, whereas in the DLB group (Figures 7.8c and 7.9c) neither seed showed connectivity with frontal regions. In contrast to controls and DLB, the AD group did not show connectivity with the anterior or posterior lobes. The AD group showed connectivity with the greatest number of brain regions, particularly for the left seed (see Table 7.4 for a summary).

Group Differences:

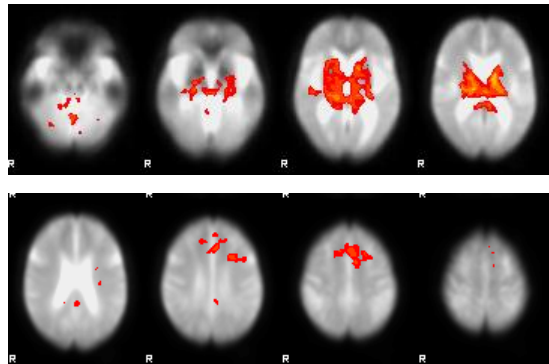
Greater connectivity with the left thalamus was reported in both the AD and DLB groups compared to controls (Figures 7.10a and b), and also for the DLB group compared to controls for the right thalamus (figure 7.10c). AD subjects showed greater connectivity than controls between the left thalamus and pre and postcentral gyrus and inferior parietal regions (all right hemisphere) (Figure 7.10a). The DLB group showed greater connectivity than controls between the left thalamus and the cingulate (bilateral), insula (right) and frontal regions (bilateral) (Figure 7.10b). For the right thalamus the DLB group showed greater connectivity than controls in frontal and limbic regions (all right hemisphere) (Figure 7.10c and Table 7.4 for a summary). The control group did not show any regions of greater connectivity with the thalamus than either dementia group.

Summary:

- Left Thalamus – AD and DLB > Controls
- Right Thalamus – DLB > Controls

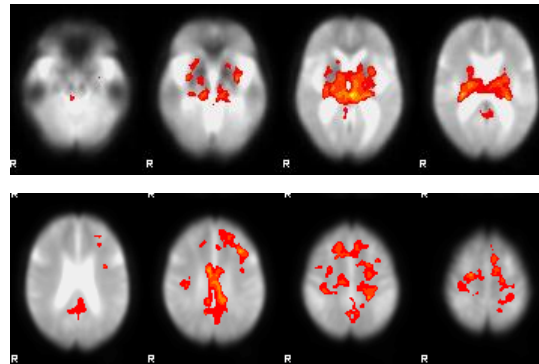
Figure 7.8: Functional Connectivity Maps for the Left Thalamus

a) Con Mean



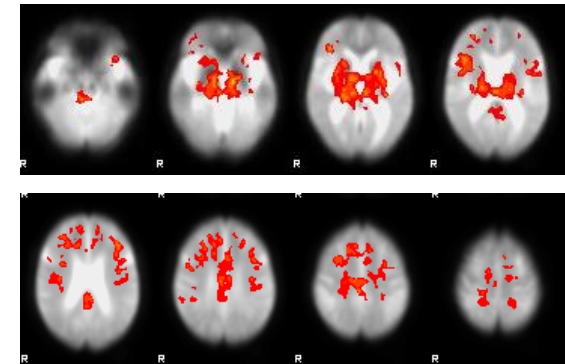
Brain Region	Coordinates	Z Stat
Thalamus	-3, -10, 9	5.87
Thalamus	8, -17, 8	5.41
Sup. Frontal	-3, 16, 49	4.33
Med. Frontal	-9, 2, 48	3.45
Sup. Frontal	10, 14, 49	3.30

b) AD Mean



Brain Region	Coordinates	Z Stat
Thalamus	16, -23, 8	5.68
Thalamus	-23, -26, 7	5.19
Caudate Tail	-27, -34, 11	5.13
Mid. Frontal	-33, 16, 38	4.92
Cingulate	6, -9, 36	4.87
Paracentral	-22, -41, 43	4.74
Sub-gyral	19, -16, 57	4.62
Precuneus	-22, -45, 48	4.58

c) DLB Mean

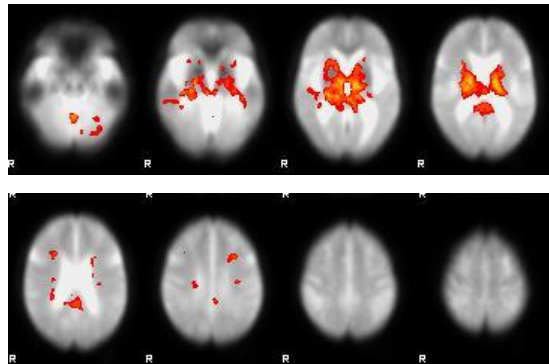


Brain Region	Coordinates	Z Stat
Thalamus	-8, -19, 8	6.0
Subthalamic N	-12, -12, -8	5.38
Thalamus	4, -23, 8	5.21
G. Pallidus	-18, -5, -2	4.89

Abbreviations: G. Pallidus = Globus Pallidus; Med. Frontal = Medial Frontal Gyrus; Mid. Frontal = Middle Frontal Gyrus; Subthalamic N = Subthalamic Nucleus; Sup. Frontal = Superior Frontal Gyrus

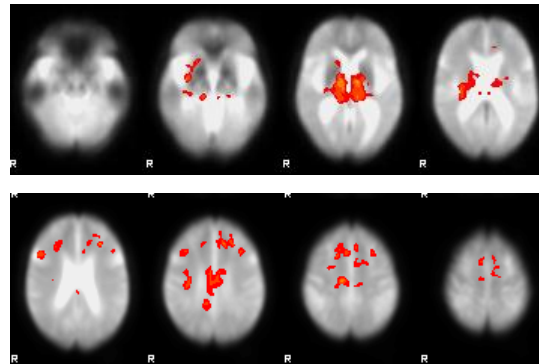
Figure 7.9: Functional Connectivity Maps for the Right Thalamus

a) Controls Mean



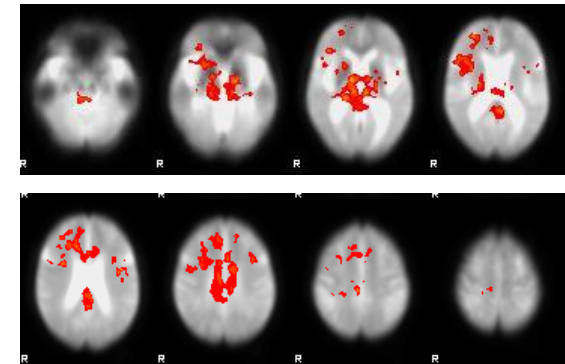
Brain Region	Coordinates	Z Stat
Thalamus	8, -19, 8	6.13
Thalamus	-16, -18, 13	5.42
Inf. S.-Lunar	-21, -67, -40	5.07
Nodule	-1, -55, -28	5.03
C. Tonsil	7, -55, -33	4.93
Tuber	-32, -64, -29	3.68
Pyramis	-23, -74, -30	3.45

b) AD Mean



Brain Region	Coordinates	Z Stat
Thalamus	-10, -13, 3	4.62
Med. Frontal	9, -21, 46	4.51
Thalamus	8, -13, 3	4.43
Clastrum	30, -22, 14	4.27
Putamen	-27, -11, 8	4.07
Mid. Frontal	-29, 26, 28	4.06
Sub-Gyral	-12, 25, 39	3.95
Sup. Frontal	4, 13, 49	3.68
Sup. Frontal	-7, 16, 54	3.51

c) DLB Mean



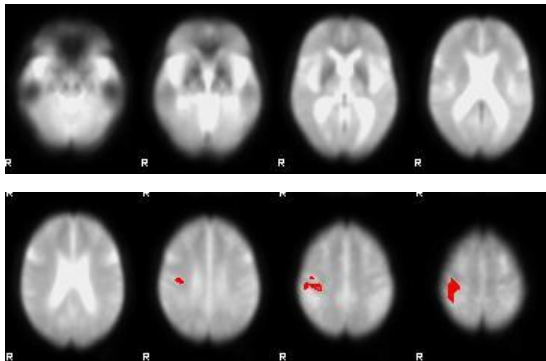
Brain Region	Coordinates	Z Stat
Thalamus	6, -21, 8	5.24
Nodule	-1, -55, -28	4.84
Thalamus	-7, -26, 7	4.45
Uvula	5, -60, -34	3.90
C. Tonsil	12, -50, -38	3.86
C. Tonsil	-10, -53, -33	3.47
Uvula	-10, -66, -29	2.92
Pyramis	-23, -72, -30	2.87

Abbreviations: C. Tonsil = Cerebellar Tonsil; Inf. S. -Lunar = Inferior Semi-Lunar Lobule; Med. Frontal = Medial Frontal Gyrus; Mid. Frontal = Middle Frontal; Sup. Frontal = Superior Frontal Gyrus

Figure 7.10: Functional Connectivity Maps Showing Group Differences for the Thalamus

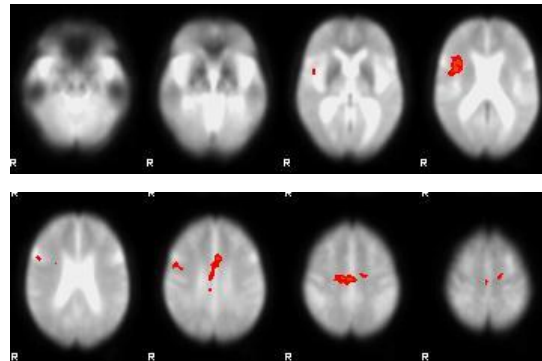
Left Thalamus

a) AD > Con



Brain Region	Coordinates	Z Stat
Postcentral	32, -34, 45	3.54
Precentral	35, -28, 56	3.06
Inf. Parietal	39, -43, 55	2.87

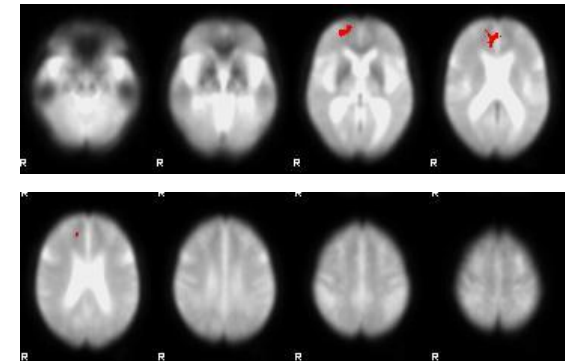
b) DLB > Con



Brain Region	Coordinates	Z Stat
Cingulate	4, -19, 40	4.04
Paracentral	0, -23, 45	3.54
Cingulate	-5, 6, 37	3.40
Precentral	-17, -19, 51	2.99
Insula	38, 1, 16	3.70
Precentral	47, -1, 37	2.82
Inf. Frontal	49, 8, 22	2.75

Right Thalamus

c) DLB > Con



Brain Region	Coordinates	Z Stat
Med. Frontal	1, 42, 19	2.92
A. Cingulate	14, 36, 24	2.89
Sup. Frontal	19, 55, 15	2.77

Abbreviations: A. Cingulate = Anterior Cingulate; Inf. Frontal = Inferior Frontal; Inf. Parietal = Inferior Parietal; Med. Frontal = Medial Frontal Gyrus; Sup. Frontal = Superior Frontal Gyrus

Table 7.4: Peak Regions of Functional Connectivity with the Left and Right Thalamus

Group Mean/ Difference	Left Thalamus	Right Thalamus
Control Mean	<ul style="list-style-type: none"> • Frontal: Medial and Superior • Sub-lobar: Thalamus 	<ul style="list-style-type: none"> • Sub-lobar: Thalamus • Anterior: Nodule • Posterior: Inferior Semi-Lunar, Cerebellar Tonsil, Tuber, Pyramis
AD Mean	<ul style="list-style-type: none"> • Frontal: Middle, Paracentral Lobule, Sub-Gyral • Sub-lobar: Thalamus, Caudate Tail • Limbic: Cingulate • Parietal: Precuneus 	<ul style="list-style-type: none"> • Frontal: Medial, Middle, Sub-gyral, Superior • Sub-lobar: Thalamus, Putamen and Claustrum
DLB Mean	<ul style="list-style-type: none"> • Sub-lobar: Thalamus and Globus Pallidus • Midbrain: Subthalamic Nucleus 	<ul style="list-style-type: none"> • Sub-lobar: Thalamus • Anterior: Nodule • Posterior: Uvula, Cerebellar Tonsil and Pyramis
AD > Con	<ul style="list-style-type: none"> • Frontal: Precentral • Parietal: Inferior and Postcentral 	
DLB > Con	<ul style="list-style-type: none"> • Frontal: Precentral, Paracentral and Inferior • Sub-lobar: Insula • Limbic: Cingulate 	<ul style="list-style-type: none"> • Frontal: Medial, Superior • Limbic: Anterior Cingulate

iv. Hippocampus

Group Means:

The functional connectivity maps in control subjects were observed to have the greatest functional connectivity for both the left and right hippocampus (Figures 7.11a and 7.12a) compared to the dementia groups (Figures 7.11b and c and 7.12b and c). The control group demonstrated connectivity between the hippocampus and sub-lobar and occipital regions which were not present in the AD or DLB groups. Generally, across all groups connectivity between the hippocampus and the rest of the brain was low compared to the other seed regions investigated. Table 7.5 summarises the brain regions showing significant connectivity.

Group Differences:

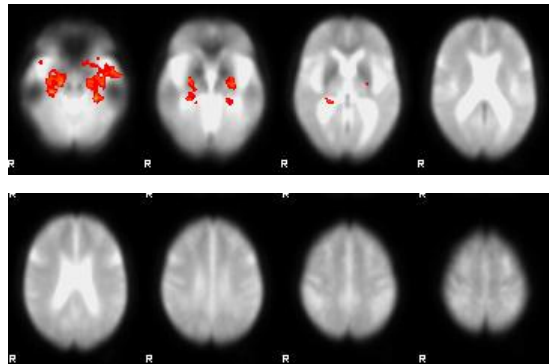
The AD group showed significantly greater connectivity than controls between the left hippocampus and the right insula and right inferior parietal regions (Figure 7.11d). These areas were not reported to show connectivity in the AD group mean results (Figure 7.11b) as their z statistic was < 2.3 . However, when comparing between groups the absence of connectivity in these regions in controls causes these regions to reach significance for the group comparison. There were no other significant differences between groups for the left or right hippocampus.

Summary:

- Left Hippocampus: AD > Con
- Right Hippocampus: No significant differences between groups

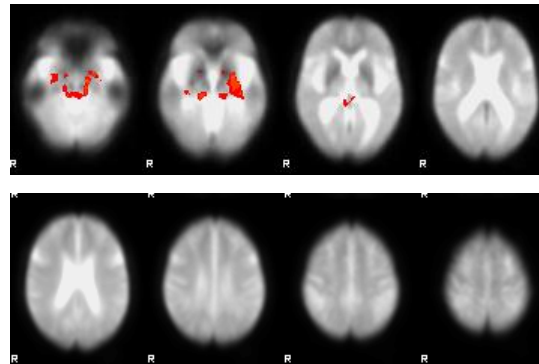
Figure 7.11: Functional Connectivity Maps for the Left Hippocampus

a) Controls Mean



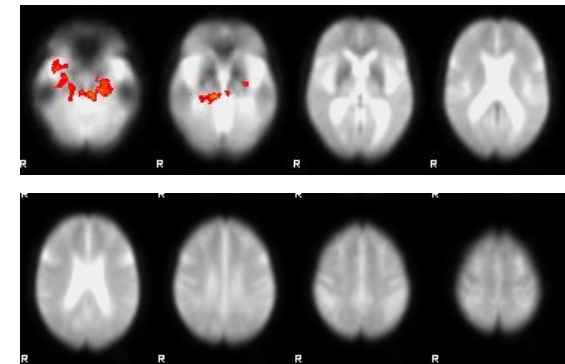
Brain Region	Coordinates	Z Stat
Culmen	-27, -31, -21	4.22
PHG	-27, -17, -14	4.15
Uncus	-34, -8, -24	4.08
PHG	21, -21, -14	4.16
Mid. Temporal	-43, 5, -28	3.92

b) AD Mean



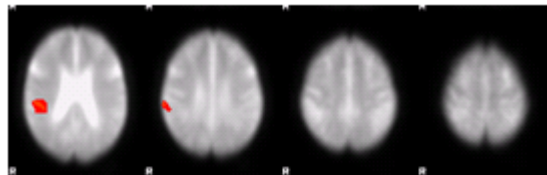
Brain Region	Coordinates	Z Stat
PHG	-23, -21, -14	5.86
Mid. Temporal	35, -1, -28	4.36
PHG	32, -17, -13	3.73
Culmen	14, -29, -9	3.66

c) DLB Mean



Brain Region	Coordinates	Z Stat
PHG	-23, -19, -14	4.92
Culmen	10, -29, -9	4.67
Culmen	-8, -29, -20	3.77

d) AD > Con

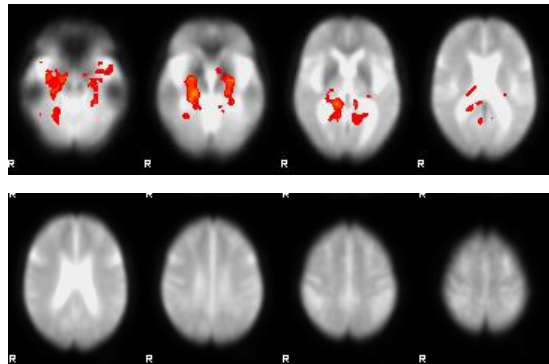


Brain Region	Coordinates	Z Stat
Inf. Parietal	49, -32, 24	3.52
Insula	39, -38, 23	3.23

Abbreviations: Inf. Parietal; Inferior Parietal; Mid. Temporal = Middle Temporal Gyrus ; PHG = Parahippocampal Gyrus

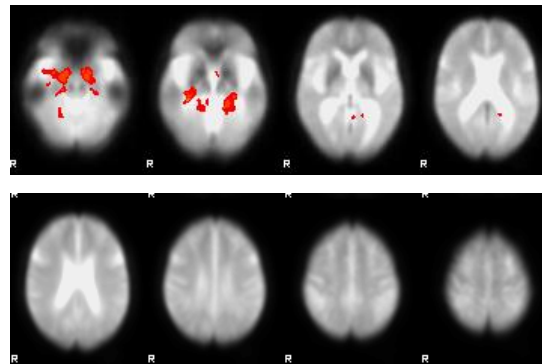
Figure 7.12: Functional Connectivity Maps for the Right Hippocampus

a) Controls Mean



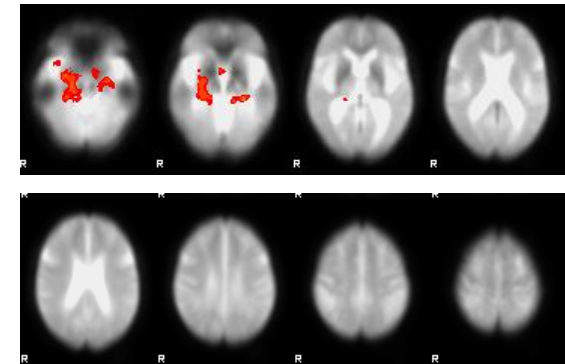
Brain Region	Coordinates	Z Stat
PHG	21, -19, -13	5.78
Culmen	6, -40, -5	4.38
Amygdala	-23, -10, -8	4.16
Putamen	-27, -10, -8	4.12
PHG	-19, -25, -9	3.74
Culmen	-25, -34, -16	3.55
Sup. Temporal	-34, 12, -22	3.48
Mid. Temporal	-39, 3, -29	3.27
Lingual	-10, -54, 4	2.64

b) AD Mean



Brain Region	Coordinates	Z Stat
PHG	23, -23, -14	5.19
Culmen	-16, -39, -16	4.46
Uncus	20, -12, -29	4.38
Mid.Temporal	40, 1, -27	4.20
PHG	-19, -13, -14	3.92

c) DLB Mean



Brain Region	Coordinates	Z Stat
PHG	25, -23, -14	5.98
Culmen	25, -31, -20	3.71
PHG	-25, -32, -10	4.76
Sup. Temporal	-30, 7, -28	3.73
Culmen	-18, -32, -15	3.61
Subcallosal	7, 5, -11	3.58

Abbreviations: Mid. Temporal = Middle Temporal Gyrus; PHG = Parahippocampal Gyrus; Sup. Temporal = Superior Temporal Gyrus

Table 7.5: Peak Regions of Functional Connectivity with the Left and Right Hippocampus

Group Mean/ Difference	Left Hippocampus	Right Hippocampus
Control Mean	<ul style="list-style-type: none"> • Limbic: Uncus, Parahippocampal Gyrus • Temporal: Middle • Anterior: Culmen 	<ul style="list-style-type: none"> • Sub-lobar: Putamen • Limbic: Parahippocampal Gyrus, Amygdala • Temporal: Superior, Middle • Occipital: Lingual • Anterior: Culmen
AD Mean	<ul style="list-style-type: none"> • Limbic: Parahippocampal Gyrus • Temporal: Middle • Anterior: Culmen 	<ul style="list-style-type: none"> • Limbic: Parahippocampal Gyrus, Uncus • Temporal: Middle • Anterior: Culmen
DLB Mean	<ul style="list-style-type: none"> • Limbic: Parahippocampal Gyrus • Anterior: Culmen 	<ul style="list-style-type: none"> • Frontal: Subcallosal Gyrus • Limbic: Parahippocampal • Temporal: Superior • Anterior: Culmen
AD > Con	<ul style="list-style-type: none"> • Sub-lobar: Insula • Parietal: Inferior 	

v. Posterior Cingulate Cortex

Group Means:

Across groups, the left and right posterior cingulate seeds showed functional connectivity with a high number of brain regions. For the left posterior cingulate, DLB subjects (Figure 7.13c) showed connectivity with the most brain regions and controls and AD showed connectivity with a similar number of brain regions (Figures 7.13a and 7.13b). For the right posterior cingulate, the AD group showed functional connectivity with the least brain regions (limbic and sub-lobar only) (Figure 7.14b), and controls and DLB subjects showed connectivity with a similar number of brain regions (Figures 7.14a and 7.14c). The DLB group showed a more widespread pattern of connectivity for the right seed involving many different brain regions and small clusters of activity, whereas the control and AD groups showed larger and more distinct clusters of activity. Table 7.6 summarises these results.

Group Differences:

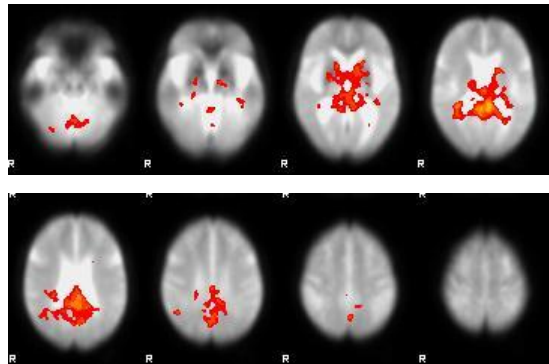
There were no significant differences in left posterior cingulate cortex connectivity between any of the groups. The AD group showed greater connectivity than controls between the right posterior cingulate cortex and the caudate head (bilateral) and body (right) and with the caudate body (bilaterally) compared to DLB subjects (Figure 7.15a and c). Although these regions appear to be localised to the cerebrospinal fluid in the AD subjects, the coordinates are localised to the grey matter region of the caudate. This is thought to be caused by greater ventricular atrophy in the dementia groups, therefore a voxel in the brain in the AD subjects (who show less atrophy) when overlayed on the mean template of all study subjects is actually placed in the cerebrospinal fluid. The DLB group showed greater connectivity than controls for a number of regions; limbic (left anterior cingulate), sub-lobar (right globus pallidus), anterior lobe (right culmen) and posterior lobe (right cerebellar tonsil) (Figure 7.15b). Controls did not show greater connectivity with any brain regions compared to the dementia groups, and the DLB group did not show greater connectivity than the AD group. Table 7.6 summarises these results.

Summary:

- Left posterior cingulate: No significant differences
- Right posterior cingulate: AD > DLB, Controls; DLB > Controls

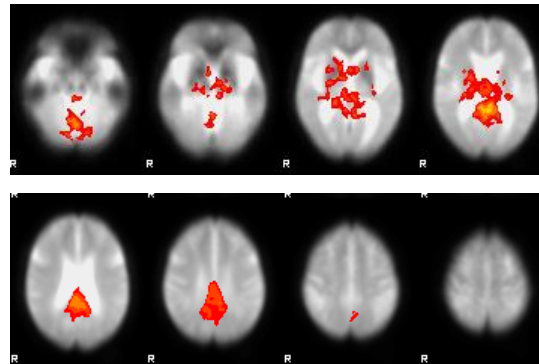
Figure 7.13: Functional Connectivity Maps for the Left Posterior Cingulate Cortex

a) Controls Mean



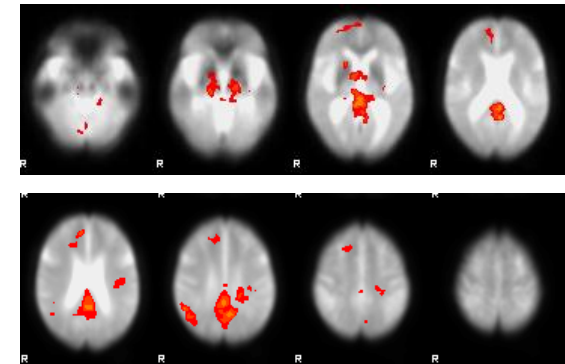
Brain Region	Coordinates	Z Stat
Cuneus	-3, -75, 19	5.57
P.Cingulate	-3, -46, 16	5.41
P.Cingulate	2, -48, 16	4.76
G. Pallidus	-10, 1, -1	4.18
Caudate Tail	32, -44, 11	4.12
C. Tonsil	-3, -53, -33	3.78
Pyramis	12, -72, -29	3.65
Inf. S.-Lunar	-27, -67, -35	3.53
Pyramis	-18, -66, -29	3.51
Nodule	-1, -59, -23	3.49

b) AD Mean



Brain Region	Coordinates	Z Stat
P.Cingulate	1, -50, 16	5.59
Precuneus	0, -46, 38	4.25
Thalamus	3, -19, 8	4.09
Thalamus	-10, -30, 7	4.04
C. Tonsil	-10, -53, -33	4.76
Pyramis	1, -65, -23	4.53
Declive	-10, -73, -19	4.50
Nodule	1, -59, -28	4.40
Declive	6, -62, -18	4.19

c) DLB Mean

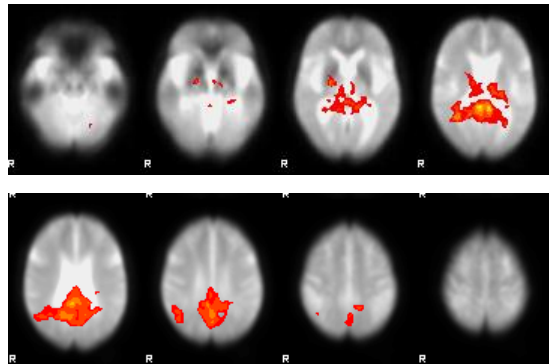


Brain Region	Coordinates	Z Stat
P.Cingulate	0, -52, 16	4.77
Lingual	-5, -60, 4	4.68
Thalamus	1, -27, 7	4.33
Culmen	4, -41, 0	4.27
Precuneus	0, -48, 32	4.24
U. of Vermis	5, -60, -34	3.96
Med. Frontal	8, 38, 35	3.63
C. Tonsil	-23, -45, -38	3.57
Nodule	1, -57, -28	3.56
Postcentral	-35, -27, 28	3.53
C. Tonsil	11, -50, -44	3.49
Cingulate	-20, -38, 33	3.34
Sup. Temporal	35, -74, 30	3.04
Sup. Frontal	15, 18, 50	3.04
Insula	-42, -19, 23	3.00

Abbreviations: C. Tonsil = Cerebellar Tonsil; G. Pallidus = Globus Pallidus; Inf. S. Lunar = Inferior Semi-Lunar Lobule; Med. Frontal = Medial Frontal Gyrus; P. Cingulate = Posterior Cingulate; Sup. Frontal = Superior Frontal; Sup. Temporal = Superior Temporal Gyrus; U. of Vermis = Uvula of Vermis

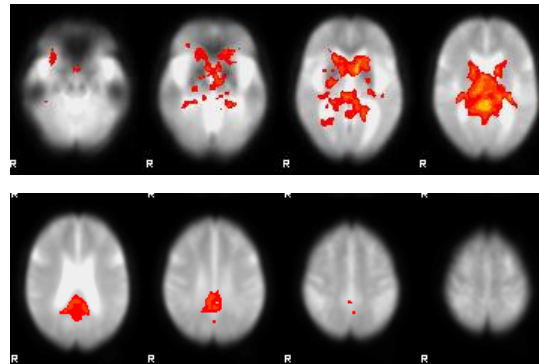
Figure 7.14: Functional Connectivity Maps for the Right Posterior Cingulate Cortex

a) Controls Mean



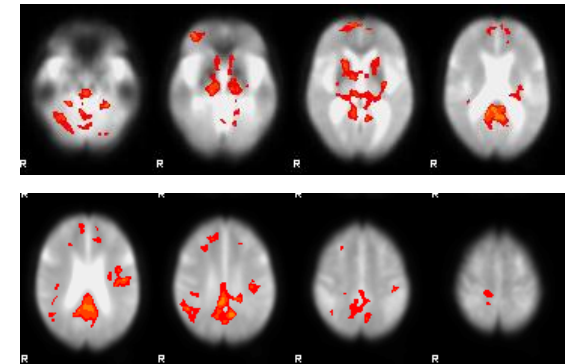
Brain Region	Coordinates	Z Stat
P. Cingulate	4, -46, 11	5.95
P. Cingulate	-7, -48, 10	5.58
Cingulate	6, -49, 27	5.08
Precuneus	13, -60, 26	4.86
Precuneus	-2, -63, 31	4.52
PHG	32, -55, 10	4.44
Inf. S.-Lunar	-23, -65, -40	3.44
Pyramis	-14, -68, -29	3.19
C. Tonsil	-25, -62, -34	3.04

b) AD Mean



Brain Region	Coordinates	Z Stat
P. Cingulate	4, -42, 11	5.27
Caudate Head	-8, 2, 4	5.12
P. Cingulate	-3, -46, 11	5.03
PHG	-10, -36, 6	4.88
Thalamus	8, -23, 13	4.69

c) DLB Mean

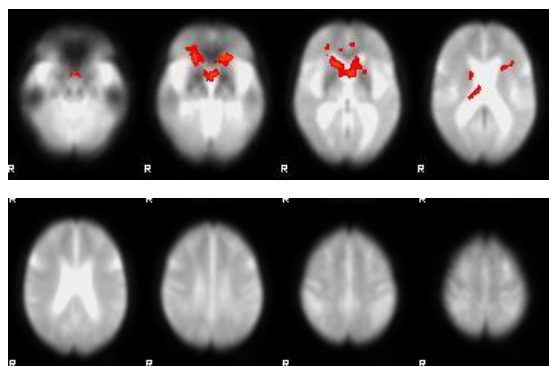


Brain Region	Coordinates	Z Stat
P. Cingulate	0, -52, 16	5.10
P. Cingulate	8, -45, 6	4.65
C. Tonsil	12, -48, -43	4.51
Precuneus	-11, -63, 31	4.51
Sub-gyral	34, 44, -2	4.45
Insula	-44, -19, 23	3.96
Postcentral	-37, -28, 28	3.85
Mid. Frontal	23, 23, 34	3.67
Med. Frontal	8, 58, 10	3.66
Inf. Parietal	-42, -32, 44	3.29

Abbreviations: C. Tonsil = Cerebellar Tonsil; Inf. Parietal = Inferior Parietal; Inf. S. -Lunar = Inferior Semi-Lunar Lobule; Med. Frontal = Medial Frontal Gyrus; Mid. Frontal = Middle Frontal; PHG = Parahippocampal Gyrus; P. Cingulate = Posterior Cingulate Cortex

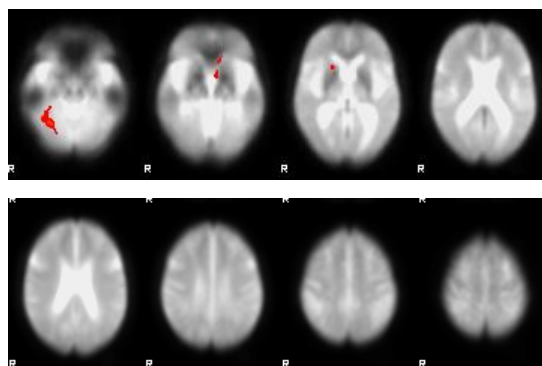
Figure 7.15: Functional Connectivity Maps showing Group Differences for the Right Posterior Cingulate Cortex

a) AD > Con



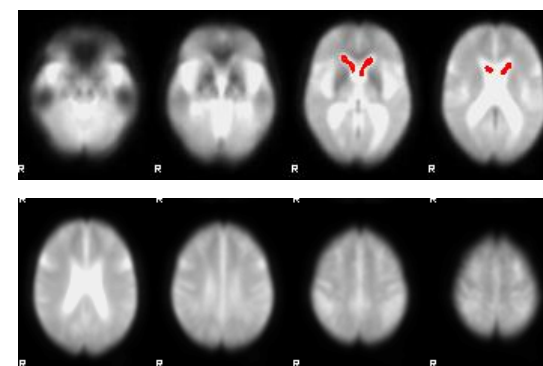
Brain Region	Coordinates	Z Stat
Caudate Head	-8, 19, 1	3.91
Caudate Head	8, 14, 0	3.74
Caudate Body	16, 15, 6	3.66

b) DLB > Con



Brain Region	Coordinates	Z Stat
C. Tonsil	25, -43, -37	3.85
Culmen	29, -56, -22	3.36
A. Cingulate	-3, 1, -1	2.91
G. Pallidus	16, 2, -1	2.82

c) AD > DLB



Brain Region	Coordinates	Z Stat
Caudate Body	-5, 5, 10	3.42
Caudate Body	5, 13, 11	3.17

Abbreviations: A. Cingulate = Anterior Cingulate Cortex; C. Tonsil = Cerebellar Tonsil; G. Pallidus = Globus Pallidus

Table 7.6: Peak Regions of Functional Connectivity with the Left and Right Posterior Cingulate Cortex

Group Mean/ Difference	Left Posterior Cingulate Cortex	Right Posterior Cingulate Cortex
Control Mean	<ul style="list-style-type: none"> • Sub-lobar: Globus Pallidus, Caudate Tail • Limbic: Posterior Cingulate • Occipital: Cuneus • Anterior: Nodule • Posterior: Cerebellar Tonsil, Pyramis, Inferior Semi-Lunar Lobule 	<ul style="list-style-type: none"> • Limbic: Posterior Cingulate, Cingulate, Parahippocampal Gyrus • Parietal: Precuneus • Occipital Lobe: Precuneus • Posterior: Inferior Semi-Lunar Lobule, Pyramis, Cerebellar Tonsil
AD Mean	<ul style="list-style-type: none"> • Sub-lobar: Thalamus • Limbic: Posterior Cingulate • Parietal: Precuneus • Anterior: Pyramis, Nodule • Posterior: Cerebellar Tonsil, Declive 	<ul style="list-style-type: none"> • Sub-lobar: Caudate Head, Thalamus • Limbic: Posterior Cingulate, Parahippocampal Gyrus
DLB Mean	<ul style="list-style-type: none"> • Frontal: Medial, Superior • Sub-lobar: Thalamus, Insula • Limbic: Posterior Cingulate, Cingulate • Parietal: Precuneus, Postcentral • Temporal: Superior 	<ul style="list-style-type: none"> • Frontal: Sub-Gyral, Middle, Medial • Sub-lobar: Insula • Limbic: Posterior Cingulate • Parietal: Precuneus, Inferior Parietal • Posterior: Cerebellar Tonsil, Postcentral

Table 7.6 (Contd.): Peak Regions of Functional Connectivity with the Left and Right Posterior Cingulate Cortex

Group Mean/ Difference	Left Posterior Cingulate Cortex	Right Posterior Cingulate Cortex
DLB Mean	<ul style="list-style-type: none"> • Occipital: Lingual Gyrus • Anterior: Culmen, Nodule • Posterior: Uvula of Vermis, Cerebellar Tonsil 	
AD > DLB		<ul style="list-style-type: none"> • Sub-lobar: Caudate Body
AD > Con		<ul style="list-style-type: none"> • Sub-lobar: Caudate Head and Body
DLB > Con		<ul style="list-style-type: none"> • Sub-lobar: Globus Pallidus • Limbic: Anterior Cingulate • Anterior: Culmen • Posterior: Cerebellar Tonsil

vi. Precuneus

Group Means:

For the control group, the left precuneus showed connectivity with the right precuneus only (Figure 7.16a), whereas AD and DLB subjects also showed connectivity with middle and medial frontal brain regions and the cingulate also (all right hemisphere) (Figures 7.16b and c respectively). The connectivity maps for the left precuneus look quite different across groups with controls showing a very large cluster of connectivity compared to AD and DLB subjects. For the right precuneus, the findings were the reverse of the left precuneus results, with AD and DLB subjects only showing connectivity with the left precuneus (Figures 7.17b and c respectively), however controls showed connectivity also with frontal regions (middle) and sub-lobar (insula and claustrum) (Figure 7.17a). Table 7.7 provides a summary of the brain regions showing significant connectivity for the group means.

Group Differences:

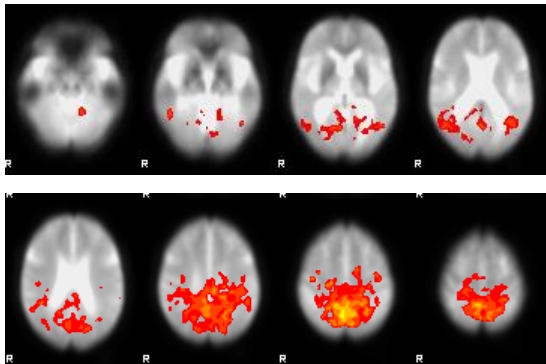
Voxelwise comparison of the group results showed that there were no significant differences between groups in functional connectivity. Though visibly, functional connectivity maps for controls do appear to show greater connectivity than AD and DLB with both the left and right precuneus.

Summary:

- Left precuneus: No significant differences between groups
- Right precuneus: No significant differences between groups

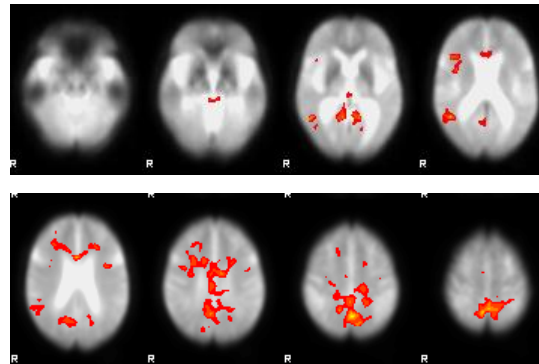
Figure 7.16: Functional Connectivity Maps for the Left Precuneus

A) Controls Mean



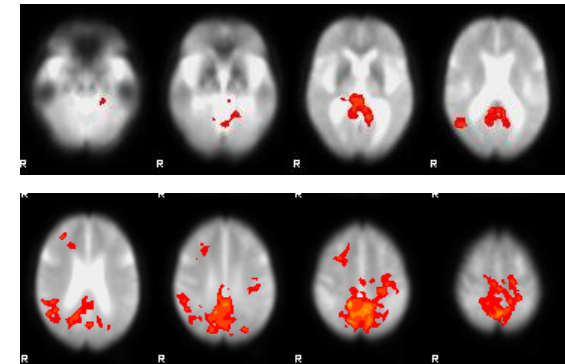
Brain Region	Coordinates	Z Stat
Precuneus	4, -66, 41	5.98
Precuneus	-7, -68, 46	5.63
Cuneus	-15, -82, 34	5.34

B) AD Mean



Brain Region	Coordinates	Z Stat
Precuneus	9, -63, 36	5.59
Precuneus	-5, -58, 42	5.54
Mid. Frontal	26, 7, 43	4.59
Med. Frontal	21, 24, 29	2.92
Cingulate	17, 22, 28	2.79

C) DLB Mean

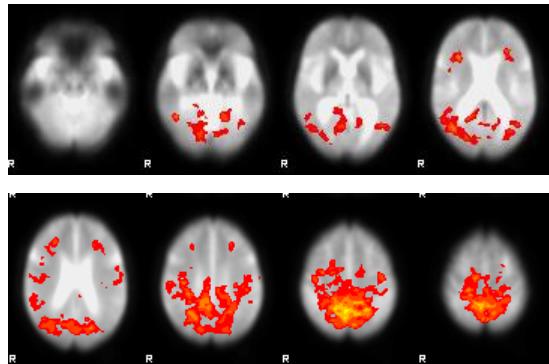


Brain Region	Coordinates	Z Stat
Precuneus	9, -63, 36	5.40
Precuneus	-5, -58, 42	4.58
Mid. Frontal	26, 7, 43	3.47
Cingulate	17, 22, 28	2.98

Abbreviations: Med. Frontal = Medial Frontal Gyrus; Mid. Frontal = Middle Frontal

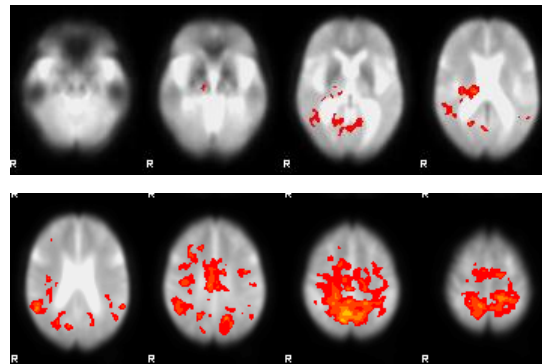
Figure 7.17: Functional Connectivity Maps for the Right Precuneus

a) Controls Mean



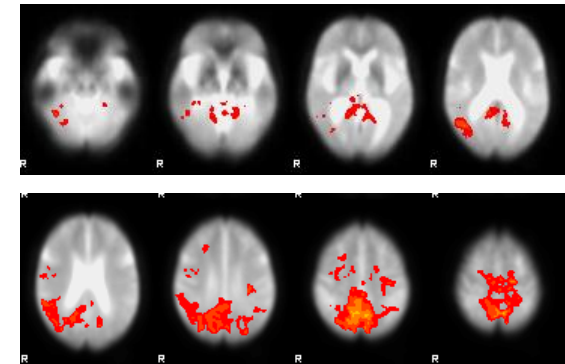
Brain Region	Coordinates	Z Stat
Precuneus	8, -54, 37	6.52
Precuneus	-7, -64, 47	6.20
Mid. Frontal	-25, 24, 33	4.95
Clastrum	-27, 16, 16	3.46
Insula	-33, 14, 16	2.87

b) AD Mean



Brain Region	Coordinates	Z Stat
Precuneus	-7, -64, 47	5.40
Precuneus	9, -65, 36	5.18

c) DLB Mean



Brain Region	Coordinates	Z Stat
Precuneus	-7, -64, 47	5.30
Precuneus	9, -65, 36	5.18

Abbreviations: Mid. Frontal = Middle Frontal

Table 7.7: Peak Regions of Functional Connectivity with the Left and Right Precuneus

Group Mean/ Difference	Left Precuneus	Right Precuneus
Control Mean	<ul style="list-style-type: none"> • Parietal: Precuneus • Occipital: Cuneus 	<ul style="list-style-type: none"> • Frontal: Middle • Parietal: Precuneus • Sub-lobar: Insula, Claustrum
AD Mean	<ul style="list-style-type: none"> • Frontal: Middle, Medial • Limbic: Cingulate • Parietal: Precuneus 	<ul style="list-style-type: none"> • Parietal Lobe: Precuneus
DLB Mean	<ul style="list-style-type: none"> • Frontal: Middle • Parietal: Precuneus • Limbic Lobe: Cingulate Gyrus 	<ul style="list-style-type: none"> • Parietal: Precuneus

vii. Primary Visual Cortex

Group Means:

For both the left and right primary visual cortex seeds, controls and DLB subjects showed a similar pattern of functional connectivity involving a few brain regions; namely cuneus, lingual gyrus and middle occipital regions (see Figures 7.18a and 7.19a for controls and Figures 7.18c and 7.19c for DLB subjects). AD subjects showed functional connectivity with more brain regions for both left and right seeds compared to control and DLB subjects (Figures 7.18b and 7.19b). Table 7.8 summarises the brain regions showing significant connectivity.

Group Differences:

There were no significant differences in functional connectivity between groups in any brain regions.

Summary:

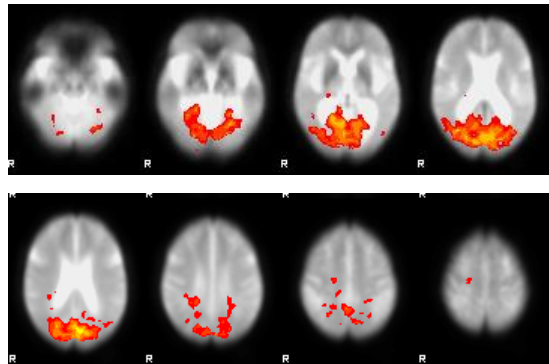
- Left primary visual cortex – No significant differences between groups
- Right primary visual cortex – No significant differences between groups

Summary of Main Findings

In summary, DLB subjects showed greater functional connectivity than controls for the highest number of seed regions, 6 in total including left and right seeds; bilateral caudate, left putamen, bilateral thalamus and right posterior cingulate cortex. The AD group showed greater functional connectivity than controls with 4 seeds; right caudate, left thalamus, left hippocampus and right posterior cingulate. AD subjects showed greater connectivity than DLB subjects for the right posterior cingulate, and the DLB group showed greater connectivity than the AD group for the bilateral putamen. No brain regions showed greater connectivity in controls compared to AD or DLB subjects. Tables 7.9 and 7.10 summarise these findings.

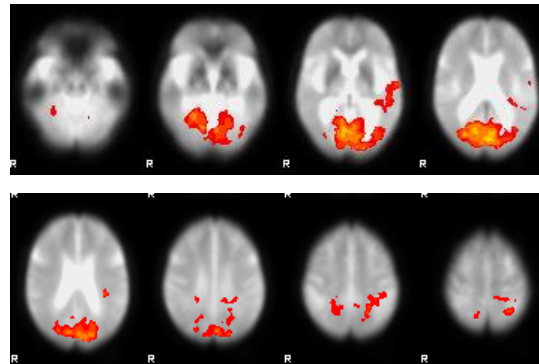
Figure 7.18: Functional Connectivity Maps for the Left Primary Visual Cortex

a) Controls Mean



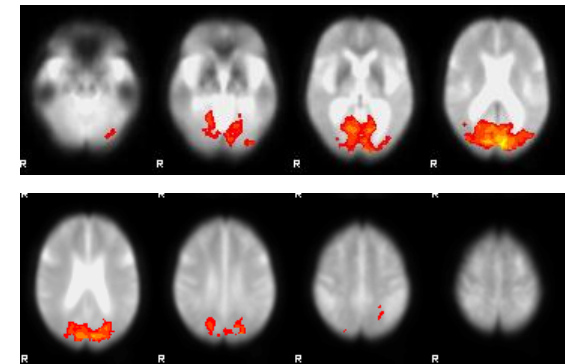
Brain Region	Coordinates	Z Stat
Cuneus	-5, -82, 18	6.26
Cuneus	12, -89, 7	5.67
Lingual Gyrus	17, -58, -1	5.56

b) AD Mean



Brain Region	Coordinates	Z Stat
Cuneus	-3, -85, 7	5.66
Cuneus	8, -84, 13	5.56
Lingual	6, -71, -2	5.24
Sup. Temporal	-36, -42, 11	3.89
Insula	-35, -35, 22	3.57
Mid. Temporal	-49, -33, 0	3.47
Caudate Tail	-33, -38, 6	3.45

c) DLB Mean

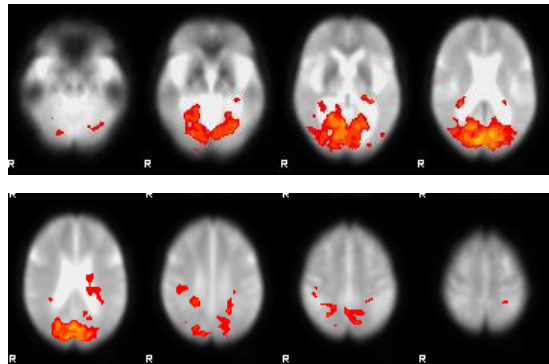


Brain Region	Coordinates	Z Stat
Cuneus	10, -84, 13	5.88
Cuneus	-9, -90, 6	5.87

Abbreviations: Mid. Temporal = Middle Temporal Gyrus; Sup. Temporal = Superior Temporal Gyrus

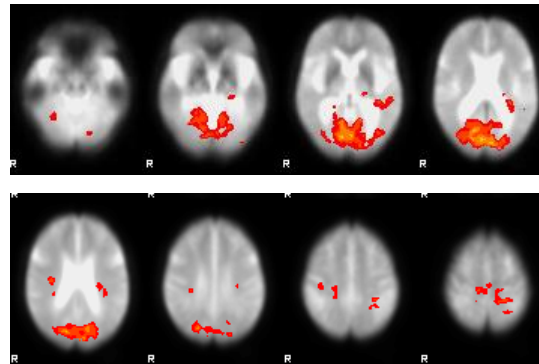
Figure 7.19: Functional Connectivity Maps for the Right Primary Visual Cortex

a) Controls Mean



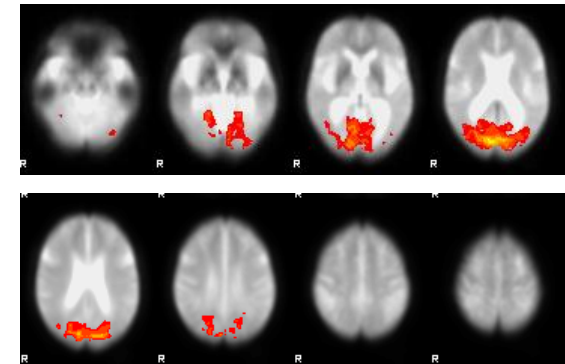
Brain Region	Coordinates	Z Stat
Cuneus	10, -87, 7	5.88
Cuneus	-11, -79, 7	5.43

b) AD Mean



Brain Region	Coordinates	Z Stat
Cuneus	13, -74, 8	5.38
Cuneus	-7, -88, 7	5.30
Lingual	2, -84, 2	5.29
Lingual	-3, -78, -3	5.01
Insula	30, -19, 25	3.95
Sub-gyral	-22, -48, 53	3.70
Caudate Tail	-31, -40, 11	3.64
Precuneus	-17, -48, 54	3.60
Inf. Parietal	-31, -45, 43	3.48
Paracent. L.	11, -34, 50	3.41
Sup. Parietal	-22, -62, 47	3.32
Mid. Temporal	-49, -35, 0	3.28
Paracent. L.	-2, -29, 56	3.02
Postcentral	35, -27, 46	2.96

c) DLB Mean



Brain Region	Coordinates	Z Stat
Cuneus	8, -87, 7	6.23
Cuneus	-11, -85, 7	5.44
Mid. Occipital	-18, -87, 17	5.40
Lingual	12, -89, -4	4.85

Abbreviations: Inf. Parietal; Inferior Parietal;
 Mid. Occipital = Middle Occipital; Mid.
 Temporal = Middle Temporal; Paracent. L =
 Paracentral Lobule; Sup. Parietal = Superior
 Parietal

Table 7.8: Peak Regions of Functional Connectivity with the Left and Right Primary Visual Cortex

Group Mean/ Difference	Left Primary Visual Cortex	Right Primary Visual Cortex
Control Mean	<ul style="list-style-type: none"> • Occipital: Cuneus, Lingual Gyrus 	<ul style="list-style-type: none"> • Occipital: Cuneus
AD Mean	<ul style="list-style-type: none"> • Occipital: Cuneus, Lingual Gyrus • Temporal: Superior, Middle, Caudate Tail • Sub-lobar: Insula 	<ul style="list-style-type: none"> • Frontal: Paracentral • Occipital Lobe: Cuneus, Lingual Gyrus • Sub-lobar: Caudate Tail, Insula • Temporal: Middle • Parietal: Postcentral, Sub-Gyral, Precuneus, Inferior, Superior
DLB Mean	<ul style="list-style-type: none"> • Occipital: Cuneus 	<ul style="list-style-type: none"> • Occipital: Cuneus, Middle, Lingual Gyrus

Table 7.9: Summary of the Differences between Groups in Functional Connectivity for Each Seed Region

Seed	Group Differences					
	Con > AD	AD > Con	Con > DLB	DLB > Con	AD > DLB	DLB > AD
Caudate Nucleus				✓		
Left				✓		
Right		✓		✓		
Putamen				✓		✓
Left				✓		✓
Right						✓
Thalamus		✓		✓		
Left		✓		✓		
Right				✓		
Hippocampus		✓				
Left		✓				
Right						
Posterior Cingulate						
Left						
Right		✓		✓	✓	
Precuneus						
Left						
Right						
Primary Visual						
Left						
Right						

Table 7.10: Summary of the Brain Regions Showing Significant Differences between Groups in Functional Connectivity for Each Seed Region

Seed	Group Differences
<p>Head of Caudate Nucleus</p> <p>Left</p> <p>Right</p>	<p>DLB > Con: Parahippocampal Gyrus (L), Precuneus (L/R), Posterior Cingulate (R)</p> <p>AD > Con: Posterior Cingulate (L/R), Precuneus (L), Cuneus (R)</p> <p>DLB > Con: Posterior Cingulate (L/R), Precuneus (L), Culmen of Vermis (R)</p>
<p>Putamen</p> <p>Left</p> <p>Right</p>	<p>DLB > Con: Precentral Gyrus (L), Postcentral Gyrus (L) Inferior Parietal (L)</p> <p>DLB > AD: Postcentral Gyrus (L) Inferior Parietal (L) Transverse Temporal (L)</p> <p>DLB > AD: Precentral Gyrus (L), Postcentral Gyrus (L), Inferior Parietal (L)</p>
<p>Thalamus</p> <p>Left</p> <p>Right</p>	<p>AD > Con: Precentral and Postcentral Gyrus (R), Inferior Parietal (R)</p> <p>DLB > Con: Precentral (L/R), Paracentral (R), Inferior Frontal (R), Cingulate (L/R), Insula (R)</p> <p>DLB > Con: Medial, Superior Frontal (R), Anterior Cingulate (R)</p>

Table 7.10 (Contd.): Summary of the Brain Regions Showing Significant Differences between Groups in Functional Connectivity for Each Seed Region

Hippocampus	
Left	AD > Con: Inferior Parietal (R), Insula (R)
Right	No significant differences
Posterior Cingulate Cortex	
Left	No significant differences
Right	AD > Con: Caudate Head (L/R), Caudate Body (R) DLB > Con: Cerebellar Tonsil (R), Culmen (R), Globus Pallidus (R), Anterior Cingulate (L) AD > DLB: Caudate Body (L/R)
Precuneus	
Left	No significant differences
Right	No significant differences
Primary Visual Cortex	
Left	No significant differences
Right	No significant differences

Neuropsychiatric Examinations

Clinical Assessment of Fluctuation Scale (CAFS) Score and Functional Connectivity

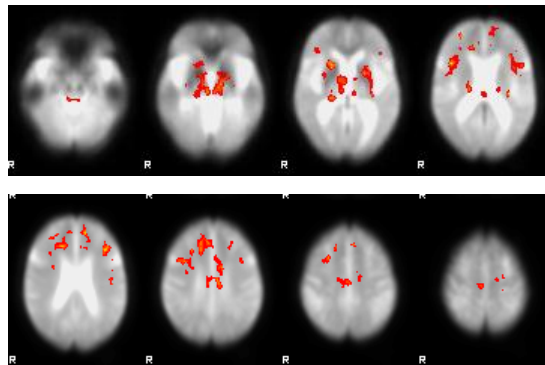
The effects of fluctuating cognition on connectivity with the mediodorsal nucleus of the thalamus were investigated in the DLB group. The thalamus has been implicated as playing a major role in the maintenance of consciousness (Perry and Perry, 2004), and at post-mortem increased nicotinic receptor binding in the mediodorsal nucleus of the thalamus is shown in DLB subjects with disturbances of consciousness than DLB without and control subjects (Pimlott et al., 2006). It was therefore expected that DLB subjects with a high CAFS score, indicating greater severity of fluctuating cognition, would have greater abnormalities in functional connectivity with the thalamus.

The DLB group was split according to their CAFS score, which ranged from 0 to 16. The mean CAFS score across all subjects (6.7) was used as a cut-off and subjects grouped as either low or high fluctuators (using the median value would have also resulted in the same grouping). Eight subjects were classified as low fluctuators (scoring 0-6 on the CAFS) and 7 subjects were classified as high fluctuators (scoring 8-16 on the CAFS).

There were no significant differences between low (Figure 7.20a for the left seed and 7.21a for the right seed) and high (Figure 7.20b for the left seed and 7.21b for the right seed) fluctuator groups in connectivity between the mediodorsal nucleus of the thalamus and all brain regions, though different patterns of connectivity were visible in the brain maps. For both the left and right seeds, the low fluctuating DLB subjects showed connectivity with more brain regions than the high fluctuating group. For both the left and right seeds, the high fluctuating DLB subjects showed a higher z statistic score (z statistic = 4.99 and 5.06) for connectivity within the thalamus compared to low fluctuating group (z statistic = 4.60 and 4.55).

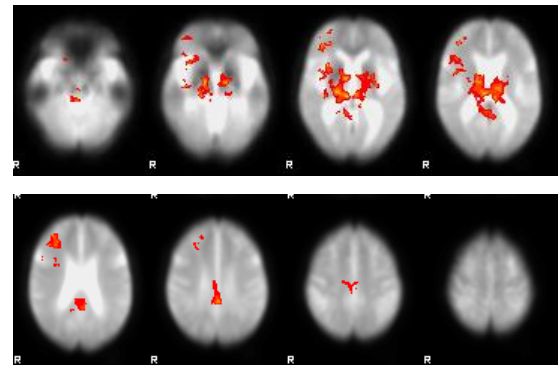
Figure 7.20: Functional Connectivity Maps for the Left Thalamus in DLB Subjects Split by Fluctuation Score

a) Low Fluctuators



Brain Region	Coordinates	Z Stat
Insula	40, 10, 17	4.51
Med. Frontal	21, 28, 24	4.38
Cingulate	17, 24, 28	4.21
Med. Frontal	-12, 41, 30	4.19
Putamen	14, 8, 0	4.74
Thalamus	-9, -19, 8	4.60
Culmen	-4, -33, -26	4.36
Insula	-31, -27, 12	4.27
Mid. Frontal	-36, 19, 27	4.12
Mid. Frontal	36, 4, 43	3.83
Precentral	32, -9, 36	2.64

b) High Fluctuators



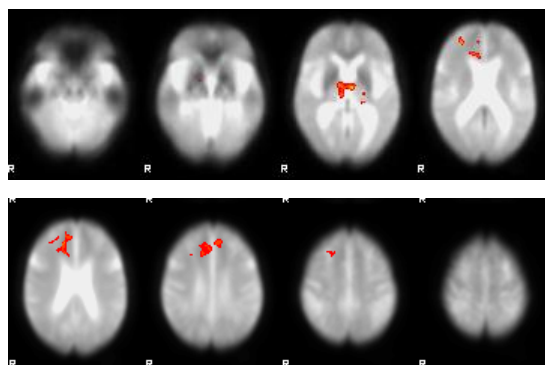
Brain Region	Coordinates	Z Stat
Thalamus	6, -30, 2	4.99
Thalamus	-1, -23, 7	4.58
Clastrum	30, 9, 6	4.53
Mid. Frontal	32, 43, 4	3.86
Inf. Frontal	44, 38, 3	3.85

Abbreviations: A. Cingulate = Anterior Cingulate Cortex; Inf. Frontal; Inferior Frontal; Med. Frontal = Medial Frontal; Mid. Frontal = Middle Frontal

Figure 7.21: Functional Connectivity Maps for the Right Thalamus in DLB Subjects Split by Fluctuation Score

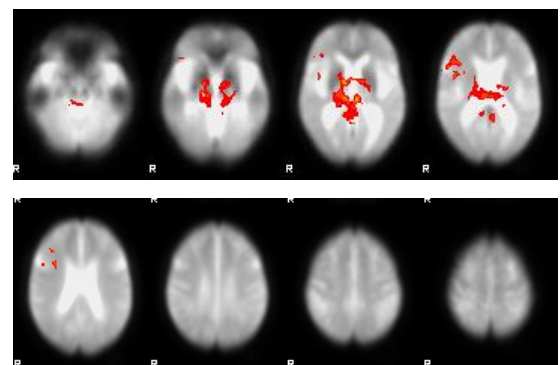
Subjects Split by Fluctuation Score

a) Low Fluctuators



Brain Region	Coordinates	Z Stat
Thalamus	-5, -13, 3	4.55
Thalamus	8, -9, -2	3.95
Mid. Frontal	27, 40, 19	3.83
Med. Frontal	8, 45, 25	3.79
A. Cingulate	12, 27, 18	3.49
Caudate Tail	-36, -29, -4	3.43
Med. Frontal	-5, 35, 35	3.38

b) High Fluctuators



Brain Region	Coordinates	Z Stat
Thalamus	4, -21, 8	5.06
Thalamus	-12, -19, 8	4.83
Precentral	49, 5, 11	4.10
Insula	40, 3, 11	4.07
Inf. Frontal	47, 22, 13	3.87
Clastrum	29, 12, 11	3.35

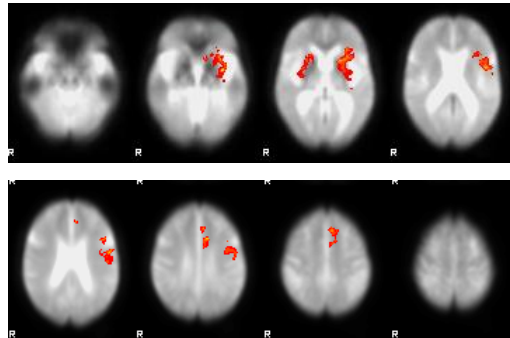
Unified Parkinson's Disease Rating Scale (UPDRS) and Functional Connectivity

Functional connectivity with the putamen was investigated in the DLB group based on their scores on the UPDRS. SPECT studies show dopaminergic loss in the putamen in DLB and Parkinson's disease compared to AD and controls (O'Brien et al., 2004a; Walker et al., 2002); therefore it was thought that connectivity with the putamen could be affected by severity of parkinsonian symptoms.

DLB subjects were split based on their median UPDRS score; 7 subjects scored ≤ 16 and so were classified in the low group (less severe parkinsonian symptoms) and 8 subjects scored ≥ 19 and so were allocated to the high UPDRS score group. No significant differences in connectivity with the putamen were found between the low and high UPDRS scoring DLB subjects. DLB subjects who had a low UPDRS score showed connectivity with more brain regions for both the left and right seeds (Figures 7.22a and 7.23a) compared to subjects who had a high UPDRS score (Figures 7.22b and 7.23b), though this was not significant. DLB subjects who had a high UPDRS score showed higher connectivity within the left and right putamen (as demonstrated by the higher z statistic score of 4.61 and 4.73), compared to the low UPDRS score group (z statistic score = 4.47 and 3.95).

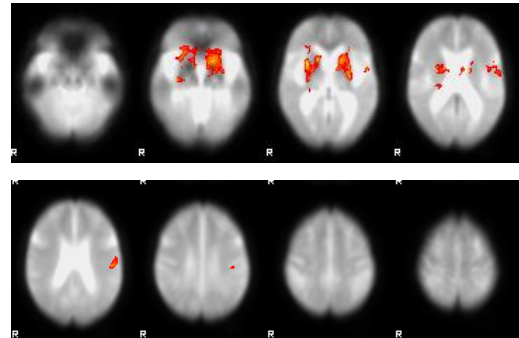
Figure 7.22: Functional Connectivity Maps for the Left Putamen in DLB Subjects Split by UPDRS Score

a) Low UPDRS



Region	Coordinates	Z Stat
Putamen	-23, 6, -1	4.47
Clastrum	-32, -4, -7	4.43
Cingulate	-13, 10, 37	4.04
Putamen	25, 14, 1	4.03
Caudate Head	12, 12, 0	4.02
Caudate Head	-10, 12, -6	3.90
Insula	-29, 21, 6	3.64
Inf. Frontal	-42, 9, 26	3.33
Sup. Frontal	-7, 20, 49	3.33
Clastrum	36, -9, 4	2.71

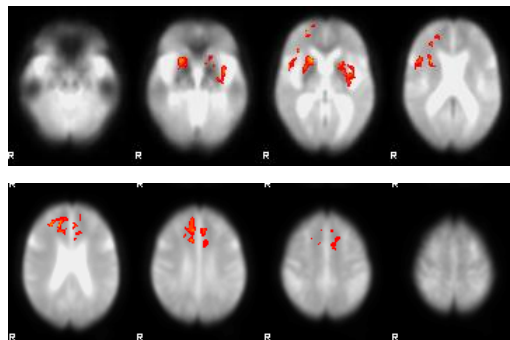
b) High UPDRS



Region	Coordinates	Z Stat
Putamen	29, 4, 5	4.61
Putamen	-25, 6, -1	4.59
Thalamus	14, -4, 10	4.44
Sup.Temp.	-51, -5, 3	3.85
Postcentral	-51, -24, 23	3.80
Precentral	-49, 0, 9	3.67
Insula	-42, -1, 14	2.78

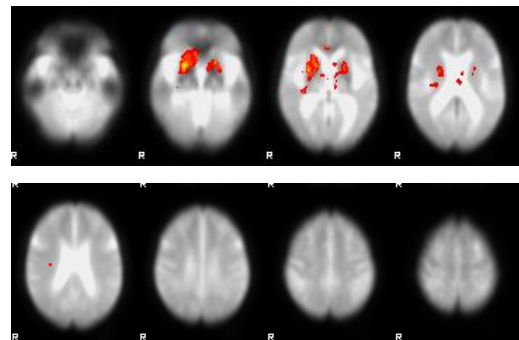
Figure 7.23: Functional Connectivity Maps for the Right Putamen in DLB Subjects Split by UPDRS Score

a) Low UPDRS



Region	Coordinates	Z Stat
Med. Frontal	16, 38, 24	4.14
Cingulate	15, 31, 29	4.06
Med. Frontal	-9, 26, 44	4.02
Sup. Frontal	27, 33, 30	3.99
Putamen	18, 14, 0	3.95
Mid. Frontal	25, 48, 9	3.64
Clastrum	28, 10, 17	3.45
Precentral	47, 2, 5	3.43
Putamen	-23, -1, -2	3.37
Clastrum	-36, -5, 3	3.33

b) High UPDRS



Region	Coordinates	Z Stat
Putamen	21, 5, -6	4.73
Putamen	-19, 9, -6	4.54
A. Cingulate	3, 28, 7	3.42

7.6 Discussion

7.6.1 Main Study Findings

This resting-state fMRI study investigated functional connectivity in control, AD and DLB subjects. The main findings of this study were abnormal functional connectivity with a number of seed regions in AD and DLB subjects compared to the control group. This abnormal pattern of connectivity in AD and DLB subjects was demonstrated by increased, or greater, connectivity than in the control subjects. Abnormal functional connectivity was most consistently seen in the DLB group with seeds in the caudate (bilateral), putamen (left), thalamus (bilateral) and posterior cingulate cortex (right) showing greater functional connectivity than in control subjects. AD subjects also showed greater connectivity than controls with a number of seed regions, namely the caudate (right), thalamus (left), hippocampus (left) and posterior cingulate cortex (right). Between the dementia groups the AD subjects showed greater connectivity than DLB subjects for the posterior cingulate cortex (right), and the DLB group showed greater connectivity than the AD group for the putamen (bilateral). The control group did not show greater connectivity than AD or DLB subjects with any seed regions.

The brain regions which AD and DLB subjects showed greater connectivity with than controls were consistent across both the dementia groups and included frontal (precentral gyrus), limbic (posterior cingulate cortex) and parietal (precuneus, inferior parietal and postcentral gyrus) regions. Between the dementia groups, the AD group showed greater connectivity between the posterior cingulate (right) and the body of caudate (bilateral) compared to DLB subjects. The DLB group showed greater connectivity between the putamen and frontal (left precentral gyrus), temporal (left transverse temporal gyrus) and parietal (left inferior parietal and postcentral gyrus) regions compared to AD subjects. For two seed regions, the precuneus and the primary visual cortex, there were no significant differences in connectivity between groups.

7.6.2 Findings in Relation to Hypotheses

It was hypothesised that functional connectivity would be abnormal in DLB subjects compared to AD and control subjects with seeds placed in the head of caudate nucleus, putamen, thalamus, posterior cingulate cortex, precuneus and primary visual cortex. It was also predicted that AD subjects' connectivity with the hippocampus, posterior cingulate cortex and precuneus would be abnormal compared to controls, and connectivity with the hippocampus would also be more affected in AD than DLB subjects. It was not certain whether abnormalities in the dementia groups would be characterised by increased or decreased functional connectivity, as some studies have reported that AD is characterised by increased connectivity whereas others have reported decreased connectivity. Hypotheses were formed based on findings from previous structural and functional studies showing abnormalities in these regions in dementia (see Chapter 4).

i. Head of Caudate Nucleus

It was predicted that DLB subjects would show abnormal connectivity with the caudate compared to control and AD subjects. This hypothesis was supported by findings from previous studies showing abnormalities in the caudate nucleus in DLB. Using SPECT, significantly reduced ligand binding (indicating dopamine transporter loss) was shown in the caudate in DLB subjects compared to AD and control subjects (O'Brien et al., 2004a), and diffusion tensor imaging has also shown abnormalities in the caudate in DLB compared to controls (Bozzali et al., 2005). Therefore, it was predicted that these abnormalities would affect the functional connectivity with this region, though a volumetric study has reported no significant differences in caudate volume between DLB, AD and controls (Almeida et al., 2003b).

The previous study in LLD, demonstrated increased/greater functional connectivity with the head of caudate nucleus in LLD versus controls (Chapter 5). It has been shown that depression is more common in DLB than AD subjects (Ballard et al., 1999) and in support of this the DLB subjects in this study had significantly higher GDS scores than the AD subjects, indicating greater depression severity. Therefore, it was expected that the caudate, a basal ganglia structure involved in emotional regulation, would be more affected in DLB than AD. However, when the DLB group was split based on median GDS score (splitting subjects using the mean would have given the same grouping), no significant differences between groups were noted for the left or right head of caudate nucleus. Though, the lack of statistically significant differences

between groups is highly likely to be due to the small group size of only 7 and 8 subjects per group.

The results from this study showed that DLB subjects' connectivity was abnormally increased compared to controls between the caudate (bilaterally) and brain regions including the posterior cingulate cortex and precuneus (bilaterally). This is similar to the findings in the LLD study, where increased caudate connectivity (bilaterally) was also reported in LLD versus control subjects. Similar to the results for the DLB subjects, the LLD subjects also showed greater connectivity with the precuneus (and a number of other regions) compared to controls, and no regions of greater connectivity in controls versus LLD (see Chapter 5). Connectivity with the right head of caudate nucleus was more affected in AD than controls, as demonstrated by increased connectivity, and similar to the results for the DLB subjects this was with the posterior cingulate cortex and the precuneus (bilaterally). A significant difference in functional connectivity with the caudate in AD compared to controls had not been predicted, but in line with the hypothesis the caudate showed more regions of increased connectivity in DLB versus controls than AD versus controls.

ii. Putamen

Similar to the hypothesis for the caudate, it was predicted that DLB subjects would show abnormal connectivity compared to control and AD subjects for the putamen also. It was hypothesised that this would most likely be characterised by decreased connectivity in DLB with the putamen, however, similar to the findings for the caudate, connectivity was increased. DLB subjects showed greater connectivity with the putamen compared to control (left only) and AD (bilaterally) subjects in similar brain regions; frontal (precentral), parietal (inferior and postcentral) and temporal (transverse) areas (all left hemisphere). Abnormally increased connectivity with the putamen was specific to DLB, with no other groups showing significantly increased connectivity.

Previous studies have reported abnormalities in the putamen in DLB. A volumetric study showed significantly decreased putamen volumes in DLB compared to AD and controls (Cousins *et al.*, 2003). Diffusion tensor imaging has demonstrated tissue organisation abnormalities in the putamen in DLB compared to controls (Bozzali *et al.*, 2005) and SPECT studies have shown significant dopamine transporter loss in the putamen in DLB compared to AD and controls (O'Brien *et al.*, 2004a). These studies show clearly that the putamen is affected in DLB, and additionally the studies by Cousins *et al.* (2003) and O'Brien *et al.* (2004) show that these abnormalities are

specific to DLB and enable differentiation from AD (O'Brien et al., 2004a; Cousins et al., 2003). This is supported also by the findings here, as abnormally increased functional connectivity with the putamen was only reported in the DLB group.

The results from the investigation of the relationship between the UPDRS score and putamen functional connectivity in DLB subjects (discussed further later) showed no significant differences between DLB subjects when split on high or low UPDRS score. Therefore the increased functional connectivity with the putamen in DLB subjects cannot solely be explained by the greater severity of motor symptoms in this disorder. Though as group sizes were small (7 or 8 subjects per group when splitting by UPDRS), the effect of severity of motor symptoms on connectivity cannot be ruled out.

iii. Thalamus

It was hypothesised that DLB subjects would show abnormal thalamic connectivity. This hypothesis was supported by previous studies showing the role of the thalamus in maintenance of consciousness (Perry and Perry, 2004) and increased nicotinic receptor binding in the mediodorsal nucleus in DLB subjects with disturbances of consciousness than DLB without and control subjects at post-mortem (Pimlott et al., 2006).

Connectivity was found to be increased in DLB subjects compared to controls between the thalamus (bilaterally) and a number of brain regions including frontal (e.g. precentral gyrus) and limbic (cingulate) regions (mainly right hemisphere). AD subjects also showed abnormal connectivity for the left thalamus compared to controls in frontal (precentral gyrus) and parietal (inferior parietal and postcentral gyrus) regions (all right hemisphere). The thalamus had not been predicted to be affected in AD, but previous studies using voxel based morphometry have shown significant grey matter loss in the thalamus in AD, and also greater loss compared to DLB (Burton et al., 2002). Similar to the findings in this study for the caudate, connectivity was affected bilaterally in DLB subjects and unilaterally in AD subjects. This supports the hypothesis for this seed region in that functional connectivity abnormalities were greater in DLB than AD subjects.

iv. Hippocampus

With the hippocampus seed, it was predicted that AD subjects would show abnormal connectivity compared to controls and DLB subjects. It was not certain whether abnormal connectivity in AD subjects would be observed as increased or decreased connectivity as previous studies have reported both functional connectivity abnormalities in AD subjects. Increased connectivity was found in AD versus control

subjects between the left hippocampus and inferior parietal and insular regions (right hemisphere only) in this study. It might have been expected that hippocampal connectivity would be more likely to be decreased in AD, as many studies have reported that the hippocampus is affected early in the disease course of AD in terms of neurofibrillary tangles and neuritic plaques and atrophy (Du et al., 2001; Killiany et al., 2000; Jack et al., 1997; Jack et al., 1992). However, this finding is consistent with the findings from this study for other seed regions, in that connectivity was increased with seeds that were expected to be functioning abnormally in dementia compared to control subjects. Similarly, others groups have also reported increased connectivity with the left hippocampus in AD subjects compared to controls (Wang et al., 2006).

It was predicted that there would be no significant difference in connectivity between DLB and control subjects, and the findings from this study support this hypothesis. A significant difference in connectivity with the hippocampus between AD and DLB subjects was also predicted, as studies have shown the hippocampus is more affected in AD than DLB (Barber et al., 2000), but no differences in hippocampus functional connectivity were reported between the dementia groups in this study.

v. Posterior Cingulate Cortex

Connectivity with the posterior cingulate cortex was hypothesised to be abnormal in dementia subjects compared to controls. The results from this study showed abnormally increased connectivity with the right posterior cingulate in DLB and AD subjects compared to controls. A significant difference in connectivity between AD and DLB subjects was also observed, with AD subjects showing greater connectivity between the right posterior cingulate and the caudate body (bilaterally). It had been hypothesised that the posterior cingulate would be more affected in DLB than AD because of the greater attentional deficits characteristic of DLB (Ballard et al., 2001). However, it seems that connectivity is more affected in AD than DLB as demonstrated by the increased connectivity.

The posterior cingulate cortex is a key region of the default mode network (Raichle et al., 2001). This network has been shown to be more active at rest and has therefore been proposed to be involved in ongoing, or intrinsic, brain activity, for example day dreaming (Raichle and Snyder, 2007; Raichle et al., 2001) (see Chapter 2). The regions showing increased connectivity in AD and DLB compared to controls included the caudate head and body and the globus pallidus. These are not regions which have been shown to form part of the default mode network. Therefore it could be that in dementia, subjects preferentially (aberrantly) connect and show greater activity

with regions which are not part of the default mode network. This abnormal connectivity in dementia could therefore compromise activity within the default mode network regions, for example the medial prefrontal and lateral parietal cortices (Raichle et al., 2001), and would mean the network may not be functioning as effectively in these subjects.

The default mode network has been shown to play a role in episodic memory processing (Greicius et al., 2004). Increased connectivity between a default mode network region (posterior cingulate) and non-default mode network regions in dementia compared to controls, and also in AD compared to DLB was reported in this study. This finding of abnormal default mode network connectivity could be associated with memory impairment, which is characteristic of AD, and could also explain why memory structures (e.g. the medial temporal lobe) are more affected in AD than DLB (Barber et al., 2000). Additionally, studies have localised amyloid beta plaques to default mode network brain regions in early stage AD (Buckner et al., 2005), providing further support to explain the prominent memory impairments characteristic of AD. The default mode network is known to be involved in attending to environmental stimuli (Gusnard et al., 2001; Raichle et al., 2001), therefore this could be associated with why abnormalities are observed in the posterior cingulate in DLB compared to controls, as attentional deficits are characteristic of DLB, and greater than in AD (Ballard et al., 2001).

These findings in AD and DLB subjects of increased connectivity between the posterior cingulate and brain regions that are not part of the default mode network propose that the default mode network is functioning abnormally in dementia, with greater abnormalities in AD compared to DLB. Previous studies have also reported that this network is affected in AD (Zhang et al., 2009; Wang et al., 2006; Greicius et al., 2004). Some studies have reported decreased connectivity (Greicius et al., 2004), whereas others have reported both increased and decreased connectivity in AD (Zhang et al., 2009; Wang et al., 2006). Similar to the findings in this study, a task-based study also reported abnormalities in connectivity in the posterior cingulate in AD and DLB, but no significant differences between AD and DLB subjects were shown (Sauer et al., 2006). As will be discussed in greater detail later, it is difficult to directly compare studies as methods of analysis have varied, Greicius *et al.* (2004) used independent component analysis, and the AD subjects in the Wang *et al.* (2006) study were younger and had a higher MMSE score than subjects in this study (Wang et al., 2006; Greicius et al., 2004).

vi. Precuneus

For the precuneus it was predicted that both AD and DLB subjects would show abnormal connectivity compared to control subjects, and additionally DLB subjects would show abnormalities in connectivity compared to AD subjects. Similar to the posterior cingulate, the precuneus has been shown to form part of the default mode network (Raichle et al., 2001) and previous studies in AD have reported reduced functional connectivity in this region (Zhang et al., 2009; He et al., 2007; Zang et al., 2004). SPECT studies in DLB report decreased perfusion in the precuneus compared to AD (Colloby et al., 2002), therefore it was expected that this might be reflected in the functional connectivity with this region.

No significant differences between groups for connectivity with the precuneus seed were found in this study. This finding highlights the specificity of the other seed regions in showing differences in functional connectivity between dementia and control subjects. Although SPECT studies report decreased perfusion in the precuneus in DLB (Colloby et al., 2002), it is not certain whether perfusion deficits also affect functional connectivity. Similar to the results reported here, task-based studies investigating functional connectivity have reported abnormalities in the posterior cingulate in DLB and AD, but the precuneus was not shown to be affected in AD or DLB (Sauer et al., 2006).

vii. Primary Visual Cortex

For the seed placed in the primary visual cortex, there were no significant differences in functional connectivity between any of the groups. It was predicted that connectivity would be normal in AD subjects as vision is not affected in this disorder. However, in DLB, resting-state SPECT studies have reported decreased perfusion in DLB compared to AD in the primary visual cortex (Colloby et al., 2002), associated with the core feature of visual hallucinations in DLB (McKeith et al., 1996). Therefore, it was thought that this abnormality in DLB subjects may be reflected in the functional connectivity results for this seed region. However, it could be that in order for DLB subjects to experience hallucinations their primary visual cortical system needs to be intact, which would explain why no significant differences were found for this seed region.

The results here showed that resting-state fMRI measures were able to report significant differences in functional connectivity in brain regions that had been hypothesised to be affected in dementia, but also showed no significant differences in brain regions which had not been expected to be affected, for example the primary

visual cortex in AD. The findings of no significant differences between groups provides further support for the differences observed between dementia groups and controls being of neuronal origin and not related to non-neuronal fluctuations or artefact.

Neuropsychiatric Measures

Within the DLB group, the relationship between scores on neuropsychiatric measures and functional connectivity were investigated. DLB subjects with a higher burden of neuropsychiatric features and cognitive impairments were hypothesised to display greater abnormalities in functional connectivity. Scores for cognitive fluctuations (clinical assessment of fluctuation scale [CAFS]) and severity of motor features of Parkinson's (unified Parkinson's disease rating scale [UPDRS]) were used to split the DLB group. No statistically significant differences between groups were reported, but visibly differences in the functional connectivity maps did seem evident.

The DLB subjects who had a high score on the CAFS (to measure fluctuating cognition) showed greater connectivity within the thalamus (bilaterally), as indicated by a higher z statistic score, compared to the low fluctuating cognition group, though this was not significant. The low fluctuating DLB subjects showed connectivity with more brain regions than the high fluctuating DLB subjects, though this was also not significant.

The thalamus has been implicated as playing a major role in the maintenance of consciousness (Perry and Perry, 2004). The group showing high fluctuating cognition was therefore expected to have greater abnormalities in functional connectivity than the low fluctuating group. However, no significant differences in functional connectivity between groups were found, but as the number of subjects in each group was low this would have made it difficult for results to reach significance.

Functional connectivity results with the putamen based on UPDRS scores showed similar results to the thalamus functional connectivity based on CAFS score. DLB subjects who had a low score (i.e. less severe parkinsonian symptoms) appeared to have connectivity with more brain regions compared to subjects who had a high UPDRS score. It could be that connectivity between distinct brain regions is important in preventing the development of parkinsonian symptoms in DLB, and due to the lack of connectivity in the high UPDRS score group the putamen is overly active and so shows a larger cluster of activity (as demonstrated by the higher z statistic score for the putamen in this group).

In support of this, a study by Wu *et al.* (2010) investigating functional connectivity in Parkinson's disease, showed that during the resting-state, subjects with Parkinson's disease show significantly decreased connectivity with the left putamen and this decreased connectivity was thought to be associated with difficulty initiating movements in this disorder (Wu *et al.*, 2010). A study by Cousins *et al.* (2003) which reported reduced putamen volume in DLB, also found no direct correlation between the degree of volume loss and severity of parkinsonism (Cousins *et al.*, 2003). The number of DLB subjects in the Cousins *et al.* (2003) study (n=14) was similar to this study (n=15).

In summary, although the connectivity maps appeared different between the DLB groups split on neuropsychiatric measures no significant differences between groups was reported. The lack of significant differences between groups is likely to be due to the sample size of only 7 or 8 subjects per group being too low for significance to be reached.

7.6.3 Findings in Relation to other Studies

Previous studies have reported some similar results to our findings. A study by Zhang *et al.* (2009), also using a seed-based correlation approach, reported increased functional connectivity in AD subjects compared to controls, which was also reported in this study. Specifically, Zhang *et al.* (2009) reported increased connectivity between the posterior cingulate and the left basal ganglia and similarly this study also showed increased connectivity between the posterior cingulate (right) and left head of caudate nucleus in AD compared to control subjects. However, Zhang *et al.* (2009) also reported decreased connectivity in AD versus controls, for example between the posterior cingulate and the precuneus. In contrast, in this present study, no regions of greater connectivity were found in control versus AD subjects. The connectivity maps in AD subjects for the left precuneus did appear to show less connectivity than controls, though this was not significant. In contrast to this study, Zhang *et al.* (2009) used a tool to overlay the whole posterior cingulate, whereas in this study seeds of 4 voxels were manually placed in both the left and right regions. Zhang *et al.* (2009) also did not include covariates of no interest (for example a global signal mask or white matter seeds) to correct for non-neuronal fluctuations, as this study did. The AD and control subjects were younger in the Zhang *et al.* (2009) study (72 and 71 years respectively),

compared to this study (77 and 76 years respectively), and the AD subjects had a slightly higher mean MMSE score (23.0 versus 21.1 in this study) (Zhang et al., 2009).

An early resting-state fMRI study by Li *et al.* (2002) reported significantly lower connectivity within the hippocampus in AD compared to control subjects. Contrary to the Li *et al.* (2002) study, this study showed increased connectivity between the left hippocampus and right inferior parietal and insula regions in AD compared to controls, and no regions of greater connectivity in controls compared to either of the dementia groups. The study by Li *et al.* (2002) used a different method and analysis approach to this study; therefore it is difficult to directly compare study findings. Li *et al.* (2002) measured the correlation between pairs of voxels within the hippocampus only, whereas in this study correlations between the hippocampus and all other brain regions were investigated. Li *et al.* (2002) did not include pre-processing steps of temporal filtering, for example, to remove non-neuronally related fluctuations, whereas the data in this study was band-pass filtered. Also, subjects were younger in the Li *et al.* (2002) study (controls mean age = 70 years and AD subjects mean age = 72 years) compared to this study, and although MMSE scores were measured they were not considered a factor for exclusion in the AD group, which could explain some of the differences reported (Li et al., 2002).

Others have also reported similar findings to Li *et al.* (2002) of reduced connectivity within/between the hippocampus and other brain regions. Wang *et al.* (2006) showed reduced connectivity between the right hippocampus and several brain regions, including limbic and temporal regions. However, similar to this study they also reported increased connectivity in AD, specifically between the left hippocampus and right dorsolateral prefrontal cortex. The Wang *et al.* (2006) study also used a seed-based correlation analysis approach, but in contrast to this study they used the whole region, whereas in this study 4 voxels were placed within the hippocampus. They also did not include covariates of no interest to correct for spurious fluctuations, as were included in this study. In comparison to the subjects in this study, the subjects in the Wang *et al.* (2006) study were younger (mean age 70 years) and the AD subjects were less cognitively impaired (MMSE score of 23.1 versus 21.1 in this study) (Wang et al., 2006).

A study by Allen *et al.* (2007) showed that in control subjects the hippocampus (bilaterally) had extensive connectivity between frontal, parietal, occipital and temporal regions, whereas in AD a more restricted pattern was seen, and an absence of connectivity with the frontal lobes (Allen et al., 2007). Similar to Allen *et al.* (2007) this

study found a more restricted pattern of connectivity in the AD group compared to controls for the right hippocampus. In this study, controls showed connectivity with sub-lobar and occipital regions which were not present in the AD group, though this was not found to be significant. Some of the methods used in the study reported here and the Allen *et al.* (2007) study were similar as they investigated connectivity with left and right hippocampi separately and placed seeds within the hippocampus, rather than using the whole region. However, the seeds Allen *et al.* (2007) placed were larger and the method of placing was different; 5 contiguous voxels, whereas in this study 4 voxels were placed in a 2 by 2 arrangement. Additionally, in contrast to this study, Allen *et al.* (2007) did not correct for global signal, and global signal correction has been shown to decrease false correlations in the data (Allen et al., 2007).

Increases in functional connectivity in AD were also reported by Wang *et al.* (2007) using an anatomic parcellation of the whole brain. In AD, they reported increased connectivity in similar regions to where this study reported increased connectivity in AD, namely the caudate, thalamus, hippocampus, precuneus, lingual and postcentral gyrus. Though, in contrast to the study here, Wang *et al.* (2007) also reported decreased connectivity in AD versus control subjects between prefrontal and parietal lobes, however as whole lobe connectivity was not investigated in this study it is difficult to compare their findings with this study. Additionally, Wang *et al.* (2007) reported decreased connectivity with the posterior cingulate cortex, a region where this study showed increased connectivity (Wang et al., 2007). The subjects in the Wang *et al.* (2007) study were younger (mean age of 70 years), and the AD subjects had a higher mean MMSE score (23.1). Wang *et al.* (2007) also averaged the time-series over all brain voxels within a brain region, whereas in this study the mean time-series in the seed region only was used, for example 4 voxels. Similar to the study reported here, Wang *et al.* (2007) followed the pre-processing steps from the Fox *et al.* (2005) study (Wang et al., 2007; Fox et al., 2005).

Comparable with the findings reported here, He *et al.* (2007) showed increased connectivity in AD subjects in the cuneus, lingual and fusiform gyrus, which were all regions where this study reported increased functional connectivity in AD compared to control subjects. In contrast, He *et al.* (2007) reported decreased connectivity in the posterior cingulate and precuneus in AD, which this study did not find (He et al., 2007). The method of analysis used by He *et al.* (2007) was different to this study. He *et al.* (2007) used a model-free approach, regional homogeneity, which measures the time-series of a specific voxel and correlates this with its nearest neighbours. Additionally,

subjects were younger (mean age of 70 years) and AD subjects were less cognitively impaired (mean MMSE score of 23.2) (He et al., 2007). Other groups have also reported decreased posterior cingulate cortex connectivity in AD compared to controls (Gili et al., 2010; Greicius et al., 2004). In contrast to this study, Gili *et al.* (2010) and Greicius *et al.* (2004) both used model-free approaches of independent component analysis, the subjects in the Gili *et al.* (2010) study were younger (controls mean age = 64 years and AD subjects mean age = 72 years) and the Greicius *et al.* (2004) study was in subjects with very mild or mild dementia (Gili et al., 2010; Greicius et al., 2004).

There have been no resting-state studies in DLB published to date. However, a task-based study in DLB, AD and control subjects showed significantly greater activity in the superior temporal sulcus in DLB compared to AD (Sauer et al., 2006). Consistent with the Sauer *et al.* (2006) finding, this study also reported increased connectivity in DLB compared to AD in temporal regions (between the left putamen seed and the left transverse temporal gyrus). Sauer *et al.* (2006) reported that the default mode network was more affected in DLB and AD compared to control subjects. Task-related deactivations of a default mode network region, the posterior cingulate cortex, were found to be significantly decreased in DLB and AD compared to controls (Sauer et al., 2006). This could be linked with the finding in this study of increased connectivity with the posterior cingulate in AD and DLB at rest, as mechanisms to suppress this resting-state network when it is not required in the task state may be inhibited, therefore the network remains abnormally increased in dementia. The mean age of subjects in the AD and DLB groups in the Sauer *et al.* (2006) study was similar to this study (78 years), though the control group was younger, mean age of 71 years, versus 76 years in this study. The dementia subjects in this study were also more cognitively impaired compared to the Sauer *et al.* (2006) study. In the Sauer *et al.* (2006) study, AD subjects showed a mean MMSE score of 22.9 (versus 21.1 in this study) and DLB subjects a mean MMSE score of 23.7 (versus 19.5 in this study) (Sauer et al., 2006).

It is difficult to directly compare findings between studies as there can be great variation, as discussed above, in subject age, stage of dementia and the methods used to analyse the data, for example. Some studies have used model-based approaches of seed-based correlation analysis, whereas others have used model-free methods of independent component analysis and additionally other model-free methods have also been used in dementia studies, e.g. regional homogeneity. Even between studies using the same methods, for example seed-based correlation analysis, there can be great variation in methodology, i.e. some will filter out spurious fluctuations and include

covariates of no interest, whereas others will not include these additional pre-processing steps.

7.6.4 Summary

This study, in general, reported abnormal functional connectivity with the seed regions that had been predicted to be more affected in DLB and AD subjects compared to controls. Abnormal connectivity was characterised by increased, or greater, connectivity in the dementia subjects compared to controls. Similarly, other resting-state fMRI studies have also reported increased connectivity in AD compared to controls (Zhang et al., 2009; He et al., 2007; Wang et al., 2007; Wang et al., 2006). The findings from this study support the compensatory recruitment hypothesis which has previously been proposed by other studies (Zhang et al., 2009; Wang et al., 2007). Brain regions which are not affected in dementia could be recruited to compensate for the poor functioning of regions which are affected by the disorder, for example temporal brain regions in AD subjects. Hence, when a seed is placed in a brain region which is not affected in dementia increased connectivity is observed, as the circuits that this seed forms connections with are increasing their activity to compensate for damage elsewhere.

Another possibility may be that there is a loss of an inhibitory function in dementia, needed to suppress certain brain regions. At rest, regions which are not needed for normal brain functioning are active in dementia because of an abnormality in inhibitory mechanisms, consequently there is no control over regions which are not needed at the time. Therefore, increases in connectivity in dementia subjects compared to healthy controls are observed.

Seeds placed in the precuneus and the primary visual cortex showed no significant differences between groups in terms of connectivity. This highlights the specificity of functional connectivity measures and the importance of seed region selection, i.e. resting-state functional connectivity is not abnormal in all brain regions in dementia. Additionally, the findings here emphasise the accuracy of functional connectivity measures as regions which had been hypothesised to show no significant differences between groups, for example the primary visual cortex (in AD versus control subjects) and the hippocampus (in DLB versus control subjects) did not demonstrate significant differences. Importantly, this study showed significant differences between the dementia groups, which proposes that certain brain regions are

more affected in AD than DLB, and in DLB than AD, which may aid in greater understanding of the neurobiology of the 2 disorders.

7.6.5 Strengths and Limitations

Strengths of this study are that the AD and DLB groups were subject to full and careful clinical and cognitive assessment and rigorous diagnosis by two independent experienced clinicians (independent of the consultant making the initial clinical diagnosis). Groups were well matched in terms of subject numbers, gender and age. The model-based analysis method used in this study enabled the investigation of the correlation of SLFs between seed regions and all other brain regions based on an *a priori* hypothesis to select the seed region. In this study, the hypotheses were based on findings from previous studies showing these regions to be functioning abnormally and/or atrophied in DLB and/or AD compared to control subjects. In contrast, some other studies in AD have only looked at correlations between specific seed regions, or just one seed and the rest of the brain (generally the hippocampus or posterior cingulate cortex in AD), or investigated connectivity within a seed region, thus potentially missing important changes elsewhere in the brain. Other studies have used model-free methods where no prior hypothesis is required and all connectivity can be searched for. The seed regions investigated in this study were all placed manually by the author. This has the advantage over automated methods as the seed placing is less likely to be affected by differences in atrophy between subjects.

Resting-state studies benefit from simplicity of experimental design and no task has to be practised or performed, which means they are advantageous in cognitively impaired patient groups for whom it may be more difficult to adhere to a task. Therefore, patient compliance and tolerance is generally high and subject head motion is reduced.

Limitations of this study are that model-based techniques are biased by the choice of seed region and so functional connectivities of interest can be missed if they do not show connectivity with the seed. Model-free methods do not require predefined seeds or a temporal model, though, the lack of specificity of model-free approaches means that results can be hard to interpret. In this study, subjects' images were registered to a mean template (comprised from all study subjects functional data), however, as atrophy has been shown to be significantly higher in dementia subjects compared to controls (O'Brien et al., 2001), for future work it may be more accurate to

have a mean brain template for each patient group. The number of subjects in each group was relatively small in this study and this could have affected the differences seen between groups, with larger numbers of subjects in each group more/greater significant differences between groups may have been observed. However, other resting-state fMRI studies have also had comparable numbers, for example the study by Zhang *et al.* (2009) investigated 16 AD and 16 control subjects (Zhang et al., 2009), whereas others have had fewer subjects, Li *et al.* (2002); 10 AD and 9 controls (Li et al., 2002), and Gili *et al.* (2010); 11 AD and 10 controls (Gili et al., 2010).

Fluctuations unrelated to neuronal activity have been shown to influence resting-state data, for example cardiac (Chang and Glover, 2009) and respiratory (Birn et al., 2006; Wise et al., 2004) related signals. These fluctuations have been shown to correlate in grey matter brain regions and as they are of non-neuronal origin they are not of interest in functional connectivity analysis (see Chapter 6 for more detail). In this study, it was aimed to correct for these spurious fluctuations by carrying out additional pre-processing and regression steps which can be incorporated within the model-based analysis. Resting-state is difficult to control, as between subjects it can vary greatly depending on how active a subjects' brain is at rest and what the subject is thinking at the time of scanning. Additionally, as there is no definitive diagnosis for AD and DLB, subject groups cannot be confirmed until autopsy; however subjects in this study met consensus criteria guidelines for AD and DLB which have previously been shown to have good sensitivity.

7.7 Conclusion

In conclusion, the main findings of this study were of significantly increased, or greater, functional connectivity in AD and DLB compared to control subjects, with greatest functional connectivity generally reported in the DLB group. DLB subjects showed greater connectivity than controls with seed regions placed in the head of caudate nucleus (bilateral), putamen (left), thalamus (bilateral) and posterior cingulate cortex (right). AD subjects showed greater connectivity than controls for the caudate (right), thalamus (left), hippocampus (left) and posterior cingulate (right). Control subjects did not show greater connectivity with any seed region compared to AD or DLB subjects. Significant differences between the AD and DLB groups in functional connectivity were also found. Specifically, the AD group showed significantly greater connectivity compared to DLB subjects with the posterior cingulate (right), and DLB subjects showed greater connectivity with the putamen (bilateral). These findings may aid in greater understanding of the neurobiology of AD and DLB, which could assist in differentiation of the disorders that commonly show similar characteristics but require different management. Further studies are needed to replicate these findings and additionally to make the methodology more consistent between studies. Chapter 8 of this thesis will discuss this in more detail.

Chapter 8

Summary

8.1 Main Findings

This research used novel magnetic resonance imaging (MRI) approaches to investigate functional connectivity between key brain regions affected by the two most common psychiatric disorders in late-life; depression and dementia, specifically Alzheimer's disease (AD) and dementia with Lewy bodies (DLB). Using functional MRI (fMRI), spontaneous low-frequency fluctuations (SLFs) in the blood oxygen level dependent (BOLD) signal were measured whilst subjects rested in the scanner. BOLD fMRI enables the measurement of neuronal activation through its coupling with the haemodynamic response (cerebral blood flow, volume and metabolism rate of oxygen). The mean BOLD signal time-series of SLFs in seed regions were cross-correlated with all other brain voxels to measure functional connectivity. The seed regions used in this research had previously been identified in neuroimaging studies as functioning abnormally in depression and dementia. SLFs represent synchronisation of neuronal activity; therefore differences between subjects reflect differences in the underlying networks.

The main aims of this work were to determine neurobiological changes in late-life depression (LLD), AD and DLB, in order to better understand brain dysfunction in these disorders. In turn it is hoped that this will inform the development of early diagnostic methods and more effective treatments to improve patient management. It is difficult to distinguish between early stage AD and DLB, both requiring different treatment strategies, and it was hoped this study would provide a differential diagnosis in these cases.

Functional Connectivity in Late-Life Depression

In the first resting-state study reported here (Chapter 5); functional connectivity between the head of caudate nucleus and all other brain regions was investigated in subjects with LLD and controls. This study showed significant functional connectivity between the head of caudate and frontal areas in controls, whereas in LLD, connectivity was observed over a much wider area. Significantly greater functional connectivity in

LLD compared to controls was demonstrated bilaterally with the head of caudate nucleus and a number of brain regions; frontal, sub-lobar, limbic, parietal and temporal. Conversely, no brain regions showed greater connectivity in controls than LLD. Additionally, depression severity was found to correlate with increased functional connectivity for the left caudate nucleus.

This study demonstrated that LLD is characterised by widespread functional connectivity with a seed region in the head of caudate nucleus, whereas in controls connectivity was frontally coordinated. These findings could be used to inform more effective treatments in LLD which target specific brain regions where significantly greater functional connectivity abnormalities are reported in LLD versus control subjects. This study confirmed findings from previous structural studies showing caudate abnormalities in LLD (Butters et al., 2009), which provides further support that specific brain regions could be more affected in LLD than early-onset depression.

Pre-Processing Methodology

The next step was to apply the same methodology to a resting-state study investigating functional connectivity in dementia subjects; however a pattern of global synchronicity was observed in some subjects, not previously seen in the LLD study. This global synchronicity is thought to be caused by spurious fluctuations, unrelated to neuronal activity, for example physiological artefacts (respiratory and cardiac related). Fluctuations from non-neuronal processes can introduce coherences in the data and increase the connectivity observed, as they have been shown to be localised to grey matter brain regions (Birn et al., 2006).

Over recent years, studies have reported methods to correct for spurious fluctuations, in order for connectivity of neuronal origin only to be investigated. These methods were investigated in detail (Chapter 6). Additional steps of pre-processing of the functional data, for example filtering, and including covariates of no interest in the regression analysis were shown to improve the accuracy of the data by removing patterns of global synchronicity related to non-neuronal signals. A method was agreed on (Fox et al., 2005) which was shown to filter out spurious fluctuations from the dementia data and which has been applied in many other resting-state studies (in younger and older subjects), and specifically in Alzheimer's disease (Wang et al., 2007), therefore the method was highly applicable to the data here.

Functional Connectivity in Dementia

The second resting-state study investigated functional connectivity in AD, DLB and control subjects (Chapter 7). Seed regions were placed in the head of caudate nucleus, thalamus, putamen, hippocampus, posterior cingulate cortex, precuneus and primary visual cortex. The approach used here involved additional pre-processing steps to correct for non-neuronally related SLFs, informed by the work carried out in Chapter 6. This resting-state study demonstrated significantly increased connectivity in AD and DLB subjects compared to controls with a number of seed regions; caudate, putamen (DLB group only), thalamus, hippocampus (AD group only) and posterior cingulate cortex. The AD group demonstrated greater functional connectivity than the DLB group with the seed placed in the posterior cingulate cortex and the DLB group showed greater functional connectivity than the AD group with the putamen. No brain regions showed significantly greater connectivity in the control group compared to the AD or DLB groups.

The findings from this study identified different patterns of connectivity between dementia subjects and controls with a number of seed regions. Specific brain regions which were more affected in AD compared to DLB were identified, and vice versa. The posterior cingulate cortex, which forms part of the default mode network, was more affected in AD compared to DLB and this network has been shown to be involved in memory processing (Greicius et al., 2004), and therefore abnormalities here may be associated with memory impairments in AD. The putamen was more affected in DLB compared to AD and controls and this structure has previously been associated with the motor features of parkinsonism (O'Brien et al., 2004a).

The results from this study may be used to differentiate between the disorders, as opposed to clinical symptoms which can greatly overlap, and consequently could inform therapeutic management of dementia by specific targeting of these brain regions. No significant differences were found between groups for connectivity with the primary visual cortex. This region was not expected to be functioning abnormally in AD, thus highlighting the sensitivity of functional connectivity measures in reporting differences between groups in brain regions which are functioning abnormally in dementia.

8.2 Strengths and Limitations

Subject Groups

The control and patient groups in this study were well matched in terms of subject numbers, age and gender and they had full and careful clinical and cognitive assessments. Ideally, subject group size could have been larger; however the number of subjects in each group matched, or was greater than, other recent BOLD fMRI studies. The subjects in this study were not medication free and therefore we cannot rule out the effect this may have on the functional connectivity results. However, the recruitment of a depression or dementia cohort who were medication free would be very difficult. Although there is no definitive diagnosis for AD and DLB, subjects in this study matched diagnostic criteria which have previously been shown to have good sensitivity.

Resting-State fMRI

Resting-state fMRI measures are advantageous because the scanning time is short and no task has to be practised or performed. This means that subject head motion is reduced and compliance is generally high. Resting-state is therefore an ideal application in older subjects and particularly cognitively impaired subjects who may find it more difficult to carry out a task whilst in the scanner. Between subjects, resting-state activity can vary depending on how active the subjects' brain is at rest. However, in comparison to task-based studies, where there can be a great difference within a subject group on task performance, resting-state enables more accurate comparisons. Also, resting-state studies enable stronger comparisons with other studies, as between different task-based studies there can be great variability in the experimental set-up of the task, for example.

Analysis Methods

A model-based approach of seed-based correlation analysis was used to measure functional connectivity in this study. This meant that we had a prior hypothesis on which seed regions to investigate based on findings from previous neuroimaging studies. In contrast, other studies apply model-free approaches with no prior hypothesis which means any correlation can be searched for with no sound background knowledge on which brain region to investigate (Sorg et al., 2007). The disadvantage of seed-based correlation analysis is that the connectivity observed can be biased by the seed region selected; however in the studies here, functional connectivity was investigated with all brain voxels in order to reduce this bias. In this study, seed regions were placed manually and by a single investigator. Other studies have used automated tools which

overlay the whole brain region under investigation (Wang et al., 2007). Older subjects, and dementia subjects in particular, are known to have greater brain atrophy (and atrophy varies between subjects) (O'Brien et al., 2001), therefore automated methods of region of interest placing can lead to inaccuracies and the seed region may overlap with the cerebrospinal fluid. In this study, connectivity with the left and right seeds was investigated separately. Other groups have investigated connectivity with bilateral regions only (Zhang et al., 2009); however studies have reported differences in functional connectivity with a left seed versus a right seed in the same brain region (Wang et al., 2006). Therefore, investigating the region bilaterally could result in these differences being missed.

For registration, and to enable group comparisons and anatomical localisation, a standard space brain template was used which was the mean of all study subjects' functional images. This was used to take into account the greater atrophy in older subjects and patient groups, as a standard brain template is based on younger subjects with less brain atrophy. For future work it may be more accurate to use group specific templates which would take into account the greater atrophy in patient groups versus controls.

Spurious fluctuations, unrelated to neuronal activity, were removed from the dementia data by additional filtering steps and regression of seed regions. These methods were found to improve the accuracy of the dementia data for the investigation of connectivity between grey matter regions only. The methodology between studies has been shown to vary greatly which makes it difficult to compare studies directly. In the LLD study reported here, high-pass filtering was included in the analysis, but regression for global or white matter signal was not carried out. Therefore, the effects of additional pre-processing steps on this data are not known, though global synchronicity had not been observed in these subjects. Some studies do not recommend global signal correction, as it has been shown to introduce anti-correlations in the data (Murphy et al., 2009). However, in this work, brain voxels which were showing a positive correlation with the seed under investigation were only measured. It is clear that consistent methodology for the analysis of resting-state data is required to enable studies to be directly compared and in order to be certain that only BOLD signal fluctuations of neuronal origin are investigated. Ideally, if cardiac and respiratory activity are monitored at the time of scanning, these signals can then be subsequently regressed out of the data using model-based approaches (Chang and Glover, 2009; Birn et al., 2008).

8.3 Future Work

A key observation from this research has been the lack of consistent methodology between resting-state studies. For example, between studies there can be great variability in the filtering and regression steps, whether model-based or model-free methods of analysis are used, and within model-based approaches if connectivity is investigated between specific seeds or with the whole brain. Therefore, for future research, greater consistency in the methodology is required to enable direct comparisons between studies and the certainty that the connectivity being measured is of neuronal origin only. The investigation of resting-state activity is a relatively recent method of research, however as there has been a rapid increase in this research area over the past few years, it seems clear that greater consistency in the methodological approaches could soon be achieved.

For future research it would be interesting to perform longitudinal studies to investigate the effects of atrophy on functional connectivity. The aim would be to determine whether increased atrophy causes functional connectivity abnormalities, or whether functional connectivity abnormalities actually precede atrophy and are therefore a more useful early stage marker of dementia. It is not known whether functional connectivity abnormalities in patient groups are directly linked with greater brain atrophy in these regions. However, if this was the case it would probably be expected that connectivity would be reduced due to volume decreases rather than increased as is reported here. Further studies may help to inform whether neuroimaging methods are a stronger measure of brain dysfunction rather than performance on cognitive tests, as patients may develop a plasticity to perform well on these tests and so scores may not truly reflect the underlying brain dysfunction.

In the LLD study, it was shown that mood state affected functional connectivity, which supports the theory that structural changes are not the only explanation for functional connectivity abnormalities. In future studies in depression it would be important to take into account the mood state of individuals and ideally image subjects when depressed and also when they have recovered to investigate which functional connectivity differences are state related and which are trait related.

Of particular importance may be the investigation of functional connectivity in subjects with mild dementia symptoms, i.e. mild cognitive impairment. This would enable the investigation of potential functional connectivity abnormalities early in the course of the disease, where treatment effects would be greater and also progression

could be more easily monitored. The drawback of this approach would be that not all mild cognitive impairment subjects go on to develop dementia (Ritchie et al., 2001).

It would be interesting to investigate other imaging measures of brain connectivity on this data, for example diffusion tensor imaging. Areas identified as functioning abnormally from this work could be used as start and end points in fibre tractography analysis to investigate the functioning of white matter tracts in depression and dementia. Diffusion tensor imaging also enables the investigation of the diffusion of water by measuring the fractional anisotropy, which can be used to measure the tendency of water to move in a single direction, and has previously been shown to be decreased (i.e. showing there are barriers to the diffusion of water) in DLB (Firbank et al., 2007). The main aims of this work would be to see if findings could be linked with the functional connectivity abnormalities found in depression and dementia.

8.4 Conclusion

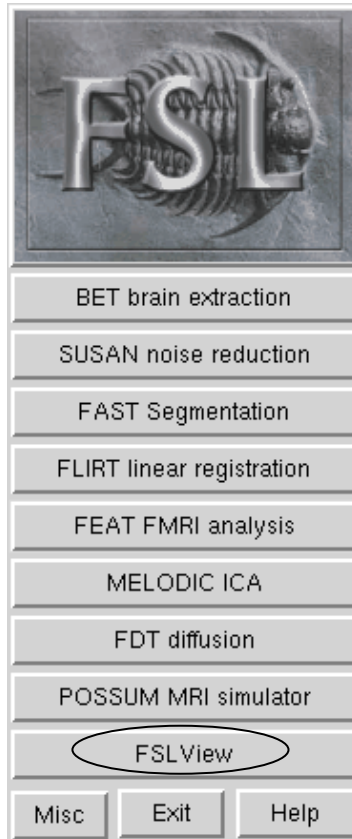
This study has demonstrated the feasibility of using resting BOLD to study functional connectivity in depression and dementia and has demonstrated different patterns of abnormalities in LLD, DLB and AD. Across the patient groups, abnormal connectivity was characterised by increased, or greater, connectivity between seed regions and the rest of the brain compared to control subjects. In both studies the control group did not show significantly greater connectivity than any of the patient groups with any seed regions.

Appendices

Appendix A

FSL Tool Methodology

- **FSLView: To place region of interest**



- 1) Load FSLView
- 2) Click File → Open → Select file → Open fMRI image file (already brain extracted)
- 3) Using movie mode the subjects' scans were viewed and commented on for motion and image quality.
- 4) Click File → Create mask → Create as 4D image
- 5) For the placing of the head of caudate nucleus seed: The head of caudate was located in the axial view. The magnification tool was used and the +/- tab to click through the slices. Using the pen function 2x2 voxels were placed on the most inferior slice where caudate and putamen were separated by internal capsule.
- 6) The left seed was placed first and saved. The left seed was then erased and the right seed drawn and saved. Note: Radiological orientation, i.e. right side of the screen is the left seed.
- 7) The rater was blinded to subject groups as the files were re-numbered by a colleague.

- **Fslmeants: To extract the time-series**

Use command line, change directory to the directory that contains the seed mask file.

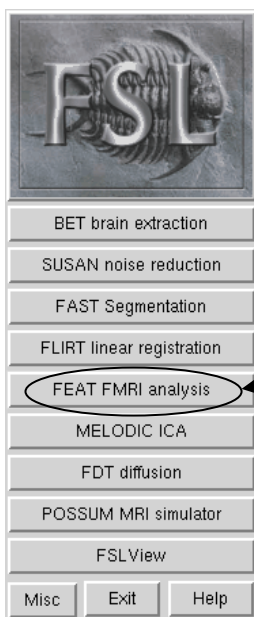
Run fslmeants

Type: **fslmeants -i <input file> -o <output file> -m <mask file>**

-i = functional scan (brain.nii.gz file), -o = plain text document, -m = left/right seed

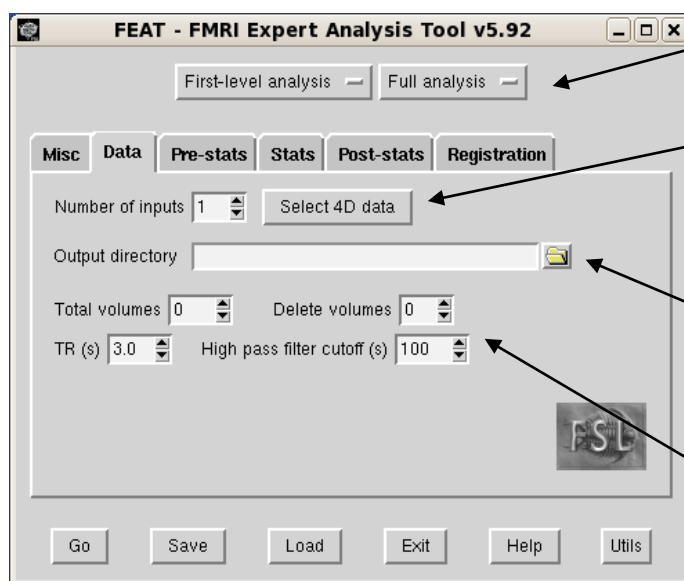
Note: Extract time-series for left and right seed separately

- **FEAT: First level fMRI analysis (model-based)**



1) Open terminal window and type 'FSL'

2) Click on FEAT FMRI analysis

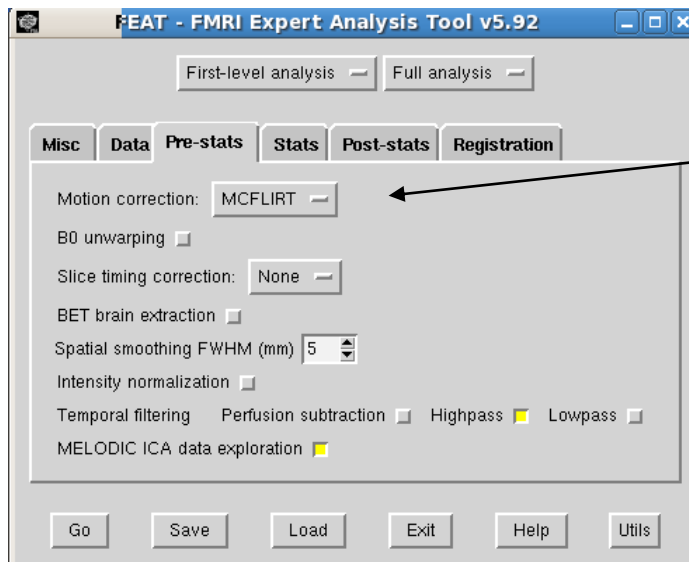


3) Select First-level analysis and full analysis

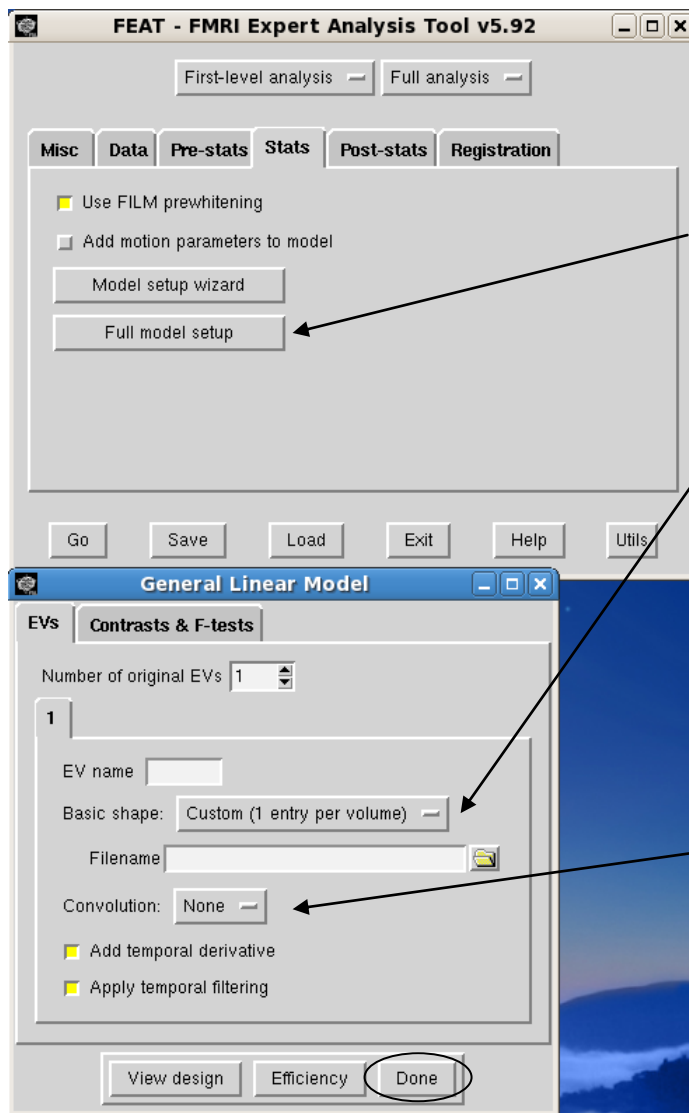
4) Select 4D data (.nii.gz file) – total volumes will change automatically, 128 for most of our data

6) Select output directory (default will be 4D data folder entered)

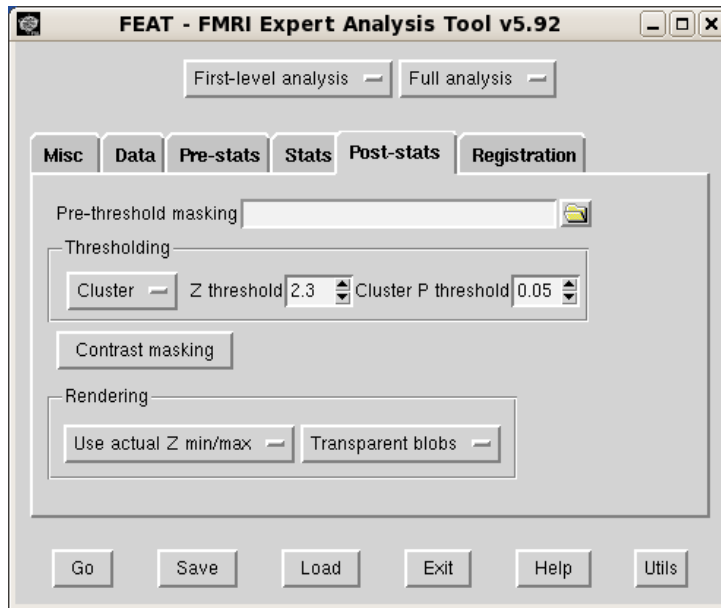
7) High pass filter cut-off – increase to 125 s



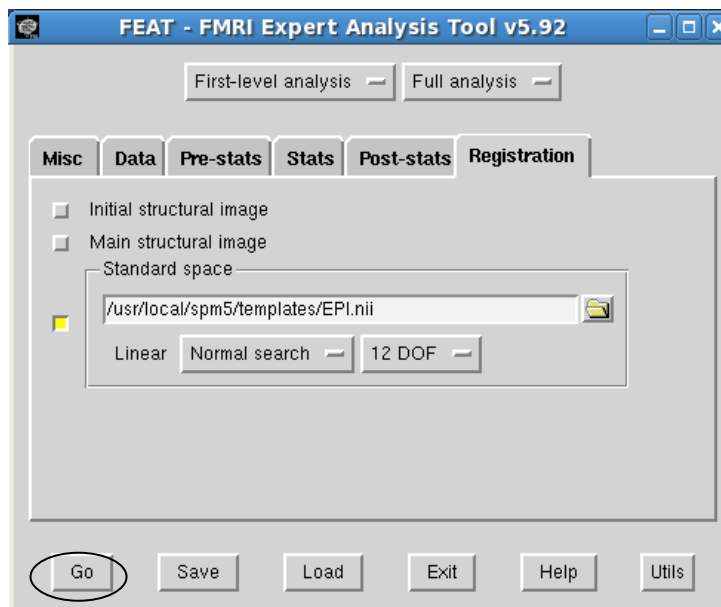
- 8) Motion correction – on
- 9) BET brain extraction – switch off as carried out already
- 10) Highpass filter – on
- 11) MELODIC ICA data exploration – on



- 12) FILM prewhitening – on
- 13) Full model setup (GLM window opens)
Basic shape: Custom (1 entry per volume)
Filename: Enter the time-series (.txt file extracted previously using fslmeans)
Note: enter left and right seed time-series separately
- 14) Convolution: None
- 15) Click Done – model produced

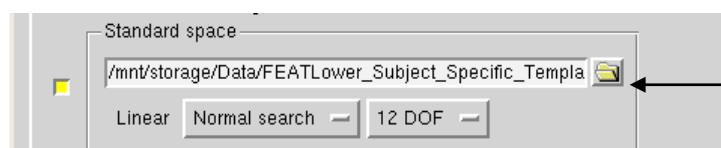


16) Default settings for thresholds used (z statistic > 2.3 and $p < 0.05$).



17) Registration to the standard space EPI template in SPM was carried out

18) Click 'Go'
The above steps were repeated for all subjects.

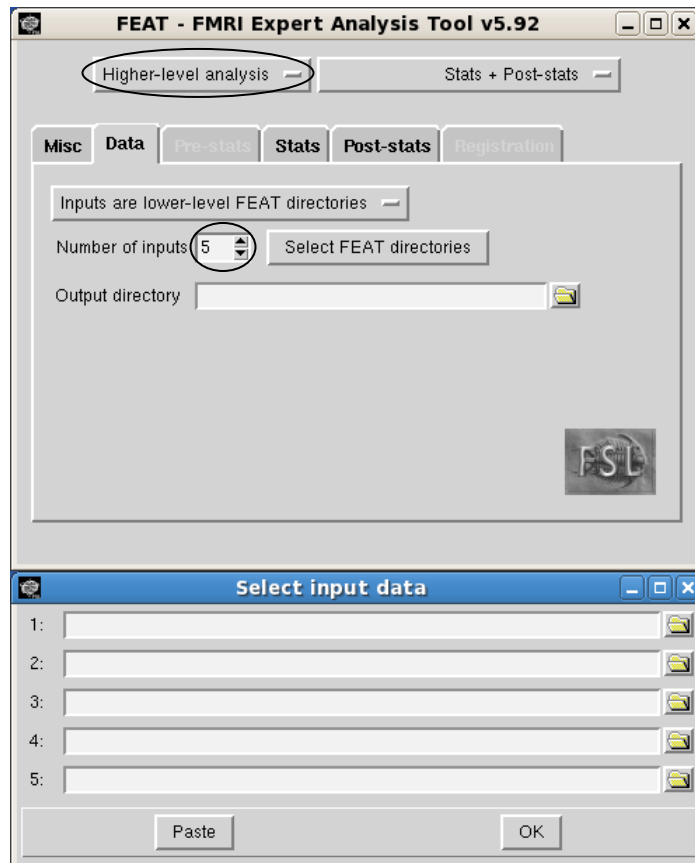


Once all above analysis steps were complete, registration only was selected to register all subjects' scans to the study specific template

- **Fslmaths: To create study specific template**

- 1) One subject was registered to the SPM EPI template and then all subjects were registered to this subject
- 2) Using fslmaths all registered images were averaged and the mean calculated

- **FEAT: Higher-level fMRI analysis**

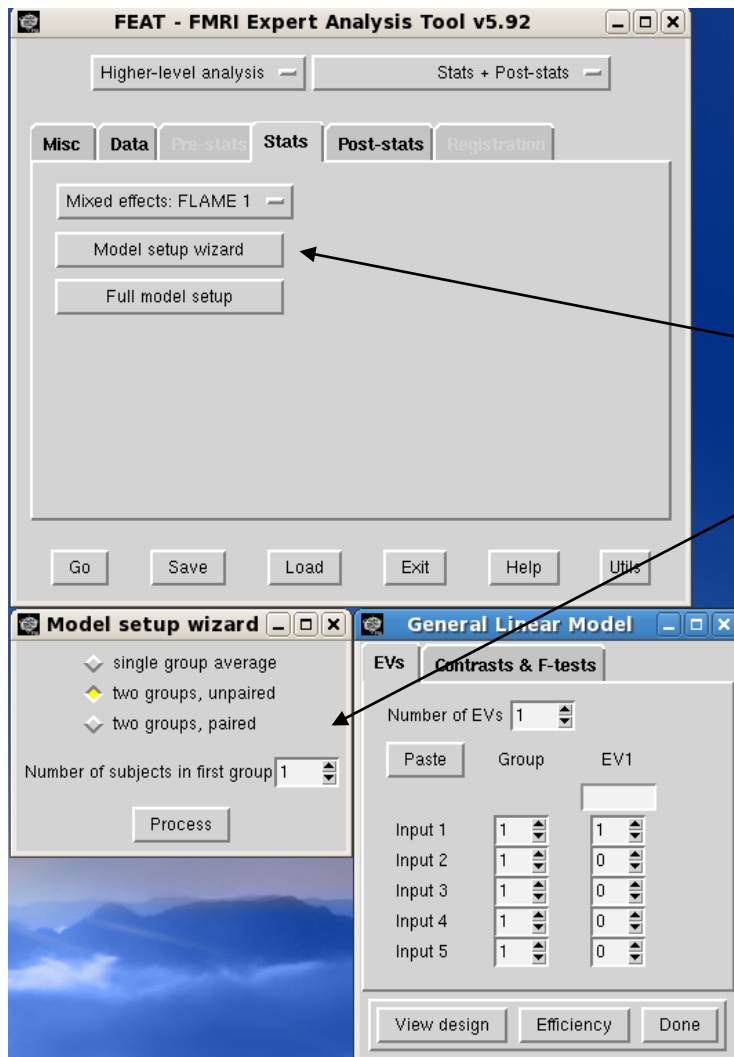


1) Enter FSL in terminal window and click on FEAT fMRI analysis. Select Higher-level analysis.

2) Enter 33 inputs (for LLD study) and select FEAT directories from lower level analysis (load left FEAT directories and run analysis, load right FEAT directories and run analysis).

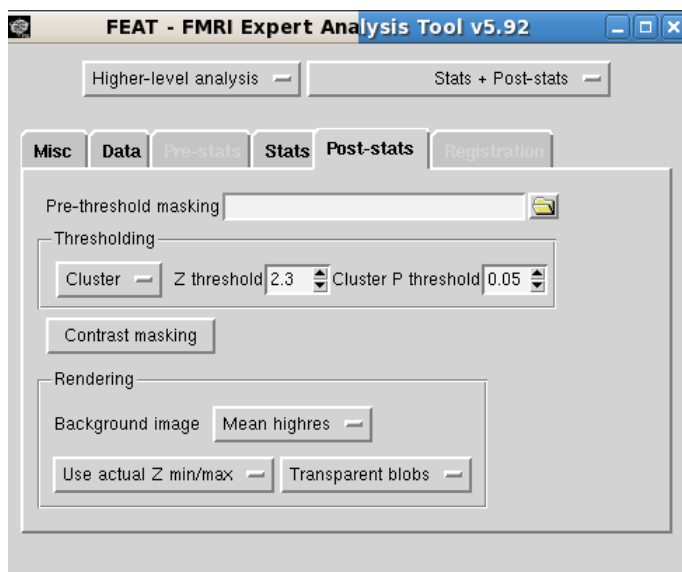
Enter all control subjects first then the patient group.

3) Select output directory.



4) Select mixed effects: FLAME 1

5) Model setup wizard – select 2 groups unpaired, then number of subjects in first group – 17



6) Default settings for thresholds used.

7) 'Go' clicked at bottom of screen

Appendix B: Functional Connectivity in Late-life Depression using Resting-state Functional Magnetic Resonance Imaging

Manuscript published in the American Journal of Geriatric Psychiatry

Eva R. Kenny, MRes¹; John T. O'Brien, DM, FRCPsych²; David A. Cousins, MRCPsych¹; Jonathan Richardson, MRCPsych²; Alan J. Thomas, PhD, MRCPsych²; Michael J. Firbank, PhD²; Andrew M. Blamire, PhD¹

¹Newcastle Magnetic Resonance Centre, Newcastle University

²Institute for Ageing and Health, Newcastle University

Corresponding author

Eva Kenny, Newcastle Magnetic Resonance Centre, Newcastle University, Campus for Ageing & Vitality, Newcastle upon Tyne, NE4 5PL

Email: e.r.kenny@ncl.ac.uk

Tel: 0191 248 1159, Fax: 0191 248 1151

Key Words – Functional MRI, Late-life Depression, Resting-state

Abstract

Objective: To investigate whether there are differences in brain connectivity in late-life depression (LLD) and non-depressed subjects using the left and right heads of caudate nuclei (hCN) as the seed regions. **Design:** Resting-state functional magnetic resonance imaging (fMRI) data were collected using a 3 Tesla MRI System. **Setting:** Subjects were recruited from primary or secondary care services in the Newcastle area. **Participants:** Thirty-three subjects aged 65 and over; 16 who had a recent episode of LLD and 17 non-depressed subjects. **Measurements:** Functional connectivity was analysed by extracting the temporal signal variation from the left and right hCN and cross-correlating with the rest of the brain. **Results:** Significant connectivity between the hCN and frontal areas was observed in the non-depressed group, whereas in LLD connectivity was seen over a much wider area. Regions showing significantly greater connectivity ($p \leq 0.05$) in LLD compared to the non-depressed group were frontal (precentral, sub-gyral, middle frontal, paracentral lobule), sub-lobar (thalamus, insula), limbic (cingulate), parietal (postcentral gyrus, precuneus, inferior parietal lobule, supramarginal gyrus) and temporal (superior temporal gyrus). Conversely, no brain regions showed greater connectivity in the non-depressed group than LLD. In both groups the right hCN showed significantly greater connectivity than the left in numerous brain regions, but connectivity for the left hCN did not exceed the right in any brain regions. **Conclusions:** This resting-state study showed increased connectivity in specific brain regions in LLD compared to the non-depressed group, which supports the view that functional connectivity is altered in depression.

Objective

Late-life depression (LLD) is a common psychiatric disorder in which the core features of low mood are often associated with impairments in attention, memory and executive function (Thomas et al., 2008; O'Brien et al., 2004b). This symptom profile is consistent with the notion that LLD results from dysfunction in frontal, striatal and limbic neural circuits that govern mood and cognition (Mayberg et al., 1999). Communication between limbic structures and neocortical areas are critical in the formation of complex behaviours and emotions, and studies of depressed subjects suggest a disruption of these functions (Alexopoulos, 2002). Positron emission tomography studies show decreased glucose utilisation in frontal regions, such as the dorsolateral prefrontal cortex (DLPFC) and anterior cingulate cortex (ACC), and increased brain activity in limbic areas such as the amygdala, pallidostriatum and medial thalamus (Mayberg et al., 1999; Drevets et al., 1997). More recently functional magnetic resonance imaging (fMRI) studies have reported similar results of decreased activity in DLPFC and in addition decreased connectivity between DLPFC and ACC in LLD (Aizenstein et al., 2009). The subgenual prefrontal cortex has attracted particular attention as metabolic increases in this area in depression (Drevets et al., 2002) correlate positively with symptom severity and the magnitude of volume reduction on structural images (Drevets et al., 1997).

LLD has been hypothesised to have a vascular basis in which cerebrovascular disease and/or ischaemic brain changes disrupt the function of mood regulating systems (Alexopoulos et al., 1997). Volume reductions in LLD have been demonstrated in frontal (orbital and medial) and temporal lobes and parts of the limbic system including the hippocampus, amygdala and parahippocampal area (Andreescu et al., 2008). Magnetic resonance imaging (MRI) studies have also shown increases in deep white matter hyperintensities (DWMH) in LLD, especially in frontal regions (Thomas et al., 2002). These DWMHs in LLD are thought to have an ischaemic basis (Thomas et al., 2002), and may arise from poor cerebral tissue perfusion associated with stroke, myocardial infarction or hypertension that often precedes LLD (Alexopoulos et al., 1997).

Cortico-cortical communication necessary for mood regulation involves connections through basal ganglia (BG) nuclei. The caudate nucleus (CN), a BG structure, is known to be involved in the control of motor, cognitive and emotional processes. In late-life depression, smaller volumes have been reported for left, right and

total CN, with reductions localised to the head of CN (hCN) and greater reduction associated with increased severity of depression (Butters et al., 2009). Negative studies have involved younger subjects (mean age 41 y) (Lacerda et al., 2003), and there is evidence that the degree of volume loss in the CN is more marked in LLD than early-onset depression (Greenwald et al., 1997), at least for the left CN. In LLD, those with smaller total and right CN volumes have a greater volume of anterior WM lesions, suggesting that the pathologies may be linked (Hannestad et al., 2006).

fMRI is widely used to investigate brain regions showing neural activity when an experimental task is performed, but more recently it has been shown that in the resting-state, i.e. when no task is performed in the scanner, spontaneous low-frequency fluctuations (SLFs) in the blood oxygenation level dependent (BOLD) signal occur at frequencies of $<0.1\text{Hz}$ (Cordes et al., 2000; Lowe et al., 1998; Biswal et al., 1995). SLFs are linked with anatomically and functionally plausible networks showing FC between brain regions. These networks have been termed resting-state networks (RSNs) (Cordes et al., 2000; Lowe et al., 1998; Biswal et al., 1995). One RSN which has received great interest is the default mode network (DMN) which shows greater BOLD signal at rest than during an experimental task (Raichle et al., 2001). The DMN includes medial prefrontal, posterior cingulate, precuneus and lateral inferior parietal cortices and has been shown to play a critical role in self-referential processing (Raichle et al., 2001).

RSNs can be analysed using model-driven or data-driven techniques. Model-driven analyses (seed region correlation) showed decreased correlations in SLFs between cortical (ACC) and limbic regions (amygdala, pallidostriatum and medial thalamus) in younger depressed subjects compared to controls at rest and during exposure to neutral, positive, and negative pictures (Anand et al., 2005a). Data-driven analyses (independent component analysis) showed increased FC in the subgenual cingulate, thalamus, orbitofrontal cortex and precuneus in younger depressed subjects compared to controls. Conversely, controls did not show significantly greater connectivity than the depressed group in any brain regions. In addition, length of depressive episode was found to correlate positively with FC in the subgenual cingulate (Greicius et al., 2007). Another study analysed SLFs for regional coherence between adjacent pixels (termed regional homogeneity or ReHo) and reported both increases and decreases in ReHo in elderly subjects with depression compared to controls. The putamen showed increased ReHo, the frontal and parietal lobes showed increased and decreased ReHo, and the temporal lobe showed decreased ReHo. The subjects had been

in remission for more than six months suggesting brain network dysfunction may persist despite clinical recovery (Yuan et al., 2008).

There is therefore evidence that alterations in connectivity may be implicated in LLD, and so we aimed to examine connectivity in LLD using model-driven analysis of resting-state fMRI data. We chose the hCN as the seed region because of its central role in mood regulating circuits and the structural and functional abnormalities in this structure previously described in studies of depression. Specifically, we hypothesised that connectivity between the hCN and the rest of the brain would be abnormal in LLD compared to age-matched non-depressed subjects. Since we hypothesised that connectivity would be trait not state dependent, we included depressed subjects who had largely recovered from their depressive episode.

Methods

Subjects & Assessment

The study involved 33 subjects aged 65 and over who were recruited from a community population in the North East of England. Sixteen patients were recruited from consecutive referrals to Newcastle and Gateshead Old Age Psychiatry Services and met diagnostic criteria for Major Depression according to DSM-IV, as assessed during a standardised interview by an experienced psychiatrist (JR). Seventeen similarly aged non-depressed subjects were recruited by advertisement, none of whom had past or present history of depression. All subjects were cognitively intact, had no history or clinical evidence of dementia and all scored 24 or more on the Mini Mental State Examination (MMSE) (Roth et al., 1986). Exclusion criteria were comorbid or previous drug or alcohol misuse; previous head injury; previous history of epilepsy; MI in the previous three months; a carotid bruit on physical examination; contraindication to MRI.

Patients were assessed using a standardised interview and received a structured physical examination. Current depression severity was rated using the Montgomery-Asberg Depression Rating Scale (MADRS) (Montgomery and Asberg, 1979). The study received ethics committee approval and all subjects gave verbal and written consent.

Imaging

Subjects were scanned on a 3 Tesla Philips Intera Achieva MRI System using an 8 channel head coil, and anatomical 3D T1-weighted and resting-state fMRI scans were acquired. FMRI scans were collected using a gradient-echo echo-planar imaging (GE-

EPI) sequence with timing and parameters informed by previous work in detection of RSNs (De Luca et al., 2006): 25 axial slices, in-plane resolution = 2 x 2 mm, slice thickness = 6 mm (contiguous), repetition time [TR] = 3000 ms; echo time [TE] = 40 ms; field of view [FOV] = 260 x 150 x 260 mm, with 128 volumes collected over 6.65 minutes.

Placing of the Region of Interest

FMRIB Software Library (FSL) (www.fmrib.ox.ac.uk/fsl) tools were used for analysis. A region of interest (ROI) of two by two pixels was defined in the hCN in the axial view on one slice of the functional image of each subject. The pixels were placed in the mid-region of the CN, and on the most inferior slice where the CN and putamen are separated by the internal capsule, similar to guidelines used in previous studies (Beyer et al., 2004). ROIs were placed in each hemisphere by a sole investigator blinded to the identity and diagnosis of each scan and guided by a standard brain atlas for reference (DeArmond et al., 1989).

Model-driven Analysis

FMRI data pre-processing steps of motion correction (Jenkinson et al., 2002), brain extraction (Smith, 2002), spatial smoothing (5 mm full width at half maximum) and high-pass temporal filtering (cut-off = 125 s) (Smith et al., 2004b) were performed using FMRI Expert Analysis Tool (FEAT) (version 5.92). The mean BOLD signal time-series was extracted from each ROI and used as the model response function in general linear modelling (GLM) analysis (Woolrich et al., 2001), effectively cross-correlating SLFs in the hCN with signal variations in all other brain areas.

Group Analysis

To perform group analysis all images were registered into standard space (Wellcome Trust Centre for Neuroimaging, 2005) using a 12 degrees of freedom affine transformation (Jenkinson et al., 2002). To take into account the age of subjects in this study a standard space template was created by calculating the mean of all subjects' functional images, and this template was then used for registration (Figure 1).

A two-sample (non-depressed and LLD groups) unpaired t-test was carried out to investigate group differences (FMRIB's Local Analysis of Mixed Effects (FLAME) (Woolrich et al., 2004). Z (Gaussianised T/F) statistic images were corrected for multiple comparisons using cluster thresholding pixels determined by $z > 2.3$ and a corrected cluster significance threshold of $p < 0.05$ (Worsley, 2001). Connectivity differences between the right and left hemisphere ROIs were also investigated using a

two-sample paired t-test (left and right ROI) for each group, with z and p thresholds as previous (Figure 1).

Localisation of Clusters

The peak connectivity cluster coordinates from the FEAT analysis are in Montreal Neurological Index (MNI) space, so coordinates were converted to Talairach space (Talairach and Tournoux, 1988) using GingerALE (Lancaster et al., 2007) and entered into Talairach Client which assigns Talairach labels (hemisphere, lobe, gyrus, tissue and cell type) (Lancaster et al., 2000).

Brain Volume Data

Anatomical T1 images were segmented into grey matter, white matter and cerebrospinal fluid (CSF) using SPM5 (Wellcome Trust Centre for Neuroimaging, 2005), and total intracranial volume (TIV) was calculated from the sum of the three components. EPI images were also analysed volumetrically using the FSL package SIENAX which calculates brain, grey and white matter, peripheral grey and ventricular CSF volumes (Smith, 2002).

Results

Demographics

Table 1 shows the clinical characteristics of the subjects. Groups were comparable for gender ($\chi^2 = 0.76$, $df = 1$), age, MMSE score and total brain volume normalised to TIV [(brain volume/total intracranial volume)*1000]. Additionally, no significant differences were found between groups in white, grey, peripheral grey matter and ventricular CSF. Mean MADRS score for LLD subjects was 7.1 (± 4.8), indicating that most had recovered from their episode of depression by the time of scanning. Mean age at onset of depression was 47.4 (± 18.5) years and the number of previous episodes of depression was 2.5 (± 2.1). At the time of the study, 12 subjects were taking antidepressants (citalopram, mirtazapine, trazodone, venlafaxine, paroxetine and lofepramine), 2 subjects were taking antipsychotics (flupenthixol and prochlorperazine), benzodiazepines (zopiclone, temazepam) and antiepileptic medication (carbamazepine and sodium valproate).

Functional Connectivity

Areas of significant connectivity with the hCN in non-depressed were predominately frontal (Figure 2) whereas in the LLD group connectivity was over a much wider area (Figure 2). Brain regions showing significantly greater connectivity

($p < 0.05$) in LLD compared to non-depressed for both left and right hCN were frontal (precentral, sub-gyral, middle frontal and paracentral lobule), sub-lobar (thalamus and insula), limbic (cingulate), parietal (postcentral gyrus, precuneus, inferior parietal lobule and supramarginal gyrus) and temporal (superior temporal gyrus). In LLD the brain regions with the most peak connectivity clusters for the left hCN were the thalamus (bilateral), precuneus (bilateral) and precentral gyrus (left), whereas for the right hCN it was the cingulate (bilateral) and the precentral gyrus (left) (Figure 2 and Table 2). There were no brain regions of significantly greater connectivity with either hCN in non-depressed compared to LLD subjects (Figure 2).

In non-depressed and LLD a number of regions showed significantly greater connectivity for the right hCN compared to the left, whereas no regions showed significantly greater connectivity for the left hCN compared to right. In non-depressed, peak areas were mainly in frontal and to a lesser extent sub-lobar areas, whereas in LLD it was sub-lobar, followed by limbic and temporal regions.

Conclusions

This resting-state fMRI study has shown increased connectivity in specific brain regions in LLD compared to non-depressed subjects, revealed by the increased spatial synchrony in SLFs. These results support the view that FC in mood regulating circuits is abnormal in depression (Drevets et al., 2002; Mayberg et al., 1999; Drevets et al., 1997). Our finding of increased FC between the hCN and the cingulate and precuneus in LLD compared to non-depressed subjects supports the theory that the DMN may be functioning abnormally in depression. Greicius *et al.* also showed increased connectivity in depression, and similarly found no areas of significantly greater connectivity in non-depressed than depressed (Greicius et al., 2007). Yuan *et al.* showed increased ReHo in LLD in similar regions to where we found increased FC with the CN, for example putamen (left) and postcentral gyrus (left). However, they also showed decreases in ReHo in depression, specifically the postcentral gyrus (right), a region where we showed increased FC (Yuan et al., 2008). The mean age of depression subjects in both of these studies was younger (39y and 67y respectively) than in our study (mean 76y) and the analysis methods different, so directly comparing the studies is difficult.

We showed greater connectivity with the right hCN compared to the left in non-depressed and depressed subjects. Similarly, rightward asymmetry has been shown in an

elderly comparison group in the hippocampus, but not in Alzheimer's disease (AD) (Wang et al., 2006).

The reasons why non-depressed subjects had a frontal predominance of connectivity whereas LLD subjects had a more diffuse pattern are not clear. We think it unlikely that differences in connectivity could be due to greater atrophy in LLD, as atrophy in AD, for example, is characterised by decreased FC, specifically within the DMN (Wang et al., 2006; Greicius et al., 2004). In addition, we found no significant difference between brain volumes in non-depressed and LLD, in particular in ventricular CSF which is of key importance due to the position of our ROI. We are confident with our ROI placing, and specifically chose a ROI size that we were certain would fit comfortably within the hCN borders and so be unaffected by brain atrophy.

Another possibility is that microvascular damage, which can alter neurovascular coupling and consequently affect the BOLD response, could be increased in LLD (D'Esposito et al., 2003), but if this was the case we would expect a delay, or a decrease in the BOLD response, and thus reduced connectivity.

The widely distributed FC seen in LLD may represent a departure from frontally coordinated suppression of brain activity, seen in the non-depressed group, which is necessary for normal rest. We show increased FC between the hCN and a number of brain regions in LLD which supports the theory of an abnormality at the circuit level rather than in a localised brain region. This finding could be caused by white matter abnormalities disrupting the normal connectivity pattern. We show increases in FC between the hCN, which controls motor, cognitive and emotional processes, and medial prefrontal regions, implicated in self referential and emotional processing. This pattern of FC could reflect increased emotional processing in depression and be responsible for the core symptom of abnormally low mood. Specifically we show increased FC in the cingulate and precuneus, which are key regions of the DMN, critical in self-referential processing. These disruptions could be aetiologically important in depression.

There has been much discussion as to the whether SLFs are of neuronal origin, as using slow sampling rates, as in this study (TR = 3000 ms), noise from the cardiac and respiratory cycles can alias into the low-frequency ranges at which resting-state FC is investigated (Lowe et al., 1998). However, studies using a high sampling rate to prevent aliasing of this activity have shown that RSNs are distinct processes, which supports the theory that they are of neuronal origin (Cordes et al., 2001). Further support comes from the correlation seen between BOLD signal and cortical electrical

activity (Goldman et al., 2002) and the changes that occur in RSNs in neurological disease (Greicius et al., 2004).

Strengths and Limitations

In our study, groups were well matched for subject number, gender and age and our analysis method enabled the investigation of time-series correlation between the hCN and all other brain regions based on an *a priori* hypothesis. This is in contrast to other studies which have only looked at correlations between a few specific regions in depression. Resting-state studies benefit from simplicity of experimental design, no task has to be practised, so patient compliance and tolerance is high and head motion is reduced. However, model-based techniques are biased by the choice of seed voxel, whereas data-driven techniques do not require predefined ROIs or a temporal model, but their lack of specificity means that results can be hard to interpret and it can be difficult to quantify the statistical significance of the spatial maps. Resting-state is difficult to control, as it is highly dependent on the subjects' definition of rest and even within subjects scans can vary greatly.

Further limitations include the effects of psychoactive medications in the LLD group, some of which are known to modulate the BOLD response to task performance and which may have an effect on connectivity (Anand et al., 2007). Our results of within group analysis showed no significant difference in connectivity between subjects taking medication and those not, however as group sizes were small and uneven we cannot draw too strong a conclusion from these results. The ideal study would have all depressed subjects in an unmedicated state but the associated practical and ethical issues would be great.

In conclusion, we report that resting-state FC is abnormal in LLD compared to non-depressed subjects. Further studies need to determine the time-series of development of changes in connectivity, the relationship with clinical and cognitive symptoms, treatment effects, and whether there is a link between connectivity and structural changes.

Figure/Table Legends

Figure 1: Overview of FEAT Analysis Steps

BET = Brain Extraction Tool, EPI = Echo Planar Imaging, FEAT = FMRI Expert Analysis Tool, FILM = FMRIB's Improved Linear Model, FLAME = FMRIB's Local Analysis of Mixed Effects, GLM = General Linear Modelling, MCFLIRT = Motion Correction FMRIB's Linear Image Registration Tool, ROIs = Region of Interests.

Figure 2: Maps Showing Regions of Significant Connectivity with Head of Caudate Nucleus in Late-Life Depression and Non-depressed Subjects

Brain regions showing significant connectivity to the left and right head of caudate nucleus in non-depressed, depressed, non-depressed greater than depressed, depressed greater than non-depressed. Images are registered to standard (MNI) space. Threshold levels are shown at the top of the figure. Voxels with a z score of 2.3 ($p < 0.05$) were considered to show significant connectivity. Slices are $z = 33, 35, 37, 39, 49, 51, 53, 55$. Note radiological orientation, i.e. left hemisphere in the image is right hemisphere in the brain.

Table 1: Demographic and Neuropsychological Data of Subjects

Values expressed as mean \pm standard deviation.

Degrees of freedom: Chi-square test = 1, Independent samples t-test = 31.

MADRS = Montgomery-Asberg Depression Rating Scale; MMSE = Mini-Mental State Examination; NA = not applicable.

^a The P value was calculated using Chi-square test

^b The P values were calculated using the Independent samples t-test.

Table 2: Brain Regions Showing Greater Connectivity in Late-Life Depression compared to Non-depressed Subjects

Figure 1

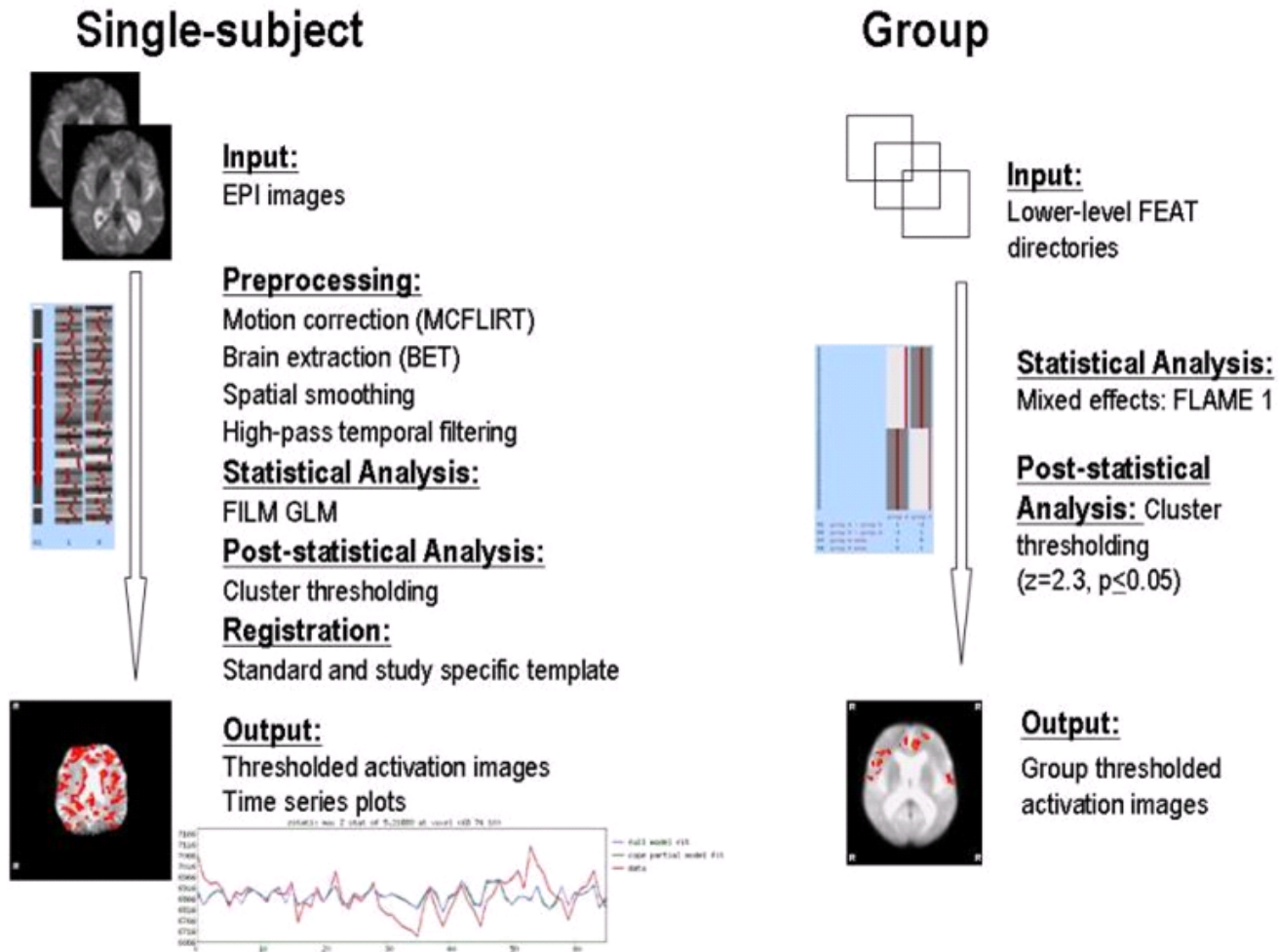


Figure 2

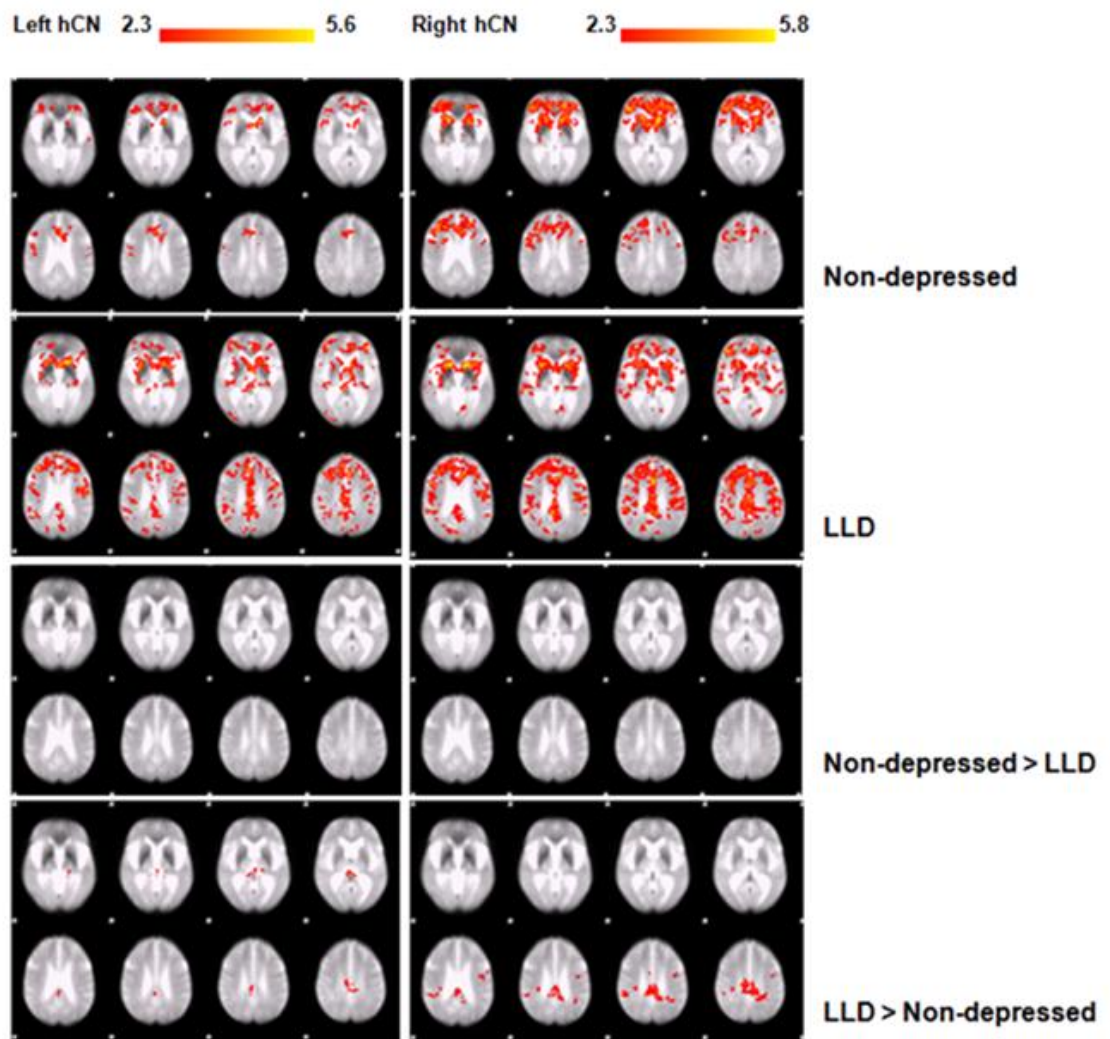


Table 1

Subject characteristics	Controls	Depressed	<i>P</i> value
Sex (M:F)	11:6	8:8	0.38 ^a
Age (Yrs)	75.7 (7.6)	76.4 (7.2)	0.76 ^b
MMSE	28.8 (1.2)	28.0 (1.8)	0.17 ^b
Brain Volume normalised to TIV	0.79 (0.05)	0.79 (0.05)	0.85 ^b
MADRS	NA	7.1 (4.8)	
Age at onset of Depression (Yrs)	NA	47.4 (18.5)	
Number of previous episodes of depression	NA	2.5 (2.1)	

^a The *P* value was calculated using Chi-Square Test

^b The *P* values were calculated using the Independent-Samples T Test.

Table 2

Left Head of Caudate Nucleus as Seed region						
Lobe	Brain Region Gyrus (Brodmann's Area/Cell type)	Side	Talairach Coordinates (mm)			Z- Statistic
			x	y	z	
Frontal	Precentral (4)	L	-16	-27	50	3.44
	Sub-Gyral (4)	R	16	-27	56	3.15
	Paracentral lobule (5)	L	-7	-40	48	3.28
	Paracentral lobule (5)	R	18	-40	50	3.01
Sub-lobar	Thalamus	R	6	-34	5	3.83
	Thalamus	L	-11	-34	8	2.92
Limbic	Cingulate (31)	R	14	-44	42	3.19
Parietal	Postcentral (3)	L	-24	-29	52	3.48
	Precuneus (7)	R	6	-36	43	3.39
	Precuneus (7)	L	-7	-48	51	3.09
Right Head of Caudate Nucleus as Seed region						
Lobe	Brain Region Gyrus (Brodmann's Area/Cell type)	Side	Talairach Coordinates (mm)			Z- Statistic
			x	y	z	
Frontal	Precentral (6)	L	-43	-6	24	3.19
	Middle Frontal (6)	L	-37	-7	41	3.19
	Paracentral lobule (5)	L	-7	-40	48	3.48
Sub-lobar	Insula (13)	R	37	-39	23	3.79
Limbic	Cingulate (31)	R	12	-20	36	3.87
		L	-7	-41	30	3.87
Parietal	Postcentral (2)	R	31	-32	38	3.56
	Inferior parietal lobule (4)	R	50	-36	30	3.21
	Supramarginal gyrus (40)	R	46	-39	32	3.08
Temporal	Superior temporal gyrus(13)	R	44	-43	22	3.09

Appendix C: Table of Dementia Study Subjects and the Medications Subjects were taking. Subjects showing Global Synchronicity are in Italics.

Subject ID	Medications
001	Dicloflex, Quinine
002	Ibuprofen, Vitamin C, Folic Acid, Cod Liver Oil, Garlic
003	Donepezil, ISMN, Aspirin, Simvastatin, Senna, Dilzem
004	Galantamine, Bendrofluazide, Lisinopril
<i>005</i>	<i>Donepezil, Vitamin B12 Injections-3 monthly</i>
006	Donepezil
007	Galantamine, Atenolol, Aspirin, Lisinopril, Simvastatin, Metformin, Omeprazole, Insulin, Bendroflumethiazide
008	Glucosamine
<i>009</i>	<i>Warfarin, Enalapril</i>
<i>010</i>	<i>Galantamine, Atenolol, Asprin, Nicorandil, ISMN, Mirtazapine, Lansoprazole, GTN</i>
<i>011</i>	<i>Donepezil, Venlafaxine, Trazodone</i>
012	Asprin, Irbesartan, Paracetamol, Tolterodine, Isphaghula, Paracetamol
013	Galantamine, Lansoprazole, Metroclopramide
014	Metformin
015	Thyroxine, Lisinopril, Amlodipine, Simvastatin, Aspirin, Senna, Fybogel

016	Donepezil, Citalopram, Propranolol, Paracetamol
017	Propranolol, Prothiaden, Nitrazepam, Bendrofluazide, Cimetidine
018	<i>Warfarin, Bendroflumethiazide</i>
019	Duloxetine, Bendroflumethiazide, Simvastatin, Perindopril Tert-Butylamine, Dorzolamide Hydrochloride, Eye drops, Glucosamine
020	Donepezil, Mirtazapine, Alendronic
021	<i>Donepezil, Glucosamine, Aspirin, Digoxin, Lansoprazole, Bisoprolol, Simvastatin, Perindopril, Nicorandil, GTN spray, Paracetamol</i>
022	Amlodipine, ISMN, Simvastatin, Prostag injection, Warfarin, Aranesp, Captopril
023	Galantamine, Aspirin, Digoxin, Furosemide, Paracetamol
024	Donepezil, Lisinopril, Simvastatin, Quinine sulphate, Paracetamol, Hydroxyzine, Bendroflumethiazide, Florazepam
025	<i>Donepezil</i>
026	Donepezil, Adcal D3, Alendronic Acid, Aspirin, Folic Acid, Mirtazapine, Ropinirole, Simvastatin, Hydroxocobalamin injection
027	Lisinopril, Simvastatin, Naproxen, Lansoprazole, Bendroflumethiazide
028	Donepezil
029	Co-Careldopa, Ramipril, Bendroflumethiazide, Galantamine, B12 injections
030	Paracetamol, Ibuprofen, Ramipril, Oxybutynin, Omeprazole, Thiamine, Galantamine, Mirtazapine, Alendronic acid, inhalers, Prednisolone
031	Olmесartan medoxomil, Allopurinol, Aspirin, Co-Careldopa, Simvastatin
032	Co-Codamol, Sinemet, Domperidone, Donepezil
033	Adalat, Perindopril, Atenolol, Bendroflumethiazide, Simvastatin, Aspirin

034	Rivastigmine, Domperidone, Madopar, Citalopram, Quetiapine, Zopiclone, Levothyroxine, Flucortisone, Calcichew D3
035	Galantamine, Omeprazole, Alendronic acid, Adcal D3, Allopurinol, Amlodipine, Aspirin, Clonazepam, Prednisolone, Simvastatin, Sertraline, Colchicine, Ventolin
036	
037	<i>Perindopril</i>
038	Sinemet, Paracetamol
039	Simvastatin
042	Co-Codamol
043	<i>Omeprazole, Isosorbide Mononitrate, Aspirin, Paroxetine, Sinemet Plus, Simvastatin tabs, Bisoprolol Fumarate, Nicorandil, Co-Beneldopa 12.5/50</i>
044	Loperamide, Lansoprazole, Bendroflumethiazide, Lisinopril, Atenolol, Aspirin E/C, Paracetamol, Epaderm ointment
045	Nefopam Hydrochloride, Aspirin, Quinine Sulphate, Peptac Liquid, Sinemet, Citalopram, Calogen Emulsion
046	Midodrine, Paracetamol, Aspirin, Fludrocortisone, Galantamine
047	<i>Aspirin, Alendronic Acid, Lansoprazole, Isosorbide Mononitrate, Calcichew D3 Forte, Donepezil, Digoxin, Furosemide, Paracetamol, Senna, GTN Spray, Lorazepam</i>
049	Atenolol, Oxybutynin, Dispersible Aspirin, Lansoprazole, Quinine Sulphate, Simvastatin, Donepezil
050	Sinemet Plus, Bendroflumethiazide, Amlodipine, Doxazosin Mesylate, Dispersible Aspirin

References

- Aarsland, D., Ballard, C., Walker, Z., Bostrom, F., Alves, G., Kossakowski, K., Leroi, I., Pozo-Rodriguez, F., Minthon, L. and Londos, E. (2009) 'Memantine in patients with Parkinson's disease dementia or dementia with Lewy bodies: a double-blind, placebo-controlled, multicentre trial', *Lancet Neurol*, 8, (7), pp. 613-8.
- Aarsland, D., Zaccai, J. and Brayne, C. (2005) 'A systematic review of prevalence studies of dementia in Parkinson's disease', *Mov Disord*, 20, (10), pp. 1255-63.
- Aizenstein, H. J., Butters, M. A., Wu, M., Mazurkewicz, L. M., Stenger, V. A., Gianaros, P. J., Becker, J. T., Reynolds, C. F., 3rd and Carter, C. S. (2009) 'Altered functioning of the executive control circuit in late-life depression: episodic and persistent phenomena', *Am J Geriatr Psychiatry*, 17, (1), pp. 30-42.
- Alexander, G. E. and Crutcher, M. D. (1990) 'Functional architecture of basal ganglia circuits: neural substrates of parallel processing', *Trends Neurosci*, 13, (7), pp. 266-71.
- Alexander, G. E., DeLong, M. R. and Strick, P. L. (1986) 'Parallel organization of functionally segregated circuits linking basal ganglia and cortex', *Annu Rev Neurosci*, 9, pp. 357-81.
- Alexopoulos, G. S. (2002) 'Frontostriatal and limbic dysfunction in late-life depression', *Am J Geriatr Psychiatry*, 10, (6), pp. 687-95.
- Alexopoulos, G. S., Kiosses, D. N., Klimstra, S., Kalayam, B. and Bruce, M. L. (2002) 'Clinical presentation of the "depression-executive dysfunction syndrome" of late life', *Am J Geriatr Psychiatry*, 10, (1), pp. 98-106.
- Alexopoulos, G. S., Meyers, B. S., Young, R. C., Campbell, S., Silbersweig, D. and Charlson, M. (1997) 'Vascular depression' hypothesis', *Arch Gen Psychiatry*, 54, (10), pp. 915-22.

- Alexopoulos, G. S., Meyers, B. S., Young, R. C., Kalayam, B., Kakuma, T., Gabrielle, M., Sirey, J. A. and Hull, J. (2000) 'Executive dysfunction and long-term outcomes of geriatric depression', *Arch Gen Psychiatry*, 57, (3), pp. 285-90.
- Alexopoulos, G. S., Meyers, B. S., Young, R. C., Mattis, S. and Kakuma, T. (1993) 'The course of geriatric depression with "reversible dementia": a controlled study', *Am J Psychiatry*, 150, (11), pp. 1693-9.
- Allen, G., Barnard, H., McColl, R., Hester, A. L., Fields, J. A., Weiner, M. F., Ringe, W. K., Lipton, A. M., Brooker, M., McDonald, E., Rubin, C. D. and Cullum, C. M. (2007) 'Reduced hippocampal functional connectivity in Alzheimer disease', *Arch Neurol*, 64, (10), pp. 1482-7.
- Allen, G. I. and Tsukahara, N. (1974) 'Cerebrocerebellar communication systems', *Physiol Rev*, 54, (4), pp. 957-1006.
- Almeida, O. P. (2008) 'Vascular depression: myth or reality?', *Int Psychogeriatr*, 20, (4), pp. 645-52.
- Almeida, O. P., Burton, E. J., Ferrier, N., McKeith, I. G. and O'Brien, J. T. (2003a) 'Depression with late onset is associated with right frontal lobe atrophy', *Psychol Med*, 33, (4), pp. 675-81.
- Almeida, O. P., Burton, E. J., McKeith, I., Gholkar, A., Burn, D. and O'Brien, J. T. (2003b) 'MRI study of caudate nucleus volume in Parkinson's disease with and without dementia with Lewy bodies and Alzheimer's disease', *Dement Geriatr Cogn Disord*, 16, (2), pp. 57-63.
- Alzheimer's Research Trust. (2010) 'Dementia 2010', *Health Economics Research Centre, University of Oxford (Luengo-Fernandez R, Leal J, Gray A)*, <http://www.dementia2010.org/>.
- American Psychiatric Association. (1994) 'Diagnostic and statistical manual of mental disorders. 4th ed.', *APA, Washington DC*.

- Anand, A., Li, Y., Wang, Y., Gardner, K. and Lowe, M. J. (2007) 'Reciprocal effects of antidepressant treatment on activity and connectivity of the mood regulating circuit: an FMRI study', *J Neuropsychiatry Clin Neurosci*, 19, (3), pp. 274-82.
- Anand, A., Li, Y., Wang, Y., Wu, J., Gao, S., Bukhari, L., Mathews, V. P., Kalnin, A. and Lowe, M. J. (2005a) 'Activity and connectivity of brain mood regulating circuit in depression: a functional magnetic resonance study', *Biol Psychiatry*, 57, (10), pp. 1079-88.
- Anand, A., Li, Y., Wang, Y., Wu, J., Gao, S., Bukhari, L., Mathews, V. P., Kalnin, A. and Lowe, M. J. (2005b) 'Antidepressant effect on connectivity of the mood-regulating circuit: an FMRI study', *Neuropsychopharmacology*, 30, (7), pp. 1334-44.
- Andreescu, C., Butters, M. A., Begley, A., Rajji, T., Wu, M., Meltzer, C. C., Reynolds, C. F., 3rd and Aizenstein, H. (2008) 'Gray matter changes in late life depression - a structural MRI analysis', *Neuropsychopharmacology*, 33, (11), pp. 2566-72.
- Auer, D. P., Putz, B., Kraft, E., Lipinski, B., Schill, J. and Holsboer, F. (2000) 'Reduced glutamate in the anterior cingulate cortex in depression: an in vivo proton magnetic resonance spectroscopy study', *Biol Psychiatry*, 47, (4), pp. 305-13.
- Aylward, E. H., Rosenblatt, A., Field, K., Yallapragada, V., Kieburtz, K., McDermott, M., Raymond, L. A., Almqvist, E. W., Hayden, M. and Ross, C. A. (2003) 'Caudate volume as an outcome measure in clinical trials for Huntington's disease: a pilot study', *Brain Res Bull*, 62, (2), pp. 137-41.
- Ballard, C., Grace, J., McKeith, I. and Holmes, C. (1998) 'Neuroleptic sensitivity in dementia with Lewy bodies and Alzheimer's disease', *Lancet*, 351, (9108), pp. 1032-3.
- Ballard, C., Harrison, R. W. S., Lowery, K. and McKeith, I. G. (1996) 'Non-cognitive symptoms in Lewy body dementia.', in Perry, R. H., McKeith, I. G. and Perry, E. K.(eds) *Dementia with Lewy Bodies*. New York: Cambridge University Press, pp. 67-84.

- Ballard, C., Holmes, C., McKeith, I., Neill, D., O'Brien, J., Cairns, N., Lantos, P., Perry, E., Ince, P. and Perry, R. (1999) 'Psychiatric morbidity in dementia with Lewy bodies: a prospective clinical and neuropathological comparative study with Alzheimer's disease.', *Am J Psychiatry*, 156, (7), pp. 1039-45.
- Ballard, C., O'Brien, J., Gray, A., Cormack, F., Ayre, G., Rowan, E., Thompson, P., Bucks, R., McKeith, I., Walker, M. and Tovee, M. (2001) 'Attention and fluctuating attention in patients with dementia with Lewy bodies and Alzheimer disease', *Arch Neurol*, 58, (6), pp. 977-82.
- Ballard, C. G., Court, J. A., Piggott, M., Johnson, M., O'Brien, J., McKeith, I., Holmes, C., Lantos, P., Jaros, E., Perry, R. and Perry, E. (2002) 'Disturbances of consciousness in dementia with Lewy bodies associated with alteration in nicotinic receptor binding in the temporal cortex', *Conscious Cogn*, 11, (3), pp. 461-74.
- Ballmaier, M., Kumar, A., Elderkin-Thompson, V., Narr, K. L., Luders, E., Thompson, P. M., Hojatkashani, C., Pham, D., Heinz, A. and Toga, A. W. (2008a) 'Mapping callosal morphology in early- and late-onset elderly depression: an index of distinct changes in cortical connectivity', *Neuropsychopharmacology*, 33, (7), pp. 1528-36.
- Ballmaier, M., Narr, K. L., Toga, A. W., Elderkin-Thompson, V., Thompson, P. M., Hamilton, L., Haroon, E., Pham, D., Heinz, A. and Kumar, A. (2008b) 'Hippocampal morphology and distinguishing late-onset from early-onset elderly depression', *Am J Psychiatry*, 165, (2), pp. 229-37.
- Ballmaier, M., Toga, A. W., Blanton, R. E., Sowell, E. R., Lavretsky, H., Peterson, J., Pham, D. and Kumar, A. (2004) 'Anterior cingulate, gyrus rectus, and orbitofrontal abnormalities in elderly depressed patients: an MRI-based parcellation of the prefrontal cortex', *Am J Psychiatry*, 161, (1), pp. 99-108.

- Bandettini, P. (2001) 'Selection of the optimal pulse sequence for functional MRI', in Jezzard, P., Matthews, P. M. and Smith, S. M.(eds) *Functional MRI An Introduction to Methods*. Oxford Medical Publishers, pp. 123-143.
- Bandettini, P. A., Jesmanowicz, A., Wong, E. C. and Hyde, J. S. (1993) 'Processing strategies for time-course data sets in functional MRI of the human brain', *Magn Reson Med*, 30, (2), pp. 161-73.
- Barber, R., Ballard, C., McKeith, I. G., Gholkar, A. and O'Brien, J. T. (2000) 'MRI volumetric study of dementia with Lewy bodies: a comparison with AD and vascular dementia', *Neurology*, 54, (6), pp. 1304-9.
- Barber, R., Gholkar, A., Scheltens, P., Ballard, C., McKeith, I. G. and O'Brien, J. T. (1999) 'Medial temporal lobe atrophy on MRI in dementia with Lewy bodies', *Neurology*, 52, (6), pp. 1153-8.
- Barber, R., Panikkar, A. and McKeith, I. G. (2001) 'Dementia with Lewy bodies: diagnosis and management', *Int J Geriatr Psychiatry*, 16 Suppl 1, pp. S12-8.
- Beckmann, C. F., DeLuca, M., Devlin, J. T. and Smith, S. M. (2005) 'Investigations into resting-state connectivity using independent component analysis', *Philos Trans R Soc Lond B Biol Sci*, 360, (1457), pp. 1001-13.
- Beckmann, C. F., Jenkinson, M. and Smith, S. M. (2003) 'General multilevel linear modeling for group analysis in FMRI', *Neuroimage*, 20, (2), pp. 1052-63.
- Beckmann, C. F. and Smith, S. M. (2004) 'Probabilistic independent component analysis for functional magnetic resonance imaging', *IEEE Trans Med Imaging*, 23, (2), pp. 137-52.
- Beckmann, C. F. and Smith, S. M. (2005) 'Tensorial extensions of independent component analysis for multisubject FMRI analysis', *Neuroimage*, 25, (1), pp. 294-311.

- Bell-McGinty, S., Butters, M. A., Meltzer, C. C., Greer, P. J., Reynolds, C. F., 3rd and Becker, J. T. (2002) 'Brain morphometric abnormalities in geriatric depression: long-term neurobiological effects of illness duration', *Am J Psychiatry*, 159, (8), pp. 1424-7.
- Beyer, J. L., Kuchibhatla, M., Payne, M., Moo-Young, M., Cassidy, F., MacFall, J. and Krishnan, K. R. (2004) 'Caudate volume measurement in older adults with bipolar disorder', *Int J Geriatr Psychiatry*, 19, (2), pp. 109-14.
- Bhasin, M., Rowan, E., Edwards, K. and McKeith, I. (2007) 'Cholinesterase inhibitors in dementia with Lewy bodies: a comparative analysis', *Int J Geriatr Psychiatry*, 22, (9), pp. 890-5.
- Binder, J. R., Frost, J. A., Hammeke, T. A., Bellgowan, P. S., Rao, S. M. and Cox, R. W. (1999) 'Conceptual processing during the conscious resting state. A functional MRI study', *J Cogn Neurosci*, 11, (1), pp. 80-95.
- Birn, R. M., Diamond, J. B., Smith, M. A. and Bandettini, P. A. (2006) 'Separating respiratory-variation-related fluctuations from neuronal-activity-related fluctuations in fMRI', *Neuroimage*, 31, (4), pp. 1536-48.
- Birn, R. M., Smith, M. A., Jones, T. B. and Bandettini, P. A. (2008) 'The respiration response function: the temporal dynamics of fMRI signal fluctuations related to changes in respiration', *Neuroimage*, 40, (2), pp. 644-54.
- Biswal, B., Yetkin, F. Z., Haughton, V. M. and Hyde, J. S. (1995) 'Functional connectivity in the motor cortex of resting human brain using echo-planar MRI', *Magn Reson Med*, 34, (4), pp. 537-41.
- Blacker, D., Albert, M. S., Bassett, S. S., Go, R. C., Harrell, L. E. and Folstein, M. F. (1994) 'Reliability and validity of NINCDS-ADRDA criteria for Alzheimer's disease. The National Institute of Mental Health Genetics Initiative', *Arch Neurol*, 51, (12), pp. 1198-204.

- Blamire, A. M., Ogawa, S., Ugurbil, K., Rothman, D., McCarthy, G., Ellermann, J. M., Hyder, F., Rattner, Z. and Shulman, R. G. (1992) 'Dynamic mapping of the human visual cortex by high-speed magnetic resonance imaging', *Proc Natl Acad Sci U S A*, 89, (22), pp. 11069-73.
- Blazer, D. (2000) 'Psychiatry and the oldest old', *Am J Psychiatry*, 157, pp. 1915-1924.
- Blazer, D. G. (2003) 'Depression in late life: review and commentary', *J Gerontol A Biol Sci Med Sci*, 58, (3), pp. 249-65.
- Bluhm, R., Williamson, P., Lanius, R., Theberge, J., Densmore, M., Bartha, R., Neufeld, R. and Osuch, E. (2009) 'Resting state default-mode network connectivity in early depression using a seed region-of-interest analysis: decreased connectivity with caudate nucleus', *Psychiatry Clin Neurosci*, 63, (6), pp. 754-61.
- Bowen, D. M., Smith, C. B., White, P. and Davison, A. N. (1976) 'Neurotransmitter-related enzymes and indices of hypoxia in senile dementia and other abiotrophies', *Brain*, 99, (3), pp. 459-96.
- Bozzali, M., Falini, A., Cercignani, M., Baglio, F., Farina, E., Alberoni, M., Vezzulli, P., Olivetto, F., Mantovani, F., Shallice, T., Scotti, G., Canal, N. and Nemni, R. (2005) 'Brain tissue damage in dementia with Lewy bodies: an in vivo diffusion tensor MRI study', *Brain*, 128, (Pt 7), pp. 1595-604.
- Braak, E., Braak, H. and Mandelkow, E. M. (1994) 'A sequence of cytoskeleton changes related to the formation of neurofibrillary tangles and neuropil threads', *Acta Neuropathol*, 87, (6), pp. 554-67.
- Braak, H. and Braak, E. (1991) 'Neuropathological staging of Alzheimer-related changes', *Acta Neuropathol*, 82, (4), pp. 239-59.
- Braak, H. and Braak, E. (1997) 'Staging of Alzheimer-related cortical destruction', *Int Psychogeriatr*, 9 Suppl 1, pp. 257-61; discussion 269-72.

- Brodsky, H., Luscombe, G., Parker, G., Wilhelm, K., Hickie, I., Austin, M. P. and Mitchell, P. (2001) 'Early and late onset depression in old age: different aetiologies, same phenomenology', *J Affect Disord*, 66, (2-3), pp. 225-36.
- Buckner, R. L., Andrews-Hanna, J. R. and Schacter, D. L. (2008) 'The brain's default network: anatomy, function, and relevance to disease', *Ann N Y Acad Sci*, 1124, pp. 1-38.
- Buckner, R. L., Snyder, A. Z., Shannon, B. J., LaRossa, G., Sachs, R., Fotenos, A. F., Sheline, Y. I., Klunk, W. E., Mathis, C. A., Morris, J. C. and Mintun, M. A. (2005) 'Molecular, structural, and functional characterization of Alzheimer's disease: evidence for a relationship between default activity, amyloid, and memory', *J Neurosci*, 25, (34), pp. 7709-17.
- Buckner, R. L. and Vincent, J. L. (2007) 'Unrest at rest: default activity and spontaneous network correlations', *Neuroimage*, 37, (4), pp. 1091-6; discussion 1097-9.
- Burton, E. J., Barber, R., Mukaetova-Ladinska, E. B., Robson, J., Perry, R. H., Jaros, E., Kalaria, R. N. and O'Brien, J. T. (2009) 'Medial temporal lobe atrophy on MRI differentiates Alzheimer's disease from dementia with Lewy bodies and vascular cognitive impairment: a prospective study with pathological verification of diagnosis', *Brain*, 132, (Pt 1), pp. 195-203.
- Burton, E. J., Karas, G., Paling, S. M., Barber, R., Williams, E. D., Ballard, C. G., McKeith, I. G., Scheltens, P., Barkhof, F. and O'Brien, J. T. (2002) 'Patterns of cerebral atrophy in dementia with Lewy bodies using voxel-based morphometry', *Neuroimage*, 17, (2), pp. 618-30.
- Burton, E. J., McKeith, I. G., Burn, D. J., Williams, E. D. and O'Brien, J. T. (2004) 'Cerebral atrophy in Parkinson's disease with and without dementia: a comparison with Alzheimer's disease, dementia with Lewy bodies and controls', *Brain*, 127, (Pt 4), pp. 791-800.
- Butters, M. A., Aizenstein, H. J., Hayashi, K. M., Meltzer, C. C., Seaman, J., Reynolds, C. F., 3rd, Toga, A. W., Thompson, P. M. and Becker, J. T. (2009) 'Three-

dimensional surface mapping of the caudate nucleus in late-life depression', *Am J Geriatr Psychiatry*, 17, (1), pp. 4-12.

Buxton, R. B. (2002a) 'Mapping Brain Activation with BOLD-fMRI', in *Introduction to Functional Magnetic Resonance Imaging. Principles and Techniques*.

Cambridge University Press, pp. 417-444.

Buxton, R. B. (2002b) 'Nuclear Magnetic Resonance', in *Introduction to Functional Magnetic Resonance Imaging. Principles and Techniques*. Cambridge

University Press, pp. 64-85.

Cabeza, R., Anderson, N. D., Houle, S., Mangels, J. A. and Nyberg, L. (2000) 'Age-related differences in neural activity during item and temporal-order memory retrieval: a positron emission tomography study', *J Cogn Neurosci*, 12, (1), pp. 197-206.

Calderon, J., Perry, R. J., Erzinclioglu, S. W., Berrios, G. E., Dening, T. R. and Hodges, J. R. (2001) 'Perception, attention, and working memory are disproportionately impaired in dementia with Lewy bodies compared with Alzheimer's disease', *J Neurol Neurosurg Psychiatry*, 70, (2), pp. 157-64.

Castellanos, F. X., Margulies, D. S., Kelly, C., Uddin, L. Q., Ghaffari, M., Kirsch, A., Shaw, D., Shehzad, Z., Di Martino, A., Biswal, B., Sonuga-Barke, E. J., Rotrosen, J., Adler, L. A. and Milham, M. P. (2008) 'Cingulate-precuneus interactions: a new locus of dysfunction in adult attention-deficit/hyperactivity disorder', *Biol Psychiatry*, 63, (3), pp. 332-7.

Chang, C. and Glover, G. H. (2009) 'Effects of model-based physiological noise correction on default mode network anti-correlations and correlations', *Neuroimage*, 47, (4), pp. 1448-59.

Collerton, D., Burn, D., McKeith, I. and O'Brien, J. (2003) 'Systematic review and meta-analysis show that dementia with Lewy bodies is a visual-perceptual and attentional-executive dementia', *Dement Geriatr Cogn Disord*, 16, (4), pp. 229-37.

- Collerton, D., Perry, E. and McKeith, I. (2005) 'Why people see things that are not there: a novel Perception and Attention Deficit model for recurrent complex visual hallucinations', *Behav Brain Sci*, 28, (6), pp. 737-57; discussion 757-94.
- Colloby, S. J., Fenwick, J. D., Williams, E. D., Paling, S. M., Lobotesis, K., Ballard, C., McKeith, I. and O'Brien, J. T. (2002) 'A comparison of (99m)Tc-HMPAO SPET changes in dementia with Lewy bodies and Alzheimer's disease using statistical parametric mapping', *Eur J Nucl Med Mol Imaging*, 29, (5), pp. 615-22.
- Colloby, S. J., Firbank, M. J., Pakrasi, S., Lloyd, J. J., Driver, I., McKeith, I. G., Williams, E. D. and O'Brien, J. T. (2008) 'A comparison of 99mTc-exametazine and 123I-FP-CIT SPECT imaging in the differential diagnosis of Alzheimer's disease and dementia with Lewy bodies', *Int Psychogeriatr*, 20, (6), pp. 1124-40.
- Comon, P. (1994) 'Independent component analysis: a new concept?', *Signal Processing*, 36, pp. 11-20.
- Corbetta, M., Kincade, J. M. and Shulman, G. L. (2002) 'Neural systems for visual orienting and their relationships to spatial working memory', *J Cogn Neurosci*, 14, (3), pp. 508-23.
- Corbetta, M. and Shulman, G. L. (2002) 'Control of goal-directed and stimulus-driven attention in the brain', *Nat Rev Neurosci*, 3, (3), pp. 201-15.
- Cordes, D., Haughton, V. M., Arfanakis, K., Carew, J. D., Turski, P. A., Moritz, C. H., Quigley, M. A. and Meyerand, M. E. (2001) 'Frequencies contributing to functional connectivity in the cerebral cortex in "resting-state" data', *AJNR Am J Neuroradiol*, 22, (7), pp. 1326-33.
- Cordes, D., Haughton, V. M., Arfanakis, K., Wendt, G. J., Turski, P. A., Moritz, C. H., Quigley, M. A. and Meyerand, M. E. (2000) 'Mapping functionally related regions of brain with functional connectivity MR imaging', *AJNR Am J Neuroradiol*, 21, (9), pp. 1636-44.

- Court, J., Martin-Ruiz, C., Piggott, M., Spurden, D., Griffiths, M. and Perry, E. (2001) 'Nicotinic receptor abnormalities in Alzheimer's disease', *Biol Psychiatry*, 49, (3), pp. 175-84.
- Cousins, D. A., Burton, E. J., Burn, D., Gholkar, A., McKeith, I. G. and O'Brien, J. T. (2003) 'Atrophy of the putamen in dementia with Lewy bodies but not Alzheimer's disease: an MRI study', *Neurology*, 61, (9), pp. 1191-5.
- Cummings, J. L., Mega, M., Gray, K., Rosenberg-Thompson, S., Carusi, D. A. and Gornbein, J. (1994) 'The Neuropsychiatric Inventory: comprehensive assessment of psychopathology in dementia', *Neurology*, 44, (12), pp. 2308-14.
- D'Esposito, M., Deouell, L. Y. and Gazzaley, A. (2003) 'Alterations in the BOLD fMRI signal with ageing and disease: a challenge for neuroimaging', *Nat Rev Neurosci*, 4, (11), pp. 863-72.
- D'Ath, P., Katona, P., Mullan, E., Evans, S. and Katona, C. (1994) 'Screening detection and management of depression in elderly primary care attenders. I: the acceptability and performance of the 15 item Geriatric Depression Scale (GDS15) and the development of short versions. ', *Fam Pract*, 11, pp. 260–266.
- Damoiseaux, J. S., Beckmann, C. F., Arigita, E. J., Barkhof, F., Scheltens, P., Stam, C. J., Smith, S. M. and Rombouts, S. A. (2008) 'Reduced resting-state brain activity in the "default network" in normal aging', *Cereb Cortex*, 18, (8), pp. 1856-64.
- Damoiseaux, J. S., Rombouts, S. A., Barkhof, F., Scheltens, P., Stam, C. J., Smith, S. M. and Beckmann, C. F. (2006) 'Consistent resting-state networks across healthy subjects', *Proc Natl Acad Sci U S A*, 103, (37), pp. 13848-53.
- De Luca, M., Beckmann, C. F., De Stefano, N., Matthews, P. M. and Smith, S. M. (2006) 'fMRI resting state networks define distinct modes of long-distance interactions in the human brain', *Neuroimage*, 29, (4), pp. 1359-67.
- DeArmond, S. J., Fusco, M. M. and Dewey, M. M. (1989) *Structure of the Human Brain: A Photographic Atlas*. Third ed New York, NY: Oxford University Press.

- Desmond, J. E., Sum, J. M., Wagner, A. D., Demb, J. B., Shear, P. K., Glover, G. H., Gabrieli, J. D. and Morrell, M. J. (1995) 'Functional MRI measurement of language lateralization in Wada-tested patients', *Brain*, 118, pp. 1411–1419.
- Devanand, D. P., Sano, M., Tang, M. X., Taylor, S., Gurland, B. J., Wilder, D., Stern, Y. and Mayeux, R. (1996) 'Depressed mood and the incidence of Alzheimer's disease in the elderly living in the community', *Arch Gen Psychiatry*, 53, (2), pp. 175-82.
- Dickerson, B. C., Salat, D. H., Greve, D. N., Chua, E. F., Rand-Giovannetti, E., Rentz, D. M., Bertram, L., Mullin, K., Tanzi, R. E., Blacker, D., Albert, M. S. and Sperling, R. A. (2005) 'Increased hippocampal activation in mild cognitive impairment compared to normal aging and AD', *Neurology*, 65, (3), pp. 404-11.
- Dotson, V. M., Davatzikos, C., Kraut, M. A. and Resnick, S. M. (2009) 'Depressive symptoms and brain volumes in older adults: a longitudinal magnetic resonance imaging study', *J Psychiatry Neurosci*, 34, (5), pp. 367-75.
- Drachman, D. A. and Leavitt, J. (1974) 'Human memory and the cholinergic system. A relationship to aging?', *Arch Neurol*, 30, (2), pp. 113-21.
- Drevets, W. C., Bogers, W. and Raichle, M. E. (2002) 'Functional anatomical correlates of antidepressant drug treatment assessed using PET measures of regional glucose metabolism', *Eur Neuropsychopharmacol*, 12, (6), pp. 527-44.
- Drevets, W. C., Price, J. L., Simpson, J. R., Jr., Todd, R. D., Reich, T., Vannier, M. and Raichle, M. E. (1997) 'Subgenual prefrontal cortex abnormalities in mood disorders', *Nature*, 386, (6627), pp. 824-7.
- Du, A. T., Schuff, N., Amend, D., Laakso, M. P., Hsu, Y. Y., Jagust, W. J., Yaffe, K., Kramer, J. H., Reed, B., Norman, D., Chui, H. C. and Weiner, M. W. (2001) 'Magnetic resonance imaging of the entorhinal cortex and hippocampus in mild cognitive impairment and Alzheimer's disease', *J Neurol Neurosurg Psychiatry*, 71, (4), pp. 441-7.

- Duda, J. E., Giasson, B. I., Mabon, M. E., Lee, V. M. and Trojanowski, J. Q. (2002) 'Novel antibodies to synuclein show abundant striatal pathology in Lewy body diseases', *Ann Neurol*, 52, (2), pp. 205-10.
- Eastley, R. and Wilcock, G. K. (2005) 'Assessment of Dementia', in Burns, A., O'Brien, J. and Ames, D.(eds) *Dementia*. Edward Arnold, pp. 38-44.
- Edwards, K., Royall, D., Hershey, L., Lichter, D., Hake, A., Farlow, M., Pasquier, F. and Johnson, S. (2007) 'Efficacy and safety of galantamine in patients with dementia with Lewy bodies: a 24-week open-label study', *Dement Geriatr Cogn Disord*, 23, (6), pp. 401-5.
- Evarts, E. V. and Thach, W. T. (1969) 'Motor mechanisms of the CNS: cerebrocerebellar interrelations', *Annu Rev Physiol*, 31, pp. 451-98.
- Fahn, S., Elton, R. and Members of the UPDRS development committee. (1987) 'Unified Parkinson's disease rating scale', in Fahn, S., Marsden, C. D., Calne, D. B. and Goldstein, M.(eds) *Recent developments in Parkinson's disease*. Florham Park; NJ: MacMillan Healthcare Information.
- Ferman, T. J., Smith, G. E., Boeve, B. F., Graff-Radford, N. R., Lucas, J. A., Knopman, D. S., Petersen, R. C., Ivnik, R. J., Wszolek, Z., Uitti, R. and Dickson, D. W. (2006) 'Neuropsychological differentiation of dementia with Lewy bodies from normal aging and Alzheimer's disease', *Clin Neuropsychol*, 20, (4), pp. 623-36.
- Firbank, M. J., Blamire, A. M., Krishnan, M. S., Teodorczuk, A., English, P., Gholkar, A., Harrison, R. M. and O'Brien, J. T. (2007) 'Diffusion tensor imaging in dementia with Lewy bodies and Alzheimer's disease', *Psychiatry Res*, 155, (2), pp. 135-45.
- Firbank, M. J., Blamire, A. M., Teodorczuk, A., Teper, E., Burton, E. J., Mitra, D. and O'Brien, J. T. (2010) 'High Resolution Imaging of the Medial Temporal Lobe in Alzheimer's Disease and Dementia with Lewy Bodies', *J Alzheimers Dis*, Aug 6 [Epub ahead of print].

- Firbank, M. J., Colloby, S. J., Burn, D. J., McKeith, I. G. and O'Brien, J. T. (2003a) 'Regional cerebral blood flow in Parkinson's disease with and without dementia', *Neuroimage*, 20, (2), pp. 1309-19.
- Firbank, M. J., Lloyd, A. J., Ferrier, N. and O'Brien, J. T. (2004) 'A volumetric study of MRI signal hyperintensities in late-life depression', *Am J Geriatr Psychiatry*, 12, (6), pp. 606-12.
- Firbank, M. J., Minett, T. and O'Brien, J. T. (2003b) 'Changes in DWI and MRS associated with white matter hyperintensities in elderly subjects', *Neurology*, 61, (7), pp. 950-4.
- FMRIB Analysis Group. (2007) 'FMRIB Software Library (FSL)', *Functional MRI of the Brain Analysis Group, Oxford University, UK*, Version 5.
- Folstein, M. F., Folstein, S. E. and McHugh, P. R. (1975) "'Mini-mental state". A practical method for grading the cognitive state of patients for the clinician', *J Psychiatr Res*, 12, (3), pp. 189-98.
- Fox, M. D. and Raichle, M. E. (2007) 'Spontaneous fluctuations in brain activity observed with functional magnetic resonance imaging', *Nat Rev Neurosci*, 8, (9), pp. 700-11.
- Fox, M. D., Snyder, A. Z., Vincent, J. L., Corbetta, M., Van Essen, D. C. and Raichle, M. E. (2005) 'The human brain is intrinsically organized into dynamic, anticorrelated functional networks', *Proc Natl Acad Sci U S A*, 102, (27), pp. 9673-8.
- Fox, M. D., Zhang, D., Snyder, A. Z. and Raichle, M. E. (2009) 'The global signal and observed anticorrelated resting state brain networks', *J Neurophysiol*, 101, (6), pp. 3270-83.

- Fox, N. C., Freeborough, P. A. and Rossor, M. N. (1996) 'Visualisation and quantification of rates of atrophy in Alzheimer's disease', *Lancet*, 348, (9020), pp. 94-7.
- Fox, P. T. and Raichle, M. E. (1986) 'Focal physiological uncoupling of cerebral blood flow and oxidative metabolism during somatosensory stimulation in human subjects', *Proc Natl Acad Sci U S A*, 83, (4), pp. 1140-4.
- Francis, P. T., Palmer, A. M., Snape, M. and Wilcock, G. K. (1999) 'The cholinergic hypothesis of Alzheimer's disease: a review of progress', *J Neurol Neurosurg Psychiatry*, 66, (2), pp. 137-47.
- Friston, K. J., Frith, C. D., Liddle, P. F. and Frackowiak, R. S. (1993) 'Functional connectivity: the principal-component analysis of large (PET) data sets', *J Cereb Blood Flow Metab*, 13, (1), pp. 5-14.
- Galasko, D. and Hansen, L. A. (1992) 'Lewy body disease', *Current Opinions in Neurology and Neurosurgery*, 5, pp. 889-894.
- Gao, S., Hendrie, H. C., Hall, K. S. and Hui, S. (1998) 'The relationships between age, sex, and the incidence of dementia and Alzheimer disease: a meta-analysis', *Arch Gen Psychiatry*, 55, (9), pp. 809-15.
- Gili, T., Cercignani, M., Serra, L., Perri, R., Giove, F., Maraviglia, B., Caltagirone, C. and Bozzali, M. (2010) 'Regional brain atrophy and functional disconnection across Alzheimer's disease evolution', *J Neurol Neurosurg Psychiatry*, Jul 16 [Epub ahead of print].
- Glover, G. H., Li, T. Q. and Ress, D. (2000) 'Image-based method for retrospective correction of physiological motion effects in fMRI: RETROICOR', *Magn Reson Med*, 44, (1), pp. 162-7.
- Goldman, R. I., Cohen, M. (2003) 'Tomographic distribution of resting alpha rhythm sources revealed by independent component analysis', *Neuroimage*, 19, pp. S412.

- Goldman, R. I., Stern, J. M., Engel, J., Jr. and Cohen, M. S. (2002) 'Simultaneous EEG and fMRI of the alpha rhythm', *Neuroreport*, 13, (18), pp. 2487-92.
- Green, R. C., Cupples, L. A., Kurz, A., Auerbach, S., Go, R., Sadovnick, D., Duara, R., Kukull, W. A., Chui, H., Edeki, T., Griffith, P. A., Friedland, R. P., Bachman, D. and Farrer, L. (2003) 'Depression as a risk factor for Alzheimer disease: the MIRAGE Study', *Arch Neurol*, 60, (5), pp. 753-9.
- Greenberg, D. L., Payne, M. E., MacFall, J. R., Steffens, D. C. and Krishnan, R. R. (2008) 'Hippocampal volumes and depression subtypes', *Psychiatry Res*, 163, (2), pp. 126-32.
- Greenwald, B. S., Kramer-Ginsberg, E., Bogerts, B., Ashtari, M., Aupperle, P., Wu, H., Allen, L., Zeman, D. and Patel, M. (1997) 'Qualitative magnetic resonance imaging findings in geriatric depression. Possible link between later-onset depression and Alzheimer's disease?', *Psychol Med*, 27, (2), pp. 421-31.
- Greicius, M. D., Flores, B. H., Menon, V., Glover, G. H., Solvason, H. B., Kenna, H., Reiss, A. L. and Schatzberg, A. F. (2007) 'Resting-state functional connectivity in major depression: abnormally increased contributions from subgenual cingulate cortex and thalamus', *Biol Psychiatry*, 62, (5), pp. 429-37.
- Greicius, M. D., Krasnow, B., Reiss, A. L. and Menon, V. (2003) 'Functional connectivity in the resting brain: a network analysis of the default mode hypothesis', *Proc Natl Acad Sci U S A*, 100, (1), pp. 253-8.
- Greicius, M. D., Srivastava, G., Reiss, A. L. and Menon, V. (2004) 'Default-mode network activity distinguishes Alzheimer's disease from healthy aging: evidence from functional MRI', *Proc Natl Acad Sci U S A*, 101, (13), pp. 4637-42.
- Grimm, S., Boesiger, P., Beck, J., Schuepbach, D., Birmpohl, F., Walter, M., Ernst, J., Hell, D., Boeker, H. and Northoff, G. (2009) 'Altered negative BOLD responses in the default-mode network during emotion processing in depressed subjects', *Neuropsychopharmacology*, 34, (4), pp. 932-843.

- Gusnard, D. A., Raichle, M. E. and Raichle, M. E. (2001) 'Searching for a baseline: functional imaging and the resting human brain', *Nat Rev Neurosci*, 2, (10), pp. 685-94.
- Haase, A., Matthaei, D., Hanicke, W. and Frahm, J. (1986) 'Dynamic digital subtraction imaging using fast low-angle shot MR movie sequence', *Radiology*, 160, (2), pp. 537-41.
- Haass, C., Koo, E. H., Mellon, A., Hung, A. Y. and Selkoe, D. J. (1992) 'Targeting of cell-surface beta-amyloid precursor protein to lysosomes: alternative processing into amyloid-bearing fragments', *Nature*, 357, (6378), pp. 500-3.
- Hannestad, J., Taylor, W. D., McQuoid, D. R., Payne, M. E., Krishnan, K. R., Steffens, D. C. and MacFall, J. R. (2006) 'White matter lesion volumes and caudate volumes in late-life depression', *Int J Geriatr Psychiatry*, 21, (12), pp. 1193-8.
- Hanyu, H., Shimizu, S., Hirao, K., Kanetaka, H., Iwamoto, T., Chikamori, T., Usui, Y., Yamashina, A., Koizumi, K. and Abe, K. (2006a) 'Comparative value of brain perfusion SPECT and [(123)I]MIBG myocardial scintigraphy in distinguishing between dementia with Lewy bodies and Alzheimer's disease', *Eur J Nucl Med Mol Imaging*, 33, (3), pp. 248-53.
- Hanyu, H., Shimizu, S., Hirao, K., Kanetaka, H., Sakurai, H., Iwamoto, T., Koizumi, K. and Abe, K. (2006b) 'Differentiation of dementia with Lewy bodies from Alzheimer's disease using Mini-Mental State Examination and brain perfusion SPECT', *J Neurol Sci*, 250, (1-2), pp. 97-102.
- Hanyu, H., Shimizu, S., Tanaka, Y., Hirao, K., Iwamoto, T. and Abe, K. (2007) 'MR features of the substantia innominata and therapeutic implications in dementias', *Neurobiol Aging*, 28, (4), pp. 548-54.
- Harding, A. J., Broe, G. A. and Halliday, G. M. (2002) 'Visual hallucinations in Lewy body disease relate to Lewy bodies in the temporal lobe', *Brain*, 125, (Pt 2), pp. 391-403.

- Haruno, M., Kuroda, T., Doya, K., Toyama, K., Kimura, M., Samejima, K., Imamizu, H. and Kawato, M. (2004) 'A neural correlate of reward-based behavioral learning in caudate nucleus: a functional magnetic resonance imaging study of a stochastic decision task', *J Neurosci*, 24, (7), pp. 1660-5.
- Hasler, G., van der Veen, J. W., Tumonis, T., Meyers, N., Shen, J. and Drevets, W. C. (2007) 'Reduced prefrontal glutamate/glutamine and gamma-aminobutyric acid levels in major depression determined using proton magnetic resonance spectroscopy', *Arch Gen Psychiatry*, 64, (2), pp. 193-200.
- Haxby, J. V., Hoffman, E. A. and Gobbini, M. I. (2000) 'The distributed human neural system for face perception', *Trends Cogn Sci*, 4, (6), pp. 223-233.
- He, Y., Wang, L., Zang, Y., Tian, L., Zhang, X., Li, K. and Jiang, T. (2007) 'Regional coherence changes in the early stages of Alzheimer's disease: a combined structural and resting-state functional MRI study', *Neuroimage*, 35, (2), pp. 488-500.
- Hedden, T., Van Dijk, K., Becker, J., Mehta, A., RA., S., Johnson, K. and Buckner, R. (2009) 'Disruption of functional connectivity in clinically normal older adults harboring amyloid burden.', *J Neurosci*, 29, (40), pp. 12686-94.
- Herrmann, L. L., Goodwin, G. M. and Ebmeier, K. P. (2007) 'The cognitive neuropsychology of depression in the elderly.', *Psychol Med.*, 37, (12), pp. 1693-702.
- Herrmann, L. L., Le Masurier, M. and Ebmeier, K. P. (2008) 'White matter hyperintensities in late life depression: a systematic review', *J Neurol Neurosurg Psychiatry*, 79, (6), pp. 619-24.
- Hickie, I., Naismith, S., Ward, P. B., Turner, K., Scott, E., Mitchell, P., Wilhelm, K. and Parker, G. (2005) 'Reduced hippocampal volumes and memory loss in patients with early- and late-onset depression', *Br J Psychiatry*, 186, pp. 197-202.

- Hirao, K., Ohnishi, T., Matsuda, H., Nemoto, K., Hirata, Y., Yamashita, F., Asada, T. and Iwamoto, T. (2006) 'Functional interactions between entorhinal cortex and posterior cingulate cortex at the very early stage of Alzheimer's disease using brain perfusion single-photon emission computed tomography', *Nucl Med Commun*, 27, (2), pp. 151-6.
- Hoge, R. D. and Pike, G. B. (2001) 'Quantitative measurement using fMRI', in Jezzard, P., Matthews, P. M. and Smith, S. M.(eds) *Functional MRI An Introduction to Methods*. Oxford Medical Publishers.
- Horn, D. I., Yu, C., Steiner, J., Buchmann, J., Kaufmann, J., Osoba, A., Eckert, U., Zierhut, K. C., Schiltz, K., He, H., Biswal, B., Bogerts, B. and Walter, M. (2010) 'Glutamatergic and resting-state functional connectivity correlates of severity in major depression - the role of pregenual anterior cingulate cortex and anterior insula', *Front Syst Neurosci*, 4, (33).
- Hort, J., O'Brien, J. T., Gainotti, G., Pirttila, T., Popescu, B. O., Rektorova, I., Sorbi, S. and Scheltens, P. (2010) 'EFNS guidelines for the diagnosis and management of Alzheimer's disease', *Eur J Neurol*, [Epub ahead of print].
- Hu, X., Le, T. H., Parrish, T. and Erhard, P. (1995) 'Retrospective estimation and correction of physiological fluctuation in functional MRI', *Magn Reson Med*, 34, (2), pp. 201-12.
- Hu, X., Le, T. H. and Ugurbil, K. (1997) 'Evaluation of the early response in fMRI in individual subjects using short stimulus duration', *Magn Reson Med*, 37, (6), pp. 877-84.
- Ishii, K., Imamura, T., Sasaki, M., Yamaji, S., Sakamoto, S., Kitagaki, H., Hashimoto, M., Hirono, N., Shimomura, T. and Mori, E. (1998) 'Regional cerebral glucose metabolism in dementia with Lewy bodies and Alzheimer's disease', *Neurology*, 51, (1), pp. 125-30.

- Ishii, K., Yamaji, S., Kitagaki, H., Imamura, T., Hirono, N. and Mori, E. (1999) 'Regional cerebral blood flow difference between dementia with Lewy bodies and AD', *Neurology*, 53, (2), pp. 413-6.
- Jack, C. R., Jr., Dickson, D. W., Parisi, J. E., Xu, Y. C., Cha, R. H., O'Brien, P. C., Edland, S. D., Smith, G. E., Boeve, B. F., Tangalos, E. G., Kokmen, E. and Petersen, R. C. (2002) 'Antemortem MRI findings correlate with hippocampal neuropathology in typical aging and dementia', *Neurology*, 58, (5), pp. 750-7.
- Jack, C. R., Jr., Petersen, R. C., O'Brien, P. C. and Tangalos, E. G. (1992) 'MR-based hippocampal volumetry in the diagnosis of Alzheimer's disease', *Neurology*, 42, (1), pp. 183-8.
- Jack, C. R., Jr., Petersen, R. C., Xu, Y. C., Waring, S. C., O'Brien, P. C., Tangalos, E. G., Smith, G. E., Ivnik, R. J. and Kokmen, E. (1997) 'Medial temporal atrophy on MRI in normal aging and very mild Alzheimer's disease', *Neurology*, 49, (3), pp. 786-94.
- Jack, C. R., Jr., Shiung, M. M., Gunter, J. L., O'Brien, P. C., Weigand, S. D., Knopman, D. S., Boeve, B. F., Ivnik, R. J., Smith, G. E., Cha, R. H., Tangalos, E. G. and Petersen, R. C. (2004) 'Comparison of different MRI brain atrophy rate measures with clinical disease progression in AD', *Neurology*, 62, (4), pp. 591-600.
- Jenkinson, M., Bannister, P., Brady, M. and Smith, S. (2002) 'Improved optimization for the robust and accurate linear registration and motion correction of brain images', *Neuroimage*, 17, (2), pp. 825-41.
- Jenkinson, M. and Smith, S. (2001) 'A global optimisation method for robust affine registration of brain images', *Med Image Anal*, 5, (2), pp. 143-56.
- Johnson, K. A., Jones, K., Holman, B. L., Becker, J. A., Spiers, P. A., Satlin, A. and Albert, M. S. (1998) 'Preclinical prediction of Alzheimer's disease using SPECT', *Neurology*, 50, (6), pp. 1563-71.

- Johnson, S. C., Schmitz, T. W., Moritz, C. H., Meyerand, M. E., Rowley, H. A., Alexander, A. L., Hansen, K. W., Gleason, C. E., Carlsson, C. M., Ries, M. L., Asthana, S., Chen, K., Reiman, E. M. and Alexander, G. E. (2006) 'Activation of brain regions vulnerable to Alzheimer's disease: the effect of mild cognitive impairment', *Neurobiol Aging*, 27, (11), pp. 1604-12.
- Jorm, A. F. and Jolley, D. (1998) 'The incidence of dementia: a meta-analysis', *Neurology*, 51, (3), pp. 728-33.
- Kang, J., Lemaire, H. G., Unterbeck, A., Salbaum, J. M., Masters, C. L., Grzeschik, K. H., Multhaup, G., Beyreuther, K. and Muller-Hill, B. (1987) 'The precursor of Alzheimer's disease amyloid A4 protein resembles a cell-surface receptor', *Nature*, 325, (6106), pp. 733-6.
- Kazee, A., Eskin, T., Lapham, L., Gabriel, K., McDaniel, K. and Hamill, R. (1993) 'Clinicopathologic correlates in Alzheimer disease: assessment of clinical and pathologic diagnostic criteria', *Alzheimer Dis Assoc Disord*, 7, pp. 152-164.
- Kemp, J. M. and Powell, T. P. (1971) 'The connexions of the striatum and globus pallidus: synthesis and speculation', *Philos Trans R Soc Lond B Biol Sci*, 262, (845), pp. 441-57.
- Kemp, P. M., Hoffmann, S. A., Tossici-Bolt, L., Fleming, J. S. and Holmes, C. (2007) 'Limitations of the HMPAO SPECT appearances of occipital lobe perfusion in the differential diagnosis of dementia with Lewy bodies', *Nucl Med Commun*, 28, (6), pp. 451-6.
- Kenny, E. R., Burton, E. J. and O'Brien, J. T. (2008) 'A volumetric magnetic resonance imaging study of entorhinal cortex volume in dementia with lewy bodies. A comparison with Alzheimer's disease and Parkinson's disease with and without dementia', *Dement Geriatr Cogn Disord*, 26, (3), pp. 218-25.
- Kenny, E. R., O'Brien, J. T., Cousins, D. A., Richardson, J., Thomas, A. J., Firbank, M. J. and Blamire, A. M. (2010) 'Functional connectivity in late-life depression

using resting-state functional magnetic resonance imaging', *Am J Geriatr Psychiatry*, 18, (7), pp. 643-51.

Khundakar, A., Morris, C., Oakley, A. and Thomas, A. J. (2010) 'Morphometric Analysis of Neuronal and Glial Cell Pathology in the Caudate Nucleus in Late-Life Depression', *Am J Geriatr Psychiatry*, Apr 27 [Epub ahead of print].

Killiany, R. J., Gomez-Isla, T., Moss, M., Kikinis, R., Sandor, T., Jolesz, F., Tanzi, R., Jones, K., Hyman, B. T. and Albert, M. S. (2000) 'Use of structural magnetic resonance imaging to predict who will get Alzheimer's disease', *Ann Neurol*, 47, (4), pp. 430-9.

Kiviniemi, V., Kantola, J. H., Jauhiainen, J., Hyvarinen, A. and Tervonen, O. (2003) 'Independent component analysis of nondeterministic fMRI signal sources', *Neuroimage*, 19, (2 Pt 1), pp. 253-60.

Klunk, W. E., Engler, H., Nordberg, A., Wang, Y., Blomqvist, G., Holt, D. P., Bergstrom, M., Savitcheva, I., Huang, G. F., Estrada, S., Ausen, B., Debnath, M. L., Barletta, J., Price, J. C., Sandell, J., Lopresti, B. J., Wall, A., Koivisto, P., Antoni, G., Mathis, C. A. and Langstrom, B. (2004) 'Imaging brain amyloid in Alzheimer's disease with Pittsburgh Compound-B', *Ann Neurol*, 55, (3), pp. 306-19.

Koch, W., Teipel, S., Mueller, S., Buerger, K., Bokde, A. L., Hampel, H., Coates, U., Reiser, M. and Meindl, T. (2010) 'Effects of aging on default mode network activity in resting state fMRI: Does the method of analysis matter?', *Neuroimage*, 51, (1), pp. 280-7.

Kohler, S., Thomas, A. J., Barnett, N. A. and O'Brien, J. T. (2010a) 'The pattern and course of cognitive impairment in late-life depression', *Psychol Med*, 40, (4), pp. 591-602.

Kohler, S., Thomas, A. J., Lloyd, A., Barber, R., Almeida, O. P. and O'Brien, J. T. (2010b) 'White matter hyperintensities, cortisol levels, brain atrophy and

continuing cognitive deficits in late-life depression', *Br J Psychiatry*, 196, (2), pp. 143-9.

Krishnan, K. R., McDonald, W. M., Escalona, P. R., Doraiswamy, P. M., Na, C., Husain, M. M., Figiel, G. S., Boyko, O. B., Ellinwood, E. H. and Nemeroff, C. B. (1992) 'Magnetic resonance imaging of the caudate nuclei in depression. Preliminary observations', *Arch Gen Psychiatry*, 49, (7), pp. 553-7.

Kumar, A., Bilker, W., Lavretsky, H. and Gottlieb, G. (2000) 'Volumetric asymmetries in late-onset mood disorders: an attenuation of frontal asymmetry with depression severity', *Psychiatry Res*, 100, (1), pp. 41-7.

Kumar, A., Newberg, A., Alavi, A., Berlin, J., Smith, R. and Reivich, M. (1993) 'Regional cerebral glucose metabolism in late-life depression and Alzheimer disease: a preliminary positron emission tomography study', *Proc Natl Acad Sci U S A*, 90, (15), pp. 7019-7023.

Lacerda, A. L., Nicoletti, M. A., Brambilla, P., Sassi, R. B., Mallinger, A. G., Frank, E., Kupfer, D. J., Keshavan, M. S. and Soares, J. C. (2003) 'Anatomical MRI study of basal ganglia in major depressive disorder', *Psychiatry Res*, 124, (3), pp. 129-40.

Lai, M. K., Lai, O. F., Keene, J., Esiri, M. M., Francis, P. T., Hope, T. and Chen, C. P. (2001) 'Psychosis of Alzheimer's disease is associated with elevated muscarinic M2 binding in the cortex', *Neurology*, 57, (5), pp. 805-11.

Lancaster, J. L., Summerlin, J. L., Rainey, L., Freitas, C. S. and Fox, P. T. (1997) 'The Talairach Daemon, a database server for Talairach Atlas Labels', *Neuroimage*, 5, pp. S633.

Lancaster, J. L., Tordesillas-Gutierrez, D., Martinez, M., Salinas, F., Evans, A., Zilles, K., Mazziotta, J. C. and Fox, P. T. (2007) 'Bias between MNI and Talairach coordinates analyzed using the ICBM-152 brain template', *Hum Brain Mapp*, 28, (11), pp. 1194-205.

- Lancaster, J. L., Woldorff, M. G., Parsons, L. M., Liotti, M., Freitas, C. S., Rainey, L., Kochunov, P. V., Nickerson, D., Mikiten, S. A. and Fox, P. T. (2000) 'Automated Talairach atlas labels for functional brain mapping', *Hum Brain Mapp*, 10, (3), pp. 120-31.
- Li, S. J., Li, Z., Wu, G., Zhang, M. J., Franczak, M. and Antuono, P. G. (2002) 'Alzheimer Disease: evaluation of a functional MR imaging index as a marker', *Radiology*, 225, (1), pp. 253-9.
- Litvan, I., Bhatia, K. P., Burn, D. J., Goetz, C. G., Lang, A. E., McKeith, I., Quinn, N., Sethi, K. D., Shults, C. and Wenning, G. K. (2003) 'Movement Disorders Society Scientific Issues Committee report: SIC Task Force appraisal of clinical diagnostic criteria for Parkinsonian disorders', *Mov Disord*, 18, (5), pp. 467-86.
- Lloyd, A. J., Ferrier, I. N., Barber, R., Gholkar, A., Young, A. H. and O'Brien, J. T. (2004) 'Hippocampal volume change in depression: late- and early-onset illness compared', *Br J Psychiatry*, 184, pp. 488-95.
- Lobotesis, K., Fenwick, J. D., Phipps, A., Ryman, A., Swann, A., Ballard, C., McKeith, I. G. and O'Brien, J. T. (2001) 'Occipital hypoperfusion on SPECT in dementia with Lewy bodies but not AD', *Neurology*, 56, (5), pp. 643-9.
- Logothetis, N. K., Pauls, J., Augath, M., Trinath, T. and Oeltermann, A. (2001) 'Neurophysiological investigation of the basis of the fMRI signal', *Nature*, 412, (6843), pp. 150-7.
- Lowe, M. J., Mock, B. J. and Sorenson, J. A. (1998) 'Functional connectivity in single and multislice echoplanar imaging using resting-state fluctuations', *Neuroimage*, 7, (2), pp. 119-32.
- Lund, T. E., Madsen, K. H., Sidaros, K., Luo, W. L. and Nichols, T. E. (2006) 'Non-white noise in fMRI: does modelling have an impact?', *Neuroimage*, 29, (1), pp. 54-66.

- Lustig, C., Snyder, A. Z., Bhakta, M., O'Brien, K. C., McAvoy, M., Raichle, M. E., Morris, J. C. and Buckner, R. L. (2003) 'Functional deactivations: change with age and dementia of the Alzheimer type', *Proc Natl Acad Sci U S A*, 100, (24), pp. 14504-9.
- Mansfield, P. (1977) 'Multi-planar image formation using NMR spin echos.', *J Phys*, C10, pp. L55-L58.
- Margulies, D. S., Kelly, A. M., Uddin, L. Q., Biswal, B. B., Castellanos, F. X. and Milham, M. P. (2007) 'Mapping the functional connectivity of anterior cingulate cortex', *Neuroimage*, 37, (2), pp. 579-88.
- Martin, J. (1996) 'The Basal Ganglia', in *Neuroanatomy Text and Atlas*. Second ed New York: Prentice Hall International.
- Masters, C. L., Simms, G., Weinman, N. A., Multhaup, G., McDonald, B. L. and Beyreuther, K. (1985) 'Amyloid plaque core protein in Alzheimer disease and Down syndrome', *Proc Natl Acad Sci U S A*, 82, (12), pp. 4245-9.
- Matthews, S. C., Paulus, M. P. and Dimsdale, J. E. (2004) 'Contribution of functional neuroimaging to understanding neuropsychiatric side effects of interferon in hepatitis C', *Psychosomatics*, 45, (4), pp. 281-6.
- Maurer-Spurej, E., Pittendreigh, C. and Solomons, K. (2004) 'The influence of selective serotonin reuptake inhibitors on human platelet serotonin', *Thromb Haemost*, 91, (1), pp. 119-28.
- Mayberg, H. S. (1994) 'Frontal lobe dysfunction in secondary depression', *J Neuropsychiatry Clin Neurosci*, 6, (4), pp. 428-42.
- Mayberg, H. S. (1997) 'Limbic-cortical dysregulation: a proposed model of depression', *J Neuropsychiatry Clin Neurosci*, 9, (3), pp. 471-81.
- Mayberg, H. S., Liotti, M., Brannan, S. K., McGinnis, S., Mahurin, R. K., Jerabek, P. A., Silva, J. A., Tekell, J. L., Martin, C. C., Lancaster, J. L. and Fox, P. T.

- (1999) 'Reciprocal limbic-cortical function and negative mood: converging PET findings in depression and normal sadness', *Am J Psychiatry*, 156, (5), pp. 675-82.
- McEwen, B. S. (1997) 'Possible mechanisms for atrophy of the human hippocampus', *Mol Psychiatry*, 2, (3), pp. 255-62.
- McKeith, I. (2005) 'Dementia with Lewy bodies', *Psychiatry*, 4, (1), pp. 52-55.
- McKeith, I., Del Ser, T., Spano, P., Emre, M., Wesnes, K., Anand, R., Cicin-Sain, A., Ferrara, R. and Spiegel, R. (2000a) 'Efficacy of rivastigmine in dementia with Lewy bodies: a randomised, double-blind, placebo-controlled international study', *Lancet*, 356, (9247), pp. 2031-6.
- McKeith, I., Fairbairn, A., Perry, R., Thompson, P. and Perry, E. (1992) 'Neuroleptic sensitivity in patients with senile dementia of Lewy body type', *BMJ*, 305, (6855), pp. 673-8.
- McKeith, I., Galasko D, Kosaka K, et al. (1996) 'Consensus guidelines for the clinical and pathological diagnosis of dementia with Lewy bodies (DLB): Report on the consortium on DLB international workshop', *Neurology*, 47, pp. 1113-1124.
- McKeith, I., O'Brien, J., Walker, Z., Tatsch, K., Booij, J., Darcourt, J., Padovani, A., Giubbini, R., Bonuccelli, U., Volterrani, D., Holmes, C., Kemp, P., Tabet, N., Meyer, I. and Reininger, C. (2007) 'Sensitivity and specificity of dopamine transporter imaging with 123I-FP-CIT SPECT in dementia with Lewy bodies: a phase III, multicentre study', *Lancet Neurol*, 6, (4), pp. 305-13.
- McKeith, I. G., Ballard, C. G., Perry, R. H., Ince, P. G., O'Brien, J. T., Neill, D., Lowery, K., Jaros, E., Barber, R., Thompson, P., Swann, A., Fairbairn, A. F. and Perry, E. K. (2000b) 'Prospective validation of Consensus criteria for the diagnosis of dementia with Lewy bodies', *Neurology*, 54, (5), pp. 1050-1058.
- McKeith, I. G., Dickson, D. W., Lowe, J., Emre, M., O'Brien, J. T., Feldman, H., Cummings, J., Duda, J. E., Lippa, C., Perry, E. K., Aarsland, D., Arai, H.,

Ballard, C. G., Boeve, B., Burn, D. J., Costa, D., Del Ser, T., Dubois, B., Galasko, D., Gauthier, S., Goetz, C. G., Gomez-Tortosa, E., Halliday, G., Hansen, L. A., Hardy, J., Iwatsubo, T., Kalaria, R. N., Kaufer, D., Kenny, R. A., Korczyn, A., Kosaka, K., Lee, V. M., Lees, A., Litvan, I., Londos, E., Lopez, O. L., Minoshima, S., Mizuno, Y., Molina, J. A., Mukaetova-Ladinska, E. B., Pasquier, F., Perry, R. H., Schulz, J. B., Trojanowski, J. Q. and Yamada, M. (2005) 'Diagnosis and management of dementia with Lewy bodies: third report of the DLB Consortium', *Neurology*, 65, (12), pp. 1863-72.

McKeith, I. G., Galasko, D., Kosaka, K., Perry, E. K., Dickson, D. W., Hansen, L. A., Salmon, D. P., Lowe, J., Mirra, S. S., Byrne, E. J., Lennox, G., Quinn, N. P., Edwardson, J. A., Ince, P. G., Bergeron, C., Burns, A., Miller, B. L., Lovestone, S., Collerton, D., Jansen, E. N., Ballard, C., de Vos, R. A., Wilcock, G. K., Jellinger, K. A. and Perry, R. H. (1996) 'Consensus guidelines for the clinical and pathologic diagnosis of dementia with Lewy bodies (DLB): report of the consortium on DLB international workshop', *Neurology*, 47, (5), pp. 1113-24.

McKhann, G., Drachman, D., Folstein, M., Katzman, R., Price, D. and Stadlan, E. M. (1984) 'Clinical diagnosis of Alzheimer's disease: report of the NINCDS-ADRDA Work Group under the auspices of Department of Health and Human Services Task Force on Alzheimer's Disease', *Neurology*, 34, (7), pp. 939-44.

Menon, R. S., Ogawa, S., Hu, X., Strupp, J. P., Anderson, P. and Ugurbil, K. (1995) 'BOLD based functional MRI at 4 Tesla includes a capillary bed contribution: echo-planar imaging correlates with previous optical imaging using intrinsic signals', *Magn Reson Med*, 33, (3), pp. 453-9.

Minoshima, S., Giordani, B., Berent, S., Frey, K. A., Foster, N. L. and Kuhl, D. E. (1997) 'Metabolic reduction in the posterior cingulate cortex in very early Alzheimer's disease', *Ann Neurol*, 42, (1), pp. 85-94.

Molloy, S., McKeith, I. G., O'Brien, J. T. and Burn, D. J. (2005) 'The role of levodopa in the management of dementia with Lewy bodies', *J Neurol Neurosurg Psychiatry*, 76, (9), pp. 1200-3.

- Molloy, S. A., Rowan, E. N., O'Brien, J. T., McKeith, I. G., Wesnes, K. and Burn, D. J. (2006) 'Effect of levodopa on cognitive function in Parkinson's disease with and without dementia and dementia with Lewy bodies', *J Neurol Neurosurg Psychiatry*, 77, (12), pp. 1323-8.
- Montgomery, S. A. and Asberg, M. (1979) 'A new depression scale designed to be sensitive to change', *Br J Psychiatry*, 134, pp. 382-9.
- Mori, E., Shimomura, T., Fujimori, M., Hirono, N., Imamura, T., Hashimoto, M., Tanimukai, S., Kazui, H. and Hanihara, T. (2000) 'Visuoperceptual impairment in dementia with Lewy bodies', *Arch Neurol*, 57, (4), pp. 489-93.
- Murphy, K., Birn, R. M., Handwerker, D. A., Jones, T. B. and Bandettini, P. A. (2009) 'The impact of global signal regression on resting state correlations: are anti-correlated networks introduced?', *Neuroimage*, 44, (3), pp. 893-905.
- Nelson, P. T., Jicha, G. A., Kryscio, R. J., Abner, E. L., Schmitt, F. A., Cooper, G., Xu, L. O., Smith, C. D. and Markesbery, W. R. (2010) 'Low sensitivity in clinical diagnoses of dementia with Lewy bodies', *J Neurol*, 257, (3), pp. 359-66.
- Nelson, P. T., Kryscio, R. J., Abner, E. L., Schmitt, F. A., Jicha, G. A., Mendiondo, M. S., Cooper, G., Smith, C. B. and Markesbery, W. R. (2009) 'Acetylcholinesterase inhibitor treatment is associated with relatively slow cognitive decline in patients with Alzheimer's disease and AD + DLB', *J Alzheimers Dis*, 16, (1), pp. 29-34.
- Nilsson, L., Nordberg, A., Hardy, J., Wester, P. and Winblad, B. (1986) 'Physostigmine restores 3H-acetylcholine efflux from Alzheimer brain slices to normal level', *J Neural Transm*, 67, (3-4), pp. 275-85.
- Nobler, M., Roose, S., Prohovnik, I., Moeller, J., Louie, J., Van Heertum, R. and Sackeim, H. (2000) 'Regional cerebral blood flow in mood disorders, V.: Effects of antidepressant medication in late-life depression', *Am J Geriatr Psychiatry*, 8, (4), pp. 289-96.

- O'Brien, J. (2007) 'Role of imaging techniques in the diagnosis of dementia', *Br J Radiol*, 80, (2), pp. S71-7.
- O'Brien, J., Ames, D., Chiu, E., Schweitzer, I., Desmond, P. and Tress, B. (1998) 'Severe deep white matter lesions and outcome in elderly patients with major depressive disorder: follow up study', *BMJ*, 317, (7164), pp. 982-4.
- O'Brien, J., Desmond, P., Ames, D., Schweitzer, I., Harrigan, S. and Tress, B. (1996) 'A magnetic resonance imaging study of white matter lesions in depression and Alzheimer's disease', *Br J Psychiatry*, 168, (4), pp. 477-85.
- O'Brien, J. T., Colloby, S., Fenwick, J., Williams, E. D., Firbank, M., Burn, D., Aarsland, D. and McKeith, I. G. (2004a) 'Dopamine transporter loss visualized with FP-CIT SPECT in the differential diagnosis of dementia with Lewy bodies', *Arch Neurol*, 61, (6), pp. 919-25.
- O'Brien, J. T., Lloyd, A., McKeith, I., Gholkar, A. and Ferrier, N. (2004b) 'A longitudinal study of hippocampal volume, cortisol levels, and cognition in older depressed subjects', *Am J Psychiatry*, 161, (11), pp. 2081-90.
- O'Brien, J. T., Paling, S., Barber, R., Williams, E. D., Ballard, C., McKeith, I. G., Gholkar, A., Crum, W. R., Rossor, M. N. and Fox, N. C. (2001) 'Progressive brain atrophy on serial MRI in dementia with Lewy bodies, AD, and vascular dementia', *Neurology*, 56, (10), pp. 1386-8.
- Ogawa, S., Lee, T. M., Kay, A. R. and Tank, D. W. (1990) 'Brain magnetic resonance imaging with contrast dependent on blood oxygenation', *Proc Natl Acad Sci U S A*, 87, (24), pp. 9868-72.
- Ogawa, S., Menon, R. S., Kim, S. G. and Ugurbil, K. (1998) 'On the characteristics of functional magnetic resonance imaging of the brain', *Annu Rev Biophys Biomol Struct*, 27, pp. 447-74.
- Ogawa, S., Menon, R. S., Tank, D. W., Kim, S. G., Merkle, H., Ellermann, J. M. and Ugurbil, K. (1993) 'Functional brain mapping by blood oxygenation level-

dependent contrast magnetic resonance imaging. A comparison of signal characteristics with a biophysical model', *Biophys J*, 64, (3), pp. 803-12.

Ogawa, S., Menon, RS, Kim, SG, Ugurbil K. (1998) 'On the characteristics of functional magnetic resonance imaging of the brain. ', *Annual Review of Biophysics & Biomolecular Structure.* , 27, pp. 447-74.

Pasley, B. N., Inglis, B. A. and Freeman, R. D. (2007) 'Analysis of oxygen metabolism implies a neural origin for the negative BOLD response in human visual cortex.', *Neuroimage*, 36, pp. 269-276.

Pauling, L. and Coryell, C. D. (1936) 'The Magnetic Properties and Structure of Hemoglobin, Oxyhemoglobin and Carbonmonoxyhemoglobin', *Proc Natl Acad Sci U S A*, 22, (4), pp. 210-6.

Perry, E. K., Gibson, P. H., Blessed, G., Perry, R. H. and Tomlinson, B. E. (1977) 'Neurotransmitter enzyme abnormalities in senile dementia. Choline acetyltransferase and glutamic acid decarboxylase activities in necropsy brain tissue', *J Neurol Sci*, 34, (2), pp. 247-65.

Perry, E. K., Haroutunian, V., Davis, K. L., Levy, R., Lantos, P., Eagger, S., Honavar, M., Dean, A., Griffiths, M., McKeith, I. G. and et al. (1994) 'Neocortical cholinergic activities differentiate Lewy body dementia from classical Alzheimer's disease', *Neuroreport*, 5, (7), pp. 747-9.

Perry, E. K. and Perry, R. H. (2004) 'Neurochemistry of consciousness: cholinergic pathologies in the human brain', *Prog Brain Res*, 145, pp. 287-99.

Perry, R. H., Irving, D., Blessed, G., Fairbairn, A. and Perry, E. K. (1990) 'Senile dementia of Lewy body type. A clinically and neuropathologically distinct form of Lewy body dementia in the elderly', *J Neurol Sci*, 95, (2), pp. 119-39.

Petersen, R. C., Smith, G. E., Waring, S. C., Ivnik, R. J., Tangalos, E. G. and Kokmen, E. (1999) 'Mild cognitive impairment: clinical characterization and outcome', *Arch Neurol*, 56, (3), pp. 303-8.

- Piggott, M. A., Ballard, C. G., Rowan, E., Holmes, C., McKeith, I. G., Jaros, E., Perry, R. H. and Perry, E. K. (2007) 'Selective loss of dopamine D2 receptors in temporal cortex in dementia with Lewy bodies, association with cognitive decline', *Synapse*, 61, (11), pp. 903-11.
- Piggott, M. A., Marshall, E. F., Thomas, N., Lloyd, S., Court, J. A., Jaros, E., Burn, D., Johnson, M., Perry, R. H., McKeith, I. G., Ballard, C. and Perry, E. K. (1999) 'Striatal dopaminergic markers in dementia with Lewy bodies, Alzheimer's and Parkinson's diseases: rostrocaudal distribution', *Brain*, 122, pp. 1449-68.
- Pimlott, S. L., Piggott, M., Ballard, C., McKeith, I., Perry, R., Kometa, S., Owens, J., Wyper, D. and Perry, E. (2006) 'Thalamic nicotinic receptors implicated in disturbed consciousness in dementia with Lewy bodies', *Neurobiol Dis*, 21, (1), pp. 50-6.
- Poline, J. B., Worsley, K. J., Evans, A. C. and Friston, K. J. (1997) 'Combining spatial extent and peak intensity to test for activations in functional imaging', *Neuroimage*, 5, (2), pp. 83-96.
- Porsteinsson, A. P., Grossberg, G. T., Mintzer, J. and Olin, J. T. (2008) 'Memantine treatment in patients with mild to moderate Alzheimer's disease already receiving a cholinesterase inhibitor: a randomized, double-blind, placebo-controlled trial', *Curr Alzheimer Res*, 5, (1), pp. 83-9.
- Raichle, M. E., MacLeod, A. M., Snyder, A. Z., Powers, W. J., Gusnard, D. A. and Shulman, G. L. (2001) 'A default mode of brain function', *Proc Natl Acad Sci U S A*, 98, (2), pp. 676-82.
- Raichle, M. E. and Snyder, A. Z. (2007) 'A default mode of brain function: a brief history of an evolving idea', *Neuroimage*, 37, (4), pp. 1083-90; discussion 1097-9.
- Rainer, M. K., Mucke, H. A., Zehetmayer, S., Krampla, W., Kuselbauer, T., Weissgram, S., Jungwirth, S., Tragl, K. H. and Fischer, P. (2006) 'Data from the

VITA Study do not support the concept of vascular depression', *Am J Geriatr Psychiatry*, 14, (6), pp. 531-7.

Raschetti, R., Albanese, E., Vanacore, N. and Maggini, M. (2007) 'Cholinesterase inhibitors in mild cognitive impairment: a systematic review of randomised trials', *PLoS Med*, 4, (11), pp. e338.

Raz, N., Rodrigue, K. M., Kennedy, K. M. and Acker, J. D. (2007) 'Vascular health and longitudinal changes in brain and cognition in middle-aged and older adults', *Neuropsychology*, 21, (2), pp. 149-57.

Reisberg, B., Doody, R., Stoffler, A., Schmitt, F., Ferris, S. and Mobius, H. J. (2003) 'Memantine in moderate-to-severe Alzheimer's disease', *N Engl J Med*, 348, (14), pp. 1333-41.

Ritchie, K., Artero, S. and Touchon, J. (2001) 'Classification criteria for mild cognitive impairment: a population-based validation study', *Neurology*, 56, (1), pp. 37-42.

Rogawski, M. A. and Wenk, G. L. (2003) 'The neuropharmacological basis for the use of memantine in the treatment of Alzheimer's disease', *CNS Drug Rev*, 9, (3), pp. 275-308.

Rombouts, S. A., Barkhof, F., Veltman, D. J., Machielsen, W. C., Witter, M. P., Bierlaagh, M. A., Lazeron, R. H., Valk, J. and Scheltens, P. (2000) 'Functional MR imaging in Alzheimer's disease during memory encoding', *AJNR Am J Neuroradiol*, 21, (10), pp. 1869-75.

Rombouts, S. A., Goekoop, R., Stam, C. J., Barkhof, F. and Scheltens, P. (2005) 'Delayed rather than decreased BOLD response as a marker for early Alzheimer's disease', *Neuroimage*, 26, (4), pp. 1078-85.

Roth, M., Tym, E., Mountjoy, C. Q., Huppert, F. A., Hendrie, H., Verma, S. and Goddard, R. (1986) 'CAMDEX. A standardised instrument for the diagnosis of mental disorder in the elderly with special reference to the early detection of dementia', *Br J Psychiatry*, 149, pp. 698-709.

- Rowe, C. C., Ng, S., Ackermann, U., Gong, S. J., Pike, K., Savage, G., Cowie, T. F., Dickinson, K. L., Maruff, P., Darby, D., Smith, C., Woodward, M., Merory, J., Tochon-Danguy, H., O'Keefe, G., Klunk, W. E., Mathis, C. A., Price, J. C., Masters, C. L. and Villemagne, V. L. (2007) 'Imaging beta-amyloid burden in aging and dementia', *Neurology*, 68, (20), pp. 1718-25.
- Roy, A. K., Shehzad, Z., Margulies, D. S., Kelly, A. M., Uddin, L. Q., Gotimer, K., Biswal, B. B., Castellanos, F. X. and Milham, M. P. (2009) 'Functional connectivity of the human amygdala using resting state fMRI', *Neuroimage*, 45, (2), pp. 614-26.
- Rylett, R. J., Ball, M. J. and Colhoun, E. H. (1983) 'Evidence for high affinity choline transport in synaptosomes prepared from hippocampus and neocortex of patients with Alzheimer's disease', *Brain Res*, 289, (1-2), pp. 169-75.
- Sanacora, G., Mason, G., Rothman, D., Behar, K., Hyder, F., Petroff, O., Berman, R., Charney, D. and Krystal, J. (1999) 'Reduced Cortical -Aminobutyric Acid Levels in Depressed Patients Determined by Proton Magnetic Resonance Spectroscopy ', *Arch Gen Psychiatry*, 56, pp. 1043-1047.
- Sauer, J., Ffytche, D. H., Ballard, C., Brown, R. G. and Howard, R. (2006) 'Differences between Alzheimer's disease and dementia with Lewy bodies: an fMRI study of task-related brain activity', *Brain*, 129, (Pt 7), pp. 1780-8.
- Scheltens, P., Leys, D., Barkhof, F., Huglo, D., Weinstein, H. C., Vermersch, P., Kuiper, M., Steinling, M., Wolters, E. C. and Valk, J. (1992) 'Atrophy of medial temporal lobes on MRI in "probable" Alzheimer's disease and normal ageing: diagnostic value and neuropsychological correlates', *J Neurol Neurosurg Psychiatry*, 55, (10), pp. 967-72.
- Schildkraut, J. J. (1965) 'The catecholamine hypothesis of affective disorders: a review of supporting evidence', *Am J Psychiatry*, 122, (5), pp. 509-22.

- Sheikh, J. I. and Yesavage, J. A. (1986) *Geriatric Depression Scale (GDS). Recent evidence and development of a shorter version.* . New York: The Haworth Press.
- Sheline, Y. I. (2003) 'Neuroimaging studies of mood disorder effects on the brain', *Biol Psychiatry*, 54, (3), pp. 338-52.
- Sheline, Y. I., Barch, D. M., Garcia, K., Gersing, K., Pieper, C., Welsh-Bohmer, K., Steffens, D. C. and Doraiswamy, P. M. (2006) 'Cognitive function in late life depression: relationships to depression severity, cerebrovascular risk factors and processing speed', *Biol Psychiatry*, 60, (1), pp. 58-65.
- Sheline, Y. I., Barch, D. M., Price, J. L., Rundle, M. M., Vaishnavi, S. N., Snyder, A. Z., Mintun, M. A., Wang, S., Coalson, R. S. and Raichle, M. E. (2009) 'The default mode network and self-referential processes in depression', *Proc Natl Acad Sci U S A*, 106, (6), pp. 1942-7.
- Sheline, Y. I., Price, J. L., Vaishnavi, S. N., Mintun, M. A., Barch, D. M., Epstein, A. A., Wilkins, C. H., Snyder, A. Z., Couture, L., Schechtman, K. and McKinstry, R. C. (2008) 'Regional white matter hyperintensity burden in automated segmentation distinguishes late-life depressed subjects from comparison subjects matched for vascular risk factors', *Am J Psychiatry*, 165, (4), pp. 524-32.
- Sheline, Y. I., Price, J. L., Yan, Z. and Mintun, M. A. (2010) 'Resting-state functional MRI in depression unmasking increased connectivity between networks via the dorsal nexus', *Proc Natl Acad Sci U S A*, 107, (24), pp. 11020-5.
- Sheline, Y. I., Wang, P. W., Gado, M. H., Csernansky, J. G. and Vannier, M. W. (1996) 'Hippocampal atrophy in recurrent major depression', *Proc Natl Acad Sci U S A*, 93, (9), pp. 3908-13.
- Shmuel, A., Yacoub, E., Pfeuffer, J., Van de Moortele, P. F., Adriany, G., Hu, X. and Ugurbil, K. (2002) 'Sustained negative BOLD, blood flow and oxygen consumption response and its coupling to the positive response in the human brain', *Neuron*, 36, (6), pp. 1195-210.

- Shmueli, K., van Gelderen, P., de Zwart, J. A., Horovitz, S. G., Fukunaga, M., Jansma, J. M. and Duyn, J. H. (2007) 'Low-frequency fluctuations in the cardiac rate as a source of variance in the resting-state fMRI BOLD signal', *Neuroimage*, 38, (2), pp. 306-20.
- Shulman, G. L., Fiez, J. A., Corbetta, M., Buckner, R. L., Miezin, F. M., Raichle, M. E. and Petersen, S. E. (1997) 'Common blood flow changes across visual tasks: decrease in cerebral cortex.', *J Cogn Neurosci*, 9, pp. 648-663.
- Smith, G., Kramer, E., Ma, Y., Kingsley, P., Dhawan, V., Chaly, T. and Eidelberg, D. (2009) 'The Functional Neuroanatomy of Geriatric Depression', *Int J Geriatr Psychiatr*, 24, (8), pp. 798-808.
- Smith, G., Kramer, E., Reynolds, C., Hermann, C., Ma, Y., Greenwald, B., Pollock, B. and D., E. (2004a) 'Positron Emission Tomography Studies of the Functional Neuroanatomy of Geriatric Depression.', *Biological Psychiatry*, 55, (181S).
- Smith, S. M. (2002) 'Fast robust automated brain extraction', *Hum Brain Mapp*, 17, (3), pp. 143-55.
- Smith, S. M., Jenkinson, M., Woolrich, M. W., Beckmann, C. F., Behrens, T. E., Johansen-Berg, H., Bannister, P. R., De Luca, M., Drobnjak, I., Flitney, D. E., Niazy, R. K., Saunders, J., Vickers, J., Zhang, Y., De Stefano, N., Brady, J. M. and Matthews, P. M. (2004b) 'Advances in functional and structural MR image analysis and implementation as FSL', *Neuroimage*, 23 Suppl 1, pp. S208-19.
- Sorg, C., Riedl, V., Muhlau, M., Calhoun, V. D., Eichele, T., Laer, L., Drzezga, A., Forstl, H., Kurz, A., Zimmer, C. and Wohlschlagel, A. M. (2007) 'Selective changes of resting-state networks in individuals at risk for Alzheimer's disease', *Proc Natl Acad Sci U S A*, 104, (47), pp. 18760-5.
- Sperling, R. A., Bates, J. F., Chua, E. F., Cocchiarella, A. J., Rentz, D. M., Rosen, B. R., Schacter, D. L. and Albert, M. S. (2003) 'fMRI studies of associative encoding in young and elderly controls and mild Alzheimer's disease', *J Neurol Neurosurg Psychiatry*, 74, (1), pp. 44-50.

SPSS for Windows. (2006) Chicago SPSS Inc (Rel 15.0.1).

Steffens, D., McQuoid, D., Payne, M. and Potter, G. (2010) 'Change in Hippocampal Volume on Magnetic Resonance Imaging and Cognitive Decline Among Older Depressed and Nondepressed Subjects in the Neurocognitive Outcomes of Depression in the Elderly Study', *Am J Geriatr Psychiatry*, Jun 1 [Epub ahead of print].

Steffens, D. C., Byrum, C. E., McQuoid, D. R., Greenberg, D. L., Payne, M. E., Blitchington, T. F., MacFall, J. R. and Krishnan, K. R. (2000) 'Hippocampal volume in geriatric depression', *Biol Psychiatry*, 48, (4), pp. 301-9.

Steffens, D. C., Chung, H., Krishnan, K. R., Longstreth, W. T., Jr., Carlson, M. and Burke, G. L. (2008) 'Antidepressant treatment and worsening white matter on serial cranial magnetic resonance imaging in the elderly: the Cardiovascular Health Study', *Stroke*, 39, (3), pp. 857-62.

Stok, C. J., Meijs, W.H. and Peters, M.J. (1987) 'Inverse solutions based on MEG and EEG applied to volume conductor analysis', *Phys Med Biol*, 32, pp. 99-104.

Strother, S. C., Anderson, J. R., Schaper, K. A., Sidtis, J. J., Liow, J. S., Woods, R. P. and Rottenberg, D. A. (1995) 'Principal component analysis and the scaled subprofile model compared to intersubject averaging and statistical parametric mapping: I. "Functional connectivity" of the human motor system studied with [15O]water PET', *J Cereb Blood Flow Metab*, 15, (5), pp. 738-53.

Taki, J., Yoshita, M., Yamada, M. and Tonami, N. (2004) 'Significance of 123I-MIBG scintigraphy as a pathophysiological indicator in the assessment of Parkinson's disease and related disorders: it can be a specific marker for Lewy body disease', *Ann Nucl Med*, 18, (6), pp. 453-61.

Talairach, J. and Tournoux, P. (1988) *Co-planar stereotaxic atlas of the human brain: an approach to medical cerebral imaging*. Stuttgart; New York: Thieme Medical Publishers.

- Tariot, P. N., Farlow, M. R., Grossberg, G. T., Graham, S. M., McDonald, S. and Gergel, I. (2004) 'Memantine treatment in patients with moderate to severe Alzheimer disease already receiving donepezil: a randomized controlled trial', *JAMA*, 291, (3), pp. 317-24.
- Taylor, W. D., MacFall, J. R., Payne, M. E., McQuoid, D. R., Steffens, D. C., Provenzale, J. M. and Krishnan, R. R. (2005) 'Greater MRI lesion volumes in elderly depressed subjects than in control subjects', *Psychiatry Res* 139, (1), pp. 1-7.
- Terry, R. D., Peck, A., DeTeresa, R., Schechter, R. and Horoupian, D. S. (1981) 'Some morphometric aspects of the brain in senile dementia of the Alzheimer type', *Ann Neurol*, 10, (2), pp. 184-92.
- Thomas, A., Burn, D. and Rowan, E. (2005) 'A comparison of the efficacy of donepezil in Parkinson's disease with dementia and dementia with Lewy bodies', *Int J Geriatric Psychiatry* 20, pp. 938-944.
- Thomas, A. J., Gallagher, P., Robinson, L. J., Porter, R. J., Young, A. H., Ferrier, I. N. and O'Brien, J. T. (2008) 'A comparison of neurocognitive impairment in younger and older adults with major depression', *Psychol Med*, pp. 1-9.
- Thomas, A. J. and O'Brien, J. T. (2008) 'Depression and cognition in older adults', *Curr Opin Psychiatry*, 21, (1), pp. 8-13.
- Thomas, A. J., O'Brien, J. T., Davis, S., Ballard, C., Barber, R., Kalaria, R. N. and Perry, R. H. (2002) 'Ischemic basis for deep white matter hyperintensities in major depression: a neuropathological study', *Arch Gen Psychiatry*, 59, (9), pp. 785-92.
- Uddin, L. Q., Kelly, A. M., Biswal, B. B., Xavier Castellanos, F. and Milham, M. P. (2009) 'Functional connectivity of default mode network components: correlation, anticorrelation, and causality', *Hum Brain Mapp*, 30, (2), pp. 625-37.

- Veer, I. M., Beckmann, C. F., van Tol, M. J., Ferrarini, L., Milles, J., Veltman, D. J., Aleman, A., van Buchem, M. A., van der Wee, N. J. and Rombouts, S. A. (2010) 'Whole brain resting-state analysis reveals decreased functional connectivity in major depression', *Front Syst Neurosci*, 4, pp. 41.
- Villringer, A. (1999) 'Physiological changes during brain activation', in Moonen, C. T. W. and Bandettini, P. A.(eds) *Functional MRI*. Berlin: Springer, pp. 3-13.
- Walker, M. P., Ayre, G. A., Cummings, J. L., Wesnes, K., McKeith, I. G., O'Brien, J. T. and Ballard, C. G. (2000) 'The Clinician Assessment of Fluctuation and the One Day Fluctuation Assessment Scale. Two methods to assess fluctuating confusion in dementia', *Br J Psychiatry*, 177, pp. 252-6.
- Walker, Z., Costa, D. C., Walker, R. W., Shaw, K., Gacinovic, S., Stevens, T., Livingston, G., Ince, P., McKeith, I. G. and Katona, C. L. (2002) 'Differentiation of dementia with Lewy bodies from Alzheimer's disease using a dopaminergic presynaptic ligand', *J Neurol Neurosurg Psychiatry*, 73, (2), pp. 134-40.
- Walter, M., Henning, A., Grimm, S., Schulte, R., Beck, J., Dydak, U., Schnepf, B., Boeker, H., Boesiger, P. and Northoff, G. (2009) 'The Relationship Between Aberrant Neuronal Activation in the Pregenua Anterior Cingulate, Altered Glutamatergic Metabolism, and Anhedonia in Major Depression', *Arch Gen Psychiatry*, 66, (5), pp. 478-486.
- Wang, K., Liang, M., Wang, L., Tian, L., Zhang, X., Li, K. and Jiang, T. (2007) 'Altered functional connectivity in early Alzheimer's disease: a resting-state fMRI study', *Hum Brain Mapp*, 28, (10), pp. 967-78.
- Wang, L., Zang, Y., He, Y., Liang, M., Zhang, X., Tian, L., Wu, T., Jiang, T. and Li, K. (2006) 'Changes in hippocampal connectivity in the early stages of Alzheimer's disease: evidence from resting state fMRI', *Neuroimage*, 31, (2), pp. 496-504.
- Weissenbacher, A., Kasess, C., Gerstl, F., Lanzenberger, R., Moser, E. and Windischberger, C. (2009) 'Correlations and anticorrelations in resting-state

functional connectivity MRI: a quantitative comparison of preprocessing strategies', *Neuroimage*, 47, (4), pp. 1408-16.

Wellcome Trust Centre for Neuroimaging. (2005) 'Statistical Parametric Mapping (SPM5)', *University College London, UK*.

Whitehouse, P. J., Price, D. L., Struble, R. G., Clark, A. W., Coyle, J. T. and Delon, M. R. (1982) 'Alzheimer's disease and senile dementia: loss of neurons in the basal forebrain', *Science*, 215, (4537), pp. 1237-9.

Whitwell, J. L., Weigand, S. D., Shiung, M. M., Boeve, B. F., Ferman, T. J., Smith, G. E., Knopman, D. S., Petersen, R. C., Benarroch, E. E., Josephs, K. A. and Jack, C. R., Jr. (2007) 'Focal atrophy in dementia with Lewy bodies on MRI: a distinct pattern from Alzheimer's disease', *Brain*, 130, (Pt 3), pp. 708-19.

Wise, R. G., Ide, K., Poulin, M. J. and Tracey, I. (2004) 'Resting fluctuations in arterial carbon dioxide induce significant low frequency variations in BOLD signal', *Neuroimage*, 21, (4), pp. 1652-64.

Woolrich, M. W., Behrens, T. E., Beckmann, C. F., Jenkinson, M. and Smith, S. M. (2004) 'Multilevel linear modelling for fMRI group analysis using Bayesian inference', *Neuroimage*, 21, (4), pp. 1732-47.

Woolrich, M. W., Ripley, B. D., Brady, M. and Smith, S. M. (2001) 'Temporal autocorrelation in univariate linear modeling of fMRI data', *Neuroimage*, 14, (6), pp. 1370-86.

Woolsey, T. A., Rovainen, C. M., Cox, S. B., Henegar, M. H., Liang, G. E., Liu, D., Moskalenko, Y. E., Sui, J. and Wei, L. (1996) 'Neuronal units linked to microvascular modules in cerebral cortex: response elements for imaging the brain', *Cereb Cortex*, 6, (5), pp. 647-60.

Worsley, K. (2001) 'Statistical analysis of activation images.', in Jezzard, P., Matthews, P. M. and Smith, S. M.(eds) *Functional MRI: An Introduction to Methods*. Oxford University Press.

- Worsley, K. J. and Friston, K. J. (1995) 'Analysis of fMRI time-series revisited - again', *Neuroimage*, 2, (3), pp. 173-81.
- Wu, T., Long, X., Wang, L., Hallett, M., Zang, Y., Li, K. and Chan, P. (2010) 'Functional connectivity of cortical motor areas in the resting state in Parkinson's disease', *Hum Brain Mapp*, Aug 25 [Epub ahead of print].
- Yang, T. T., Gallen, C. C., Schwartz, B. J. and Bloom, F. E. (1993) 'Noninvasive somatosensory homunculus mapping in humans by using a large-array biomagnetometer', *Proc Natl Acad Sci U S A*, 90, (7), pp. 3098-102.
- Yuan, Y., Zhang, Z., Bai, F., Yu, H., Shi, Y., Qian, Y., Liu, W., You, J., Zhang, X. and Liu, Z. (2008) 'Abnormal neural activity in the patients with remitted geriatric depression: a resting-state functional magnetic resonance imaging study', *J Affect Disord*, 111, (2-3), pp. 145-52.
- Zang, Y., Jiang, T., Lu, Y., He, Y. and Tian, L. (2004) 'Regional homogeneity approach to fMRI data analysis', *Neuroimage*, 22, (1), pp. 394-400.
- Zhang, H. Y., Wang, S. J., Xing, J., Liu, B., Ma, Z. L., Yang, M., Zhang, Z. J. and Teng, G. J. (2009) 'Detection of PCC functional connectivity characteristics in resting-state fMRI in mild Alzheimer's disease', *Behav Brain Res*, 197, (1), pp. 103-8.
- Zhou, Y., Yu, C., Zheng, H., Liu, Y., Song, M., Qin, W., Li, K. and Jiang, T. (2010) 'Increased neural resources recruitment in the intrinsic organization in major depression', *J Affect Disord*, 121, (3), pp. 220-30.